Wardah Tahir
Sahol Hamid Abu Bakar
Marfiah Ab. Wahid
Siti Rashidah Mohd Nasir
Wei Koon Lee   *Editors*

ISFRAM 2015

Proceedings of the International Symposium on Flood Research and Management 2015

Springer

ISFRAM 2015

Wardah Tahir · Sahol Hamid Abu Bakar
Marfiah Ab. Wahid · Siti Rashidah Mohd Nasir
Wei Koon Lee
Editors

ISFRAM 2015

Proceedings of the International Symposium
on Flood Research and Management 2015

Springer

Editors
Wardah Tahir
Faculty of Civil Engineering
Universiti Teknologi MARA
Shah Alam, Selangor
Malaysia

Sahol Hamid Abu Bakar
Universiti Teknologi MARA
Shah Alam, Selangor
Malaysia

Marfiah Ab. Wahid
Universiti Teknologi MARA
Shah Alam, Selangor
Malaysia

Siti Rashidah Mohd Nasir
Universiti Teknologi MARA
Shah Alam, Selangor
Malaysia

Wei Koon Lee
Universiti Teknologi MARA
Shah Alam, Selangor
Malaysia

Preface

With increasing urbanization and the rise of more densely populated cities around the world, human civilization is becoming more vulnerable to disasters. Years of development and prosperity can be wiped away in minutes as a consequence of disasters such as tsunami and earthquake. Flood, meanwhile, is another natural hazard which continuously affects many parts of the world. The increasing magnitude and frequency of flood disasters can be attributed to the combined impacts of several factors, including climate change, global warming effects (e.g. glacier melting and sea-level rise), land-use changes, and poor watershed management, amongst others. The problem is evermore pressing today and calls for comprehensive study and in-depth research to arrive at feasible and practical solutions.

The Second International Symposium on Flood Research and Management 2015 (ISFRAM 2015) is organized by the Flood Control Research Center (FCRC), Universiti Teknologi MARA to promote advances in flood research and management for improving resilience towards flood disasters. The objective of ISFRAM 2015 is to provide a forum for researchers, scientists and engineers to share and exchange their views, experiences, and researches in flood-related areas and sustainable management. The symposium presents innovative work and best practices in managing flood and recommendation of flood solutions.

Full paper submissions to the symposium were reviewed by a qualified panel of reviewers before final acceptance. Selected papers were evaluated based on research content, relevance, and originality of contribution. Papers selected cover a broad range of topics from fundamental theories to state-of-the art technology in areas related to flood research and management. The proceedings will serve as a valuable source of reference in managing flood for the betterment and quality of life.

This symposium is supported by FCRC collaborators—Colorado State University, IIT Roorkee, AIT Thailand, Stuttgart University, Asian Core Program (ACP) Kyoto University, Institute of Water Modeling (IWM) Bangladesh, and locally, National Hydraulic of Research Institute, Malaysia (NAHRIM), and the Drainage and

Irrigation Department (DID). I would like to express my deepest gratitude to all committee members, panel of reviewers, authors, session chairs, delegates, and everyone who had contributed directly and indirectly to make ISFRAM 2015 a success.

Wardah Tahir

About FCRC

Flood Control Research Centre, Faculty of Civil Engineering, Universiti Teknologi MARA was established in collaboration with Stuttgart University, Colorado State University, Asian Institute of Technology (AIT) and Indian Institute of Technology (IIT) Roorkee. The objectives of the center are:

- To identify important issues on flood
- To provide the solutions for flood problems in Malaysia
- To train young researchers and staff
- To share the pool of expertise
- To go beyond the Malaysian border
- To get national and international research grants

FCRC local national research collaborators include the National Hydraulic Research Institute Malaysia (NAHRIM), Drainage and Irrigation Department (DID), Lembaga Urus Air Selangor (LUAS), Malaysian Meteorological Department (MMD), Department of Environment (DOE), National Security Council, and Local City Councils. The contributions of these agencies include:

- To share resources, data, and expertise
- To act as the push factor to the government for implementation of the proposed flood solution
- To engage in joint research and supervision
- To engage in joint publication
- To co-organize events and activities

Current and future activities of FCRC include:

(I) **Operate a Flood Library which is equipped with:**

- Simulation models (e.g: HEC-RAS, HEC-HMS, Info works, Mike-11, TREX)
- Collection of structural solutions and key methodologies for flood problem

- Repositories of technical papers
- Open access to other libraries, especially to the partner universities

(II) **Define methodology in master planning of flood, including:**

- Flood risk and damage assessment
- Flood plan to incorporate the entire flood hydrological regime
- Economic analysis of cut-off point for extending flood plan using non-structural method
- Nonstructural flood planning

(III) **Provide training program**

- To increase capacity building for those involved in flood control and management
- To enable access to experts in the consortium of the 5-university collaboration

(IV) **Organizing annual meeting and symposium.**

ISFRAM 2015 Organizing Committee

Patron
Y. Bhg. Tan Sri Dato' Sri Prof. Ir. Dr. Sahol Hamid Abu Bakar FASc

UiTM Advisor
Prof. Dr. Azmi Ibrahim

International Collaborators
Dr. Daniel Gunaratnam, USA
Prof. Dr. Pierre Y. Julien, Colorado State University
Prof. Dr. Silke Wieprecht, Stuttgart University, Germany
Prof. Dr. M. Perumal, Indian Institute of Technology (IIT), Roorkee, India
Prof. Dr. Mukand Singh Babel, Asian Institute of Technology (AIT), Thailand
Institute of Water Modelling (IWM) Bangladesh
Asian Core Program, Kyoto University

National Collaborators
National Hydraulic Research Institute Malaysia
Department of Irrigation and Drainage (DID) Malaysia

General Chair
Assoc. Prof. Dr. Wardah Tahir

General Co-chair
Dr. Siti Rashidah Mohd Nasir

Secretary
Dr. Marfiah Ab. Wahid

Treasurer
Jurina Jaafar

Technical Program Chair
Dr. Mohd Fozi Ali
Dr. Janmaizatulriah Jani

Dr. Lee Wei Koon
Assoc. Prof. Dr. Ramlah Tajuddin

Publication Chair
Dr. Rohana Hassan

Finance Chair
Ros Mini Ismail

Secretariat
Suzana Ramli
Dr. Jazuri Abdullah
Nurulhuda Imran
Sharifah Nurul Huda Syed Yahya

Information and Website Chair
Dr. Ihsan Yassin
Dr. Khasiah Zakaria
Bahroni Moojee

ISFRAM Reviewers

Dr. Mokhtar Guizani, SET King Saud University Saudi Arabia,
e-mail: g_mokh@yahoo.fr
Dr. Milad Jajarmizadeh, UNITEN, e-mail: milad_jajarmi@yahoo.com
Assoc. Prof. Dr. Marlinda Abdul Malik, UNITEN, e-mail: marlinda@uniten.edu.my
Assoc. Prof. Dr. Wardah Tahir, UiTM, e-mail: wardah_tahir@yahoo.com
Mrs. Azlinda Saadon, UNISEL, e-mail: azlinda303@gmail.com
Prof. Dr. Abdul Halim Ghazali, UPM, e-mail: abdhalim@eng.upm.edu.my
Mr. Fauzi Baharudin, UiTM, e-mail: fauzi1956@yahoo.com
Prof. Dr. Faridah Othman, UM, e-mail: faridahothman@um.edu.my
Mrs. Azinoor Azida Abu Bakar, UiTM, e-mail: azinoor@salam.uitm.edu.my
Prof. Dr. Ahmad Khairi Abd Wahab, UTM, e-mail: drakaw@gmail.com
Dr. Marfiah Ab. Wahid, UiTM, e-mail: ce_marfiah@yahoo.com
Dr. Mohd Fozi Ali, UiTM, e-mail: mohdfozi@salam.uitm.edu.my
Dr. Suzana Ramli, UiTM, e-mail: suzana799@salam.uitm.edu.my
Prof. Dr. Ahmad Yahya, USM, e-mail: ceshukri@usm.my
Assoc. Prof. Dr. Ramlah Tajuddin, UiTM, e-mail: reviewramlah2014@gmail.com
Dr. May Raksmey, UiTM, e-mail: may_raksmey@salam.uitm.edu.my
Dr. Lee Wei Koon, UiTM, e-mail: leewei994@salam.uitm.edu.my
Mrs. Nuryazmeen Farhan Haron, UiTM, e-mail: neemzay@yahoo.com
Prof. Dr. Muthiah Perumal, IIT Roorkee, India, e-mail: p_erumal@yahoo.com
Assoc. Prof. Dr. Sucharit Koontanakulvong, Chulalongkorn University, Thailand,
e-mail: sucharit.K@chula.ac.th
Mrs. Caroline Peter Diman, UiTM, e-mail: carolinepeter968@ppinang.uitm.edu.my
Dr. Jazuri Abdullah, UiTM, e-mail: jazuri.abdullah@yahoo.com
Dr. Chia Chay Tay, UiTM, e-mail: taychiay@perlis.uitm.edu.my
Prof. Krzysztof S. Kulpa, Warsaw University of Technology, Poland,
e-mail: K.Kulpa@elka.pw.edu.pl
Prof. Dr. Md Azlin Md Said, USM, e-mail: azlin@eng.usm.my
Assoc. Prof. Dr. Sayang Mohd Deni, UiTM, e-mail: sayang@tmsk.uitm.edu.my
Sharifah Nurul Huda Syed Yahya, UiTM, e-mail: sharifahnurulhuda@hotmail.com
Dr. Nor Aizam Adnan, UiTM, e-mail: nor_aizam@salam.uitm.edu.my

Contents

Part II   Water and Flood Modelling

Part III   Rainfall-Runoff Modelling

Part V   Weather and Climate

Part I
Flood Forecasting and Management

Recent Application of Weather Radar Observation into Hydrologic Forecasting in Japan

Eiichi Nakakita and Sunmin Kim

Abstract This paper introduces recent research efforts on hydrologic flood forecasting in Japan using multiple weather radar observation networks. After illustrating the details of weather radar observation systems in Japan, several noticeable researches of the authors are introduced.

Keywords Weather radar · X-band · C-band · Dual polarization · Early detection · Rain cell · Flood forecasting · Ensemble forecasting

1 Introduction

Advances in weather radar observation techniques have allowed us to expect significant improvement in flash flood forecasting with a distributed hydrologic model. More accurate and localized flood predictions (in terms of estimating flood peak time and magnitude) are now available, by applying state-of-the-art knowledge and technology to hydrology and meteorology. Weather radar has been a widely used tool for precipitation observation for the last several decades, and much research effort has been applied to improve the accuracy of quantitative precipitation estimation (QPE) and quantitative precipitation forecasting (QPF) using weather radar (e.g., [1, 3, 7]).

The radar observation system in Japan is operated by two governmental groups: Japan Meteorological Agency (JMA) and the Ministry of Land, Infrastructure, Transport and Tourism (MLIT) of Japan. The JMA radar observation network is

E. Nakakita (✉)
Disaster Prevention Research Institute, Kyoto University, Gokasyo,
Uji, Kyoto, Japan
e-mail: nakakita@hmd.dpri.kyoto-u.ac.jp

S. Kim
Graduate School of Engineering, Kyoto University, KyotoDaigakuKatsura,
Kyoto, Japan
e-mail: kim.sunmin.6x@kyoto-u.ac.jp

comprised of 20 C-band radars (with a wavelength of 5.6 cm), which cover most of the Japan Islands and observe rainfall intensity and distribution. Radar data are digitized to produce special radar echo composite maps every five minutes for the purpose of monitoring precipitation throughout the country. The data are also calibrated using the gauged point rainfall intensities. On the other hand, the MLIT's radar observation system is composed of 26 C-band radars throughout Japan. The observed radar echo from each radar unit is first modified and then sent to the National Bureau of Synthesis Process within the MLIT. Through several steps for homogenizing observation accuracy, including distance and elevation correction, synthesized rainfall intensity maps for the entire nation of Japan are generated every five minutes.

Those two radar networks of Japan are characterized by their respective observation purposes. The radar observation conducted by the JMA is intended to provide basic information for short-term precipitation forecasting. Thus, it focuses on rainfall distribution and is therefore more sensitive in order to capture the low rainfall intensity values. On the other hand, the observation conducted by the MLIT is intended to assist the flood forecasting system of the River Bureau, MLIT, and is focused on capturing an accurate measurement of rainfall intensities during heavy rainfall. As will be discussed in the following section, the conventional C-band radar observation conducted by the MLIT tends to overestimate rainfall intensities.

The MLIT has recently launched a new radar observation network system designed for flash flood observation and forecasting in small river basins within urban areas. It is called the X-band multi-parameter radar network and is distinguished by its dual polarimetric wave pulses of short length (3 cm). Attenuation problems resulting from the short wave length of radar echo are strengthened by polarimetric wavelengths and very dense radar networks. In total, 39 X-band MP radars have been established around many cities in Japan by 2015, since it was firstly introduced in 2009. Each observation in area around many cities is conducted by 3–4 X-band radars with very fine spatial resolution (250 m) in every one minute.

The details of the X-band radar network are summarized in Table 1, comparing it with the conventional C-band radar observation conducted by the JMA and the

Table 1 Characteristics of each radar observation in Japan

Details	C-band radar network of the JMA	C-band radar network of the MLIT	X-band radar network of the MLIT
Observation interval (min)	10	5	1
Data distribution (min)	5–10	5–10	1–2
Spatial resolution	1 km	1 km	250 m
Wave length (cm)	5–6	5–6	3
Observation range	120 km radius	120 km radius	60 km radius
Dual polarization	No	Partially	Yes
Doppler function	Partially	Partially	Yes
Volume scanning	Yes	Partially	Yes

MLIT. While conventional radar observation takes 10–15 min to observe, collect, and distribute the information to the public, the new radar networks require only 2–3 min for full distribution. At the present time, the observation network is in a testing phase for operational usage, checking the observation accuracy and applicability in a wide variety of aspects.

2 Utilization of X-Band MP Radar

2.1 Background of XRAIN Utilization

On July 28, 2008, about 50 people who were enjoying a sunny day along a small river channel (Toga-gawa) near their residential area in Kobe City, Japan, were swept away by a flash flood caused by the sudden development of a convective rainstorm; five were later found dead. It took only 16 min for the water level of the channel to increase 1.4 meters after the rainstorm started in the small, 8.7 km^2 catchment area [6].

Later, it was found that a single cumulonimbus cloud developed about 30 min before the heavy rain started and induced the flash flood [2]. In the same year, another five people working in an underground sewage pipe system in Tokyo City were swept away and lost their lives because of flash flood in an urbanized area induced by a suddenly developed cumulonimbus cloud.

Intensive investigations and research were done to figure out the exact procedure of the tragic accidents and to prevent those kinds of disasters in the future. Among the information, the first echo of the Toga-gawa rainstorm event was detected with a three-dimensional volume scan image from a C-band radar [2]. The first echo of the rainstorm was detected at a 5 km height in the atmosphere at 14:14 p.m. that day, which was 15 min before the rain started on the ground and 31 min before the flash flood occurred.

Even considering a certain amount of time lapsed for a warning to be issued and evacuation to occur, this early detection could have provided enough time to save all those people. There have been continuous research efforts to provide precise short-term rainfall forecasting based on real-time radar observation data (e.g., [1, 3]) as well as combining with numerical weather prediction model outputs (e.g., [7]). However, the conventional nowcasting skills are not able to predict such a suddenly developed convective rainstorm, since the conventional methods are based on already developed rainstorms.

Meanwhile, as a nationwide countermeasure, the Japanese government has been installing a new weather radar network called X-band polarimetric radar information network (XRAIN) around the major urban areas in Japan since 2010 to prevent flash flood disasters with more accurate and faster observations of rainstorms. For the last 4 years, the Ministry of Land, Infrastructure, Transport and Tourism (MLIT) of Japan has equipped 14 major cities, including Tokyo, Nagoya, Osaka, and Kobe, with 39 XRAIN radars (see Fig. 1).
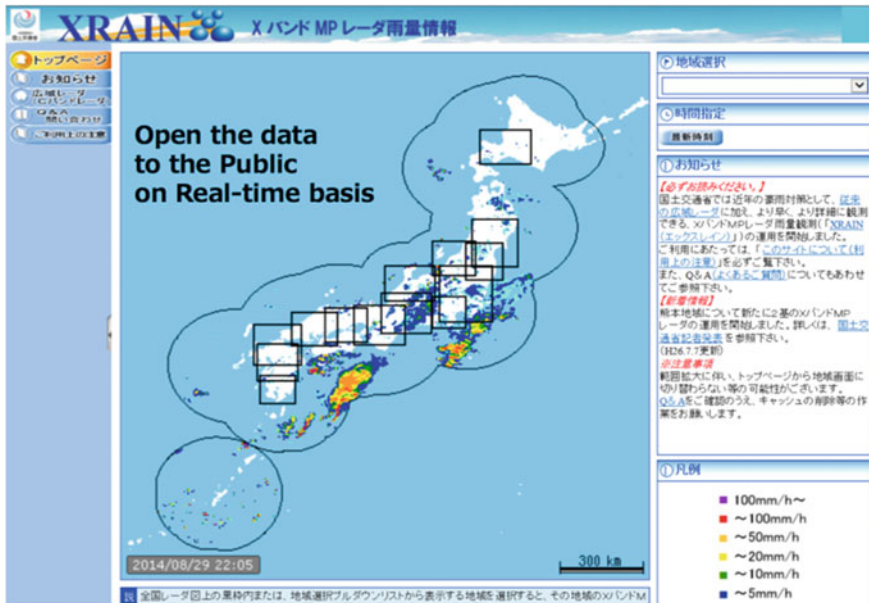
Fig. 1 Screen shot of XRAIN Web site to public. Solid rectangular line shows 14 areas covered by 39 XRAIN radars

The XRAIN radar is characterized by high spatial resolution (250 m) and frequent observation interval (1-minute) with X-band wavelengths (3 cm) within the densely overlapped observation network, allowing us to overcome the attenuation and short observation range problems. The dual-polarized radio waves of XRAIN provide improved polarimetric functions, such as ZDR and KDP, which provide higher accuracy of quantitative precipitation estimations (QPEs) compared to the conventional QPE based on the Z–R relationship. Superiority of polarimetric weather radar has been well known for its improved accuracy of QPEs as well as its applicability for detecting hazardous convective rainstorms. Additionally, Doppler velocity of rain cells is observed with three-dimensional volume scanning. One of the best merits of XRAIN is that it takes only one minute to get the composed horizontal distribution of rainfall intensity from the observation network, and one cycle of the three-dimensional volume scan is available every five minutes.

2.2 Early Detection of Baby Rain cell

Based on the newly equipped radar observation network of Japan, our research team has been developing an effective algorithm to detect a baby rain cell, which is the early stage of a single-cell rainstorm (refer to Fig. 2). The definition of a

Fig. 2 Radar depiction of a rainstorm, showing life cycle of radar cross section. Early detection algorithm is able to detect the first echo in the stage of 1 or 2 and is also able to evaluate whether it will be developed to heavy rainfall
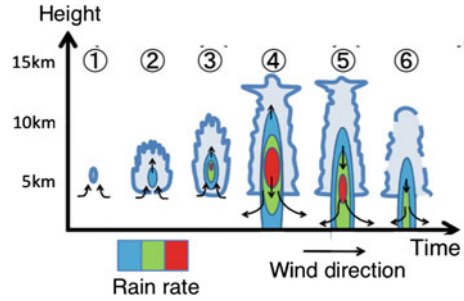
single-cell rainstorm in this study is a rainstorm generated from an independently developed cumulonimbus cloud having more than 50 mm/h of rainfall intensity. The criteria to select baby rain cells from numerous radar echoes are set empirically as a first echo having more than 20 dBZ of intensity when there was no precedent reflectivity in the previous volume scan (5 min before) within a 5 km radius. The reflectivity criteria were set as a relatively low value to detect very early stages of baby rain cells while trying to avoid interruption from noise echo.

The microscale vertex in the early stage of rainstorms was observed in our previous study [4], and it was able to estimate pseudo-vorticity using the Doppler velocity observation. Based on the introduced early detection algorithm, it was able to detect baby rain cells 5–15 min before their development, and it was successful at determining the danger level for whether the rain cells would finally downpour to the ground as heavy rainfall (see Fig. 3).
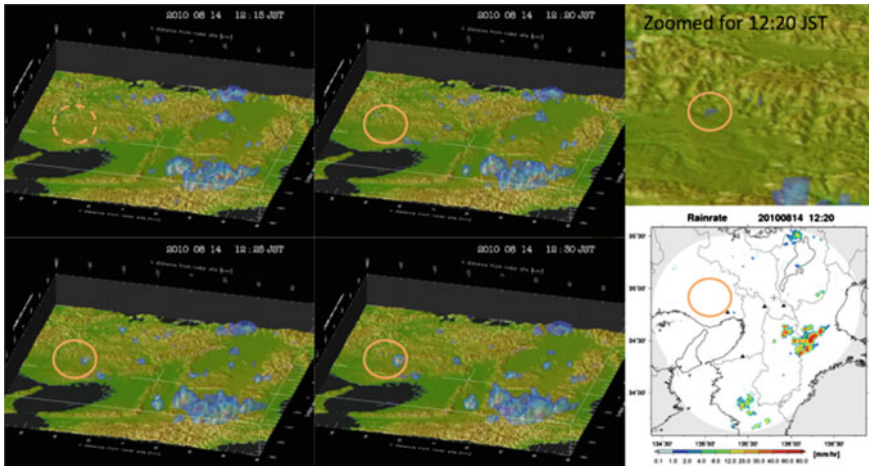
Fig. 3 An example of a detected baby rain cell at 12:20 p.m. on Aug. 14, 2010. The baby rain cell was first detected at 12:20 p.m. (*upper right*), while there was no rainfall on the ground yet (*bottom right*). The baby rain cell showed its increased volume and reflectivity strength while it moved eastward between 12:25 p.m. and 12:30 p.m. (*bottom left* and *bottom center*)

The evaluation results from the collected 35 single-cell rainstorm events so far showed that every event had a strong vertical vorticity in the early stage of its evolution. Average time until the first detection of vorticity was 1.7 min after the detection of baby rain cells, while the average time of maximum rainfall intensity appeared 25.3 min after the detection of baby rain cells. In the end, vorticity detection occurred 23.6 min before the maximum rainfall intensity on the ground.

Currently, an automatic rainstorm nowcasting system is under developing based on the baby rain cell detection and the vorticity estimation algorithm. The purpose of the rainstorm nowcasting system development is to provide early warnings of single-cell rainstorms even before it starts to rain. The major algorithm of the system is divided into three steps: (1) to detect a baby rain cell in the early stage of a single-cell rainstorm, (2) to decide its danger level with the vorticity estimation, and (3) to trace the baby rain cell until it develops into a rainstorm and finally disappears.

It is noteworthy that only 10 min or even 5 min of earlier detection could give us enough time to save lives from a natural disaster. And, the presented algorithm and system are based on the ongoing collaborative research with the Ministry of Land, Infrastructure, Transport and Tourism (MLIT) of Japan, with continuous upgrading of the equipped XRAIN observation system.

3 Ensemble Forecasting with Multiple Input

3.1 Combination of X-Band and C-Band Radar Input

This study is designed to evaluate the new radar observation network from a hydrologic perspective. First of all, the accuracy of the X-band radar observation was determined by comparing its results with the rainfall intensities as observed by ground gauge stations. It was also compared with conventional C-band radar observation of MLIT. The rainfall information from the new radar network was then provided to a distributed hydrologic model to simulate river discharges. The simulated river discharges were evaluated again using the observed river discharge to estimate the applicability of the new observation network in the context of operations regarding flood forecasting.

The tested rainfall data in this study, which was derived from X-band radar and the conventional C-band radar, are provided by the MLIT as synthesized rainfall intensities within rectangular coordinates. However, both data sets are not bias corrected using the ground-gauged data. We adopted an already-built-up rainfall–runoff simulation system on the Yodo River Basin of Japan for the hydrologic evaluation of the radar-observed rainfall data. The Yodo River Basin is in the Kansai District, located in the midwest region of Japan, and is one of the X-band observation networks covering the river basin (the sixth rectangular section from the left in Fig. 1). Details of the selected events are provided in Table 2.

Table 2 Rainfall event utilized in hydrologic evaluation

Event	Event duration	Maximum rainfall intensity
Event 1	02:00–14:00, Aug. 12, 2010	Up to 50 mm/h
Event 2	00:00–18:00, Oct. 09, 2010	20–30 mm/h
Event 3	12:00–24:00, Oct. 31, 2010	10–20 mm/h

Ground gauging observation data from the AMeDAS were collected for the evaluation of the X-band radar observation's accuracy. Ten gauging stations are available within the X-band observation network of the Kansai District. Each AMeDAS observation station offers 10-min intervals of rainfall intensity data, and this data were utilized to evaluate both the X-band radar observation and the C-band radar observation. Figure 4 shows an example of the comparison of the rainfall intensities observed by the AMeDAS ground gauging station, X-band, and C-band radar networks. As the representative example shown in Fig. 4 (up), both observations made by the X-band radar and the C-band radar show a high degree of agreement and accuracy when compared to the ground gauge station values. However, the C-band radar observations show overestimated values in many cases,

Fig. 4 Rainfall intensity comparison using the X-band radar and C-band radar observations compared to the observations at the ground gauging stations (AMeDAS) of Hirakata (*up*) and Kyoto (*down*)
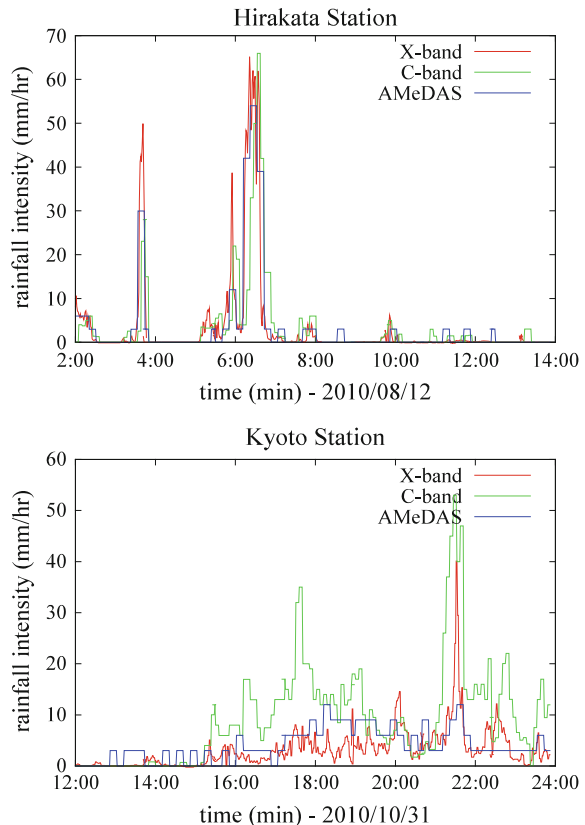
and the X-band radar observations provide underestimated rainfall intensities in some cases.

The rainfall information gathered from the both radar observations was evaluated from a hydrologic perspective. Both rainfall input data sets were provided to the hydrologic model and the simulated river discharges were compared with the observed discharge data to determine the input accuracy. The hydrologic model utilized here was a physically based distributed hydrologic model using one-dimensional kinematic wave equation. For the hillslope runoff simulation using 250-m resolution DEM, the model utilizes the kinematic wave equation, which incorporates a stage discharge relationship for subsurface and surface flow. Channel flow simulation was also conducted by solving the kinematic wave equation and the model produced hourly based hydrographs at each river segment.

The hydrologic model was calibrated manually using the observed point-gauged rainfall data and river discharge data from the Yodo River Basin. There are five parameters to be optimized in the model: roughness coefficient n, soil depths ds and dc, and hydraulic conductivities k_a and k_c [5]. For the evaluation of the radar-observed rainfall data, inflows at the multiple dam sites were simulated using the distributed hydrologic model. Figure 5 (up) shows one of the typical simulation results and their comparison with the observed river discharge at both checkpoints.

The X-band radar-observed rainfall data provide very good simulation results in most cases when those are compared to the observed discharges. The simulation results using the C-band radar-observed rainfall data also give considerably good simulation results. However, the accuracy of the simulation results is diverse in each event and each catchment.

According to the evaluation test on the both radar observations, it was able to understand that the newly equipped X-band polarimetric radar network shows somewhat improved observation accuracy compared to conventional C-band radar observation. However, it has a tendency to underestimate the rainfall, and the accuracy is not always superior to that of the C-band radar.

Based on the evaluation information, we have tested couple of methods to blend the advantages of the both radar networks, one is to synthesize the radar-observed rainfall intensities and the other one is to synthesize the simulated river discharges from each rainfall information. It was found that the both blending methods show improved forecasting accuracy compared to the independent utilization of radar information as shown in Fig. 5 (down).

3.2 Combination of Radar Observation and NWP Output

Many river basins in Japan are characterized by steep mountains in many regions, which are generating orographic rainfall significantly. Because of this orographic effect in the rainfall, it was not easy to get good enough accuracy of radar-based rainfall prediction. To overcome this prediction huddle, [3] proposed an improved radar image extrapolation method by combining orographic rainfall identification
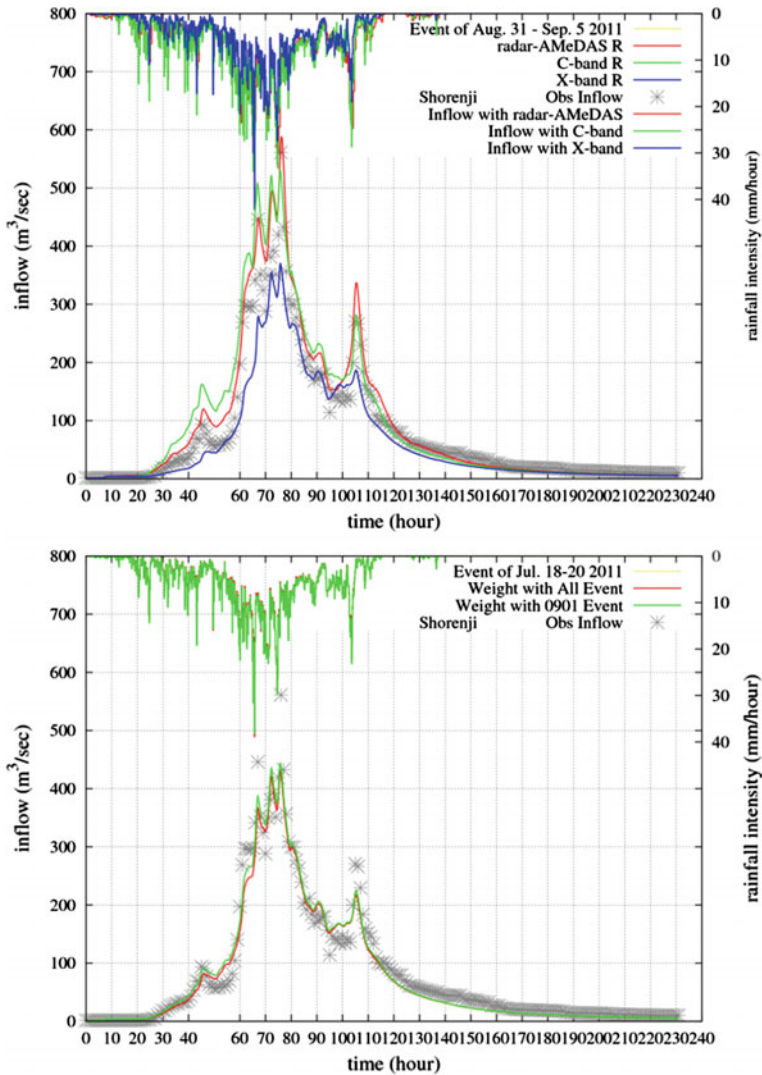
Fig. 5 Runoff simulation results with independent utilization of radar information (*left*) and with the blended radar information (*right*) that shows improved forecasting accuracy

scheme and the error-field scheme considering prediction error structures (Fig. 6). The method was able to improve the prediction accuracy in mountainous areas by separating radar rainfall into orographic and non-orographic rain fields. And consideration of future prediction error using the characteristics of the recent prediction error has been showing robust accuracy improvements [1, 3].
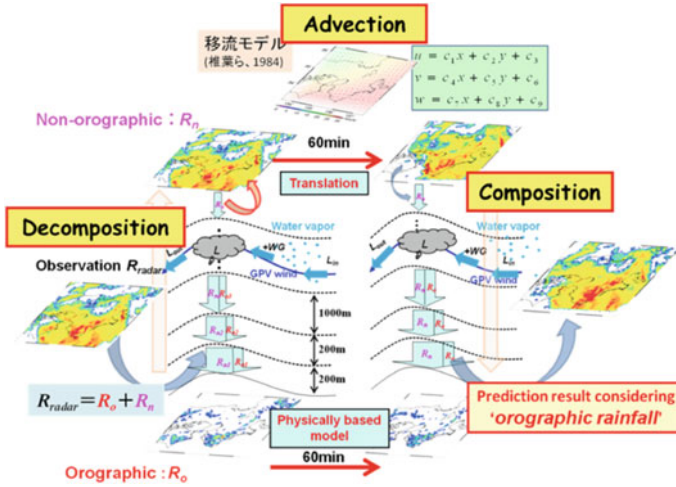
Fig. 6 Schematic drawing of delineation for orographic rainfall amounts [3]

However, the accuracy of radar-based rainfall prediction decreases drastically while the prediction lead time getting longer. It is generally believed that the radar image extrapolation method is proper for short lead time, e.g., up to 3 h. As an alternative to provide longer lead time predictions, QPFs from NWP models are widely utilized. NWP (numerical weather prediction) models simulate the dynamics and physics of the atmosphere, and therefore, they are able to produce more reliable forecasts over longer lead times.

The combination of radar-based prediction with NWP model output, which is known as hybrid forecasting scheme, has been provided for the last several decades. The combination of the data is based on the merging of rainfall prediction outputs through radar image extrapolation method with outputs of an NWP model. Hybrid forecasting of radar-based prediction with NWP rainfall has shown that it provides more skillful forecasts than either NWP forecast or radar prediction alone. However, the accuracy improvement of each prediction method with NWP and radar prior to blending technique has not been addressed well in the related previous researches.

The main objective of this study was to blend the advantages of ensemble information of radar-based prediction with NWP rainfall for the accuracy improvement of rainfall and flood forecasting using the hybrid forecasting scheme. At first, the accuracy of radar image extrapolation method is improved by considering orographic rainfall identification and the error-field updating scheme. The accuracy of ensemble NWP output was also improved by utilizing the error-field updating scheme based on the concept of [1] (Fig. 7).
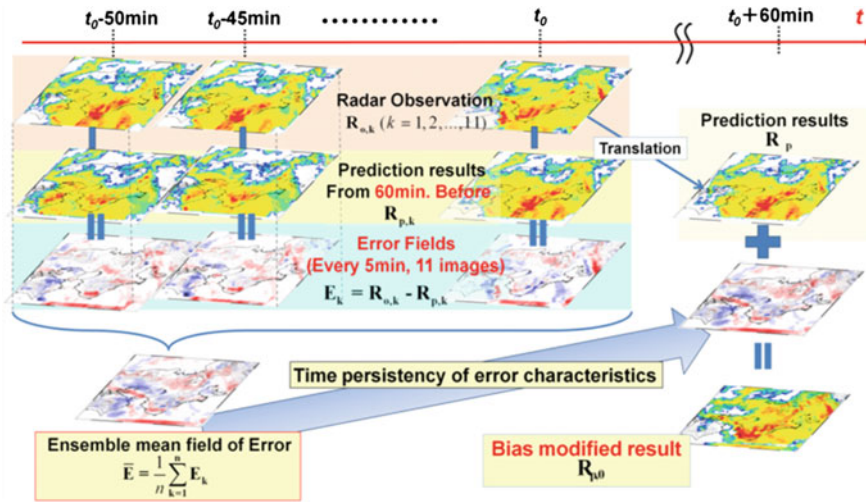
Fig. 7 Schematic drawing for the error-field update scheme in the radar image extrapolation method [1]

Finally, improved radar-based prediction and updated ensemble NWP rainfall forecast were merged with a time-variant weight function through Critical Success Index (CSI) and root mean square error (RMSE) indexes from the previous 3 h forecasting results. The proposed blending method was verified through 2011's largest rainfall event for Typhoon Talas and was applied to the hybrid flood forecasting on dam catchments in Kii Peninsula, Japan.

Based on the successful application results, improved radar image extrapolation method with the consideration of orographic rainfall identification and the error fields showed better performance than other radar prediction methods in spatial forecast location in verification results of accumulated rainfall distribution, correlation coefficient, CSI, and RMSE indexes. And ensemble NWP rainfall was improved with quantitative bias correction using mean field bias of error fields, and updated NWP rainfall produced higher performances than radar prediction results considering the orographic rainfall and the error-field scheme.

The improvement achieved by merging the radar prediction with the updated NWP rainfall becomes prominent for longer lead times and for stronger rainfall intensities in case of both the error-field schemes. And hybrid flood forecasting with combination of blending and updated NWP rainfall by error-field scheme could improve the underestimated part of original ensemble NWP rainfall in rising limb and peak discharge period over the two catchments (Fig. 8). In overall, the bias correction by error-field scheme added to each ensemble member appears to significantly enhance the ensemble's utility and provide a more effective way for accuracy improvement in rainfall and flood forecasting in the subject basin.
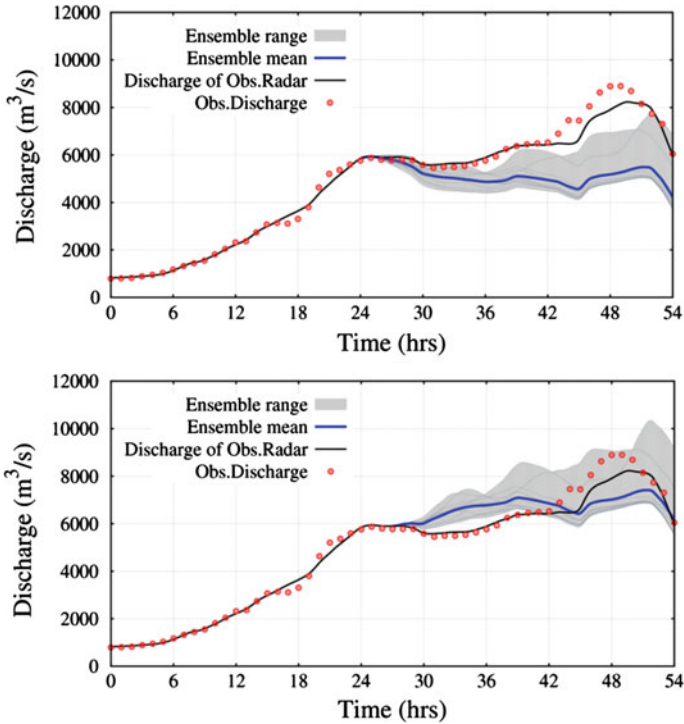
Fig. 8 Runoff simulation results with NWP ensemble output without error correction and blending scheme (*up*) and with the blended radar information (*down*) that shows improved forecasting accuracy

References

1. Kim S, Tachikawa Y, Sayama T, Takara K (2009) Ensemble flood forecasting with stochastic radar image extrapolation and a distributed hydrologic model. Hydrol Process 23:597–611. doi:10.1002/hyp.7188
2. Nakakita E, Yamabe H, Yamaguchi K (2010) Earlier detection of the origin of very localized torrential rainfall. J Hydraul Eng JSCE 54:343–348
3. Nakakita E, Yoshikai T, Kim S (2012) Application of error-ensemble prediction method to a short-term rainfall prediction model considering orographic rainfall. Weather Radar Hydrol 351:317–322
4. Nakakita E, Nishiwaki R, Yamabe H, Yamaguchi K (2013) Research on the prognostic risk of baby cell for Guerilla-heavy rainfall considering by vorticity with Doppler velocity. J Hydraul Eng JSCE 57:307–312
5. Tachikawa Y, Nagatani G, Takara K (2004) Development of stage-discharge relationship equation incorporating saturated–unsaturated flow mechanism. Ann J Hydraul Eng JSCE 48:7–12 (in Japanese with English abstract)

6. Tachikawa Y, Esaki S, Shiiba M, Ichikawa Y (2009) Rainfall-runoff analysis of the Toga river flush flood in July 2008 to prevent the water accident. J River Eng JSCE 15:43–48

7. Yu W, Nakakita E, Kim S, Yamaguchi K (2015) Improvement of rainfall and flood forecasts by blending ensemble NWP rainfall with radar prediction considering orographic rainfall. J Hydrol. doi:10.1016/j.jhydrol.2015.04.05

An Overview: Flood Catastrophe
of Kelantan Watershed in 2014

**Aminah Shakirah Jaafar, Lariyah Mohd Sidek, Hidayah Basri,
Nazirul Mubin Zahari, Milad Jajarmizadeh, Hanapi Mohamad Noor,
Sazali Osman, Abdul Hafiz Mohammad and Wan Hazdy Azad**

Abstract One of the challenging topics in Malaysia is flood occurrence, which have important impacts in human life and socioeconomic subjects. Malaysia, periodically, have faced with huge floods since previous years. Kelantan river basin, which located in the northeast of Peninsular Malaysia, is prone to flood events in Malaysia. Kelantan River has been badly affected with flood during recent monsoon season on December 2014 due to heavy monsoons rainfall and climate change issues. In this study, available rainfall and water-level data are analyzed and presented based on the flood event on December 2014. Generally, the flood area affected includes the districts of Kota Bharu, Kuala Krai, Machang, Pasir Mas, Pasir Puteh, Tanah Merah, Gua Musang, and Tumpat at Kelantan State. In the northeast monsoon season, the Kelantan State suffers from two phase of flood. The first phase began on December 14–17, 2014, and the second phase occurred on December 20–24, 2014. A comparison between accumulated rainfall on December and whole year of 2014 at Gagau station shows that contribution of rainfall on December is roughly 50 % of all of 2014. Overview of water-level results at Kelantan watershed shows that all areas are involved with highest record in 2014 in comparison with previous decades except Golok area. Results of water-level ranges show that most of the parts of Kelantan watershed are involved with over danger values for flood in 2014, which Lebir and Kelantan rivers have high increasing. In conclusion, it is suggested that there is a need to have study on flood mitigation and recognition of critical hydrological phenomena for sustainable strategies in Kelantan watershed. Consequently, this research provides primary information as baseline study for upcoming research for water resource management projects.

Keywords Flood · Rainfall · Kelantan · Water level · Malaysia

A.S. Jaafar (✉) · L.M. Sidek · H. Basri · N.M. Zahari · M. Jajarmizadeh
Centre for Sustainable Technology and Environment (CSTEN), Universiti Tenaga Nasional (UNITEN), Selangor Bandar Baru Bangi, Malaysia
e-mail: Aminahshakirah91@gmail.com

H.M. Noor · S. Osman · A.H. Mohammad · W.H. Azad
Department of Irrigation, Drainage Malaysia (DID), Kuala Lumpur, Malaysia

1   Introduction

Natural disasters happened every year and their impact seem to have greatly increased in recent decades, mostly because of environmental degradation, deforestation, intensified land use, and the increasing population [1]. Climatic events such as heavy rainfall and floods usually rise upon the arrival of monsoonal season in the eastern part of Peninsular Malaysia. Usually, rainfall is the main factor of flood event and other main that gives rise to main contributory factors might be intensity and duration of rainfall, the wetness of the ground, and the response of the rainfall catchment. Moreover, flood events are controversial natural disaster owing to human and economic losses to the country. Flood has caused considerable financial damages to roads, highways, villages, agriculture, and livelihood. Some of the human actions that have contributed to the event are deforestation and squatters' residence location that was built along riverbank. Besides, other structural component such as most of the drainage pipelines that were old designed is also one of the contributions to this flood event [2]. Furthermore, Sani [3] investigated case study of one of the most extreme flood events occurred at Kelantan river basin during flood event 1967. Sani [3] also discussed about the "six factors" that reasoned the contribution to 1967 flood such as the unusual heavy rain, the closing up of the Kelantan estuary by sand bars, the very low ground level along main riverbanks, the poor conditions of the various drainage systems, the small tidal range along the Kelantan coast and finally the indiscriminate developments of the upper reaches of the river and throughout its catchments resulting in rapid runoff from the hills and heavy silting in the rivers. The magnitude of the flood impacts that resulted about 84 % of the population and at least about 125,000 people were affected and had to be evacuated during the 1967 flood [3].

Moreover, the condition of precipitation in Malaysia is greatly under the influence of monsoon. There are typically three phases of monsoon seasons that Malaysia undergoes in a year such as the southwest monsoon, northeast monsoon, and transitional monsoon. Southwest monsoon starts from the mid of May or early of June and ends in the end of the September. Meanwhile, northeast monsoon starts from early of November and ends in the end of the March. For the transitional monsoon, it starts from the mid of September and ends in the end of the October. Furthermore, in this modern highly risk societies, it is not peculiar to define "extreme" hydrological events in higher recurrence intervals of more than 100 ARI [4]. Average recurrence interval (ARI) is the average or expected value of the periods between exceedances of a given rainfall total accumulated over a given duration. It is implicit in this definition that the periods between exceedances are generally random [5]. Average recurrence interval (ARI) is one of the critical elements in water resource management and are calculated or projected with the assumption of a stable and stationary climate and the stationarity assumption requires that the mean and variance of climatic conditions do not change over time [6].

There are a few of rainfall and stream flow stations in the catchment area including telemetry devices as shown in Fig. 2. In this study, application of chronological information and primary analysis on past hydrometeorological extreme events such as rainfall and flood is presented. The hydrometeorological data required for this study were collected from the Department of Irrigation and Drainage (DID) Malaysia from 1965 to 2014 [7].

2 Materials and Methods

2.1 Case Study

Kelantan is located at the eastern region of peninsular Malaysia shown in Fig. 1. Kota Bharu is the capital of Kelantan as well as the growth development in North Kelantan. The area of Kelantan State is of 15,099 km^2 which is equivalent to 4.4 % of Malaysia's area [8]. The population of Kelantan State is 1.539 million [2], and Kelantan river basin has annual rainfall of about 2500 mm and most of rainfall during northeast monsoon events that is between mid-October and mid-January. Kelantan river basin has four main tributaries, namely Galas, Nenggiri, Lebir, and Pergau. The length of the Kelantan River from the upstream to downstream is 388 km and drains area about 13,000 km^2 occupying more than 85 % of the Kelantan State [9]. The Kelantan River is approximately 105 km, and it includes Lebir and Galas rivers at Kuala Krai. Kelantan River passes through the several urban areas, namely Kuala Krai, Tanah Merah, and Kota Bharu. Downstream of Kelantan River has a population around 0.5 million which can be in a medium level of population. Roughly, population density (ppl) in the urbanized most downstream area is exceeding 20,000 ppl/km^2 [3, 10]. Figure 2 shows the river network of the Kelantan basin and location of hydrological stations. Based on previous rainfall records, Kelantan River is potential to have severed flood frequently. Therefore, study on flood events and attributed research are required as baseline in Kelantan River such as flood early warning system because evaluation of Kelantan River based on hydrological and flood studies offer to provide sufficient time for the authorities to evacuate the downstream communities to safer places and take necessary measures to protect physical properties in vulnerable areas. For hydrometeorological studies in Kelantan river basin, there are water-level stations under authority of Department of Irrigation and Drainage (DID) of Malaysia that provides previous flood records and attributed information for public view. Usually, water-level stations are used to issue flood warnings to the downstream communities [7].

Fig. 1 Map of Malaysia highlighting the Kelantan State as the study area

2.2 *Accessible Data and Primary Assessment*

In this section, it comprises of the overall information regarding the contribution of rainfall and water levels for Kelantan State in 2014. Satellite imagery related with the government agencies Malaysian Meteorological Department Malaysia (MetMalaysia) in Fig. 3 that functions in providing climatological services to users in all sectors and monitors the atmospheric composition in Malaysia and provides information and other meteorological aspects. Review of Radar image of MetMalaysia shows the cumulus clouds have formed on December 20, 2014, until December 25, 2014 [11]. Moreover, Fig. 3 also shows that Kelantan River has involved with more rainfall during the period December 20–23, 2014, which leads flood in downstream of the Kelantan River. It shows that the cloud formation began on the December 20 until December 25, 2014. The green and blue patterns show the rainfall rate in mm/h for the flood event in 2014. The blue pattern indicates the intensity of the rainfall between the ranges of 0.05–0.5 mm/h. Meanwhile, the green pattern indicates the rainfall rate between 0.5 and 8 mm/h. From the weather

Fig. 2 Location of hydrometeorological stations at Kelantan State

status, heavy rain warning (red level) is released at 8:58 am on December 24, 2014, by the Malaysian Meteorological Department. Warning situation reported as intermittent rain occasionally occurring in Kelantan State (Tumpat, Pasir Mas, Tanah Merah, Machang, Pasir Puteh, Jeli, Kuala Krai, and Gua Musang) is expected to continue until December 24, 2014 [11].
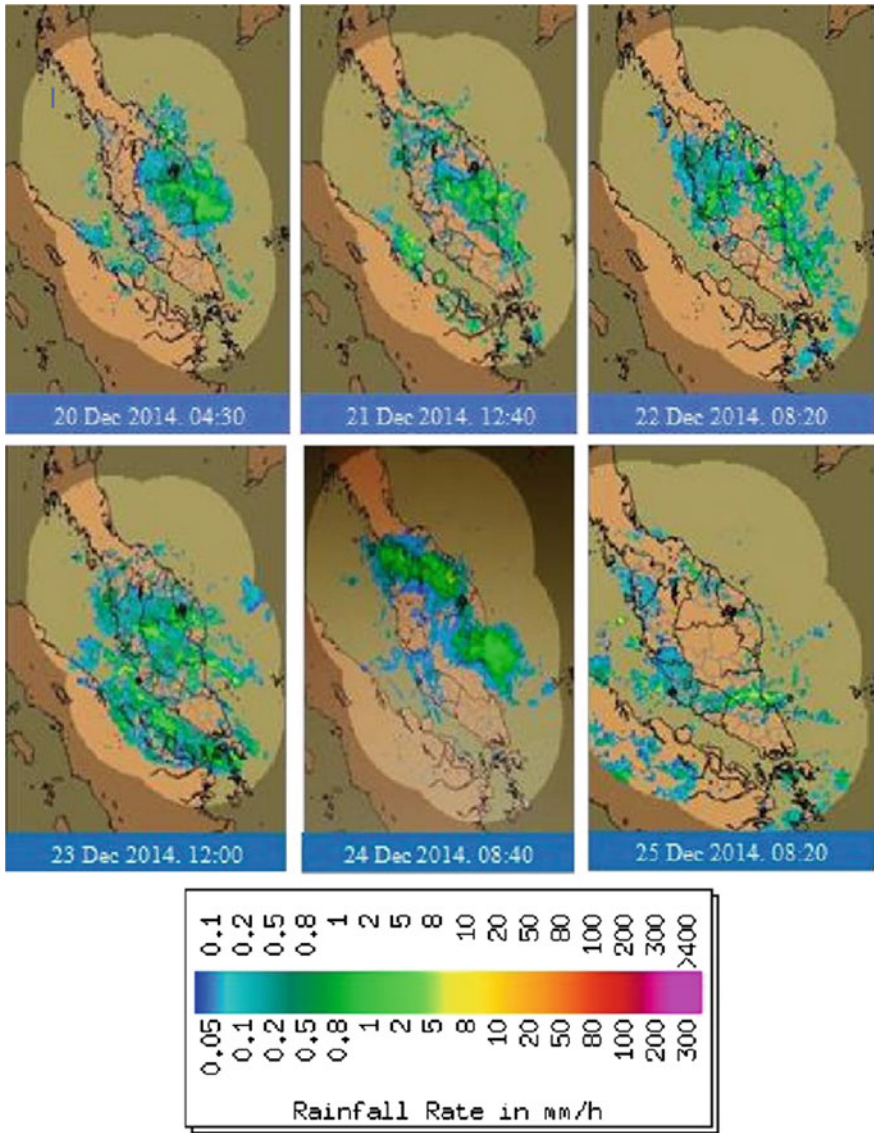
Fig. 3 The cloud formation images on December 20–25, 2014 [11]

The recorded rainfall from telemetry station at Kelantan shows that the highest amount of rainfall is during the period December 15–25, 2014. The highest value of accumulated rainfall recorded during the flood event on December 2014 for duration of 10 days is at Gunung Gagau station about 1898 mm, while the lowest value of accumulated rainfall during the flood event is at Lojing station about 476 mm. Figure 4 represents Isohyetal map for Kelantan State on December 20–25,
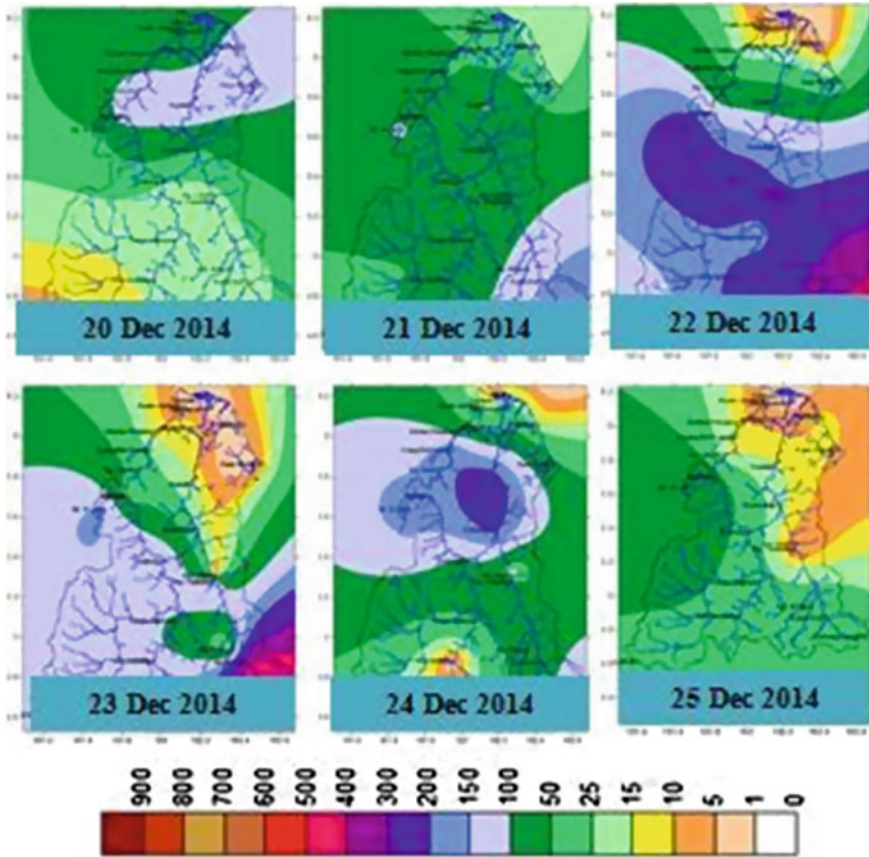
Fig. 4 Isohyte map for Peninsular Malaysia started during the period December 20–25, 2014 [12]

2014. It shows that on December 22, 2014, the heavy rainfall estimated more than 150 mm for a day especially at Gunung Gagau station and along the Golok River. However, on the December 24, 2014, the rainfall intensity is concentrated near Kelantan River especially at Kusial and Kuala Krai rainfall stations. It is clear that the total rainfall recorded during every flood is different. It mostly do not follow a fixed trend of neither ascending nor descending since rainfall amount is greatly dependent on atmosphere climate during flood event.

Table 1 shows the comparison between accumulated rainfalls for 10 days from December 14 to December 24, 2014, during the massive flood event on December 2014 for the rainfall stations with the comparison of average rainfall for December since previous years. It indicates that the comparison of accumulated rainfall of 10 days for Gunung Gagau station is 2.7 times with the average rainfall for

Table 1 Rainfall Station at Gunung Gagau, Kusial, and Kuala Krai [12]

Rainfall station	Accumulated rainfall of 10 days during flood event December 2014 (mm)	Annual average rainfall for December year 1965–2013 (mm)	Comparison of accumulated rainfall of 10 days during flood event December 2014 with the average rainfall for December
Gunung Gagau	1898	700	2.7
Kuala Krai	848	585	1.5
Kusial	1048	757	1.4

December while Kusial rainfall station is 1.4 times the annual average rainfall for December.

Table 2 shows the comparison between the accumulated rainfalls within 10 days on December 2014 with the accumulated annual rainfall for 365 days at Gagau Rainfall Station. Accumulated rainfall for the period of 10 days at Gunung Gagau Station shows that during December 2014 flood event, it already achieved 50 % of

Table 2 Comparison of accumulated rainfall of 10 days with an annual rainfall [12]

Rainfall station name	Gagau station	
Duration of rain (days)	10 days	365 days (1 Year)
Accumulated rainfall (mm)	1898	4000
Comparison with the annual rainfall	~ 50 % of annual rainfall	
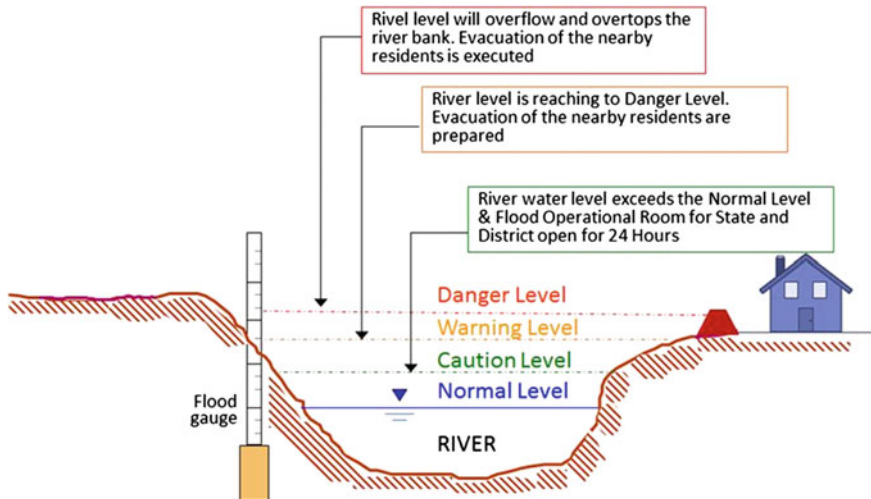
Fig. 5 The standard of critical river levels termed by DID Malaysia [7]

the total annual rainfall. This value shows extreme and huge amount of precipitation that occurred during the event. Based on the standard of critical river levels termed by the DID Malaysia organization shown in Fig. 5, there are 4 types of level such as normal level, caution level, warning level, and danger level. These standards are followed for the implementation of flood forecasting and public evacuation. Caution level alerts the public when the river level exceeds the normal level. Meanwhile, warning level alerts the public when the river level is reaching to danger level and evacuation of the nearby residents is prepared. Danger level is when the river level will overflow and overtops the riverbank and the evacuation of the public is executed.

Table 3 shows the recorded water level on December 2014 for Kelantan river basin in line with the standard critical river levels set by DID for each rivers. Clearly, Lebir and Kelantan rivers are involved with over danger level values. Lebir River has an over danger level value roughly 9.51 m which is highest in comparison with other stations while Golok River at Rantau Panjang exceeds danger level by 1.84 m.

Figure 6 shows the accumulated rainfalls for each rainfall stations for duration of 10 days from December 14 to December 24, 2014, during the flood event December 2014. It shows that Gunung Gagau station received the highest amount of rainfall in value of 1898 mm and Kg. Laloh station received the least amount of precipitation in value of 476 mm. Gunung Gagau station situated at the upstream part of Kelantan river basin and it experienced the most rainfall during the December 2014. However, Kg. Laloh station caters the least amount of rainfall during the December 2014.

Figure 7 shows that Galas and Lebir River experienced the highest water-level flows during the December 2014 flood event while Semarak and Golok rivers

Table 3 Recorded maximum water level for Kelantan river basin [12]

No	River	Location	Normal level (m)	Warning level (m)	Danger level (m)	Water level on December 2014	
						Date and time	Water level (m)
1	Galas	Dabong	28.00	35.00	38.00	24/12/14 16:00	46.47
2	Lebir	Tualang	23.00	31.00	35.00	27/12/14 04:00	44.51
3	Kelantan	Tangga Krai	17.00	22.50	25.00	25/12/14 15:00	34.17
4	Kelantan	Guillemar d Bridge	10.00	14.00	16.00	26/12/14 00:00	22.74
5	Kelantan	Tambatan DiRaja	1.00	4.00	5.00	27/12/14 07:00	6.96
6	Golok	Jenob	19.00	22.50	23.50	11/1/14 21:00	25.44
7	Golok	Rantau Panjang	5.00	8.00	9.00	18/12/14 11:00	10.84
8	Semerak	Pasir Putih	0.40	2.30	3.00	18/12/14 07:00	2.67
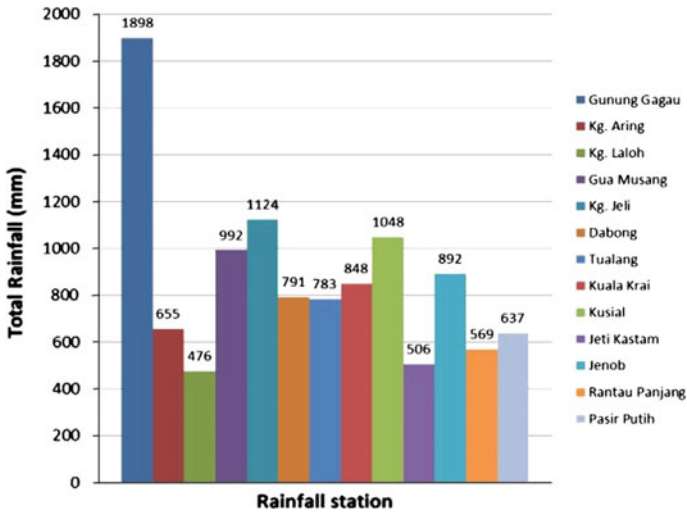
Fig. 6 Accumulated rainfall for 10 days from December 14 to December 24, 2014
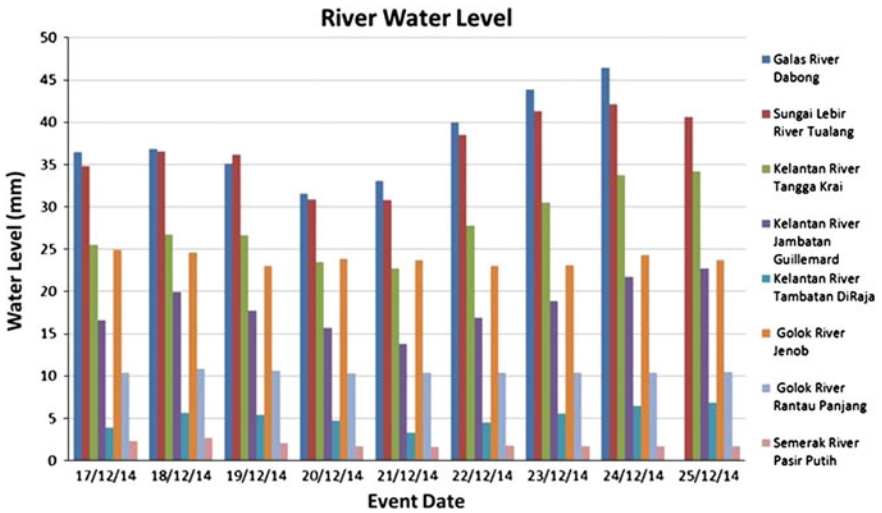
Fig. 7 The water level in Galas, Lebir, Kelantan, Golok, and Semerak rivers on December 17–25, 2014

experienced the least flows during the flood event. It seems that urban and rural area around two rivers Lebir and Galas might be vulnerable for flood event because the area experienced high level of flow in rivers.

3 Discussion and Conclusion

Floods can have decimating results and consequences for the economy, environment, and individuals. Indeed, disadvantages of flood can be transmission of pollution, erosion, and losing freshwaters as well financial and lives damages. The recent flood in December 2014 at Kelantan State seemed to have taken Malaysians by surprise, including the authorities responsible for disaster management. It is vital in ensuring that during flood event, the Disaster Operation Control Centers is functioning immediately in affected areas to coordinate and provide accurate information about where the affected people were so that relief efforts could be directed there. It is important to convey immediate information on central portal or Web site providing daily updates on the flood situation, road accessibility, where relief effort can be taken and location of any stranded victims can be identified. However, institutional capacity and preparedness of agencies in responding to disasters should be further enhanced through the improvement of overall capacity and preparedness of response agencies, procurement of high tech equipment, conducting seminars/drills and exercises to reflect the complexity of disasters. The disaster management framework should be strengthened, especially at the local government level. Therefore, the government should conduct activities that could enhance inter-agency cooperation especially at the local level. Based on the evaluation from the impacts of Kelantan Flood 2014, it actually results in a challenging enforcement, operation, and implementation for upcoming years at national and international scale for study such as vulnerable urban area, contribution of flood on landscape, socioeconomic influenced by flood and damages on human life and infrastructures.

This research is done to prepare the vital information regarding the flood event happened at Kelantan State on December 2014 as a baseline for future studies. Two sets of data such as rainfall and water-level data are obtained and analyzed to get the general idea on the flood event for Kelantan State on December 2014. Kelantan watershed is roughly 13000 km^2, which include urban and rural area in up and down streams. Major rivers, namely Nenggiri, Lebir, Galas, and Kelantan, are located at Kelantan watershed that is flood prone area. Further study reveals that highest accumulative rainfall is related with Gunung Gagau in December 2014. Evaluation of water-level records illustrates that highest water level is for Kuala Krai (34.17 m) on December 2014. Analysis on available data of water level

illustrates that most rivers experienced with phenomenon of exceedance of danger level during the December 2014. Statistic shows that Lebir River experienced highest rate accordance over danger warning value of about 9.51 more than danger level. Most rainfall stations have received high rate of rainfalls showing that Gunung Gagau had highest record at Kelantan watershed which value is 1898 mm.

Therefore, there is a need to encourage and highlight more study on flood protection and warning systems. In addition, stream flow modeling and recognition of flooded area can be an optimistic method along the Kelantan River from upstream to downstream. Hence, it is crucial to compile and analyze major hydrological extreme events, which could serve as a reference in the planning, and management of water resource projects especially for introducing additional safety factors in the design of water resource projects.

References

1. Lavanya K (2012) Urban flood management-case study of Chennai city. Archit Res, 1–18
2. Chan N (1995) Flood disaster management in Malaysia: an evaluation of the effectiveness of government resettlement schemes. Disaster Prev Manage 4(4):22–29
3. Sani S (1973) The 1967 flood in Kelantan, West Malaysia. Akademika 3:1–14
4. Hafiz I, Sidek LM, Basri H, Fukami K, Hanapi MN, Livia L, Jaafar AS (2014) Hydrological extreme event in Dungun River Basin Region. In: 13th international conference on Urban Drainage ICUD 2014, Sarawak, Malaysia
5. Tao D et al (2015) Return period and risk analysis of nonstationary low-flow series under climate change. J Hydrol 527:234–250
6. Australian Water Information Dictionary, Australian Government Bureau of Meteorology. Retrieved from Australian Government Bureau of Meteorology, http://www.bom.gov.au/water/awid/id-704.shtml. Accessed on 2015
7. Department of Hydrology, Department of Drainage and Irrigation Kelantan (2014) Rainfall & water level data. Department of Drainage and Irrigation Kelantan, Kota Bharu
8. Pradhan B, Youssef A (2011) A 100 year maximum flood susceptibility mapping using integrated hydrology and hydrodynamic models: Kelantan River Corridor Malaysia. J Flood Risk Manage 1–14
9. Hafiz I, Sidek LM, Basri H, Fukami K, Hanapi MN, Livia L, Jaafar AS (2014) Integrated Flood Analysis System (IFAS) for Kelantan River Basin, IEEE International Symposium on Telecommunication Technologies ISTT 2014, Langkawi Island, Malaysia
10. Mohammad M, Nor A, Arham Muctar A, Baten MA, Dony Andriansyah N (2014) Flood impact assessment in Kota Bharu, Malaysia: a statistical analysis. World Appl Sci J 32 (4):626–634

11. Malaysian Meteorological Department, Malaysian Meteorological Department. Retrieved from Official Website of Malaysian Meteorological Department Malaysia, http://www.met.gov.my/index.php. Accessed on 2013
12. Malaysia Department of Irrigation and Drainage (2015) Laporan Banjir Negeri Kelantan 2014. Department of Irrigation and Drainage, Kuala Lumpur

Flood Disaster Management in Malaysia: Standard Operating Procedures (SOPs) Review

Wardah Tahir, Janmaizatulriah Jani, Intan Rohani Endut, Mazidah Mukri, Nurul Elma Kordi and Nur Eizati Mohd Ali

Abstract Flood is a natural weather-related disaster frequently occurring in Malaysia. One of the greatest challenges that Malaysia faces today is recognizing the magnitude of risks posed by flooding. The public, private and NGOs should deliberate the amount of investments required to reduce the flood risk, including making appropriate emergency preparations, strengthening the existing Standard Operating Procedures (SOPs), and finding new solution for minimizing risk related to flood disaster. The current existing SOPs indicate that there is still lack of holistic flood risk management system to minimize this problem. The country should be committed to establish a national policy on flood risk management that requires effective, economical, sustainable, and consistent management of flood risk to people, properties, and communities. Risk management has been established as a well-defined procedure for handling risks due to natural, environmental, and man-made hazards. A risk management can be applied at every level of the action: planning, design, and operation level. A holistic flood risk management system will evaluate the potential risk before, during, and after the flood disaster. The paper reviews the current SOPs implemented by the agencies dealing with flood disaster in Malaysia.

Keywords Flood · Standard operating procedures (SOP) · Flood risk management

1 Introduction

Almost every end of the year during the northeast monsoon, the east states of Peninsular Malaysia will be inundated by flood water. Flooding is the most significant natural hazard in Malaysia, as evidenced by the history recorded since 1920, in which the country had experienced major floods in 1926, 1963, 1965, 1967, 1969, 1971, 1973, 1979, 1983, 1988, 1993, 1998, 2005, and most recently was in December 2014. The main causes of flood occurrence in Malaysia are the

W. Tahir · J. Jani (✉) · I.R. Endut · M. Mukri · N.E. Kordi · N.E.M. Ali
Faculty of Civil Engineering, Universiti Teknologi MARA, Shah Alam, Malaysia
e-mail: j_jan2000@yahoo.com

abundant amount of rainfall, in addition to other factors such as deforestation, tidal effect, lack of maintenance to the river system, and increased number of urbanized areas with inadequate drainage that cannot support the amount of flow during the heavy rainfall. The combination of natural and human factors has produced different types of floods such as monsoon, flash, and tidal flood. Flood had caused extensive damages to property, road and railways system, agricultural land, crops, and loss of life. Following the disastrous 1971 flood, the government had established the Disaster Management and Relief committee (NDMRC) in 1972 for coordinating the flood relief operations at national, state, and district levels.

The main purpose of the study is to produce a holistic flood risk management system (HFRM) for flood disaster in Malaysia. The HFRM system can become a very useful tool for the public, private, and other related agencies to assess the risk before, during, and after the flood disaster. In Malaysia, National Security Council (NSC) together with other agencies such as Department of Irrigation and Drainage (DID) are the responsible parties for coordinating all relief operation before, during, and after flood events. To achieve this aim, the study will examine the current SOPs related to flood disaster. The focus of this paper was to review the current SOPs implemented by the country and assess the need of HFRM system to improve the flood management in the country.

2 Flood Disaster Management in Malaysia

Disaster had and will always be a part of life so long as hazards and risks exist. Many developed countries nowadays are still challenged with problems when faced with the flood disaster although they are well-equipped with sophisticated structural and non-structural measures and defense systems. The flood hazards are almost certain; what we can do is to minimize the impact of disaster in order to save people and properties. Risk assessment and validation of flood disasters are a worldwide problem in the field of natural science and technology.

In Malaysia, floods occur frequently in urban or rural areas and cause the greatest damages among all natural disasters. The damages caused by floods estimated annually were MYR 1 billion that affect 21 % of Malaysia's population [1]. Floods occurred at varying severities in East Coast of Peninsular Malaysia especially in Kelantan. There are three types of flood in Malaysia: the monsoonal flood, flash, and tidal flood [2]. Monsoonal flood is due to heavy rainfall usually occurs in a longer period from one week to a month. In urban areas, flash floods normally occur during a short period within two or three hours due to highly intense rainfall.

Floods are not new to the country, but what have been done to mitigate and manage this disaster. There is a need to understand the concept of disaster and what it entails, as well as the country's flood risk management system which covers the activities before, during, and after a flood disaster tragedy.

In Malaysia, the Natural Management and Relief Committee (NDMRC) coordinates flood relief operations at every level: national, state, and district levels [3].

The flood disaster management is based on National Security Council (NSC) Directive No 20 and Fixed Operating Regulations (PTO). It describes the responsibilities of various agencies and the cooperation of these agencies in managing disaster. The National Flood Disaster Relief Machinery (NFDRM) is the committee that reacts to major floods based on reactive system [3]. This committee is responsible for operations at national, state, district, mukim, and village levels [2]. The relief machinery and emergency flood management covers the flood forecasting and warning system (pre-disaster), flood relief machinery (during disaster), flood management emergency (during disaster), and funding and aid delivery system (post disaster).

3   Malaysian Flood Disaster Management Model

For pre-disaster flood management, flood forecasting systems have been developed and used by the Department of Irrigation and Drainage such as linear transfer function model and tank model to forecast for future flood in the flood prone areas. Information from the model was used for flood preparation to the potential area to be hit. Dissemination systems such as SMS, telephone, warning sirens, fax, and Web site were also used as flood warning system. Although there is a system for pre-disaster flood management, the data used as input for flood forecasting models are only based on river level and rain gauge data. The total number of telemetric stations for rainfall and river flow seems large enough at populated area, and telemetric rain gauge stations should also be installed at sparsely populated areas such as highland watershed areas [2].

Integrated flood forecasting and river monitoring (IFFRM) is a project that integrates flood forecasting model and monitoring the water resource-related issues such as water quality, drought, and debris flow. Through this project, a total of 88 hydrological stations have been set up across Klang River Basin to record and monitor rainfall, water level, soil moisture, water quality, water flow, and weather (using met stations). These data will be used as input for flood forecasting model to give efficient and accurate flood forecasting and warning to relevant agencies related to water, namely DID Kuala Lumpur, DID Selangor, Kuala Lumpur City Hall (DBKL), Local authority, dam operators, and media. With this information, the agencies can make decision and make preparation for incoming flood to reduce the impact of flood in the affected area.

Flood mitigation policy in Malaysia has progressively improved. Since the first Malaysia Plan (1971–1975), the country's expenditure on flood mitigation has increased substantially. Many structural and non-structural measures have been implemented for flood control and relief. However, there are many areas that need to be improved. The government has introduced a flood management program using holistic approach with respect to five strategies, namely prevention, protection, preparedness, emergency, and recovery [2]. These strategies involve the collaboration among government, private sector, non-governmental organization

(NGO), and community. However, the success of this flood disaster management depends on its implementation on the affected areas.

The current flood disaster management is focusing on the strategies to manage the flood disaster during the flooding. The implementation normally is focusing on the rescue shelter, food, and medical supplies for the victims during the flood events. There is no risk management system in place to evaluate the disaster before, during, and after the flood disaster. Current flood management model also lacks multidisciplinary approach, in which there is no balanced mixture between structural and non-structural measures. In addition, there is lack of integration among various agencies that are responsible for flood management.

4   Disaster Management Mechanism

In general, any disaster management mechanism should involve four stages. First, preparation before disaster includes flood event forecasting, early flood warning, and decision making by experts to prevent further problem [4]; secondly, preparation for the arrival of the disaster; thirdly, the disaster emergency response; and fourthly, the disaster recovery response [5].

In Malaysia, the National Security Council (NSC) is the coordinating body in disaster management and also the lead policy maker. All activities involved in the disaster prevention, preparedness, response operation, and recovery are coordinated by the NSC [6]. The National Security Council had established the Directive No. 20 to integrate and coordinate the management of disasters on land in an organized and systematic way. The directives provide comprehensive set of guidelines during disasters in Malaysia based on Hyogo Framework for Action as Malaysia is a member to the World Conference [7]. The guidelines become the main instrument in activating flood management with the support of various other legislations though it is not specifically enacted for flood management [8]. Other related acts such as Land Conservation Act 1960, Town and Country Planning Act 1976, Environment Quality Act 1974, Local Government Act 1976, Irrigation Areas Act 1953, Drainage Works Act 1954, National Forestry Act 1984, and Uniform Building By-Laws 1984 are important in the flood disaster management [8].

The disaster management in the country is dependent on the assessment of the current situation. The assessment shall be based on the complexity and magnitude of the disaster, destruction, and damage caused by the ability of financial resources, manpower and equipment, expertise, assistance, and the time frame for response (Directive 20, MKN). The Directive 20 advocates an integrated management of responsibilities and functions of various agencies involved. Three levels of management are established to manage the disasters based on the severity level of the disaster itself. The directive is also supported by other Standard Operating Procedures (SOPs) stipulated by various agencies which outline the mechanism of disaster management as well as their duty and responsibility [6]. The three levels of management and their scope are shown in Table 1.

Table 1 Disaster management committee level

Disaster level	Management
Level I District Disaster Management Committee (DTCP)	Chaired by District Disaster Management—to ensure all actions are standardized asset and human resources are enough, communicate with mass media
Level II State Disaster Management Committee (JPBN)	Chaired by State Government Secretary—to give aids to the affected area such as monetary aids, asset, and human resource
Level III Central Disaster Management Committee (JPBP)	Chaired by the Minister at Department of Ministry to determine the national disaster management policy, the assets, financial, and human resources

Source Disaster Management in Malaysia, NSC, 2011

Table 2 Action procedures and relief operation at each level of Disaster Management Committee

Action at each level
District level
(i) Any disaster incident at initial stage should be managed by the relevant agencies by means of the facilities and resources at District Level Management
(ii) On receiving a disaster report, District Police Officer Chief and District Fire Brigade Chief should take suitable steps by the assistance from key rescue agencies and subsidiary agencies and other organization and voluntary bodies in charge in giving aid and rehabilitation to disaster victims. District Police Officer Chief and District Fire Brigade Chief would be commander and deputy commander of disaster operation, respectively
(iii) District Disaster Management Committee (JPBD) which is led by District Officer should be organized to ensure all activities of search and rescue operation, taking over, and preparation of facilities and machinery and other emergency aid, i.e., food and treatment could be implemented and managed in good order and fully coordinated
(iv) JPBD Chairman together with the commander and deputy commander would evaluate the disaster to identify the level of the disaster and capability of local agencies at District Level in handling it. After evaluation is completed and initial step is taken, but it is found that the disaster could not be handled at district level or needs assistance from state level, JPBD should inform State Disaster Management Committee (JPBN) to get quick help and taking over the disaster management
State level
1. The whole management and control of Level II Disaster will be taken over by the State Level Authority or by mobilizing some sources beneath the state control. State Police Chief and Director of State Fire Brigade will be a commander and deputy commander of disaster operation, respectively, at this stage
2. JPBN lead by State Secretary should be mobilized to ensure that all disaster management run efficiently and coordinated. For Federal Territory of Kuala Lumpur, the chairman of JPBN is the mayor while for Federal Territory of Labuan is the Director of Administration Federal Territory, Labuan
3. JPBN on assistance by Disaster Operation Commander shall decide on capability rescue agencies to handle disaster incident as required, so JPBN should notify Central Disaster Management Committee (JPBP) instantly through a fixed information and communication channel

Table 2 (continued)

Action at each level
Central level
1. When the disaster administration is taken over by central level (Level III Disaster), all correlated agencies and sources that include search and rescue team, emergency assistance, etc., at district and state level shall be united to face disaster that occurred under JPBP. The Director of Internal Security and Public Order, Royal Malaysia Police (PDRM), and Deputy Chief Director of operation, JBPM, respectively, will be the commander and deputy commander of disaster operation
2. JPBP headed by a minister selected by the prime minister should be mobilized to guarantee that entire aspect with respect to policy and decision in search and rescue operation is carried out in a professional and effective manner

The action procedure and the relief operation by the government authority level for each stage in overcoming the disaster are shown in Table 2. As with the case in Kelantan on December 2014, the disaster management had gone up to Level III, the Central Level headed by a minister appointed by the Prime Minister. The operation had been implemented satisfactorily though there are many unexpected problems due to the unprecedented scale of the event such as insufficient shelter, food, and rescue transport. The action procedures and relief operation had also been implemented to its optimum capability and capacity regardless of the different party that rule the state.

5   Roles and Duties of Agencies

Various agencies need to work together to ensure flood victims safety and relief during a flood event. Ref. [7] has the opinion that the government officials involved during flood event are purely exercising their standard official responsibility as members of the civil service, army, or police. Table 3 lists the responsibilities of various agencies during a disaster.

Table 4 shows the SOPs from different agency involved in disaster management referring from document PTO (Peraturan Tetap Operasi) Flood Disaster Response (Tindakbalas Menghadapi Bencana Banjir). As shown in Tables 3 and 4, the roles and responsibilities of the agencies are well established and it is only a matter of good coordination during a disaster that will ensure these operating procedures are effectively executed.

Table 3 Various agencies and the related roles and responsibilities

Responsibilities of agency

Special Malaysia Disaster Assistance and Rescue Team (SMART)

To search and rescue victims in any disaster which need the help of special skill, expertise, tools, and equipment

Royal Malaysia Police (PDRM)

1. To inform the relevant agencies of the occurrence of the disaster
2. To coordinate disaster operation at the scene of incident with other agencies
3. To establish Control Post on Scene
4. To control and cordon special areas at the sight of incident
5. To search and rescue lives and properties
6. To control movement at the scene of disaster
7. To carry out investigation on the disaster
8. To protect unclaimed properties and to trace their owner
9. To help in protecting lives/properties.
10. To collect and protect information and exhibits for the use of investigation/litigation.
11. To give air transport service through the PDRM Air Unit whenever necessary.

Malaysian Fire and Rescue Department (JBPM)

1. To search and rescue victims
2. To prevent incident from being spread by fighting the fire, control any chemical leakage, and other dangerous situation
3. To collect information and study the risk in order to advice the police on evacuation step
4. To cooperate with the police in establishing operation border/zone (inner cordon) around the proper place of incident to enable JBPM carry out surveillance and control operation
5. To ensure the security of workers involved in rescue operation
6. To take into account the incident effect on environment and take action to reduce the effect of incident
7. To cooperate with incident medical officer and other medical officer and the ambulance in helping the victims who need such help and removing patients from place of incident
8. To support the police in searching killed victims
9. To carry out investigation whenever necessary and prepare report and evidence
10. Always being ready at the proper place of incident to ensure that the situation is safe and under control

Malaysian Armed Forces (ATM)

1. To support by offering services of members from all ranks during disaster
2. To support in providing transportation vehicles for land, air, or sea at all levels of disaster
3. To assist with preparing machinery equipment facilities to be used in relation to disaster at all levels
4. To provide skilled services, such as experts in explosive, engineering, communication, and any form of aid if necessary
5. To assist with construction works if needed to facilitate the operation during a disaster
6. To provide divers services
7. To carry out search and rescue operation based on necessity during a disaster
8. To prepare Air Ambulance as first aid and to evacuate victims
9. To provide liaison officers at all levels
10. To offer emergency relief services when ATM is the first agency to reach the place of incident and will only hand over the responsibility when official authority on disaster arrived to continue works according to the issued directive

Table 3 (continued)

Responsibilities of agency

Emergency medical services

I. *Emergency and rescue services*

1. To offer skilled services on emergency treatment in rescue operation hand-in-hand with rescue workers from other agencies
2. To give emergency treatment service to the trapped victims
3. To provide ambulance, pre-hospital, and transport services

II. *Medical depot service*

1. To provide emergency treatment service to victims and rescuers
2. To give forensic services including identification, morgue and evidence documentation
3. To give medical supply
4. To give health services and to control infections disease
5. To give psychological services, such as post-trauma disorder, psychotherapy, counseling, and debriefing

Civil Defense Department

1. Assisting in operations to save life and property
2. Assisting in preparation and maintenance of evacuation centers and provision of food for the victims
3. Assisting in providing first aid service to the victims, if necessary

Public Works Department (JKR)

1. Providing stores, transport, and work force from JKR to do the jobs of cleaning up the scene of incident and transportation
2. Providing temporary shelter as canopy or tent
3. Supplying water and to raise water pressure at places where such services are needed (where water supply is under the supervision of JKR/Water Supply Department (JBA)
4. Providing technical and skill services in the fields of forensic, geotechnics, structures, etc., as in landslide or structure failure cases

Social Welfare Department (JKM)

1. Prepare and maintain the evacuation centers

2. To make an arrangement and distributing food, clothing, and other necessities

3. To carry out registration on the victim for the purpose of rehabilitation

4. To offer guidance, advice/counseling to victims

Malaysia Red Crescent Society (PBSM)

1. To assist the Social Welfare Department with maintaining evacuation centers, cooking and serving food, distributing clothes, blankets and doing registration, and rehabilitation works for the victims
2. To assist other agencies with rescuing and evacuating victims
3. To assist emergency medical service (hospital) with offering first aid and other emergency relief and health care at the evacuation centers

Source [6]

Table 4 SOPs of various agencies

Standard operating procedures (SOP) by agency

JKM

1. Identify evacuation centers in accordance with the type of disaster
2. To inform the public in a region the location of evacuation centers that has been determined
3. Facilities are sufficient and in a satisfactory condition
4. Determine the layout (by lot) in the relief center to ensure the victims' comfort
5. Determine the layout of the work area (where the prayers, the woman, a cook, a registration period, the activities, etc.) in the evacuation centers
6. Determine supervisors as the leader of staff at each relief center

Bilik Gerakan Bencana will be opened 24 h after Level II was announced by National Security Council

Supply stock at keeping depot

• The front base is added to optimum level
• The numbers of stocks at front base satisfy the requirement set (5000 victims × 3 days used)
• Adequate list of suppliers to support relief operation

Short-term relief

– Food relief; dried food, mat, blanket, and disaster kit are given as soon as possible to victims at the relief center

Long term relief

– Aids for victims' recovery will be announced in not more than 30 days from the date of request after the disaster has end

Counseling and psychology

– The result to get counseling and psychology service will be announced not more than 5 days from the date of request

Source Customer Charter Achievement Report (2015)

DID

1. To run State and Federal Bilik Gerakan for 24 h
2. To observe more frequently telemetry and river gauges and river gauges to ensure the system works properly
3. To give report about the water level routinely and to advise indication for immediate evacuation action
4. Disseminate widely the information to the public
5. Review the effectiveness of RTB project to reduce disaster risk and assess additional needs RTB projects. Study non-structural measures to reduce disaster risk

MKN

1. To be the lead agency (focal point) in the national disaster management regional and international levels
2. Remove the strategy, direction, action plans, and policy direction in Disaster management
3. Ensure the adoption and implementation of policies and management mechanisms Disaster running smoothly
4. To monitor and make auditing in disaster management run by government agencies and ordered improvements to enhance the effectiveness of the national disaster management
5. Provide secretariat services to committees disaster management at all levels
6. Manage and move SMART teams for search and rescue at home and abroad when necessary
7. Manage KWABBN subject to financial rules and procedures in force from time to time
8. Coordinate the handling of practical sessions and search and disaster management rescue from time to time

Table 4 (continued)

Standard operating procedures (SOP) by agency

9. To monitor and ensure the implementation of measures reduction disaster to prevent or reduce the impact of disasters are ongoing by government agencies
10. Plan, coordinate, and monitor the implementation of educational strategies, training, and awareness to officials and members of government agencies, agency statutory, private and voluntary bodies, and the public in face and reduce the risk of disasters.
11. To provide advice on the conduct and management of disasters
12. Provision of post-mortem handling of the aftermath of disasters held a disaster
13. Evaluate, coordinate, and lead a humanitarian aid mission and Disaster response abroad
14. Evaluate and coordinating humanitarian assistance from foreign countries

<div align="center">(Directive 20, MKN)</div>

Also in charge in:

– Coordination of air asset
– Disaster statement through Portal Bencana
– Update and finalize the list of names of the victims that were moved to evacuation centers
– Update and finalize the list of names of victims who are not moved to evacuation centers

Private sectors
(Tenaga Nasional Berhad TNB)

1. Suggest together with the justification for the proposal to stop the supply of utilities should be communicated immediately to the PKOB
2. The implementation of contingency plans for ensuring continuity of supply
3. The utility area/important facilities disclosure of the period dismissal, the expected duration reconnection, and rational stopping the supply of utilities to the public

<div align="center">Source Peraturan Tetap Operasi Tindakbalas
Menghadapi Bencana Banjir</div>

JPBN/JPBD

1. Ensuring that all logistic assets can be operated
2. All assets are placed in an area (staging point) that has been set
3. The area is divided into sub-regions and determined government agency responsible
4. Aircraft placed at strategic locations
5. The role of each aircraft has been assigned according to priority situations
6. Designated areas to facilitate the operation
7. Directory roles, according to the specific functions and roles
8. Update the contact directory regularly

6 Flood Risk Management

The process to manage flood risk situation involves activities that are intended to improve the capability in coping with the flood event [8]. In flood risk management, recovery process after a disaster is equally important as the process to reconstruct and rehabilitate after the flood [7]. The objective of having a holistic flood risk management is to control any flood event, in terms of flood preparedness to reduce the flood impact [8]. This includes the process of risk analysis, which offers the basis for elongated term management decisions for the present flood protection system.

Fig. 1 The critical water level at flood warning station. *Source* Kesiapsiagaan Bencana Semasa Monsun Timur Laut, MKN

Figure 1 shows The Critical Water level at Flood Warning Station. The water levels are divided into several stages which are the normal level, the caution level, the warning level, and the danger level. Based on these levels, the specific appropriate acts can be identified. This kind of information is critical in providing early warning of flood risks for improved flood preparedness. Besides that, different organizations are responsible for warning and evacuation orders for different disaster as shown in Table 5.

Table 5 Organizations responsible for warning and evacuation orders

Severe weather phenomena	Organization responsible for warning	Organization responsible for evacuation order
Tropical cyclone	Malaysian Meteorological Department	National Security Council of Malaysia
Heavy rain	Malaysian Meteorological Department	National Security Council of Malaysia
Strong wind	Malaysian Meteorological Department	National Security Council of Malaysia
River flood	Department of Drainage and Irrigation Malaysia	National Security Council of Malaysia
Storm surge	Malaysian Meteorological Department	National Security Council of Malaysia

Source [6]

Effective disaster risk management contributes to sustainable development. To achieve sustainable development, resilience and disaster risk reduction must be part of urban design and this requires strong unions and broad participation [9]. Resilience can be defined as the capability of a system, community or society to struggle, absorb, accommodate to, and recover from the impact of a hazard in a timely and efficient manner, (UNISDR 2009).

7 Conclusion

The paper presents a comprehensive information and review on the flood disaster management in Malaysia. The roles and responsibilities of the leading and supporting agencies involved in the flood rescue and relief operation are described. The current SOPs are also listed for each agency involved. In general, the flood disaster management in Malaysia is well defined and established, comprising district, state, and central levels and the supporting agencies with their comprehensive SOPs. However, the records show that the flood disaster management in the country is still having problem. There is a need to identify the best coordination system between all the agencies including non-government organizations (NGOs). The currently executed SOPs had not shown good coordination among the NGOs. Based on the previous experience especially during December 2014 flood, the involvement of NGOs is huge and significant. Future work is going to be executed in defining and establishing holistic risk management system in Malaysia. Hopefully with this kind of system, the coordination in managing flood disaster in Malaysia will be enhanced.

References

1. Othman M (2014) COBIT principles to govern flood management. Int J Disaster Risk Reduct 9:212–223
2. Chan NW (2012) Impact of disasters and disasters risk management in Malaysia: the case of floods in Sawada. In: Sawada Y, Oum S (eds), Economic and welfare impacts of disasters in east Asia and policy responses. ERIA Research Project Report 2011-8, Jakarta: ERIA, pp 503–551
3. Khalid MS, Shafiai S (2014) Flood disaster management in Malaysia: an evaluation of the effectiveness flood delivery system. Int J Soc Sci Human 5(4):398
4. Zakaria N, Mustaffa CS (2014) Source credibility, risk communication and well-being: a conceptual framework. Procedia Soc Behav Sci 155:178–183
5. Tingsanchali T (2012) Urban flood disaster management. Procedia Eng 32:25–37

6. Abdullah MH, Tussin AM (2014) Tropical cyclone, rough seas and severe weather monitoring and early warning system in Malaysia. JMA/WMO Workshop on effective tropical cyclone warning in Southeast Asia
7. Hamin Z, Othman MB, Elias Z (2013) Floating on a legislative framework in flood management in Malaysia: lessons from the United Kingdom. Procedia Soc Behav Sci 101(2013):277–283
8. Zaharah Elias ZH (2013) Sustainable management of flood risks in Malaysia: some lesson from the legislation in England and Wales. Procedia Soc Behav Sci 491–497
9. ISDR (2011) Strategic framework 2025. Work Programme 2012–2015

Development of MSMA SME Design Aid Tools and Database System: Analysis and Design Stage

L.M. Sidek, H. Haris, H.A. Mohiyaden, H. Basri, Z.A. Roseli and M.D. Norlida

Abstract Rapid urbanization has many negative effects on environment such as deterioration of water quality contributed by pollution. In terms of stormwater management, even with the introduction of Manual Saliran Mesra Alam (MSMA) in 2000 (Urban Stormwater Management Manual for Malaysia), numerous new technologies have yet to be examined in detail, especially the relationship between water quantity and quality. Implementation is based on the restoration and optimization of the ecosystem. In this study, it has been reviewed and introduced the MSMA software in regard to water quality and discharge analysis for the future study. MSMA SME Design Aid and Database System knowledge base consists of a compilation of information and data relevant to stormwater treatment including algorithm for components, available design standard, technical guidelines, components design, supplier contact information, and images of each components and drawings. MSMA SME Design Aid and Database System framework consists of four main modules: user requirement input, analysis and design phase, prototype phase and user testing. There are 28 main components which have important role for visualization of any given catchment such as rainfall data, green roof, bioretention, constructed wetland, porous pavement, rainwater harvesting system, grey water reuse system and checking tools items. Currently, the 4 key components, such as bioretention system, water quality volume, lined drain design and bridge afflux estimator, have been developed in this study. MSMA SME Design Aid and Database System is able to assist engineers and developers in terms of management and improvement of water quantity and quality

L.M. Sidek (✉) · H. Haris · H.A. Mohiyaden (✉) · H. Basri
Centre for Sustainable Technology and Environment, Universiti Tenaga Nasional, Jalan IKRAM-Uniten, 43000 Selangor, Malaysia
e-mail: lariyah@uniten.edu.my

H.A. Mohiyaden
e-mail: hairun@uniten.edu.my

H. Haris
e-mail: harizah@uniten.edu.my

Z.A. Roseli · M.D. Norlida
Humid Tropics Centre Kuala Lumpur, No. 2 Jalan Ledang off Jalan Duta, 50480 Kuala Lumpur, Malaysia

entering urban rivers from urban regions. This system is also helpful when an expert-level judgment is needed repetitively for a large amount of cases, like in the planning of stormwater BMPs systems for an entire city catchment.

Keywords Stormwater management · Urban flood · Design aid expert system

1 Introduction

One of the main concerns in Malaysia is urbanization which is fast and progressive. Rapid urbanization has many negative effects on environment such as deterioration of water quality contributed by pollution. One of the common negative impacts of urbanization is the congestion of the drainage system which leads to produce unmanaged freshwater and consequently flash flood. This circulation has caused trouble for water quality and related issues whether in urban or rural area. Generally, in the past, urban drainage systems have been built to narrow the riverbeds by the inclusion of concrete and other man-made materials. These types of drainage systems in urban area and the waterways were influenced by the solids in stormwater runoffs [1]. Moreover, the inclusion of litter, debris and sediments in drainage system will lead to the enhancement of the flood and decreasing quality of the water. These days, urban rivers have mostly been changed into artificial channels, and they collect both freshwaters and urban sewage from urban locations.

Pollution loading usually results in poor water quality. Consequently, the downstream areas obtain more effects derived from contaminated materials inside freshwaters in channel flow. In Malaysia, pollution of freshwaters in open channels is considered as one of the important topics for review and study in the future. It is clear that bacteriological or chemical quality of urban streams may cause a severe risk to public health. The result is that many urban watercourses have not had any amenity value to support the range of an ecosystem at least. Also, the quality of water in open channel flows does not meet the water quality objectives that have been offered by the Department of Irrigation and Drainage (DID), Malaysia. To perform a research on management of freshwaters, DID and related organizations such as Universiti Tenaga Nasional Malaysia have made an agreement to design a toolbox, namely MSMA Integrated Stormwater Management Eco Hydrology Design Aid and Database System (MSMA SME Design Aid and Database System). The MSMA SME Design Aid and Database System knowledge base consists of a compilation of information and data relevant to stormwater treatment. The MSMA SME Design Aid and Database System algorithm includes MSMA SME Design Aid and Database System components, available design standard, technical guidelines for MSMA SME Design Aid and Database System, components design, supplier contact information and images of each component and drawing.

MSMA SME Design Aid and Database System categorizes as one of the expert systems. Expert system is an interactive computer software/paradigm incorporating judgment, experience, rules of thumb, intuition and other expertise to provide

knowledgeable advice about a variety of tasks to non-specialists [2]. Expert systems can cooperate as experts to make higher level decisions based on varying performance levels [3]. They can be described as new software technology that allows the formalization and representation of knowledge as well as experts. The objectives of this study are to assist in the solution development of MSMA SME Design Aid and Database System components and integrated stormwater management based on expert data and user input and to provide better understanding on the MSMA SME Design Aid and Database System components which cover all aspects including concepts, detailed design and performances. MSMA SME Design Aid and Database system is able to assist engineers and developers in terms of management and improvement of water quantity and quality entering urban rivers from urban regions.

2 Materials and Methods

2.1 Introduction of MSMA SME Design Aid and Database System Design Framework

The aim of the development of MSMA SME Design Aid and Database System is to assist in the solution development of MSMA SME Design Aid and Database System components and integrated stormwater management based on expert data and user input. Figure 1 shows the framework of four modules for MSMA SME Design Aid and Database System Design. Module 1 is related with feeding the input data and specification of catchment features. Next, module 2 is involved with the configuration of structural and non-structural component and attributed assessments. Module 3 includes with prototyping or providing first sampling of the integrated of model and database. Finally, module 4 is considered as evaluation of results or outputs with observed data which related with water quality and peak discharge.

2.2 Framework Module 1 (Database): Development Database for MSMA SME Design Aid and Database System

Indeed, the information is basically related to the MSMA SME Design Aid and Database System design standards available, MSMA SME Design Aid and Database System component factsheet and MSMA SME Design Aid and Database System design step and typical drawing. The input data is important prior to further analysis in the MSMA SME Design Aid and Database System as well as to forecast the model output and result analysis. The model input data includes appropriate rainfall data, infiltration rate and soil properties, inflow hydrograph and initial water
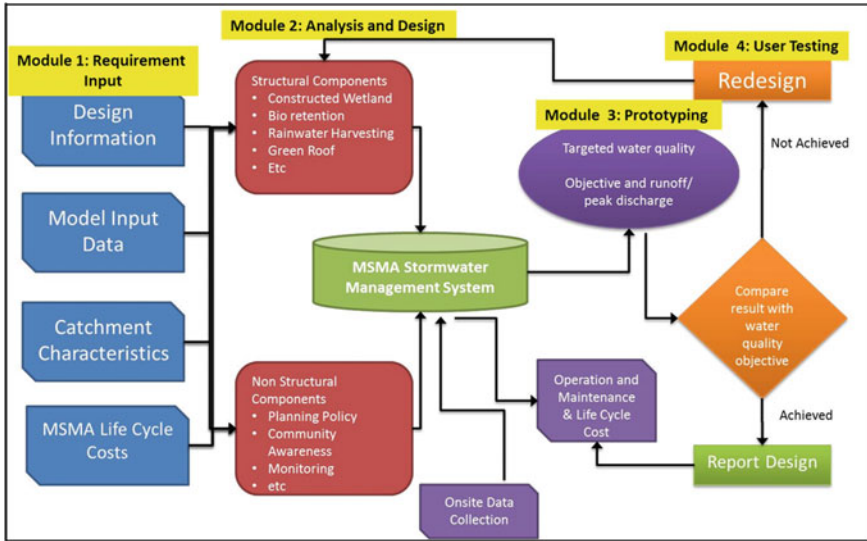
Fig. 1 Design framework for MSMA SME Design Aid and Database System

quality data. The infiltration rate is the velocity or speed at which water enters into the soil. It is usually measured by the depth in millimetre of the water layer that can enter the soil in one hour. Inflow hydrograph is important parameter for measuring the rainfall capacity and flood routing. The catchment characteristics input includes catchment area, site analysis, and the selection of MSMA SME Design Aid and Database System components are needed in order to predict and analyse the performance of specific MSMA SME Design Aid and Database System components.

2.3 Framework Module 2: MSMA SME Design Aid and Database System Treatment Approach/Technologies

The MSMA SME Design Aid and Database System results will be evaluated and compared with the performance targets such as water quality objective and stormwater runoff or peak discharge to minimize the impacts on receiving waters crossing of change in land use and management. Based on the performance targets, it is expected that around 90 % of the average annual runoff volume will need to be treated [4]. This is approximately equivalent to treating the 3-month average return interval (ARI) event. The actual on-site data of all MSMA SME Design Aid and Database System components will be collected during the monitoring stage. This data varies in provisions of the components performances in terms of water quality

improvement, reduced stormwater runoff, heat reduction, water storage allotment, etc. These on-site data will then be analysed and integrated in the MSMA SME Design Aid and Database System.

2.4 Framework Module 3 (Optimization): Performance MSMA SME Design Aid and Database System

The performance of MSMA SME Design Aid and Database System can be compared with the Model for Urban Stormwater Improvement Conceptualization (MUSIC) software to evaluate the reliability of outputs in terms of the urban stormwater systems for this study. MUSIC model was developed by the Cooperative Research Centre (CRC) for Catchment Hydrology in Australia. MUSIC is designed to simulate urban stormwater systems operating at a range of temporal and spatial scales. MUSIC provides evaluation of conceptual designs for stormwater management systems in any given catchment to meet specified water quality [5].

3 Discussion and Conclusion

MSMA SME consists of six modules: database, hydrology, design quantity control, design quality control, conveyance design and checking tools. Figure 2 shows the general and detail module for MSMA SME.
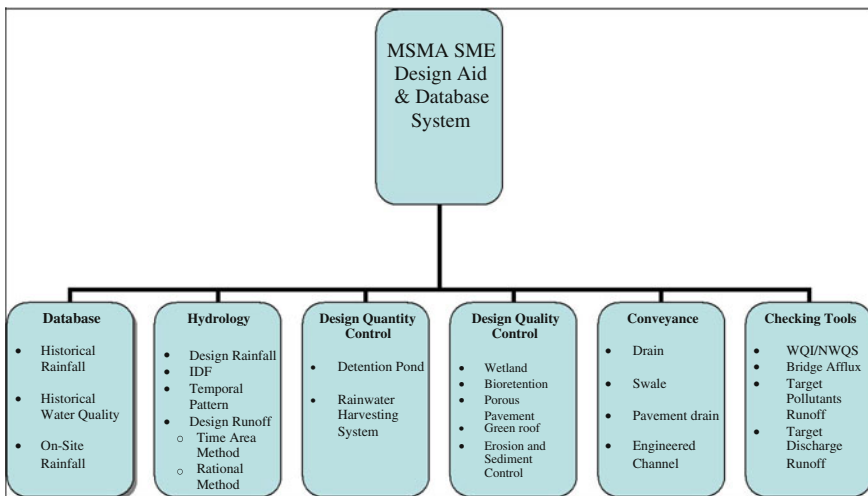
Fig. 2 MSMA SME design aid and database system module flowchart

3.1 Interface of MASMA SME Design Aid and Database System

MSMA SME software is a comprehensive program to assist engineers and developers in terms of management and improvement of water quality entering urban rivers from urban regions. It provides detailed design of the proposed rehabilitation works to improve the water quality and quantity and the riverbank rehabilitation in the developed areas. It is also equipped with the calculation functions to achieve the most optimum value for the design purpose (Fig. 3).

A few functions such as time–area method, detention pond, IDF curves creator and bridge afflux estimator have compiled with the database systems. Indeed, every function has specified database system to save every data that is important. The above-mentioned functions require a database system due to the production of tabulate data and visualization of values for any attributed calculation. For instance, the time–area method as a function requires sufficient rainfall data to create the temporal pattern. Therefore, it is very important to have a complete database system in regard to rainfall data. The sub-interfaces are the introduction of MSMA SME concept, MSMA SME components, MSMA SME design, database, analysis result, report, maintenance and references. The project 'Open' and 'Save' function is also included in this menu tools strip. Figure 4 shows the MSMA SME menu tool strip.
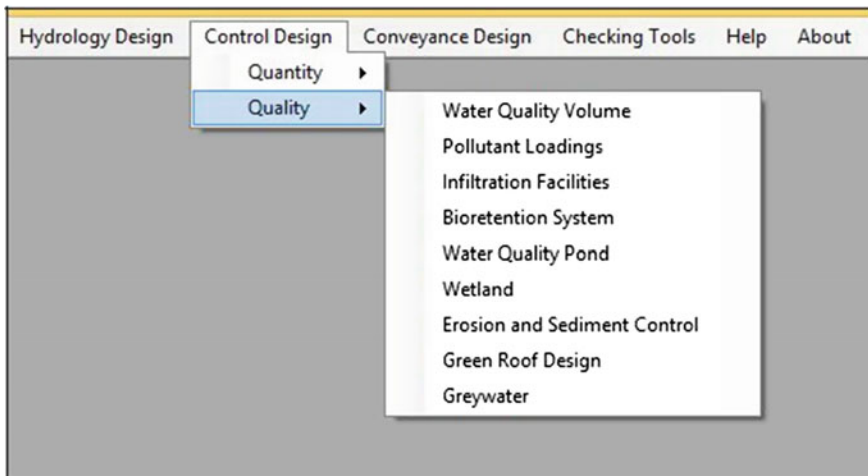
Fig. 3 MSMA SME menu tool strip
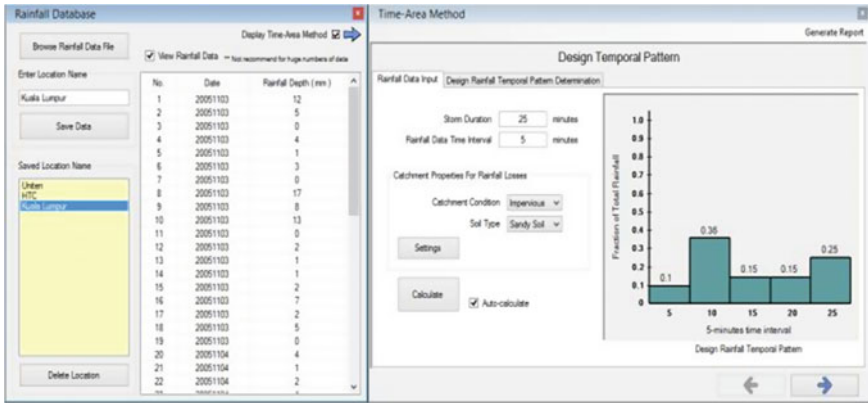
Fig. 4 Time–area method component interface with attributed database system

3.2 MSMA SME Components

There are 28 MSMA SME components that have been completely compiled in the software. Figure 5 shows an example of the components interface.
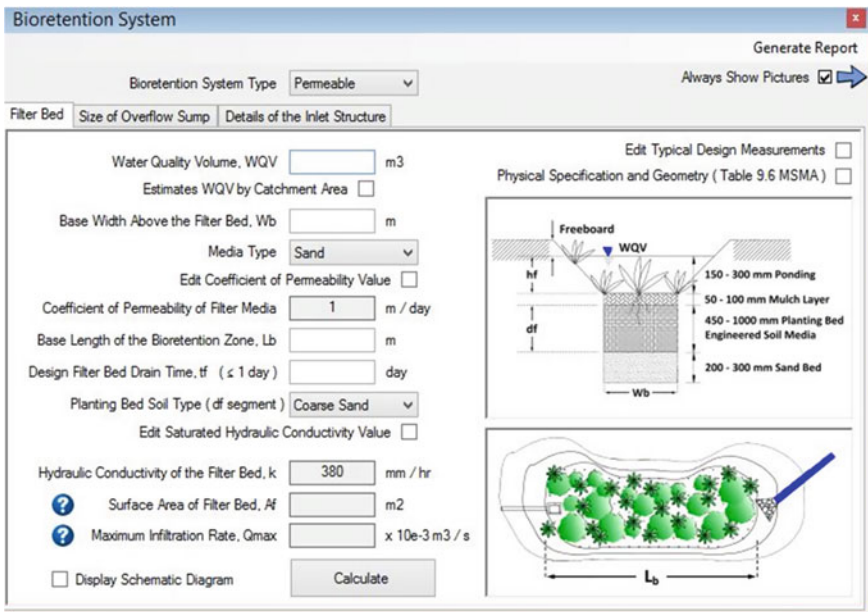
Fig. 5 Bioretention system component interface

3.3 Developed Time–Area Method

This is hydrological calculation method to determine the runoff value due to iso-chrones in given catchment. It is a common solution in generating the design temporal pattern from raw rainfall data and in generating the hydrograph easily. This rainfall data system is specially designed for all states in peninsula Malaysia in order to create the distribution of designed rainfall. Figure 5 shows time–area method component interface with the database system which is used in MSMA SME.

3.4 Bioretention System

Based on the literature, bioretention system is water best management practices (BMPs) that use filtration to treat stormwater runoff [6]. These systems use vegetation, such as trees, shrubs and grasses, to remove pollutants water runoff. Sources of runoff are diverted to bioretention systems directly as overland flow or through a stormwater drainage system. Bioretention system in this study can be a shallow-dish design. Bioretention operates by filtering the stormwater runoff through the surface vegetation, followed by the stormwater percolating into filter media, where filtration detention treatment, denitrification and some biological
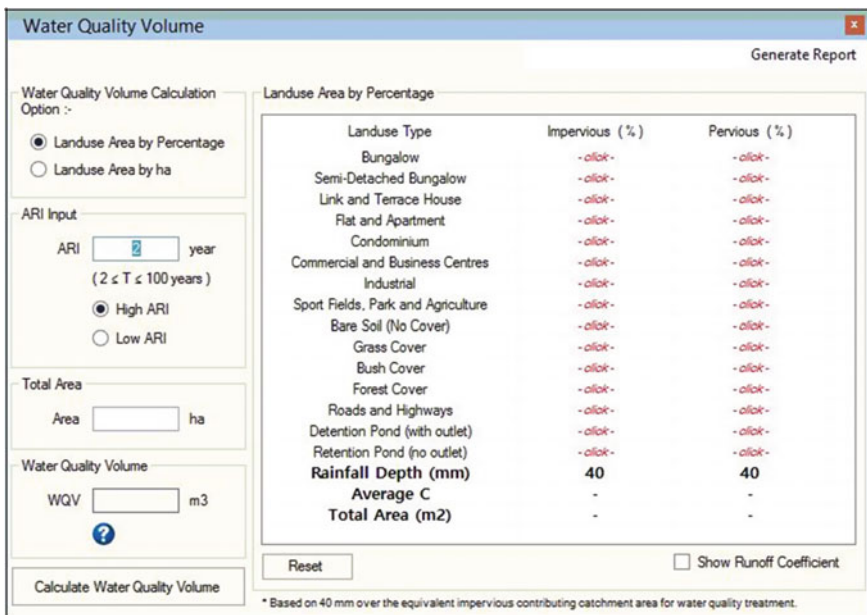
Fig. 6 Water quality volume component interface

uptake occur. The monitoring plan for bioretention systems means to prove that the system can improve water quality and detainment of pollutants through several treatment mechanisms. It consists of permeable and impermeable type of system. MSMA SME software complies with orifice and weir type of overflow structure, and also, it can be editable due to the typical design measurements and coefficient values. Figure 6 shows the bioretention system component interface.

3.5 Water Quality Volume

Water quality volume is a function to estimate runoff volumes before any assessment can be made of pollutant loads which is depending on land-use type. In this software, it consists of two calculation methods due to land-use area either by percentage or by hectare. Figure 7 shows the water quality volume component interface.

3.6 Lined Drain Design

This rectangular-shaped drain is one of the simplest types of constructed drain, and it is highly resistant to erosion with a very low maintenance cost. It also comply with typical drain surface types such as short grass cover, tall grass cover, smooth
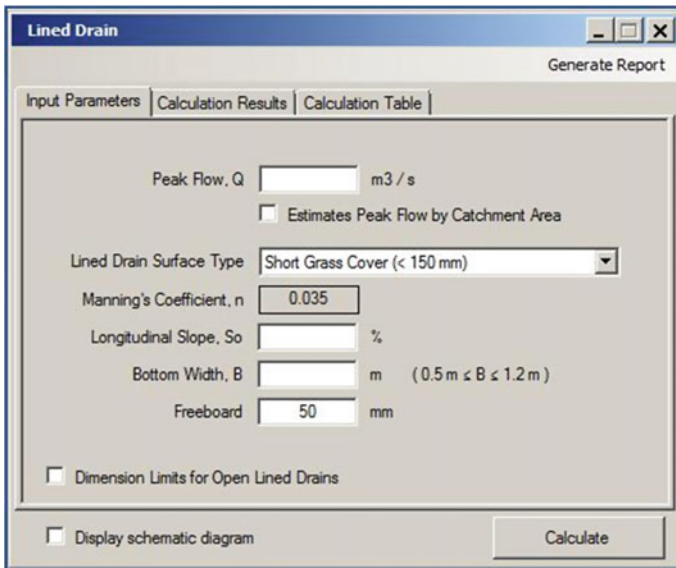
Fig. 7 Lined drain design component interface
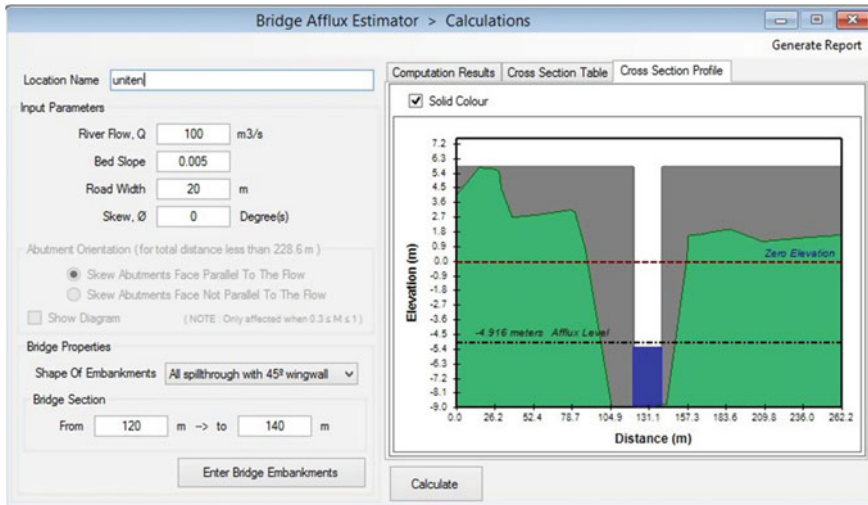
Fig. 8 Bridge afflux estimator component interface calculation part

finished concrete and rough finished concrete. The calculation result includes the complete details of calculation tables. Figure 8 below shows the lined drain design component interface.

3.7 Bridge Afflux Estimator

In this component of this module, it is particularly to estimate the value of afflux prior to the bridge construction process. Afflux is the distance between normal water surface and the bridge freeboard which is the lowest surface of bridge. This is the fundamental criteria in bridge design concept, as the procedure of flood management. In other words, it is to avoid flood occurrence that comes because of the bridge. It can determine the value of afflux due to the design water flow. This software is very easy to use, and it is useful to help the engineer to design work easier. The calculation steps, graphs, formulas and guidelines are based on the Road Engineering Association of Malaysia (REAM). This is one of the critical MSMA SME components to develop. Bridge afflux estimator contains 36 graphs that have been digitized into programmatically coding forms. It also consists of three graphical parts for the river cross-sectional profile. For instance, by a calculation, 16 graphs have to be interpolated with plenty of repeating loops' process and many equations involved. In short, this part of MSMA SME component involves numerous very complicated complex processes. This component also compiled with attributed database system because it needs the river cross-sectional data. River cross-sectional data contains the elevation level and the distance of riverbed profile. This software complies with two shape of bridge embankment properties whereby all spill through with '45° wingwall' and '90°

wingwall', and it supports the skewed orientation of abutments (or embankments) in its calculation. By using this software, those difficulties of the calculation process to estimate the bridge afflux value can just easily be achieved in just a few clicks.

3.8 Conclusion

In order to control the stormwater quality problem due to nonpoint source (NPS) pollution generated from stormwater in urban areas, Department of Irrigation and Drainage of Malaysia (DID) has taken serious actions by creating Manual Saliran Mesra Alam (MSMA) to monitor the stormwater quantitatively and qualitatively. Thus, MSMA Manual recommended various BMPs to improve the flooding and water quality problems. However, the performance of stormwater BMPs is intensely reliant on specific location conditions such as type of land use, hydrological data and maintenance frequency. Moreover, the data should be captured in the knowledge management expert system. To fulfil this task, the MSMA SME Design Aid and Database System is created. One of the advantages of the MSMA SME is to provide automation of expert-level judgment, and also, it has its own database system. MSMA SME Design Aid and Database System is able to assist engineers and developers in terms of management and improvement of water quantity and quality entering urban rivers from urban regions. This system is also helpful when an expert-level judgment is needed repetitively for a large amount of cases, like in the planning of stormwater BMPs systems for an entire city catchment.

References

1. Roesner LA, Pruden A, Kidner EM (2007) Improved protocol for classification and analysis of stormwater borne solid, Water Environment Research Foundation. Colorado State University, Fort Collins
2. Gasching J, Reboh R, Reiter J (1981) Development of knowledge-based system for water resources problems: SRI international. Menlo Park, California
3. Basri N (1999) An expert system for the design of composting facilities in developing countries. PhD Thesis, Department of Civil Engineering, University of Leeds
4. DID (2010) Guideline for erosion and sediment control in Malaysia. Department of Irrigation and Drainage Malaysia
5. Wong THF (2002) A model for urban stormwater improvement conceptualization. Urban Drainage 2002, pp 115–115. doi:10.1061/40644(2002)115
6. DID (2000) Urban stormwater management manual, Vol. 13, Chapter 34, Malaysia

A Model to Determine the Degree of Housing Damage for Flood-Affected Area: A Preliminary Study

Thuraiya Mohd, Mohamad Haizam Mohamed Saraf, Siti Fairuz Che Pin, Dzulkarnaen Ismail, Tajul Edrus Nordin and Mohd Nasurudin Hasbullah

Abstract Recent years, global warming and ozone depletion had impacted people's lives in many ways. In Malaysia, floods have become a common phenomenon caused by a combination of natural factors such as heavy monsoon rainfall and human factors like poor drainage system and deforestation. Heavy year-round rainfall has led to "spillover" effect bringing heavy rains and subsequent flooding. Floods can cause damage to housing and its possession as well as disruption to communication. At times, relocation is deemed necessary. In reality, flood victims are relocated or evacuated to a safe area provided by the authorities but some run to their own shelter. Therefore, the focus of the government is to accelerate the construction of permanent houses for the affected people. The question arises whether the estimated replacement needs took into account the degree of damage to the affected homes? Do they really deserve to receive the permanent house based on the condition of their house post-flood? Is the condition of the house deemed acceptable by end users? Thus, this preliminary study emphasizes on the understanding of the degree of housing damage after a flood, and the findings provide a conceptual model for the degree of housing damages in the Malaysian context.

Keywords Flood · Flood disaster · Flood housing damages · Damage assessment · Degree of housing damages

1 Introduction

The past few decades have witnessed a rapid expansion of population in Malaysia. The population was 10,881,000 in 1970, but in 2013, the statistics indicated that the population in Malaysia has risen to 29,947,600 (Malaysian Department of Statistics [1]). The increasing population has resulted in an increase in the number of property

T. Mohd (✉) · M.H.M. Saraf · S.F.C. Pin · D. Ismail · T.E. Nordin · M.N. Hasbullah
Faculty of Architecture, Planning and Surveying, UiTM Perak, Perak, Malaysia
e-mail: thura231@perak.uitm.edu.my

ownership. Therefore, a greater percentage of the country's land area, often in areas that previously were as being unsuitable for urban development and human settlement, are taken up to cater to the need for accommodation [2,3]. This increased number of properties, changes in water collection and flows and poor drainage system coupled with heavy monsoon rainfall, intense convection rainstorms, and other local factors have caused seasonal floods in Malaysia [3,4]. In recent years, floods have become very common. Following such disaster, there is often a tally of the preliminary damage assessment with respect to the injuries, loss of lives, cost of damage, and destroyed properties. With these disasters attracting considerable media attention, people are more aware of the damage that occurred at the affected area [5]. There have been numerous studies pertaining preliminary damage assessment to buildings after a flood. A variety of damage assessments had been carried out in different countries after the event of a natural disaster. There are several guidelines for assessing the degree of building damage prepared by government agencies, researchers, local authorities, and nongovernmental organization (NGO). In 2009, Attaullah Shah, Hamid Mumtaz Khan, and Ehsan U. Qazi outlined the evaluation of the buildings destroyed or damaged due to the flooding in Pakistan. The evaluation of damage is made on mud houses which are the most common type of building structure in Pakistan [6]. In USA, Federal Emergency Management Agency (FEMA) has developed an operations manual to standardize the procedures in preliminary damage assessment nationwide. There are several state authorities in USA, like New Jersey and Florida, which reviewed this operation manually and did some modification to suit the type of disasters that their states often experienced. Apart from that, there are also numerous literatures that emphasized on residential properties damaged from hurricanes and floods [7, 8]. In concordance with the variety of the degree of housing damage, different countries are likely to have different construction methods, materials used, and the nature of the flood. A general assessment that determines the extent of flood-hit houses seems irrelevant in other countries. Moreover, in Malaysia, there is still no standardized damage assessment used by the authorities or relevant agencies in assessing the degree of housing damages after a disaster. As a result, errors in assessing the degrees of housing damages and providing inaccurate type of assistance might occur. Furthermore, the attributes for each degree of damage are not coherent because a detailed description on the attributes for each degree of damage has not been prepared yet. Thus, the attribute model from a synthesis of existing eight degrees of housing damages will be laid out. These models might not be comprehensive in listing the attributes, in which many could be added, but these attributes are sufficed to illustrate the research aims and objectives of this research.

2 The Attribute Model of the Degrees of Housing Damages for Flood-Affected Area

2.1 European Macro-Seismic Scale 1998 (EMS-98)

The EMS-98 is the basis for the evaluation of seismic intensity in European countries and is also used in a number of countries outside Europe. The category of disaster to apply this model is primarily for earthquake and post-earthquake disaster such as tsunami, landslide, and flooding. However, this model only applies to reinforced concrete type of buildings. The first scale has 12 divisions for seismic loads, but for flood disaster, the damage classification scale is only classified into six divisions: Grade 0, Grade1, Grade 2, Grade 3, Grade 4, and Grade 5. The grade takes into consideration structural and non-structural elements. Structural elements are the main structures such as foundation, beams, columns, roofs, floors, and load-bearing walls, whereas non-structural elements are gutters, chimneys, plaster ceilings, siding, and others.

According to the EMS-98, *Grade 5* refers to destruction which means very heavy structural damage. The attributes for *Grade 5* include structures that are totally destroyed or nearly collapsing. The function of the affected house is no longer usable and restored. For *Grade 4*, EMS-98 indicates that the building structures received very heavy damage which consist of heavy structural damage and very heavy non-structural damage. The attributes for *Grade 4* are serious failure of walls and partial failure of roofs and floors. Meanwhile, in *Grade 3*, the structures dealt with substantial to heavy damage which means the affected house has moderate structural damage and heavy non-structural damage. The attributes are fractured at the roofline, failure of non-structural elements like partitions and gable walls. There is a large and extensive crack in most walls. Roof tiles detached. *Grade 2* damage scale means the affected house is moderately damaged with slight structural damage and moderate non-structural damage. The attributes are cracks in many walls, fall of fairly large pieces of plaster, and partial collapse of chimneys. Last but not the least is *Grade 1*. In *Grade 1*, there is no structural damage but only slight non-structural damage. The attributes are hairline cracks in very few walls, fall of small pieces of plaster, and loose stones from upper parts of buildings in very few cases.

2.2 Green Alert Damage Assessment Manual

The Damage Assessment Manual by Green Alert in the UK is based on Windshield Survey (2004) that provides information to determine the severity of the disaster and type of disaster assistance that may be required. In this manual, the person responsible will assess the affected house caused by natural or man-made disasters. The type of building structure is for masonry and wood frame buildings. The degree

of damage is destroyed 80 %, major 30 %, minor 5 %, affected but habitable, and inaccessible [9].

Destroyed 80 % indicates that the building structures no longer exist or are severely damaged to the extent that it is no longer usable and that restoration is not technically possible or economically feasible. The attributes for destroyed 80 % damage are moved off foundation, two exterior walls collapsed, second floor is gone, structure leveled above foundation, or two or more basement walls collapsed. *Major* damage indicates the structure cannot be used or may be used under limited conditions or reduced levels of service or may be restored to a mere dwelling with extensive repairs. The structure damage is over 10 % but less than 80 % and averages at 30 %. The affected house cannot be occupied within a short period, if ever, because the necessary repairs are too time-consuming or not practical. The attributes for major damage may constitute utility damages such as well, septic system, electrical service, or gas. One or more rooms destroyed, one exterior wall collapsed, or exterior frame damaged. Roof off or collapsed and foundation damaged, bowed or collapsed wall. *Minor* damage means the structure may still be used for its intended purpose or may be repaired with minimal repairs, and the damage is less than 10 % and averages about 5 % damage. The affected house with minor damage may be occupied after repairs have been accomplished. These repairs should be accomplished within one or two weeks. The attributes for minor damage may constitute roofing/shingles removed or exposing sheathing, exterior or interior wall cracks. *Affected but habitable* damage is the affected house is habitable with no repairs needed. The attributes for affected but habitable damage are cosmetic damages such as shutters, gutters, shingles, and siding. *Inaccessible* degree of damage is the condition when the affected house is not accessible due to damage to a road or bridge, or the affected house is surrounded by water and only accessible by boat.

2.3   Florida Division of Emergency Management

In Florida (USA), as it is vulnerable to a host of natural and man-made disasters, local governments may contact Florida Department of Community Affairs, Division of Emergency Management, to initiate assistance for damage assessment. Immediately following a disaster, an initial damage assessment must be carried out by them to estimate the type and extent of damages [10]. The degree of damage model they use is sorted into five degrees of damage levels: destroyed, major, minor, affected but habitable, and inaccessible. The model is influenced by the Federal Emergency Management Agency (FEMA) of USA, however, with few improvements on the structure damage attributes.

The most sever level of damage is *destroyed*. According to the Florida Emergency Management Division, destroyed indicates that the structure of a particular affected house is not economically feasible for reparation, permanently inhabitable. The damage will consist of a complete failure of major structural

components or attributes such as collapse of basement, foundation, walls, basement walls, or roof. For *major* degree of damage, they outlined that the affected house has sustained significant damage to the building structures, becomes inhabitable, and requires extensive repairs. The damage on the structures will take more than 30 days to repair. The damage will have substantial failures to walls, floors, foundation, or roof that has more than 50 % damage to the structure. *Minor* degree of damage, as it is the most common type of damage, exists when the affected house has less than 50 % damage to structure like floors and walls that are habitable after repairs in 30 days. *Affected* degree of damage means that the affected house is still habitable with some damage to structure and contents. The affected house may be hit by flood, but only damage its contents. In the event of *inaccessible* degree of damage, the house is inaccessible by normal means due to road closure and road covered by water; the road is impassable of a landslide or bridge collapse.

2.4 Earthquake Engineering Field Investigation Team of Japan (EEFIT)

EEFIT was formed as a joint venture between industries and universities. Each country has their own team that will visit affected regions for data collection to improve the understanding of structural behavior of natural disasters especially seismic loads. In Japan, EEFIT mission team made some modification to the damage assessment model from EMS-98. The degree of damage is divided into 5: no damage (DM0), light damage (DM1), moderate damage (DM2), heavy damage (DM3), and collapse (DM4).

DM4 or destroyed refers to complete structural damage or collapse. The attributes are foundations are visible, floor slabs are exposed, heavy foundation damage, collapse of large sections of foundations, and structures due to heavy scouring. Next is *DM3*. *DM3* or heavy damage refers to inhabitable after disaster. The attributes are collapse of masonry wall panels beyond repair and structural integrity compromised. Most parts of the structure suffered collapse. There is excessive foundation settlement tilting beyond repair. The wall sections collapsed due to scouring and the damage is non-repairable. The affected house requires demolition since it is not suitable for occupancy. Then, *DM2* refers to moderate damage which the structures dealt with collapse of parts of masonry wall panels without compromising structural integrity. The attributes include that most parts of the structures are still intact with some parts suffering heavy damage. Scouring at corners of the structures leaving foundations partly exposed but could be repaired by backfilling. Cracks caused by undermined foundations are clearly visible on walls but not critical. The affected house is not suitable for immediate occupancy. Light damage or *DM1* refers to slight non-structural damage. The damage attributes are only limited to chipping of plaster on walls, minor and very few visible cracking, damage to windows and doors. The damage is repairable and the building can be occupied immediately and

therefore no damage. There is no visible damage to the building main structures during the survey.

2.5 National Disaster Management Agency of Indonesia (BNBP)

In the event of natural disaster in Indonesia, especially earthquakes which are more common than floods, the National Disaster Management Agency (BNPB) will lead in coordinating and facilitating the recovery, reconstruction, and rehabilitation process. Preliminary damage and needs assessment are necessary in the delivery of assistance addressing the specific needs for particular vulnerable groups of affected victims. In assessing the damage, BNPB uses a model that distinguishes three degrees of property damage: light damage, moderate damage, and heavy damage [11]. *Heavy damage* refers to total collapse or destruction that it seems economically unwise to restore the condition of the affected house. The attributes that belong to heavily damaged degree of damage are large openings at the ground floor or collapse of first floor and leveled building structure. *Moderate damage* means the building structure is still habitable with major reparation and is economically wise. However, no attributes or detailed description of this degree of damage were given. *Light damage* indicates that the affected house is still habitable with only minor damage to non-structural elements. Attributes for the non-structural damage were also not provided.

2.6 New Jersey State Police Office of Emergency Management

New Jersey State Police Office of Emergency Management produced a preliminary damage assessment in any event of natural disasters, especially in the event of a hurricane. Based on FEMA Preliminary Damage Assessment (PDA), they did some modification on damage scale and only categorized it into 4 degrees: affected, minor, major, and destroyed. The attributes are similar with the FEMA's PDA and therefore only discuss the damage scale descriptions. The only missing damage scale is inaccessible damage scale as in FEMA's PDA, and inaccessible is one of the damage scale that constitutes the damage assessment model. *Destroyed* means the structures of the affected house are totally loss or damaged to the extent that it does not function as a place to dwell and also not economically repairable. Next is *major*. The structures are damaged to the extent that it is no longer usable and may return to its existing functions only with extensive repairs. *Minor* damage is when the structure is slightly damaged but may be occupied under limited conditions, whereby restored within a short period of time. Lastly, it is *affected*. Some damage

to the structure but still habitable and only slight damage to building contents. This kind of damage requires no reparation and can be occupied immediately.

2.7 Henry B. Hodde III Damage Assessment Model

Although FEMA has prescribed specific guidelines for the damage assessment procedure, Henry [2] stressed that most communities or state organizations use slightly different protocols and methods in assessing property damage caused by natural disasters. In his research, he laid several damage assessment models from thirteen local governments and came out with an improvised degree of damage assessment. He further categorized the damage into four degrees: category 1, category 2, category 3, and category 4. However, this category of damage only described the structure damage but did not explain the details of structure damage attributes. In *category 4*, the structures identified have been completely destroyed and/or washed away. In *category 3*, the structures identified to have major damage and considered to be unsafe and/or experienced substantial damage. By all means, the affected house needs major repairs or rebuilding, whereas in *category 2*, the structures identified with some damage could be considered to be safe and structurally sound. The damages would not be considered as being substantially damaged. Lastly, *category 1* is identified as minimal damage on structures.

2.8 Federal Emergency Management Agency (FEMA) Operations Manual

This operation manual was developed by FEMA to standardize the procedures in preliminary damage assessments nationwide. This manual was prepared and reviewed by FEMA regional officers with vast experience in performing damage assessment through many types of disasters. The model these manuals use to distinguish the type of damage is categorized into destroyed, major, minor, affected, and inaccessible [8].

Destroyed degree of damage means the structure is a total loss to such an extent that repairs are not economically feasible. It may constitute two or more walls destroyed. The roof has totally collapsed or substantially damaged and could no longer function as it is. The damage might have washed all building structures and only the foundation remains. The affected house is pushed off the foundation. Major degree of damage exists when the affected house has sustained more than 50 % structural damages, becomes inhabitable, and requires extensive repairs. It may constitute walls, roof, floors, and foundation substantial failure to function. *Minor* degree of damage generally is not habitable after flood damage, but may be made habitable in a short period of time with house repairs. It may constitute windows or

doors blown in. The furnace or water heater at the basement is broken. *Affected* degree of damage includes dwellings with minimal damage to structure and/or contents, and the house is habitable without repairs. *Inaccessible* degree of damage is the condition when the affected house is not accessible due to damage to a road or bridge.

3   Methodology

This paper seeks to perform a comprehensive assessment on the degree of housing damage after a flood. This research involves only qualitative description in the analysis. It involves reviews on eight (8) models from the literature study and experts' views, i.e., interviews with parties involved in MERCY in order to assess the housing damage post-flooding. In order to obtain validation of proposed model of degree of housing damage, the researcher has conducted a "model validation" by forming focus groups among selected panels to evaluate and provide personal views on the proposed model. These focus groups consist of ten (10) technical experts involved in MERCY Malaysia to assess the housing damage post-flooding.

4   Findings and Discussion

From the eight (8) reviews of the attribute model, with a comprehensive summary based on the feedback from experts, the frequency of the degree of housing damage attributes and the suitability of flood disaster and building structure in the Malaysian context suggested that degree of housing damage is as follows (Table 1).

In this paper, eight (8) attribute models of damage assessment from UK, USA, Indonesia, Japan, and European countries were reviewed and came out with a suggested degree of housing damage. This conceptual model is categorized into four degrees of damage: inaccessible, minor, major, and destroyed.

First degree of damage is inaccessible. This degree indicates that the residence is not accessible by normal means with supporting attributes, for example, due to the building being flooded or submerged, road or bridge being out, and the flood-affected area becoming ground zero. It is recommended for the relevant authorities to assist in the preliminary damage assessment.

Next is minor. The damage is described as slight damage to building structure; however, the building still can be occupied within a short period after some minor reparation. The attributes of damage are only minor damage to partitions, infills, ceilings, doors, and windows that are repairable within one to two weeks.

Major is the third degree of damage. The building has sustained structural or significant damage that made it unsuitable to be occupied. Despite that, the building can be occupied after extensive repairs. The recommendation is that the affected building with major degree of damage is to undergo extensive repair and could be occupied after 30 days.

Table 1 Suggested degrees of housing damages

Suggested degree of damage	Description of damage	Attributes of damage	Recommendation
Inaccessible	The residence is inaccessible by normal means	The house is flooded or submerged	Authorities to assist
		Road and bridge is out	
		Ground zero	
Minor	Slight damage to building structure can be occupied within a short period after minor reparation	Minor damage in partitions, infills, and ceilings	Can be repaired within one to two weeks
		Minor damage to door and windows	
Major	The building has sustained structural or significant damages, becomes inhabitable, and requires extensive repairs. Could be occupied after extensive repairs	Substantial failure of walls, floors, foundation, or roof	Habitable after extensive repairs more than 30 days
		Utilities damaged (Electrical, surface water drainage, sewerage reticulation system, water reticulation)	
Destroyed	Total loss	Null	Recommended for temporary shelter

The last degree of damage is destroyed. The description for this degree of damage is that a particular building experienced total loss or has been completely destroyed. It is recommended as a temporary shelter.

5 Conclusion and Future Research

In this paper, based on the qualitative description analysis, we have explored various literatures on eight (8) models of degree of housing damage as a tool to develop a conceptual model that is applicable to the Malaysian context. This suggested model is not being tested yet as this is only the preliminary study. With this suggested model, it will allow the researchers to examine and develop a housing damage assessment model in evaluating the degree of housing damage after a flood in the Malaysian context.

References

1. Malaysia flood damage to cost $560 m. Post Magazine. 13 January 2015. Retrieved 13 January 2015 (subscription required)
2. Chan NW (1998) Institutional arrangements for flood hazard management in Malaysia: an evaluation using the criteria approach. Disasters 21(3):206–222
3. Eves C, Wilkinson SJ (2014) Assessing the immediate and short-term impact of flooding on residential property participant behaviour. Natural Hazards DOI: 10.1007/s11069-013-0961-y
4. Chan, NW (1995) Flood disaster management in Malaysia: an evaluation of the effectiveness of government resettlements schemes. Emerald Insight 22–29
5. Wittaya D, Hokao K (2012) Assessing the flood impacts and the cultural properties vulnerabilities in Ayutthaya, Thailand. In: The 3rd international conference on sustainable future for human security. Sciverse ScinceDirect, pp 739–748
6. Shah A, Khan HM, Qazi EU (2009) Damage assessment of flood affected mud houses in Pakistan. J Himalayan Earth Sci 46(1):99–110
7. Hodde, BH (2012, November) The damage assessment process: evaluating coastal storm damage assessments in Texas After Hurricane IKE. The University of Houston Publication. Clear Lake, Texas, USA: Proquest LLC 2013
8. Federal Emergency Management Agency U (2005) Preliminary damage assessment for individual assistance. Federal Emergency Management Agency, USA
9. Damage assessment manual (2004). www.greenalert.net
10. Division of Emergency Management F (2004) Handbook for disaster assisstance. Florida: Division of Emergency Management, Florida
11. BNPB, Bappenas and Government of Indonesia (2009) West Sumatra and Jambi natural disasters: damage, loss and preliminary needs assessment. West Sumatra: Badan Nasional Penanggulangan Bencana, Indonesia

Identification of Vulnerable Regions for TNB's Electric Substations during Flood in Peninsular Malaysia

Nurul Elyeena Rostam, Lariyah Mohd Sidek, Hidayah Basri, Milad Jajarmizadeh, Ming Fai Chow, Radin Diana R. Ahmad and Shyong Wai Foon

Abstract Flood is usually an environmental hazard which has been increased in recent years by forcing the pushing factors such as climate change and urbanization. This study presents flood-prone area related to the electric substations for Tenaga Nasional Berhad (TNB) in Peninsular Malaysia. The objective of this research was to identify the related regions that the electric substations are in vulnerable condition by flood risk. For this research, two types of maps are generated, namely flood inundation map (FIM), which indicates the area and capacity of the flood, and flood hazard map (FHM), which provides the area, depth, velocity, and extension of the flood for the TNB's location of substation. For this issue, different classes of substations are involved in analysis, namely transmission main intake (PMU), main distribution (PPU), main switching station (SSU), and distribution substation (PE). An integration of TNB's substation maps performed with FIM and FHM due to identify substations which are in flood-prone regions. Generally, result shows that Kelantan is classified as the highest flood-prone region for TNB's infrastructures especially for PMU which they are affected by flood. Kelantan, Terengganu, and Perlis are involved with the highest flooded, respectively, based on PPU and SSU infrastructure. Finally, for PE substations, Kelantan, Perlis, and Terengganu have the highest contribution for flooded substations for TNB's structures.

Keywords Flood · Tenaga Nasional Berhad · Electric substation · Inundation area

N.E. Rostam (✉) · L. Mohd Sidek · H. Basri · M. Jajarmizadeh · M.F. Chow
Centre for Sustainable Technology and Environment (CSTEN), Universiti Tenaga Nasional, Jalan IKRAM-UNITEN, 43000 Kajang, Selangor, Malaysia
e-mail: lyeena14@gmail.com

R.D. R. Ahmad
TNB Research Sdn Bhd, 43000 Kajang, Selangor, Malaysia

S.W. Foon
TNB Distribution Sdn Bhd, 46200 Petaling Jaya, Selangor, Malaysia

1   Introduction

Flood is a serious and frequent natural disaster in Malaysia. In Malaysia, 9 % or 29,720 km^2 of the country is located in flood-prone regions with total 4.915 million people affected by floods. Totally, 21 % of the Malaysian regions are affected by floods [1]. Flood occurrence can be categorized into flash and monsoon types in Malaysia [2]. Flash floods usually happen in urban areas with high rainfall intensity, which normally occurs 4–6 h after the rainfall event. On the other hand, monsoonal floods occur during the wet seasons in Malaysia, especially at the east coast of the Peninsular [3]. Usually, flash flood is generated faster than monsoonal flood and has high impact on infrastructure of urban area. The reason might be related to limited time available to prepare mitigation actions and evacuation. In rapid urbanized region like Kuala Lumpur, flash floods usually have significant impact on urbanized area and infrastructure. For instance, in 2012, 6 flash floods have been recorded at Kuala Lumpur and the worst event recorded at May 2, 2012, which results to some financial damage [4].

Between the urbanized infrastructures, the electricity infrastructure is the major element of fundamental facilities during the development in each country. With the increasing of demand, the safety and continuity of electricity become the huge issue. The interruption of the electricity due to the natural disasters such as flood can cause huge impact to the economic and safety of the country. In Malaysia, the electricity is used based on the grid system and there are three classifications. For peninsular Malaysia, National Grid is operated and owned by Tenega Nasional Berhad (TNB). The National Grid is responsible for the interconnected power systems for the Peninsular Malaysian states. It is the area of 131,598 km^2, a population of 21 million approximately. It has been reported a peak demand of 16,901 megawatts occurred on June 11, 2014 [5]. While the other two electrical grids in Sabah and Sarawak operate by Sabah Electricity Sdn Bhd and Sarawak Energy Berhad, respectively.

As the largest utility company in Malaysia, Tenaga Nasional Berhad (TNB) is faced a major threats due to the rising severity and frequency of flood poses to their supply performance, inflicting unexpected revenue loss, and high repair and maintenance cost. During the flood, electricity infrastructures have been cut off due to safety issues. For instance, during the flood in December 2013, TNB had spent RM10 million for the repair of all their substations affected in the floods at Johor, Pahang, and Terengganu [6]. While for floods in December 2014, TNB's losses are RM10 million at Kelantan [7]. TNBs are under pressure to limit the number of customer outages and minimize the outages time.

It has been reported, during the extreme flood events in Kelantan, PMU substations (*Pencawang Masuk Utama*) have been shut down. PMU Tanah Merah and PMU LMAL are located in Pasir Mas. PMU Tanah Merah plays the major role in National Grid since it is connected to north and east part of Peninsular Malaysia. The interruption operation of Tanah Merah PMU can cause problem to the National Grid overall and can cause harm to the Malaysia security. Owing to the flood on PMU Tanah Merah, it has been shut down on December 25, 2014 (3.41 am).

Fig. 1 **a** Flood mark located in PMU Tanah Merah. **b** Flood mark located at PMU LMAL located in Pasir Mas

Similarly, PMU LMAL was shut down on December 25, 2014 (10.55 pm). Both the PMUs had been fully normalized in less than a week. PMU Tanah Merah had been fully normalized on December 31, 2014 (11.30 pm) while PMU LMAL on December 30, 2014 (6.37 pm) [8]. Figure 1a and b show the flood mark recoded during the site visit to this location.

In fact, natural disaster cannot be stopped and only can be minimized by having sustainable plan. Usually, there are structure and non-structured mitigation methods, but TNB provides one type of measure for mitigation process as structure forms. By past experiences in regard to flood, TNB provides a substation

construction guideline in the flood-prone area, e.g., water barrier or flood wall at the substations' door, rise of substations floor and use of pole mounted substations [9].

The existing substation based on the standardized designs may not provide the best approach for critical substation that located in the flood-prone area [10]. Literature brings some common solutions for any disaster for urbanized infrastructure which is related to flood hazard [10]. It can be as follows:

1. Identify all substation switchyard elevations and control house elevations that do not meet current industry standards for coastal, river, or inland waterway flooding.
2. Evaluate the risk of loss of specific equipment and/or systems to determine the scope of flood mitigation activities required to maintain acceptable levels of service for all substations impacted by flood immunity to provide the necessary reliability for the increasing public demands, and more critically for emergency response.
3. Determine the worst-case storm scenario based on the recorded data.
4. Design critical coastal or critical aging substations in accordance with the result of the worst-case scenario analysis, tempered by the risk of loss determination for equipment loss, and acceptable service levels.

Non-structured measuring is based on the modeling such as flood hazard map (FHM), master plan, and flood forecasting and warning system. In Malaysia, the flood mapping is developed by Department of Irrigation and Drainage (DID). Flood inundation map (FIM), flood hazard map (FHM), and flood risk map (FRM) are the main types of mapping that be practice in Malaysia [11]. Many electrical substations were built before the existence of flood hazard and flood inundation maps in Malaysia. Due to rapid urbanization, a significant number of substations are situated in flood-prone areas. This conditions result in TNB's electricity supplier infrastructure at high risk. By review the reports and literature, currently, there are not any predictions of flood events to enhance the understanding and awareness of flood-risk zones which may affect TNB substations in Peninsular Malaysia.

This paper presents the location of each TNB's substations that are exposed to flood risks. This research, as fundamental study, helps to understand the risk of each flooded substation. In first phase (in this study), importance of vulnerable regions in Peninsular Malaysia is identified for future outline of TNB's program owing to mitigation of flood risk on infrastructure.

2 Methodology

2.1 Electric Substations

A substation or switching station is a connection and switching points for transmission lines, subtransmission feeders, generating units, and transformers [12]. The substations can be classified depending on the purpose or the types. For this study, the substations are categories based on the purpose. There are various types of

Table 1 TNB's substation (PMU/PPU/SSU/PE) [13]

Type of substation	Function	Average cost range
PMU *Pencawang Masuk Utama*—transmission main intake	Distribution bulk power substation that provide interfacing between transmission network and distribution network where the transmission voltage is step down to. It is the first level of distribution primary network (33, 11 kV)	More than RM30 Millions depending on the transformer
PPU *Pencawang Pembahagi Utama*–Main distribution substation	Distribution primary substation that distributes power by stepping down 33 kV voltage to 11 or 22 kV voltage as a second level of distribution primary network	RM7 Millions—RM10 Millions depending on the transformer size
SSU *Stesen Pembahagi Utama*–Main switching station	Distribution substation that further distributes power without voltage transformation within the distribution primary network (33 kV, 22 kV, 11 kV). It provides interfacing between various PMUs and/or various PPUs within the distribution primary network	RM500 K to RM1 Million depending on the number of switchgear and voltage level
PE *Pencawang Eleterik*—distribution substation	Low-voltage substation provides interfacing between primary network and secondary network in distribution system where the 11 or 22 kV voltage is step down to 415 V	RM100 K to RM250 K depending on the transformer size and size of building

TNBs, namely transmission main intake or Pencawang Masuk Utama (PMU), main distribution substation or Pencawang Pembahagi Utama (PPU), main switching station or Station Suis Utama (SSU), and distribution substation or Pencawang Elektrik (PE). The digitized location of the existing substation is used to overlay with the FIM. This digitized location information of the substations is collected from TNB-GIS unit. Table 1 shows details of each substation with the average cost range.

2.2 Flood Inundation Map and Flood Hazard Map

Flood Inundation Map (FIM) indicates the geographical areas which covered by flood according to the flood report done by DID. This map only shows the flood area and capacity of the flood. Figure 2 shows that the area of FIM is covered with TNB's PMU substation in Peninsular Malaysia as an example. The total area of FIM is 19,412.57 km^2 that covers almost 15 % area of Peninsular Malaysia. Flood hazard map (FHM) is the flood-extend presentation that is generated by a combination of river basin model and hydrology input using hydrodynamic modeling.

Fig. 2 Flood inundation map lay with TNB's PMU substations in Peninsular Malaysia

Flood hazard map (FHM) is used with information of 2010 as latest available by DID for this study. Up to 2014, it has been completed 28 river basins by DID for FHM. At the earlier production of FHM, it only be generated for 100 ARI (average rainfall intensity). Since 2012, DID provides a guideline that all FHM must be generated for different ARIs (e.g., 5,10,20,50, and 100 ARI).

The FHM provides the area, depth, velocity, and extent of the flood.

2.3 Overlaying Process

The overlaying process is the important part of determining substations that they are in flood risk. This process is performed with GIS due to integration of different data prepared and generated. For the beginning, all the data needed such as the TNB substation location and the flood map are gathering. The location of substation in digitize format is collected from TNB-GIS while the flood map is obtained from DID.
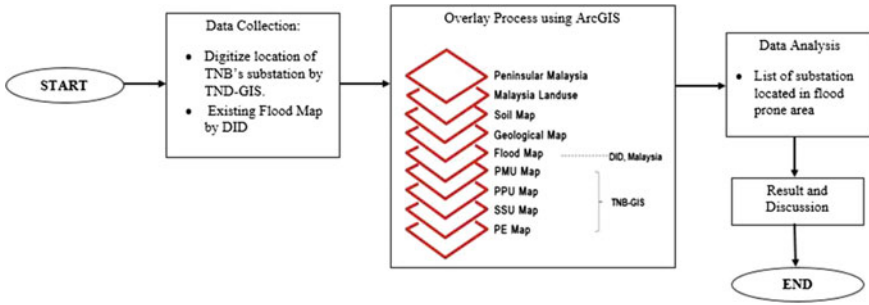
Fig. 3 Flowchart on process of identified TNB's substation located in flood-prone area

Next step is to produce the flood mapping for the TNB's substation. The GIS is used in this overlaying process due to the wide application in Malaysia. Furthermore, the GIS can provide better mapping drawing with the user-friendly tools. List of the substations located in flood-prone area is collected in GIS based on the intersection of TNB's substation with the flood map. Figure 3 shows summary process of identifying the TNB's substations that located in flood-prone area.

3   Result and Discussion

Figure 4 is the presentation of FIM with the TNB's substation located in Kelantan as an example, while Table 2 shows the overall TNB's substation located in flood-prone area based on FIM analysis. Table 2 shows that Kelantan has the highest percentages of substation located in flood-prone area totally. For PMU substations, Kelantan has the highest record of flooded electric infrastructures (100 %). Other states have similar result for flood-prone area involved with electric infrastructure. Based on PPU and SSU, Kelantan (89 %), Trengannu (47.5 %) and Perlis (42.8 %) are involved with the highest contribution of drowned infrastructure
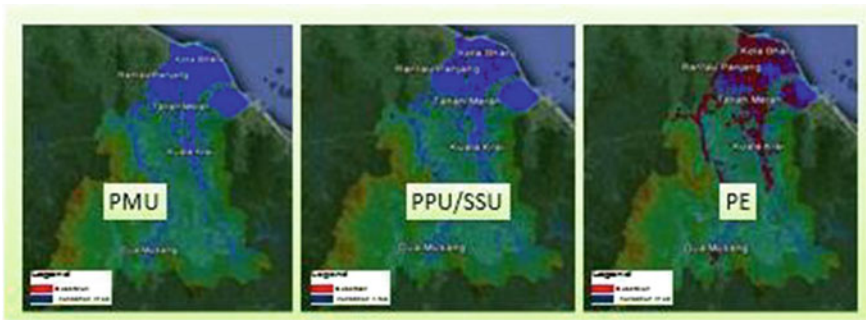
Fig. 4 Substation located in flood-prone area in Kelantan
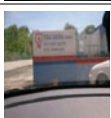
Table 2 Summary of substation located in the flood-prone area

States	Substation in flood-prone area/overall substations			Percentages of substations in flood-prone area (%)		
	PMU	PPU and SSU	PE	PMU	PPU and SSU	PE
Perlis	2/6	3/7	362/581	33.33	42.86	62.31
Kedah	6/26	18/77	1423/4962	23.08	23.38	28.68
Pulau Pinang	8/22	38/151	800/3406	36.36	25.17	28.68
Perak	3/54	29/214	775/5789	5.56	13.55	13.39
Kelantan	11/11	57/64	1511/1801	100.0	89.06	83.90
Terengganu	4/13	57/120	948/2284	30.77	47.50	41.51
Pahang	6/26	26/108	654/2189	23.08	24.07	29.88
Selangor	5/90	11/442	683/17058	5.56	2.49	4.00
Kuala Lumpur	2/28	12/172	158/4021	7.14	6.98	3.93
Negeri Sembilan	4/37	16/284	219/2860	10.81	5.63	7.66
Melaka	6/19	50/233	676/2507	31.58	21.46	26.96
Johor	16/51	77/234	2308/8207	31.37	32.91	28.12

for TNB. Finally for PE, Kelantan (83 %), Perlis (62 %), and Trengannu (41.5 %) are the highest vulnerable area for structures of TNB. On the other hand, the lowest risk for TNB's structures is for Kuala Lumpur. The reason might be related to the recent constructions of TNB's structures including flood evaluations and identification of flood-prone area. Also, development of mitigation system has important role for this modern urbanized region.

List of substations located in the flood-prone area has been produced, and the site verification is done to identify the flood risk of each substation. This site verification is really important in providing the significant data such as the substation elevation, severity of flood occurred, and the highest flood depth that had been recorded at that substation. Based on the site visit, it shows that the elevation of the height of substation and attributed location can prevent the substation from drowned condition. Table 3 shows the example of data collected during the site visit in summary. Figure 5 is the list of software that is used for this study.

Table 3 Example of site verification from the collected data

Substation	Elevation of substation platform (m)	Verification on site	Flood defense method	Picture
PMU Geliga, Kemaman	9.78	In flood-prone area 2013 & 2014	Use sandbag to close all doors	
PMU Gong Badak	6.38	Yes, access road only	Stand by	
PPU Kustem	7.33	Yes, 1 meter	Inform TNB to switch off the power supply	
SSU Kustem	6.73	Yes, 1 meter	Inform TNB to switch off the power supply	
PPU Saujana	11.29	Yes	No	
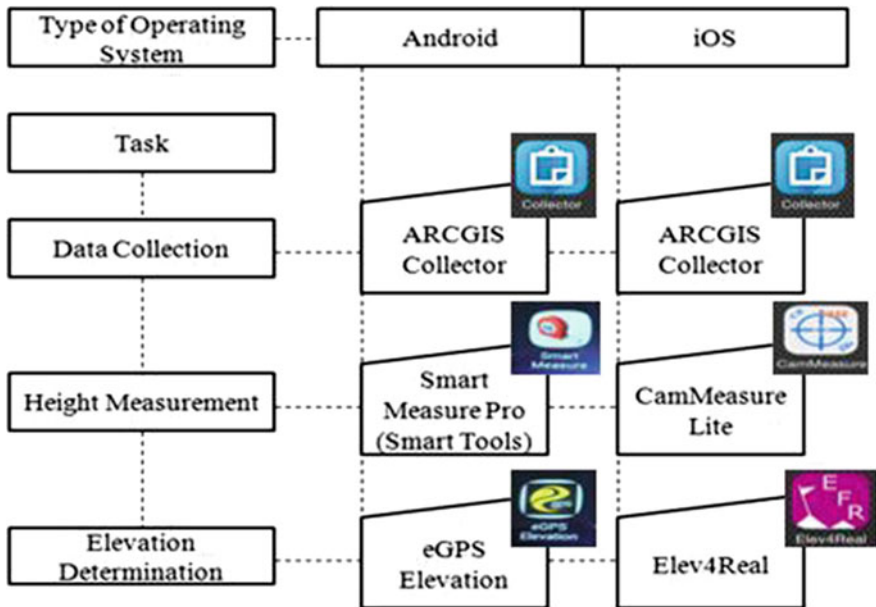
Fig. 5 List of softwares used in data verification

Consequently, the continuation of this study can be followed by identification of the flood-risk level for each substation. This study can provide the indicator safety based on the flood region. With availability of data, the new mitigation methods can be suggested to TNB for minimizing the flood impact on electric substation. Current study can be used as guideline for development of TNB's substation by contribution of flood-risk priority for different regions.

4   Conclusion

One of the challenging topics for tropical climate and developing countries are identification of flood-prone area based on the electric power substations. In Malaysia, Tenaga Nasional Berhad has the highest responsibility for distribution of electric power; however, some of the infrastructures are located in flood-prone area. Flooded electric substation leads to cut off electricity and potential danger for human life during flood events. Therefore, it is required to study the flood-prone electric substations. The objective of this study was the identification of TNBs substations in flood-prone area by using the flood inundation map and flood hazard map. Also, location of substation has been identified by available data. Using GIS and integration of maps on TNB's substations reveals that contribution of different regions in Peninsular Malaysia for potential-drowned substation. In conclusion, results show that Kelantan has been identified as the most vulnerable state for most types of TNBs, namely transmission main intake, main distribution substation, main switching station, and distribution substation. Moreover, the results illustrate that the shortest flooded infrastructure of TNBs is related to Kula Lumpur. The reason of this procedure might be related to the recent analysis on location and identification of flood-prone area and developed proper mitigation systems such as drainage systems in Kuala Lumpur. Therefore, it is required to consider the flood analysis related to TNBs structure in other developing state in Malaysia owing to protect dangerous results during flood.

References

1. Department of Irrigation and Drainage (2009) Volume 1—flood management 2–5
2. Department of Irrigation and Drainage (2010) Urban storm. Water Management Manual for Malaysia, Kuala Lumpur, pp 2–12

3. Noorazuan MH (2003) Flash flood, imperviousness and urban drainage in Malaysia: the geographical perspective. Universal Publishers, Malaysia, p 105
4. Department of Irrigation and Drainage (2013) Flood management approaches. Available at: http://www.water.gov.my. Accessed 25 June 2015
5. Peninsular Malaysia Grid System Operator online. Available at: gso.org.my. Accessed June 2015
6. Malaymail online (2013) Deputy minister: TNB spend RM10 m to repair flood hitarea. Available at: http://m.themalaymailonline.com. Accessed Oct 2014
7. Malaymail online (2015) Chairman of Kelantan's Flood Disaster Operations Committee: TNB suffered losses RM10 m in flood hit area. Available at: http://m.themalaymailonline.com. Accessed Feb 2015
8. Tenaga Nasional Berhad (2014) Kronologi Gangguan & Pemulihan Bekalan Elektrik Negeri Kelantan
9. Tenaga Nasional Berhad (2012) Pekeliling PBK(Pengurusan Aset) Bil.A22/2012-Kaedah Mitigasi Pencawang 11 kV dan 22 kV di Kawasan yang Dilanda Banjir 105
10. Boggess JM, Becker GW, Mitchell MK (2014) Storm and flood hardening of electrical substations, T&D conference and exposition, 2014 IEEE PES, vol., no., pp 1.5, 14–17 April 2014. doi:10.1109/TDC.2014.6863387
11. Ketua Pengarah Jabatan Pengairan & Saliran Malaysia 2007 draft text speech: flood and drought management in Malaysia 6
12. Singh SN (2008) Electric power generation, transmission and distribution. PHI Learning Pvt. Ltd, p 368, New Delhi
13. Rahman S (2013) Overview of distribution network [PDF document]. Rev on 3 Dec 2013

Part II
Water and Flood Modelling

Mathematical Modeling in Irrigation and Flood Management

**A.F.M. Afzal Hossain, S.M. Shah-Newaz
and Muhammad Hassan Bin Afzal**

Abstract The economy of Bangladesh predominantly depends upon agriculture. About 70 % of the population is dependent on agriculture. In the next 25 years, the population of the country is expected to increase by 40 %. This increase of population will increase the food demand of about 29 %. The changes in the agricultural area have important implications for food production as the reduced area implies an increase in cropping intensity on the remaining land. Planned utilization and efficient management of water resources for irrigation is one of the most crucial elements for achieving desired changes in agricultural production which calls for application of an integrated hydrological modeling tool. Most of the irrigation projects in Bangladesh are implemented 30–40 years ago. Nowadays, lots of infrastructural changes have been occurred. The irrigation canal command area conceived earlier has been changed, and many drainage routes have been blocked. As the hydraulic events are dynamic and changes occur every year, it is very difficult to provide solution of these complex situations for the normal prevailing method without modeling technique. Modeling technique can provide sustainable solution considering impacts of different scenarios for irrigation, flood, and drainage improvements. This paper highlights the case study of Teesta Barrage Project (TBP) Phase-I. This case study shows how the state-of-the-art technologies could be used for irrigation and flood management in irrigation project. The application of modeling tool in TBP phase-I opens up a new dimension of models as a very useful tool in Command Area Development Project. After the completion of TBP Phase-I, the project experienced water-logging problems at several locations coupled with

A.F.M. Afzal Hossain (✉)
Planning and Development, IWM, Dhaka, Bangladesh
e-mail: afh@iwmbd.org

S.M. Shah-Newaz
Irrigation Management Division, IWM, Dhaka, Bangladesh

M.H.B. Afzal
EEE Department, Primeasia University, Dhaka, Bangladesh
e-mail: hassan.afzal@primeasia.edu.bd

M.H.B. Afzal
University of Dhaka(DU), Dhaka, Bangladesh

the fact that the potential irrigable areas did not get irrigation. Under CAD project of TBP phase-I, IWM carried out detailed hydraulic model study for the irrigation and drainage systems in an integrated way to find remedial measures. A comprehensive data collection program including topographic survey has been carried out in connection with this study. Updated topographic map has been developed, and command area has been redelineated based on this map. A number of problems were identified, and corresponding solutions have been established based on the study. Most of the suggestions related to irrigation and drainage have already been implemented, and the results are found very much satisfactory. These are definitely positive indications of the successful utilization of modeling tool for better management of water resources projects. Computer-based interactive information system (IIS) for the whole project area and decision support system (DSS) for a pilot area have been developed for better management of the project.

1   Introduction

The economy of Bangladesh predominantly depends upon agriculture. In Bangladesh, potential cultivable area is about 8.3 Million hectors (Mha) of which 7.7 Mha are considered irrigable as per NWMP [1]. About 70 % of the population is dependent on agriculture. In the next 25 years, the population of the country is expected to increase by 40 %. The agricultural land will be reduced by about 4.4 % (Technical Report # 7, National Water Management Plan [1]. This increase of population will increase the rice demand in the next 25 years about 29 %. The changes in the agricultural area have important implications for food production as the reduced area implies an increase in cropping intensity on the remaining land.

Development of agriculture through irrigation, drainage, and flood control has got priority in the national development plans to attain food adequacy. The central strategy for the water resources development would be expansion coverage and proper utilization of water resources conjunctively to increase area under effective cultivation for the improvement in agricultural productivity [2]. Water management for the following issues needs to be considered to attain food adequacy.

- Increase irrigation coverage up to the potential;
- Achieve full potential benefit of irrigation;
- Minimize crop damage by flooding;
- Minimize crop damage by drought forecasting;
- Crop diversification based on available resource; and
- Increase cropping intensity.

In Bangladesh, total irrigated area has been estimated to be 4.11 Mha as per BADC [3] and NWMP [1] and the remaining 3.6 Mha area is available for irrigation. With existing easily accessible water resources, a major source of irrigation is groundwater available in the northern parts of the country, major portion of which is already now being used. About 2.7 Mha areas are solely dependent on surface water for irrigation. Moreover, there is scope of diversifying crops with irrigation, which may accrue more benefit [4].

Planned utilization and efficient management of water resources for irrigation is one of the most crucial elements for achieving desired changes in agricultural production which calls for the application of an integrated hydrological modeling tool. Most of the irrigation projects in Bangladesh were implemented 30–40 years ago when planning, and the design of the projects had been done based on the then available conventional methods. Those methods were based on many assumptions and limitations where analysis of project was not possible in a holistic approach considering all the project parameters at a time. Nowadays, lots of infrastructural changes have been occurred. The irrigation canal command area conceived earlier has been changed, and many drainage routes have been blocked. As the hydraulic events are dynamic and changes occur every year, it is very difficult to provide solution of these complex situations for the normal prevailing method without modeling technique. Modeling is such an approach by which it is possible to investigate the whole project in a holistic way considering all the project parameters at a time. In this approach, the impact of different option scenario is also possible to visualize beforehand. As such, the modeling technique can provide sustainable solution in water management problems for irrigation and drainage improvement.

IWM began its journey in 1990 with the commitment to provide scientifically based analytical tools, models, and decision support services that would help planners, designers, engineers, and scientists to understand, describe and manage the complex water resources and ecosystem which would ultimately contribute to:

- Minimize losses of lives, crops, and properties;
- Enhance and protect quality of life; and
- Sustainable economic development toward poverty alleviation.

Since 1996 IWM has been providing modeling support in irrigation, drainage, and flood management. It has been observed that in many irrigation and drainage projects, benefits have been achieved after the implementation of IWM's suggestions. This credit also goes to the design cell of BWDB and project-level implementation. The hydrological modeling has become now a proven tool in the water resources management aspects such as irrigation, drainage, and flood management.

The committed role of IWM and benefit using the modeling tools for irrigation management of command area development project and flood management projects have been discussed in this paper.

1.1 Application of Mathematical Model in Command Area Development Project

1. Teesta Barrage Project Phase-I

The Teesta Barrage Project (TBP) has been planned to provide primarily supplementary irrigation for transplanted Aman. In addition, irrigation to Rabi and Aus crops may also be possible in a limited scale depending on the availability of surface water resources. The Phase-I of TBP has been completed in June 1998 covering a gross benefited area of 154,250 ha and a net irrigable area of 111,406 ha. Study area is shown in Fig. 1.

The main objective of this project is to increase the productivity of the land by achieving the full potential benefit of irrigation in the project area. But after the completion of TBP Phase-I, the project experienced water-logging problems at several locations coupled with the fact that the potential irrigable areas did not get irrigation. The project authority tried their best at micro-level to solve the problems. They dealt discretely with individual problems using available conventional methods. But as they had no such tool like mathematical model to investigate the whole project in an integrated way, they could not find the complete solution. Solution of one problematic area would create new problem to another area, and as such problems were persistent [5].

A. *To attain the objectives of TBP by overcoming the problems, mathematical model study was identified to review and evaluate the performance of the existing irrigation and drainage systems thus to find out problems and suggest remedial measures. IWM developed mathematical models of the irrigation and drainage systems by incorporating all the rivers, canals, road networks, and hydraulic structures within the project area, topographic and hydro-meteorological data, cropping pattern, crop water requirements, and all other project elements necessary to describe the real situation.*

IWM carried out a comprehensive modeling study of the Command Area of TBP Phase-I. The study includes seven major components, which are as follows.

- Survey and mapping;
- Irrigation study;
- Drainage study;
- Groundwater study [6];
- Development of a decision support system (DSS) for a pilot area;
- Development of interactive information system (IIS); and
- Development of structure operation rule curves.
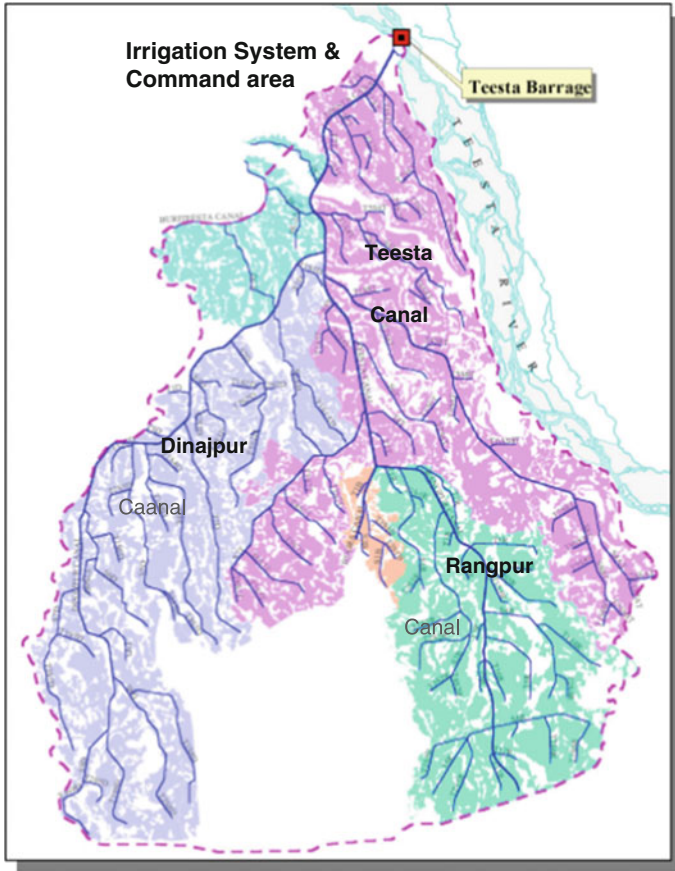
Fig. 1 Command area development of Teesta Barrage project

1.2   Survey and Mapping

Survey and data collection work started at the very beginning of the study. Data collection includes water level and discharge observation in the drainage channel and irrigation system, topographic survey for an area of 1542 km^2, inventory of existing structure on irrigation and drainage channels, groundwater-level observation, and soil testing. Detailed topographic survey work comprised of benchmark establishment, land-level survey and plotting of contours, delineation of homestead area, water bodies, alignment of roads, embankments, railway lines, irrigation canals, and drainage channels. The survey works have been carried out by using

sophisticated satellite-based survey equipment, digital total station, and conventional optical levels. The collected data have been organized in a relational database, and an interactive information system (IIS) has been developed.

1.3 Irrigation Study

The four main irrigation system of the project are as follows:

(i) Teesta irrigation system, (ii) Dinajpur irrigation system, (iii) Rangpur irrigation system, and (iv) Bogra irrigation system

As Bogra system is not fully developed, here only the performance of the existing three irrigation systems has been evaluated integrating tertiary, secondary, and main canal systems applying hydraulic modeling. During both Kharif-I and Kharif-II, it has been observed that in the Teesta and Rangpur main canals, full supply level cannot be achieved in a dynamic head for the required flow of Phase-I. The reason behind the fact is that these canals were designed for larger flow to cover the areas of both phases (Phase-I and II). A number of bottlenecks have been identified in the Teesta, Rangpur, and Dinajpur canal systems, i.e., less flow into the secondary and tertiary canal at optimum gate operation of main canal, improper size, vent and sill level of structures, and insufficient tertiary canal length to cover full command area. A number of improvement scenarios have been developed and studied in consultation with the field officials and Design VI of BWDB to find optimum solution. The model study reveals the need of some interventions to achieve full supply level and required flow in the canal system. On the basis of detail hydraulic model study and interactions with local people, officials of TBP and Design VI, remedial measures have been suggested for improving the irrigation canal systems to bring potential irrigable area under irrigation. Figure 2 shows that FSL is not achieved at the dynamic head in the existing system of S7T canal. The study-suggested solution is shown in Fig. 3 where FSL is achieved with two additional check structures and optimized operation of structures.
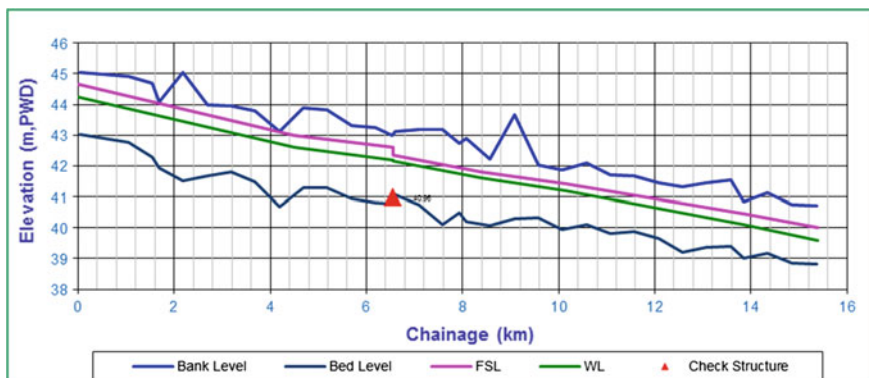
Fig. 2 Comparison of FSL and WL at S7T canal in the existing condition
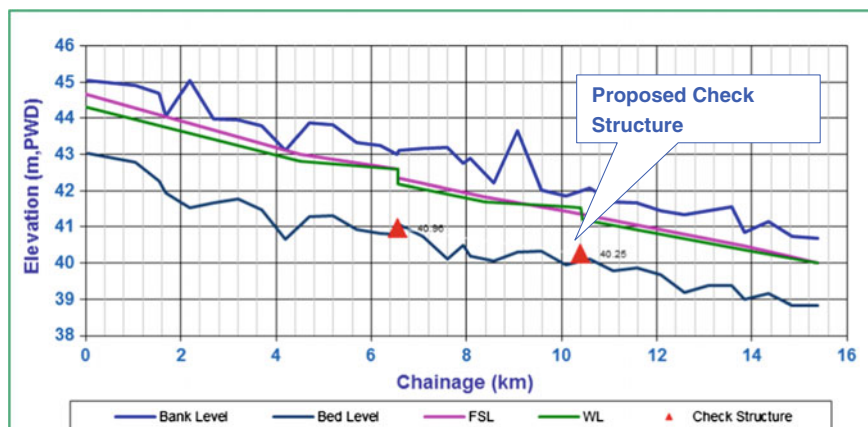
Fig. 3 Comparison of FSL and WL at S7T canal at the optimized condition

1.4   Post-Project Evaluation of Irrigation

Most of the recommendations related to problems associated with the irrigation system have already been implemented by BWDB. A field visit was made by IWM professional along with BWDB officials to evaluate the performances of the recommendations. Interactions with local people were also made in this regard. Summary of the overall field observation is given in the table below.

Sites visited	Previous problem	IWM's recommendation	Status of implementation	Improvement obtained
CKD1S4T	Insufficient flow to the downstream	Addition of two pipes	Implemented and operated	Enough flow to the downstream
S6T bypass canal	Insufficient flow into the canal	Bypass canal from u/s of R3T	Implemented but not operated yet	Required flow and FSL are expected in the canal
S8Tcanal at 14.1 km	FSL is not achieved	Construction of new check structure	Implemented except vertical gates	FSL is expected to be achieved by operating the gates
T2R bypass canal	No flow in the canal	Bypass canal from u/s of R2R	Implemented and operated	Enough flow in the canal
Offtake of T4T	Higher sill level, no flow into the canal	Lowering of sill by 70 cm	Implemented and operated	Enough flow in the canal
T1D bypass canal	No flow in the canal	Bypass from u/s of R3D	Implemented and problem removed	Enough flow in the canal

1.5 Drainage Study

The river systems that drain the project area are as follows:

(i) Buriteesta–Naotara–Dhum System, (ii) Aulikhana–Ghagot System, (iii) Deonai–Charalkata–Jamuneswari System, (iv) Dhaijan–Bullai–Jamuneswari System, (v) Burikhora–Old Jamuneswari–Chickly System, and (vi) Kharkharia–Ichmati Jamuna System.

The irrigation canals cross the natural rivers at many locations. The cross-drainage structures have been provided at the meeting point of river and canal. The irrigation canal dyke interrupts the natural overland drainage. For smooth overland flow, siphons under the irrigation canal bed were provided at the flood plain. These siphons do not have defined drainage channel at the upstream or downstream. No proper annual maintenance is being practiced to clean and flush the siphons for functioning with full capacity, which results in blockage of the siphons to some extent such as Naotara siphon.

The design drainage coefficient was calculated on the basis of 5-day accumulated rainfall of 5-year return period considering three-day submergence [7]. In the Teesta Barrage Project area, most of the homesteads are only at 0.3 m or 0.45 m above the ground level. So in a number of places, homesteads get inundated at water level of 3-day duration such as Hajarihat. There are many areas of drainage congestions, which are localized problems.

1. *The major identified drainage congestion areas within TBP Phase-I are as follows:*
2. *(i) Naotara siphon, (ii) Dhodrar River, (iii) T6S7T at Hajarihat, (iv) Mirkabeel area, and (v) Ghugumari River at Kaimari*

A comprehensive modeling study has been carried out to investigate the drainage problems and suggests solution in an integrated way. A set of drainage options has been developed in consultation with officials of Design VI and Teesta Barrage Project, BWDB. Flood management model study to assess the impact of all options was carried out. The results of the options have been consulted with design engineers and field officials of TBP. It has been revealed from this study that all major drainage structures are adequate for 5-year flow with 3-day submergence. But nowadays, the project people expects one-day submergence. It has been also observed that siphon gets siltation in each year. Annual flushing is essential for smooth functioning of the siphon with its full capacity.

Drainage congestion along Dhodrar River was a common phenomenon in the past. There are eight water control structures and ten culverts over its 20-km length most of which are not adequate to drain u/s area. Different local government agencies built all the culverts; out of these, the culverts at changes 19.3 and 20.45 km are found quite inadequate to accommodate u/s flow generated from a drainage area of 5500 ha. Figure 4 shows newly constructed 2-vent box culvert (left side) as per the recommendation of IWM along with the existing inadequate one

(right side) on Dhodrar River at 19.3 km. It has been reported that there is no more drainage congestion at this location after the construction of the new culvert.

To identify the drainage problems and to find the probable optimal solutions, six scenarios have been developed. Hydraulic model simulations were made for each option to generate and analyze information on water level, inundation depth, discharge, and flow velocity. The final option for implementation has been selected on the basis of draining the runoff within 1 day causing no drainage congestion.

Figure 5 shows the flood map of existing condition at Dhodrar River [8] and study-suggested solution where drainage congestion is removed with design

Fig. 4 Drainage improvement of Dhodrar River at 18.0 km
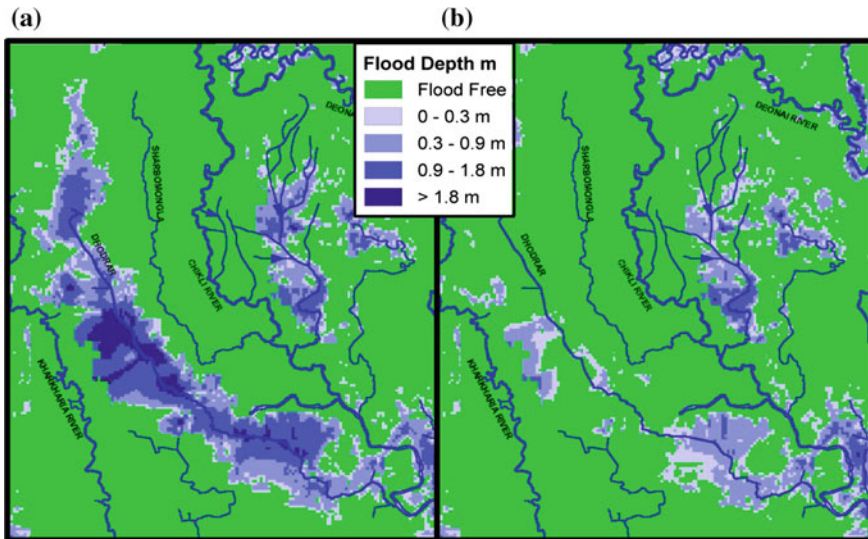
Fig. 5 **a** and **b** Flood map for the existing condition and suggested option

cross-section and additional one vent at 4.1 km, two additional vents at 10, 10.9, 12.68, 13.8, 18, 19.3, and 20.45 km, and three additional vents at 15.3 km.

Similarly, several improvement options were carried out for the existing drainage problem of each area. Merits and demerits of each option were analyzed, and findings were shown in a local workshop in Dalia. Views of beneficiaries project officials and concerned design cell were considered, and finally, hydraulic parameters for optimum option were suggested.

2   Post-Project Evaluation of Drainage

Most of the IWM's recommendations related to drainage problem have also been implemented by BWDB. Professionals from IWM and BWDB visited several sites to evaluate the effectiveness of the recommendations, which have been implemented. The visiting team also collects opinion of the local people. Summary of the findings of field visit is given in the table below.

Sites visited	Previous problem	IWM's recommendation	Status of implementation	Improvement obtained
Drainage siphon at 12.5 km of S8T canal (Kaimari)	Drainage congestion at u/s of Siphon	Addition of 2-vent box siphon	Implemented	No congestion observed in monsoon of 2004
Dhodrar River at 15.3 km and 18 km	Drainage congestion	Addition of 3 vents at 15.3 km and 2 vents at 18 km	Implemented	No congestion observed in monsoon of 2004
Mirkabeel Siphon at 0.41 km of S6R	Drainage congestion at u/s of Siphon	Addition of 1 vent box siphon	Implemented	No congestion observed in monsoon of 2004

3   Conclusions

Application of mathematical modeling in water resources project is very beneficial for the decision makers to observe the impact of any intervention or modification in the project infrastructure at different stages of the project, e.g., prefeasibility, feasibility, implementation as well as rehabilitation stages.

The application of modeling tool in TBP phase-I opens up a new dimension of models as a very useful tool in Command Area Development Project, which may be replicated in other CAD projects, e.g., G-K CAD, Barisal, Manu CAD, and

WMIP projects. The effectiveness of modeling tool has been proven to be convenient, cost effective, and quantitative with regard to the aspects on assessments.

Models can be used effectively for people's participatory-based irrigation and drainage management studies. It was observed that through adopting a series of options and demonstrating their effective outcome to the beneficiaries save lot of efforts in resolving conflicting issues and complex situations regarding water management problems.

Groundwater model study will provide Thana (Sub-district) wise available water resources, recharge mechanism, zoning plan, and indication of future expansion.

Surface water and groundwater are interlinked, sometimes withdraw from one source has an impact on the other. An integrated model study can give an overall picture on the water resources availability and management considering total demand from different sources.

References

1. NWMP (2001) Draft development strategy for national water management plan, 2001
2. Hossain AFMA (2015) Flood Management to Reduce Flood Hazards of Gumti River Using Mathematical Modelling. Isfram 2014 31–40
3. BADC (2002) Survey report on irrigation equipment and irrigated area in Boro/2001 season
4. Hossain AA, Afzal MHB (2013) Management of irrigation and drainage systems using mathematical modelling. J Appl Water Eng Res 1:129–136
5. IWM (2004) Development of decision support services using mathematical modelling technique and topographic survey, mapping & development of interactive information system, final report, CAD of Teesta Barrage Project Phase-I, 2004
6. IWM (2004) Groundwater management and zoning study for repair and rehabilitation of deep Tubewell project in greater Dinajpur District under post drought agricultural rehabilitation programme, Interim Report, 2004
7. Afzal MHB, Bhuiyan M (2015) Sustainable Trend Analysis of Annual Divisional Rainfall in Bangladesh. Isfram 2014 257–270
8. IWM (2004) Feasibility and model study for rehabilitation of flood control embankment on both banks of Gumti River, Final Report, 2004

Modeling Optimal Water Allocation by Managing the Demands in Selangor

Nurul Nadiah Mohd Firdaus Hum and Suhaimi Abdul-Talib

Abstract Water in Selangor is getting scarce, yet it is the key to its economic development. A fast-growing population and expanding industrialization in the state creates demands for new water sources and innovative management of water resources and services. The goal of this study was to calculate the impact on the supply—demand gap for the city and industry sectors in Selangor by the year 2050. To achieve this, two main simulations involving groundwater application using the Water Evaluation and Planning (WEAP) model, this, integrate an economic optimization model and a hydrology water management model. First simulation involves business as usual scenarios while the second incorporates the water saving measures into the simulation via the demand side management (DSM) analysis. Both simulations were carried out in the Selangor and Langat catchment as both catchments represent the main catchments for the state of Selangor. Such detailed simulation and inclusion of previously unaccounted for factors can help to create awareness of potential future problems, inform water practices, and suggest management alternatives. Results show that with the groundwater as an alternative resource and proper water saving measures, water deficit within Selangor can be significantly reduced.

Keywords Groundwater · Hydroeconomics · Selangor · Water allocation · WEAP

N.N.M.F. Hum (✉)
Faculty of Applied Sciences, Universiti Teknologi MARA (UiTM), Shah Alam, Selangor, Malaysia
e-mail: nadiah0978@gmail.com

S. Abdul-Talib
Faculty of Civil Engineering, Universiti Teknologi MARA (UiTM), Shah Alam, Selangor, Malaysia
e-mail: ecsuhaimi@salam.uitm.edu.my

1   Introduction

As a vital resource, water plays a role in every part of the livelihood and socioeconomic development of a country. Rapid population rise together with the improved standards of living, city, and industrial growth has led to the increase of pressure on water resources as well as the demands and conflicts among competing water use sectors [1, 2].

Water demand when it is less than its availability does not create any issues of conflicts as all of its users can access to its water supply. However, when the demand exceeds the available supply and its water allocation fails to meet the demand, water conflicts would be noticeable [1]. Thus, in order to avoid the present as well as the future water conflicts between the competing demands, researchers and scientists have given increased emphasis in developing tools and techniques to improve the management of the water resources [1]. The development and applications of various models, which provide a good insight into the intricacies of various problems related to proper water allocations besides balancing its mismatch between the supply and demand in an integrated water management, is therefore necessary [3].

Among the different existing methods for integrated water management (mental models, Bayesian networks, metamodels, risk-assessment approaches, knowledge elicitation tools, Artificial Neural Network, among others), hydroeconomic tools provide relevant insights about how to best optimize the use of water resources and constitute useful tools to help policy-makers identify the most efficient and sustainable water management strategy [3–6]. Reca et al. [7] and Bielsa and Duarte [8] developed a hydroeconomic model on economic optimization for agricultural water resources planning. Besides, the integration of these hydroeconomic models has been widely and successfully used to study water quality problems [9, 10], global water and food policy questions [11, 12], the impact of drought [13], land use changes [14], and water management and policy strategies [15, 16].

The present study analyzes the water allocation in Selangor by using two main simulations. First, simulation includes groundwater application through the case of business as usual which is later referred to as reference and the case of higher population growth. While the second simulation analyzes the demand side management (DSM) that incorporates the groundwater on the supply and demand in the state of Selangor. Both simulations used a novel hydroeconomic model based on the integration of an economic optimization model and a hydrology water management model built on the Water Evaluation and Planning (WEAP) model. Application of the model was carried out in the Selangor and Langat catchments, which are the main catchments for the state of Selangor which then are used to calculate the impact on the supply–demand gap by the year 2050.

2   Materials and Method

2.1   Study Area

Representing the state of Selangor is the Selangor and Langat River catchments as the case study catchment as both catchments constitute the largest water supply and demand in the state. The total area of the both catchments is 2514.13 km^2 and the climate is tropical with hot, dry season and wet, monsoon season. The catchment is divided into 34 sub-catchment areas (20 in Selangor catchment and 14 in Langat catchment), each of which is a source of surface runoff as well as an independent groundwater aquifer.

2.2   Data Collection and Analysis

Data sets for the years 1990–2010 were used in this study. Table 1 summarizes the type of input data required for the development of the economic and hydrology models, data sources used and methodology employed to process all information.

2.3   Model Development

The Water Evaluation and Planning Model (WEAP), developed by the Stockholm Environment Institute (SEI), is designed to evaluate water resources development and the management scenarios associated with the changes in the biophysical and socioeconomic conditions [17]. In this model, water supply is defined by the amount of precipitation that falls on a catchment or a number of catchments. This supply can be enhanced through the accumulation of the supply or the increase in the storage. On the other hand, it can also deplete progressively through natural processes and human withdrawals such as for city and industry usage. Furthermore, WEAP adopts a broad definition of water demand, where the catchment itself is the first point of depletion through evapotranspiration. The core of the model is a water balance equation that includes such components as catchment scale rainfall–runoff processes, groundwater recharge, evaporative demands, surface and groundwater withdrawals, and return flows. Water supplies and demands are linked to the stream network and water allocation components via the WEAP interface, which would then keep track of water allocations and accounts for the groundwater and streamflow depletion and addition [17, 18]. The model optimizes water use in a catchment using an iterative Linear Programming algorithm which seeks to maximize the water delivered to the demand sites according to the user-defined priorities. Demand sites are assigned to a priority ranges between 1 and 99, where 1 is the highest priority and 99 is the lowest priority. When water is limited, the model

Table 1 Input data required for the development of the economic and hydrologic models

Type of data	Source	Format/methodology	Used in hydrology/economic model
Land use data			
Digital elevation and land cover	Agensi Remote Sensing Malaysia (ARSM)	Digital maps processed in GIS	Hydrology model
Climate data			
Precipitation, temperature, humidity, wind speed, evaporation, soil moisture	National Hydraulic Research Institute Malaysia (NAHRIM)	Monthly time series processed in PRECIS model	Hydrology model
Water supply data			
Rivers, stream gauges, groundwater	Department of Drainage and Irrigation Malaysia (DID)	Data records in Excel	Hydrology model
Reservoirs	Suruhanjaya Perkhidmatan Air Negara (SPAN)	Excel files	Hydrology model
	Syarikat Bekalan Air Selangor (SYABAS)	Excel files	
Water demand data			
Land use data	Jabatan Pertanian Negeri Selangor	Text files	Hydrology model
City sector –Population –Water use rates –Water consumption Industry sector –Population –Water use rates –Water consumption	Malaysian consensus (Jabatan Statistik Malaysia) Suruhanjaya Perkhidmatan Air Negara (SPAN)	Excel files Excel files	Economic model Economic model Economic model Economic model Economic model Economic model

would progressively restrict the water allocation to the demand sites of the lowest priority [19]. A schematic representation of the Selangor and Langat catchments using WEAP application is depicted in Fig. 1 [3]. In this study, emphasis was given to the city and industries. Hence, city and industries are the main consumers of the treated water and given priority "1" while agricultural irrigation is given priority after the two main demands are met.

2.4   Hydrology Model

The area for the hydrology study includes 7 main rivers in the Selangor catchment (Sg. Batang Kali, Sg. Serendah, Sg. Kuang, Sg. Ranching, Sg. Buloh, Sg. Kerling, and Sg. Garing) while the Langat catchment contains 3 main rivers (Sg. Langat,

Sg. Semenyih, and Sg. Lui); 5 reservoirs with a total storage capacity of
468.08 Mm^3 and 10 key stream flow gauges. Four groundwater stations were used
in the study which consists of two points in each catchment. In addition, the study
area had been characterized into fractional sections that represent areas of similar
land use classes (city, industrial area, irrigated agricultural land, and forest). Natural
hydrology processes within each catchment unit and fractional area have been
simulated on a monthly time step using WEAP 2-bucket hydrology module (see
[17, 18] for details).

2.5 Economic Model

The economic model in this study represents the water demand nodes in Selangor.
The water demand is the total water required to meet the city and industry needs
which then are presented as city and industrial nodes in the WEAP model. The
current water demand for the city sector is 1735 MLD while for the industrial sector
is 1254 MLD. Estimated population for both catchments was 1.153 million (2015)
and the population is projected to increase with the growth rate of 2.2 per annum
[3]. Major districts that involved in the calculation of the model are Hulu Langat,
Putrajaya, Cyberjaya, Kuala Langat, Sepang, Seremban, Hulu Selangor, and Kuala
Selangor. Under this model simulation, two scenarios would be used for all of the
economic analysis. The first scenario is business as usual scenario that is used to
represent the reference analysis which would be later referred to in this study. Water
usage for the year span of 1991–2050 is used to project the water supply and
demand network in Selangor while current scenario is set at 1990 for the purpose of
calibration and validation while the projection growth rate is set at 2.2 %. Second
scenario is higher in population growth rate, which is done in order to foresee the
impact of possible population rate growth at densely populated areas. Higher
population growth rate is set at 7 % for the study.

2.6 Scenarios Simulation

In order to assess whether the groundwater does posed an impact on the growing water demand in Selangor, two main scenarios were simulated:

Scenario 1 *Groundwater application.* Effects of the groundwater application toward the water demand sectors (city and industry) in Selangor were analyzed through the reference and higher population growth scenarios.

Scenario 2 *Demand side management.* Water saving initiatives were taken into the calculation of the model (13.79 % from toilet water savings, 4.09 % from washing machines, 7.33 % from shower heads and faucets), usage of groundwater on the DSM, and the amount of water demand that can be reduced was translated in this scenarios.

3 Results and Discussion

3.1 Model Testing: Calibration and Validation

The hydroeconomic model was calibrated and validated for the period of 1990–2010 for both hydrology and economic data used in the study. The accuracy of the model was quantified using the Bias and the Nash-Sutcliffe model accuracy statistics [20, 21]. The values of bias ranged between −9 and +12 % with an average of 2 %, while the Nash-Sutcliffe Efficiency (NSE) varied from 0.86 to 0.97 with an average of 0.9098.

Besides, the economic and hydrology models were coupled together and validated for the base year 1990. The optimal water usage from both industry and city sectors obtained from the calibrated economic model was replicated into the hydrology model, which in turn estimates the net water requirements as in Fig. 2.

3.2 Scenario 1—Groundwater Application

Under this scenario which incorporates the groundwater data into the economic model, reference scenarios for both city and industry project no difference between the addition of groundwater and the model without the groundwater effect. Higher population growth on the other hand projects similar results before and after the implementation of groundwater for city node. However, industry water demands projections as in Fig. 3 indicate significant difference between before and after the implementation of the groundwater with the difference of 10.13 %.
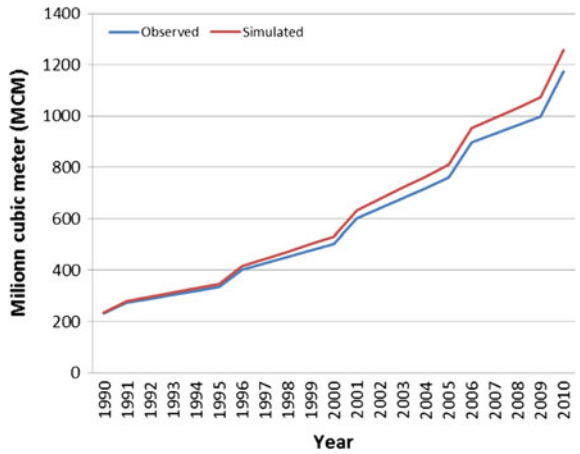
Fig. 2 Simulated WEAP and observed water requirement for Selangor
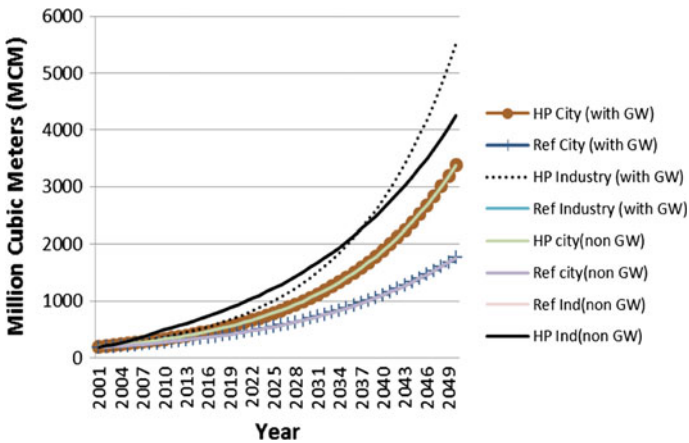
Fig. 3 Effects of groundwater on water demand in Selangor

Unmet demand analysis simulation was done in order to highlight the amount of deficits that arises from the implication of groundwater into the water allocation study. Hence in this analysis, two scenarios were presented in Figs. 4 and 5, namely unmet demand for the city sector and unmet demand for the industrial sector.

Figure 4 illustrates the amount of unmet demand through the reference and higher population growth for both with and without groundwater study. Results show that the reference scenario differs by 28.81 % while the higher population growth differs by 33.41 % in relation to the application without the implementation of the groundwater. All analysis under this scenario, however, managed to keep the deficits as "0" as an indicator that all demands are fully met until the year 2030.
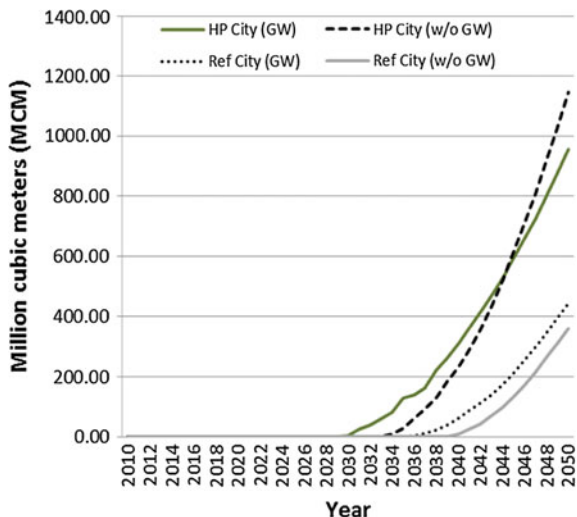
Fig. 4 Unmet demand for city sector in Selangor
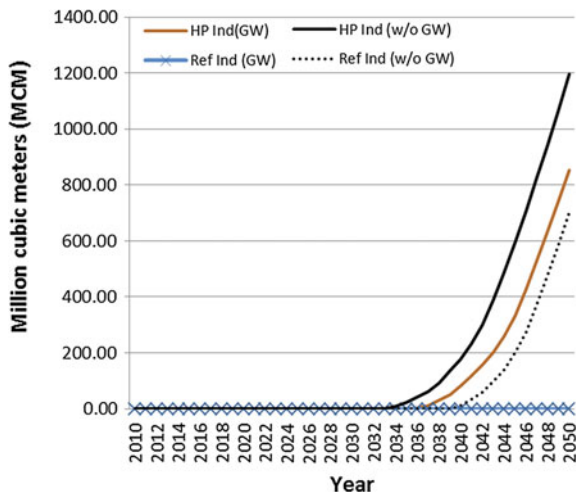
Fig. 5 Unmet demand for industry sector in Selangor

Higher population growth with groundwater implementation starts to have deficit of
9.38 MCM at 2030 while under the reference scenario, deficit of 7.36 MCM was
observed in 2036. Both scenarios that imply groundwater start to have deficits four
years earlier than without the implementation of groundwater.

Figure 5 illustrates the unmet demand for the industrial sector in Selangor. With
a difference of 69.34 % (reference) and 54.58 % (higher population growth)

between the scenario that implement groundwater and the one that does not implement, reference scenario that implement the usage of groundwater managed to keep the deficit "0" throughout the analysis. As for the higher population growth scenario that implements groundwater, deficit of 10.46 MCM was observed at the year of 2037 as compared to the same scenario that does not implement the groundwater measures of 9.96 MCM at the year 2034.

3.3 Scenario 2: Demand Site Management (DSM)

Through this scenario, implementation of water saving devices and usage of groundwater as part of the initiatives in reducing the water demand in Selangor has been analyzed. Figures 6 and 7 show the amount of water savings that can be achieved through the implementation of DSM and groundwater onto the city and industry sectors. Should the Selangor and Langat catchments applies the water saving devices by half of the population, the amount of water that can be saved is 13.79 % for the city sectors for both reference and higher population growth simulation as in agreement to Mohd Firdaus Hum and Abdul-Talib [3]. Industrial sector water savings totaled for 9.12 % (86.97 MCM) for reference simulation and 8.00 % (43.96 MCM) for the higher population growth simulation.

With the addition of groundwater into the city's simulation calculation, the amount of savings that can be achieved averaged at 63.65 MCM for reference and 88.44 MCM for higher population growth. Total savings via this simulation with
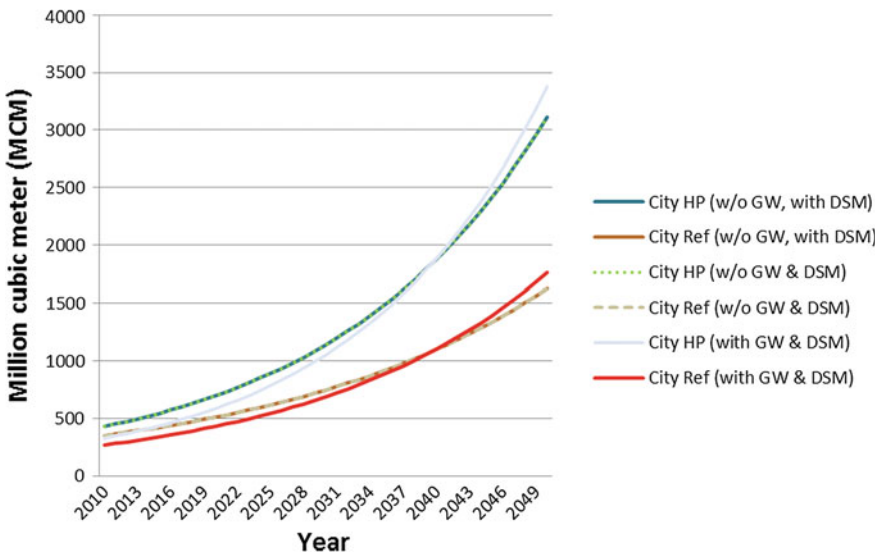
Fig. 6 DSM implementation on city scenario
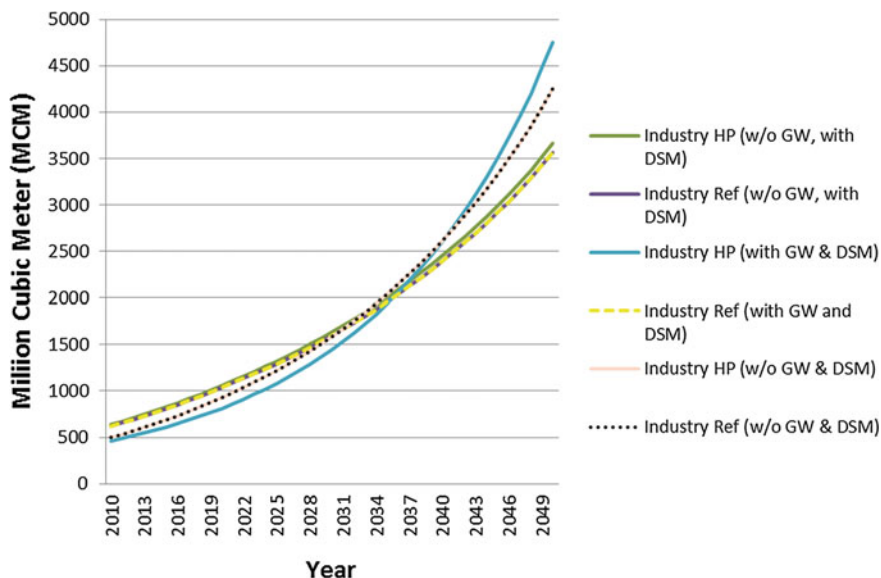
Fig. 7 DSM implementation on industry scenario

the addition of groundwater is 13.23 %. Industry on the other hand, although projects no difference in the addition of groundwater into the reference DSM simulation, under the higher population growth simulation significant change in the savings was recorded. Being the only simulation with a significant water savings of 20.4 % as observed in Fig. 7, industrial higher population growth simulation manages to reduce water demand by an average savings of 195.51 MCM until the year 2036.

4   Conclusion

This study used the WEAP model to evaluate the water supply and demand in the state of Selangor. Based on the reference projections, the water availability of Selangor is adequate until the year of 2036 while based on the higher population projections, the water availability is shorten to 2034 due to higher growth in the population. However, with the implementation of DSM and the addition of groundwater into the water economics, the savings that can be achieved for the city areas are 88.44 MCM under the reference and 63.65 MCM under the higher population simulations. However, the industrial sector records water savings of 160.32 MCM for the higher population growth simulations.

References

1. Babel MS, Das Gupta A, Nayak DK (2005) A model for optimal allocation of water to competing demands. Water Resour Manage 19:693–712
2. Gleick HP, Cooley H, Cohen M, Morikawa M, Morrison J, Palaniappan M (2009) The World's water 2008–2009: The Biennial report on freshwater resources. Island Pr, Washinton DC
3. Mohd Firdaus Hum NN, Abdul-Talib S (2015) Modelling water supply and demand for effective water management allocation in Selangor (in press)
4. Keshtkar AR, Salajegheh A, Sadodin A, Allan MG (2013) Application of Bayesian network for sustainability assessment in catchment modeling and management (case study: the Hablehrood river catchment). Ecol Model 268:48–54
5. Brouwer R, Hofkes M (2008) Integrated hydro-economic modelling: approaches, key issues and future research directions. Ecol Econ 66:16–22
6. Babel MS, Maporn N, Shide VR (2014) Incorporationg future climatic and socioeconomic variable in water demand forecasting: a case study in Bangkok. Water Resour Manage 28:2049–2062
7. Reca J, Roldan J, Alcaide M, Camacho E (2001) Optimization model for water allocation in deficit irrigation system: I. Description of the model. Water Manage 48(2):103–116
8. Bielsa J, Duarte R (2001) An economic model for water allocation in North Eastern Spain. Water Res Dev 17(3):397–410
9. Volk M, Hirschfeld J, Dehnhardt A, Schmidt G, Bohn C, Liershch S, Gassman PW (2008) Intergrated ecological-economic modelling of water pollution abatement management options in the Upper Ems River Basin. Ecol Econ 66:66–76
10. Harou JJ, Pulido-Velazquez M, Rosenberg DE, Medellin-Azuara J, Lund JR, Howitt RE (2009) Hydroeconomic models: concept, design, application and future prospects. J Hydrol 375:627–643
11. Rosegrant M, Cai X, Cline S (2002) World water food to 2025: dealing with scarcity. International Food Policy Research Institute (IFPRI), Washington DC, p 338
12. De Fraiture C (2007) Integrated water and food analysis at the global and basin level. An application of WATERSIM. Water Resour Manage 21:185–198
13. Maneta MP, Torres MO, Wallender WW, Vosti S, Howitt R, Rodrigues L, Bassoi LH, Panday S (2009) A spatially distributed hydroeconomic model to assess the effects of drought on land use, farm profits and agricultural employment. Water Resour Res 45:W11412
14. Ahrends H, Mast M, Rogers C, Kunstmann H (2008) Coupled hydrological-economic modelling for optimised irrigated cultivation in a semi-arid catchment of West Africa. Environ Model Softw 23:1327–1337
15. Jenkins MW, Lund J, Howitt R, Draper A, Msangi S, Tanaka S, Ritzema R, Marques G (2004) Optimization of California's water supply system: results and insights. Journal of Water Resources Planning and Management 130:271–280
16. Qureshi M, Qureshi S, Bajracharya K, Kirby M (2008) Integrated biophysical and economic modelling framework to assess impacts of alternative groundwater management options. Water Resour Manage 22:321–341
17. Yates D, Sieber J, Purkey D, Huber AL (2005) WEAP21: a demand, priority and preferences driven water planning model: part 1 model characteristics. Water Int 30:487–500

18. Yates D, Sieber J, Purkey D, Huber AL, Galbraith H (2005) WEAP21: a demand, priority and preferences driven water planning model: part 2, aiding freshwater ecosystem service evaluation. Water Int 30:501–512
19. Bharati L, Smakhtin VU, Anand BK (2009) Modelling water supply and demand scenarios: the Godavari—Krishna inter basin transfer, India. Water Policy 11(Supplement 1):140–153
20. Blanco-Gutiérrez I, Vartega-Ortega C, Flichman G (2011) Cost-effectiveness of groundwater conservation measures: a multi-level analysis with policy implications. Agric Water Manag 98:639–652
21. Nash JE, Sutcliffe JV (1970) River flow forecasting through conceptual models part I—A discussion of principles. J Hydrol 10:282–290

Sediment Load Distribution Analysis of Langat River Basin, Selangor

Mohd Fozi Ali, Siti Maisarah Ahmad, Khairi Khalid and Nor Faiza Abd Rahman

Abstract Rapid development in urban areas and uncontrolled deforestation are among the factors that contribute to the pollution of rivers through the process of erosion and sedimentation resulting from such activities. Stormwater runoff will flash out all the eroded soil and sediments to the downstream area, and sedimentation will occur in rivers and lead to other environmental problem. This research aims to evaluate the formation of suspended sediment and bedload sediment at the upper part of Langat River Basin, one of the most important river water catchments in Peninsular Malaysia. Sediment samples were collected using sediment grabber and analyzed in the laboratory. Three parameters were quantified throughout this study, namely concentration of suspended sediment (mg/L), river discharge values (m^3/s), and grain size distribution (g). The result showed that the estimated mean sediment load flow into Langat River is 5267.73 ton/km^2/year. Distributions of sediment grain size in upstream of Langat River consist of very rough sediment grains, showing a possibility of logging and deforestation activities within the catchment area. Hence, a long-term preventive measure such as environmental policies regulating land use development and management practices should be formulated and implemented to fix the sedimentation problems in Langat River Basin.

M.F. Ali (✉) · S.M. Ahmad · N.F.A. Rahman
Faculty of Civil Engineering, Universiti Teknologi MARA, Shah Alam, Malaysia
e-mail: mdfozi@salam.uitm.edu.my

S.M. Ahmad
e-mail: sara_maisara17@yahoo.com

N.F.A. Rahman
e-mail: doctor_cute84@yahoo.com

K. Khalid
Faculty of Civil Engineering, Universiti Teknologi MARA Pahang, Jengka, Pahang, Malaysia
e-mail: khairikh@pahang.uitm.edu.my

1   Introduction

Sediments are defined as the materials deposited at the bottom of water bodies [1]. It is in solid fragments of organic or inorganic material form produced from the weathering processes of rocks and minerals, aided by the natural occurring agents such as the wind, water, ice, or others. Deposited material has varies shape and size. In other words, the size of sediment can be small such as silt, medium such as sand, or large such as boulders. Mostly, an estuary found to have fine-grained, such as sand and silt, sediments. The quantity of sediment to be carried away depends on the speed of water flows in a stream. The slower moving flows will have a lower rate sediment movement and adversely for faster moving flows [2].

River discharge from different rainfall distributions is being the important part in determining the sediment loads. In particular, the higher discharge value would increase the water velocity, thus will result in higher sediment load. Furthermore, time is also a vital factor where the higher amount of sediment relies on the longer duration of sediment process. The river is being the one of the essential sources of water for living thing beside lakes, sea, underground water, and other water catchment. However, some processes reduce the river water quality concerning the sedimentary product. These involve erosion, mobility, and deposition. This situation is closely related to a unidirectional flow, where the river will experience water level fluctuations, rates of flow, and rates of erosion during monsoons and droughts. Human activities are the major issue in clearing the natural resources. Urbanization is increasing the impermeable surface that potentially blocks the water penetrates through. It even increases the scale of surface runoff. Furthermore, agricultural practices such as mulching and contour terrace reduce erosion even so decrease the runoff [3]. Nevertheless, the higher the velocity and volume of surface runoff, the higher rate of erosion will increase the amount of soil will be carried away down the slopes. As a result, suspended sediment content will increase as well as the water turbidity of the stream channel, thus lowering the water quality status [4].

Langat River Basin, a tropical river watershed in Malaysia, is chosen for the study in accessing the sediment load distribution analysis. Several studies have been conducted on the basin related to water resources and hydrological behavior of the basin. The basin became a first watershed in the country is initiated toward implementing of Integrated River Basin Management (IRBM) [5]. Many researchers were studied on the hydrological processes of the basin. It includes a historical water discharge study [6] and the impact of land used change on discharge and direct runoff [7, 8, 9]. This study was carried out to determine the suspended sediment yields, the factors that are affecting sediment transport, and finally to assess the particle size range of bedload sediment in Langat River Basin.

Fig. 1 Land used map of the study area
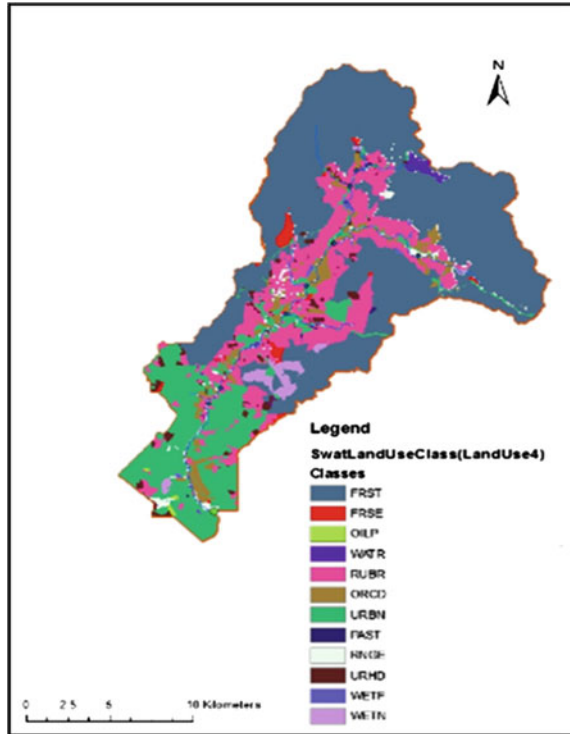
2 Study Area

The Langat River Basin is one of the most important river water catchments in Malaysia. Situated in Selangor state, the catchment is drained by three main tributaries: Langat River, Semenyih River, and Labu River [10]. The mainstream of the Langat River, which stretches for 141 km, has a total catchment area of 2271 km^2 and lies within latitudes of 2° 40′ 152″N–3°16′ 15″N and longitudes of 101° 19′ 20″E–102°1′10″E. Langat catchment presently consists of two reservoirs, the Langat Reservoir and the Semenyih Reservoir, respectively, and eight water treatment plants [11]. The upper part of Langat River as in Fig. 1 has a total catchment area approximately 331.9 km^2 [12]. The catchment area was found to have 12 broad classes of land cover [13] as shown in Fig. 1. The hilly part locates the study area was covered by steep land.

3 Methodology

A four sampling stations representing the length of the Langat River were selected: Station 1 (S1) at upstream Pangsun, Station 2 (S2) at Sg. Lui, Station 3 (S3) at mid-stream of Dusun Tua, and Station 4 (S4) at downstream Kajang as shown in

Fig. 2 Graphical location and sampling point of study
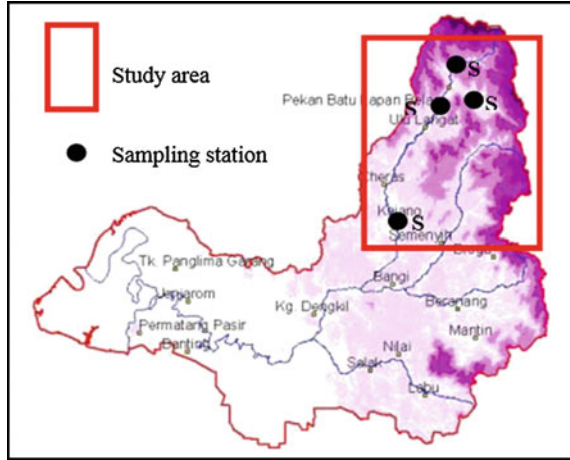
Fig. 2. Water samples were taken from each station and kept in polyethylene bottles for analysis to find the total suspended sediments (TSS) in the upper part of Langat River. Sediment samples were also collected using sediment grabber. The samples taken were analyzed in the laboratory. The cross-sectional length and water velocity were also measured at each station using several types of apparatus such as the measuring tape, poles, and stopwatch.

For the stream flow measurement, floating object (orange) was applied in this study to obtain the stream discharge value. Parameters, such as the flow velocity, width, and depth of the river, were determined in situ and used for purposes of measuring specific discharge values. Discharge value (Q) was calculated using several variables including stream cross-sectional area, stream length, and water velocity. Discharge was measured by solving the following equation:

$$Q = ALC/T \tag{1}$$

where

A Average cross-sectional area of the stream (stream width multiplied by average water depth)
L Length of the stream reach measured (usually 20 ft.)
C A coefficient or correction factor (0.8 for rocky-bottom streams or 0.9 for muddy-bottom streams)
T Time, in seconds, for the float to travel the length of L
Q Discharge value (m^3/s)

The photometric method applied by spectrophotometer was used to determine the TSS value directly. This study required a 10 ml water sample for each study area plot. The measurement of suspended solids needs a blank sample of 10 ml of deionized water as an indicator. After both samples were completely prepared, the

machine is ready to be set up for the testing. The blank sample should be assigned to zero by means of 0 mg/L. The real sample is then inserted, after the blank sample is removed. The TSS value is shown in the screen directly in mg/L.

The calculation of suspended sediment load value (SL) is based on the discharge value, TSS value, and area of sampling catchment. The data to be analyzed would be used to detect changes in the concentration of suspended matter and its relationship to hydrological parameters and other variables.

$$SL = (Q \times TSS)/\text{area of sampling point}$$
$$= (L/\text{day} \times kg/L)/km^2$$
$$= kg/km^2/\text{day} \times 365 \text{ days}$$
$$= kg/km^2/\text{year}$$

The sieving method was done by spreading the sediments into the aluminum trays and marked them with each station representative. Grain samples then were put into an oven and leaving them to dry at 105 °C for 24 h. The grain samples collected from all stations mostly showed the coarser grain; that is, the greatest particle size is 4.75 mm. Therefore, for easy handling, the soil sample was approximately weighed into 500-g samples using an electronic weighing machine and sieved 15 min with a mechanical shaker. The sizes of sieve tray utilized in this study were 4.75, 3.35, 2, 1.18, 0.6, 0.425, 0.212, 0.15, 0.063 mm. Once all grain samples had been separated according to size, they were weighed on an electronic weighing balance to the nearest two-point decimal. The weight of each sample size represented a percentage size of the soil.

The Udden-Wentworth scale as rewritten in Table 1 and sorting classification in Table 2 are referred in this study. The graphical representations do simplify the analysis made. The x-axis scale is the phi value while the y-axis is the cumulative percentage scale value (0–100 %) using a linear scale is shown in Fig. 3. The cumulative curve was used to determine the phi size of each phi value (phi at 5 %, phi at 16 %, and so on, where % refers to cumulative percentage) is recorded in Table 3. The various statistical values above are used to calculate the following equations of statistical parameters:

Table 1 Distribution size of mean value

Distribution size of mean value	
Phi value (ϕ)	Udden-Wentworth size class
−2 to −1	Gravel
−1 to 0.0	Very coarse sand
0.0 to 1	Coarse sand
1 to 2	Medium sand
2 to 3	Fine sand
3 to 4	Very fine sand

Table 2 Sediment sorting range

Sediment sorting range	
Sorting range (φ)	Description of sorting
<0.35	Very well sorted
0.35–0.50	Well sorted
0.50–0.71	Moderately well sorted
0.71–1.00	Moderately sorted
1.00–2.00	Poorly sorted
2.00–4.00	Very poorly sorted
>4.00	Extremely poorly sorted
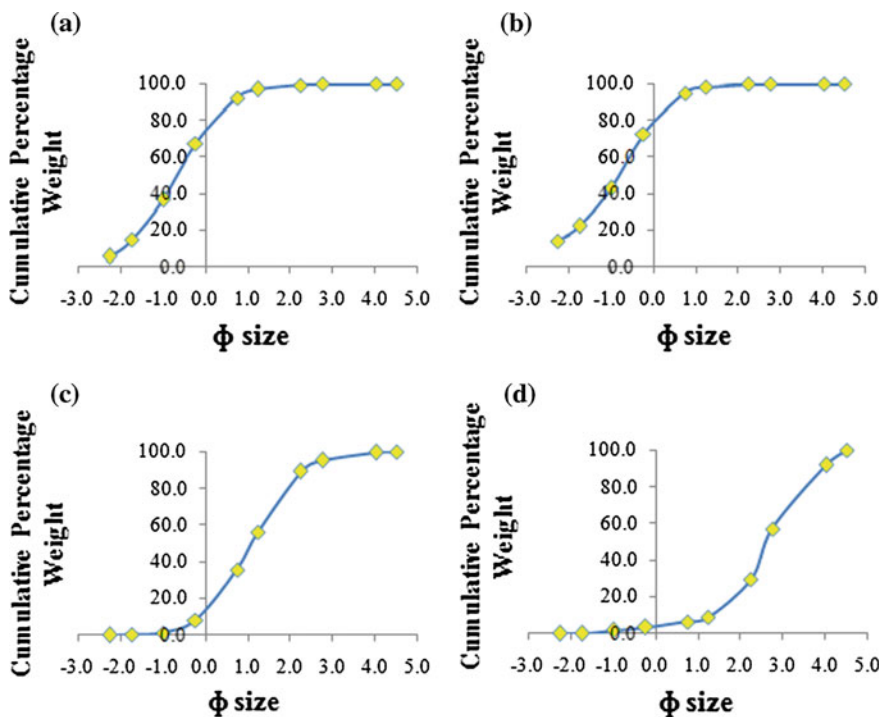
Fig. 3 Soil grain size graph obtained through the calculations in sieving analysis. **a** Station 1. **b** Station 2. **c** Station 3. **d** Station 4

$$\text{Median} = \phi\,50 \tag{2}$$

$$\text{Mean (M)} = (\phi\,16 + \phi\,50 + \phi\,84)/3 \tag{3}$$

$$\text{Standard deviation } (\sigma) = [(\phi\,84 - \phi\,16)/4] + [(\phi\,95 - \phi\,5)/6.6] \tag{4}$$

Table 3 Phi value derived from sieving analysis

Phi value derived from calculations in sieving analysis							
Station 1		Station 2		Station 3		Station 4	
Perc. (%)	Phi	Perc. (%)	Phi	Perc. (%)	Phi	Perc. (%)	Phi
5	−2.3	5	−3	5	−0.4	5	0.4
16	−1.7	16	−2.1	16	0.1	16	1.7
50	−0.7	50	−0.8	50	1.1	50	2.6
84	0.4	84	0.2	84	2.1	84	3.7
95	0.9	95	0.8	95	2.8	95	4.2

4 Results and Discussion

The observed discharge value was measured to be higher at the Kajang station compared to the other three stations on the upper of the watershed. The station is the largest area of sampling point where the difference in depth and width of the river significantly influences the flow value of the river. The average value of discharge was measured to be at 15.4, 6.8, 2.78, and 2.65 m³/s for a Kajang station, Dusun Tua, Sg. Lui, and Pangsun station, respectively.

The results of TSS are shown in Table 4. Station 4 was found to have the highest average of TSS value at 326.91 mg/L. In contrast, the lowest value was recorded at the Station 2 with the mean TSS value of 9.53 mg/L. This sampling station was identified as the station located at the lower part of the area of the study placed within the greatest catchment area. The finding views a maximum amount of 780.33 mg/L suspended sediment on November 5, 2014, compared to September 9, 2014 (192.87 mg/L) at Station 4. This could have been due to the consequence of stream flow that was suddenly increased on November 5, 2014. Sedimentation is a complex problem in humid tropical areas such as Malaysia as the soil erosion often occurs when the presence of very high precipitation will increase a river discharge straight away deteriorating the river water quality.

The correlation between streamflow and suspended sediment values in Langat River has been analyzed in order to determine their relationship. A significant association of $R^2 = 0.998$ between observed discharge values and TSS values was

Table 4 Total suspended sediment (TSS) at Langat River Basin

Sta.	TSS (mg/L)						
	24/9	30/9	15/10	29/10	5/11	12/11	Mean
S1	8.96	10.27	10.97	12.67	12.91	13.33	11.5
S2	6.00	8.73	9.00	10.33	10.85	12.25	9.5
S3	104.33	117.3	122.20	156.04	168.3	172.40	140.1
S4	192.87	214.6	404.00	177.33	780.3	192.35	326.9
Total	312.16	350.8	546.17	356.37	972.3	510.33	–
Max.	192.87	214.6	404.00	177.33	780.3	192.35	326.9

gained for the Langat River. Linear graph exhibits that an increase in stream flow value would cause an increase in TSS value, leading to a higher value of water turbidity. Therefore, flow capacity value is the factor that could affect the mobility or TSS values. As a result, the higher velocity of water induced by river discharge will increase the rate of soil detachment and produce more suspended sediment yield in a river.

Sediment load is defined as the total mobility of sediment scoured onto the riverbed. The annual increase in suspended sediment load would leave a significant impact on the drainage system. Alluvial deposition, if not persistently controlled, will be an increasingly serious problem from now on. Consequently, a water quality of a river will decrease. Furthermore, a reduction of river's depth will lead to surface overflow or flooding within the surrounding area. Hence, it will adversely impact all living things, including demolishing the local inhabitants. Throughout this study, daily and yearly sediment yields were calculated at certain sampling stations due to the limitation of data as shown in Table 5. The catchment area of stations 2 and 4 has been identified as their watershed area of 68.1 and 331.9 km^2, respectively. The highest sediment load (9,322,032.31 kg/km^2/year) was observed at Kajang mainstream and the lowest (235,569.91 kg/km^2/year) at Lui River. High sediment load at Kajang stream was due to higher precipitation and probably related to the higher flow and concentration of sediment. The increase in water level during the monsoon season is owing to the softening of soil slopes, aided by the nearest human activities, causing them to be eroded easily, thus decreasing the depth of a river [2]. Therefore, it is reasonable that Station 4 shows the highest suspended sediment load values (owing to the higher TSS value at 326.91 mg/L). Other factors including the dumping of garbage and other domestic activities by residents also contribute to the increase of the sediment deposition in the catchment area.

The analysis of sediment grain size in this study is shown in Table 6. The measurement of phi (ϕ) introduced by Wentworth was used in the study. The median value is the mid-value in a set of data arranged in ascending order.

Table 5 Suspended sediment load

Sampling station	TSS (mg/L)	TSS (kg/L)	Total sediment per day (kg/km^2/day)	Total sediment per year (ton/km^2/year)
Station 2	9.53	0.00000953	654.36	259.67
Station 4	326.91	0.00032691	25,894.53	10,275.78

Table 6 Sediment grain size distribution

Station	Median	Mean	Standard deviation
S1	−0.7	−0.667 (very coarse sand)	1.010 (poorly sorted)
S2	−0.8	−0.900 (very coarse sand)	1.151 (poorly sorted)
S3	1.1	1.100 (medium sand)	0.985 (moderately sorted)
S4	2.6	2.667 (fine sand)	1.076 (poorly sorted)

The mean size of an individual grain size is the baseline for comparing the weight force and flow force needed before water movement would occur. Typically, rough grains demonstrate a strong energy flow, whereas fine grains demonstrate weak energy flow. As specified in Table 6, the median value of Station 4 situated at Langat downstream is the highest of the four stations at phi 2.6. The mean size analysis at the upstream mainly exhibited very coarse sand sizes between phi −1.00 and phi 0.00. The average values of the downstream and midstream stations of Langat River show fine sand at phi 2.667 and medium sand at phi 1.100. The values, therefore, indicated that energy flow at the two upstream stations was high. Otherwise, the downstream station experiences low energy flow. Thus, the overall energy flow of the Langat River at the time of the study (29/10/14) was varied depends on the elevation of the stations.

The standard deviation indicates the sorting classification of the grain size distribution. For instance, high amount of rough grain size would be having a huge value of standard deviation represents as poorly sorted. As exhibited in Table 6, it is discovered that three stations which are stations 1, 2, and 4 were having poorly sorted of sediment. Only the middle sampling station has moderately sorted. In short, this kind of condition justifies that the Langat River has poorly sorted of sediment that is possible from the influence of the surrounding activities. In brief, the study shows the sediment grain size in the Langat River is varied from very coarse-to-fine sand and having poor levels of uniformity.

5 Conclusion

The study shows that the suspended sediment concentrations of the four stations along Langat River are increasing to the downstream. According to the data tabulation, the average value of TSS obtained in the upper part of Langat River is relatively moderate (122.01 mg/L) compared to the other water column in Malaysia. Langat River also demonstrates that one of the stations exhibits the highest sediment production that is 10,275.78 ton per year within 331.9 km^2 of the area. Therefore, necessary steps toward its rehabilitation and prevention must be initiated and implemented immediately as suspended sediment load would affect water quality and aquatic life. The factor of sediment mobility at the Langat River was controlling with the observed streamflow value. Significantly, the increased rate of stream flow could influence the production of suspended sediment. Nevertheless, the reason for sedimentation increase through the Langat River was not due to flow alone. The adjacent activities such as urban development, agriculture, and logging do contribute to the increasing level of riverbed sediments. Based on the observations during the sampling days, Langat River experienced recurrent flooding and overflows from the Station 4 during the monsoon period.

A study on the distribution of sediment grain size was found that the upstream of Langat River consists of very rough sediment grains, showing a possibility of logging and deforestation activities within the catchment. The fine grains found an

increase in the downstream locations demonstrate the presence of urban development including construction projects which owing to the major problem of flash flood occurrence. Therefore, a long-term preventive measure such as environmental policies regulating land use development and management practices should be formulated and implemented immediately to fix the sedimentation problems in Langat River.

References

1. Oxford Dictionary, Retrieved 20 March 2014, from http://www.oxforddictionaries.com
2. Toriman ME, Kamarudin MKA, Idris M, Jamil NR, Gazim MB, Abd Aziz NA (2009) Sediment concentration and load analyses at Chini river, Pekan, Pahang Malaysia. Res J Earth Sci 1(2):43–50
3. Goh E, Hui TK (2006) Soil erosion engineering: Pulau Pinang. Universiti Sains Malaysia, Malaysia
4. Toriman ME, Jauhir H, Mokhtar M, Gazim MB, Abdullah SMS, Jaafar O (2009) Predicting for discharge characteristics in Langat river, Malaysia using neural network application model. Res J Earth Sci 1(1):15–21
5. Mokhtar MB, Elfithi R, Shah AHH (2004) Collaborative decision making as a best practice in integrated water resources management: a case study on Langat Basin, Malaysia. In: Proceeding of the 1st Southeast Asia Water Forum, Chiang Mai, Thailand, pp 333–354
6. Hai HY, Jaafar O, El-Shafie A, Sharifah Mastura SA (2011) Analysis of hydrological processes of Langat river sub-basins at Lui and Dengkil. Int J Phys Sci 6(32):7390–7409
7. Hafizan J, Sharifuddin MZ, Ahmad ZA, Mohd KY, Mohd AS, Mazlin M (2010) Hydrological trend analysis due to land use changes at Langat river basin. Environ Asia 3:20–31 (special issue)
8. Amini A, Thamer MA, Abdul Halim G, Bujang KH (2009) Adjustment of peak streamflows of a tropical river for urbanization. Am J Environ Sci 5(3):285–294
9. Khalid K, Ali MF, Abd Rahman NF, Abd Rasid MZ (2014) The importance and role of infiltration approaches in hydrological modeling: A case study in Malaysia river basin, ICOST 2014, pp 76–80, March 7–8, 2014, Penang, Malaysia
10. Khalid K, Ali MF, Rahman NFA, Mispan MR, Rasid MZA, Haron SH, Mohd MSF (2015) Optimization of spatial input parameter in distributed hydrological model. In: International conference on marine science and environmental engineering (MAROCENET 2015), June 2015, Sea Sun Sand Resort and Spa Phuket, Phuket, Thailand
11. Ali MF, Saadon A, Abd Rahman NF, Khalid K. (2014) An assessment of water demanding Malaysia using water evaluation and planning (WEAP) system. In: CIEC 2013, proceedings of the international civil and infrastructure engineering conference 2013, Part VIII, pp 743–755
12. Khalid K, Ali MF, Abd Rahman NF (2015) The development and application of Malaysian soil taxonomy in SWAT watershed model. In: ISFRAM 2014, proceedings of the international symposium on flood research and management. ISBN 978-981-287-365-1
13. Ali MF, Abd Rahman NF, Khalid K (2014) A discharge assessment by using integrated hydrologic model for environmental technology development. J Adv Mater Res 911:378–382

Comparison of a Hybrid Neural Network and Semi-distributed Simulator for Stream Flow Prediction

Milad Jajarmizadeh, Lariyah Mohd Sidek, Sobri Harun, Shamsuddin Shahid and Hidayah Basri

Abstract Hydrological models are widely used for the simulation of stream flow in order to aid water resources planning and management in catchment or river basin. Numerous hydrological models have been developed based on different theories. Performance of such models depends on hydro-climatic setting of a catchment. In the present study, performance of a widely used physically based distributed model known as Soil and Water Assessment (SWAT) and a data-driven model, namely hybrid artificial neural network (HANN), has been evaluated to simulate stream flow in an arid catchment located in the south of Iran. Data related to topography, hydrometeorology, land cover, and soil were collected and processed for this purpose. The models were calibrated and validated with same time period to evaluate the advantage and disadvantages of different models. The results showed SWAT outperformed HANN in terms of relative errors such as Nash-Sutcliffe efficiency and percent of bias during model validation. Other error indicates, namely root mean square error (RMSE), mean square error, and mean relative error (MRE), were found close to zero for SWAT during both model calibration and validation. The study suggests that both models have their own promising flow prediction due to their own features and capabilities for daily flow.

Keywords SWAT · Hybrid neural network · Hydrologic modeling · Streamflow

1 Introduction

Estimation of mean and seasonal or daily fluctuation of stream flow is essential for water managers, planning authorities, and disaster mitigation authorities. Long-term simulation of stream flow in catchment or river basin is also required for water

M. Jajarmizadeh (✉) · L.M. Sidek · H. Basri
College of Engineering, Universiti Tenaga Nasional Malaysia, Putrajaya, Malaysia
e-mail: milad_jajarmi@yahoo.com

S. Harun · S. Shahid
Faculty of Civil Engineering, Universiti Teknologi Malaysia, Skudai, Malaysia

resource management, sustainable development, evaluation of hydrologic cycle, and related details such as the storage capacity, power generation, release pattern for irrigation, and municipal demands [1]. These pieces of information are particularly important for arid region, where less reliability of stream flow due to little and erratic rainfall is a major concern. Water scarcity is a common problem in such region. At the same time, erratic rainfall often causes prolonged drought or severe flood in such region. It is anticipated that global-induced climate change will make the water resource management in arid or semiarid region more challenging in near future.

Iran is facing increasing challenge due to aridity in recent years. Declination of groundwater and reduction of freshwater resources is a growing concern in the country. The literature review shows that Iran is a water-deficit country since 1999. The World Water Council [2] ranked Iran as one of the highest water stress country in Asia. The increasing water scarcity compelled Iranian government to accept international help [3]. The recent policy of Iranian government is to use new technologies for the evaluation of water resources in order to aid better planning and management of this precious resource.

As a background, in previous decades, the application of digital calculators has over whelmed sophisticated circulation for rainfall-runoff visualization in hydro-logical sciences. In the field of hydrology, privileges of using digital calculators can be proceeded to vast numbers of consequent calculation and to be able to respond to an answer whether it is 'positive' or 'negative' and to be specifically designed interrogations [4]. Hence, the development or application of hydrological tools is a challenging topic owing to monitor of hydrological phenomena [5]. To date, the applicability of various kinds of hydrological tools is a concern owing to have a review on the advantages and disadvantages on such subjects such as streamflow-modeling and attributed topics such as prediction of peakflows and the capability of the runoff volume prediction. Therefore, the availability of different hydrological tools is required to this application for regional and global scales owing to explore the compatibility and applicability in regard to specific objectives in water projects.

Hydrological models are generally used for evaluation of available water resources in a catchment or river basin. Various lumped, semi-distributed and distributed models have been proposed for catchment stream flow simulation and water budgeting. Models have been developed based on knowledge or data. In knowledge-based model, conceptuality on physical relation between stream flow and various hydro-meteorological variables and catchment physical properties are established. On the other hand, in data-driven model, statistical relation between stream flow and various hydro-meteorological variables is established. Models based on both concepts have been found suitable in simulation of stream flow in different parts of the world. However, both the modeling approaches have their own advantages and disadvantages. Suitability of a modeling approach depends on various factors including hydro-meteorology of the region, catchment type, and various catchment properties. Therefore, it is always suggested to use more than one model to assess the performance in order to select the most suitable model for simulation of stream flow. Therefore, selection of most suitable model by

comparing various models is considered as one of the most challenging tasks for hydrologist [6–11].

Recently, two groups of hydrological models are increasingly used for stream flow simulation, namely data-driven and knowledge-driven models. In this research, a knowledge-driven model known as soil and water assessment tool (SWAT) and a data-driven model known as hybrid artificial neural network (HANN) were used to assess their performance in simulating stream flow in Roodan River Basin located in arid region of Southern Iran. Both the models were used to simulate daily stream flow in order to evaluate their performance in simulating various properties of stream flow. It should be noted that there are not too many research for comparison of flow accuracy between SWAT and data-driven techniques [12]. Demirel et al. [12] compared the performance of SWAT and data-driven technique in simulating stream flow of a small basin located in temperate climate. They reported that data-driven model was more successful than SWAT in term of forecasting the peak flows. Srivastava et al. [13] explored the capability of a data-driven tool and SWAT in an agriculture watershed. They reported that monthly runoff prediction capability of data-driven model outperformed SWAT. They proposed less capability of SWAT is due to its weakness in using snowmelt procedure during winter. Morid et al. [14] compared the performance of SWAT and a data-driven model for simulating daily runoff in a snow-bound ungauged catchment in Iran. They reported that the performance of both models was more or less same, but the data-driven technique outperformed the SWAT in simulating low stream flows; meanwhile, SWAT simulated the high flows better. The often contradictory results as mentioned above emphasize the need of comparison of different hydrological models.

Stream flow modeling of Roodan River Basin is highly crucial due to increasing water stress in the context of increasing population, urbanization, and unmanaged changing ecosystem [15, 16]. Few studies have been carried out on hydrological modeling in south Iran. This study is the consequent of the previous research in Roodan River Basin [17, 18]. It can be expected that present study will help to identify suitable hydrological model which can be used for the estimation of freshwater flow in arid catchments of south Iran which in turn will help in water resources management and mitigating the impacts of water scarcity.

2 Materials and Methods

2.1 Case Study

Roodan River Basin is located in the Kerman and Hormozgan states of southeastern Iran. The area of the river basin is 10,570 km^2. The basin lies between northern geographical latitude of 26°57′–28°31′ and the eastern longitude of 56°47′–57°54′ (Fig. 1). The annual average rainfall is in the area is approximately 215 mm.
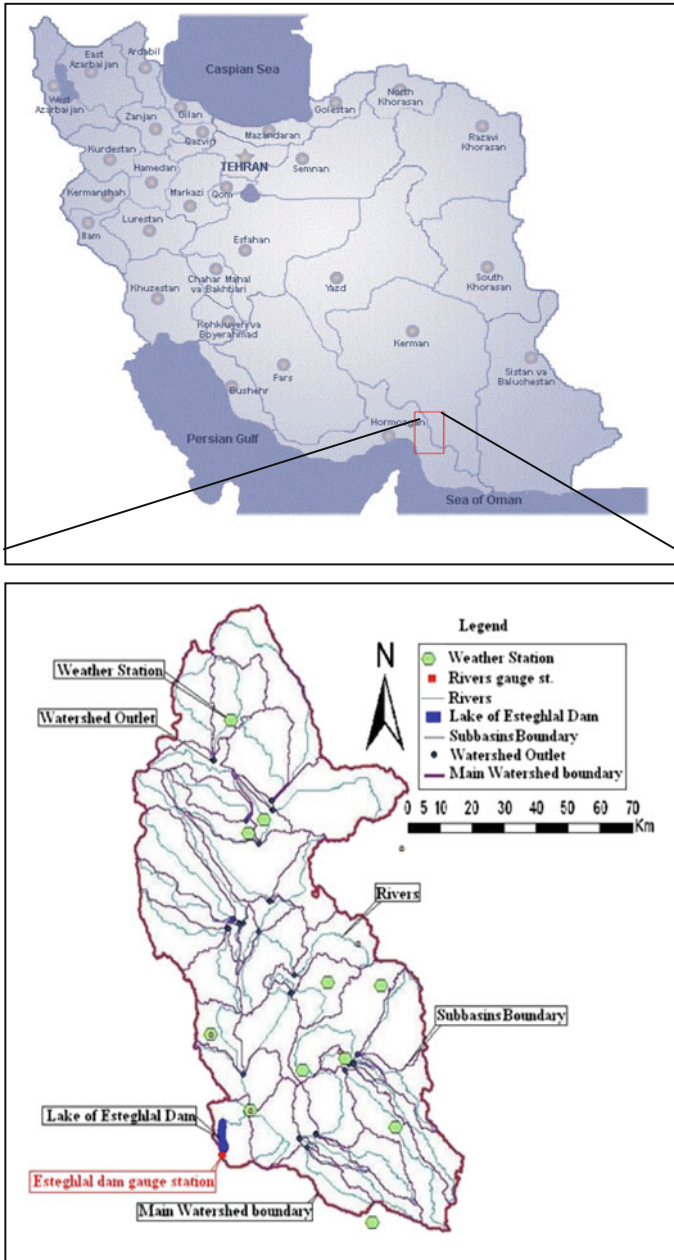
Fig. 1 Site location of Roodan River Basin in Iran

The climate of Roodan is a trade-off from semiarid to arid with high-intensity short-duration precipitation, which provides considerable freshwaters for saving in seasonal and perennial rivers. Major land uses are range brush, mixture of grassland with range brush. Three dams were built in the downstream of basin for water preservation, among which Esteghlal Dam (Minab Dam) is the biggest. Esteghlal Dam located after main outlet of Roodan watershed and delivers major part of freshwater for the city of Bandar Abbas.

2.2   Soil and Water Assessment Simulator

SWAT is a watershed scale hydrologic simulator for visualization of the land management for different scales of basin. It is a public domain hydrological simulator developed by the Agricultural Research Service at the Grassland and Soil and Water Research Laboratory in Temple, Texas, USA [19]. It is widely used for hydrological simulation and environmental impact assessment. SWAT visualizes the hydrologic cycle, freshwaters, return flow, infiltration, evapotranspiration, transmission losses, pond and tank storage, plant/crop growth and irrigation planning, groundwater routing and river routing, nutrient and pesticide loading, and water allocation using with component of meteorological data. This model is applied worldwide and is continuously under development and application owing to reduce of weakness and increasing the applicability in different regions across the globe [19]. Thus, SWAT can be a simulator for monitoring water resources and different management policies in water resource management. SWAT requires hydro-meteorological and catchment physical data such as elevation, land use, and soil. In addition, for better recognition of river streams, digital river map can be used as supplementary data.

In the present study, required data of Roodan river basin were collected and processed for stream flow simulation in the basin. Soil map was prepared from the map of soil distribution, geological map, and available soil samples. The landuse map of Roodan was prepared from Landsat 7 satellite image of the year 2007–2008 and agricultural statistics available from the agriculture organization of Hormozgan, Iran [18, 20].

All available information was used to prepare the Geo-Database for SWAT to visualize the watershed and related features. Meteorological data, namely precipitation and temperature, were used as input to the model. Discharge was modeled based on curve number method of soil moisture condition II for Roodan River Basin [21]. Details of the development of SWAT for Roodan River Basin can be found in [18, 20–23].

2.3   Semi-automatic Calibration Method for SWAT

SWAT conventionally calibrated manually. However, recently a separated program has been developed to calibrate and validate the model, which is known as Sequential Uncertainty Fitting program (SUFI-2). Usually, semi-distributed models such as SWAT need to calibrate many parameters which is very difficult to do manually. Semi-automatic calibration method SUFI-2 provides a faster procedure for SWAT calibration [19]. Moreover, SUFI-2 as semi-automatic calibration method is beneficial for monitoring the calibration procedure and exploring the optimal parameters for validation. Furthermore, SUFI-2 calibration is based on the calculation of potential sources on uncertainties inherent to parameters and variables, conceptual model, and measured data. Propagation of uncertainties in SUFI-2 can be presented at 95 % probability distribution [24]. The criteria of 95 % probability distribution referred to as the 95 % prediction uncertainty (95PPU). Details of the theory and development of SUFI-2 can be found in Abbaspour [25].

In the present study, twenty-six parameters [18], which have direct and indirect influence on flow simulation, are used for calibration of model. SUFI-2 performs number of iterations to find the optimum calibration and optimum parameter ranges for flow simulation. In each iteration, the range of parameters gradually becomes narrower within the parameter space. Usually, a shorter parameter space produces better outcome as the objective function is close to better value. Details of calibration of Roodan River Basin can be found in [18, 20–23].

2.4   Development of Hybrid Network

One of the generations in data-driven techniques is hybrid network, which includes different configuration of the combination of two or more kinds of neural networks or any set of module in input, hidden, or output layers. Hybrid networks are followed to learn of relationships through the data (input–output) and then it generalizes of features to rest of data. Usually, development of data-driven approach includes distinguished stages such as data collection, selection of predictors, and configuration of selected network [26]. To date, various data-driven networks, both simple and hybrid types, have been used in hydrology, meteorology, and water resource management [27, 28].

The HANN used in the present study is the combination of Multilayer perceptron [17]. This configuration provides more flexibility to build hidden layer in creating some structures such as distinguished transfer functions correspond with given neuron [29]. One of the privileges for HANN is speeding up of computation, especially, when there are many input data used for model development.

In the present study, precipitation and discharge data were used as input and output of HANN model. The structure of the network was chosen on tried and error basis. In the present study, hybrid network with three layers, namely the input,
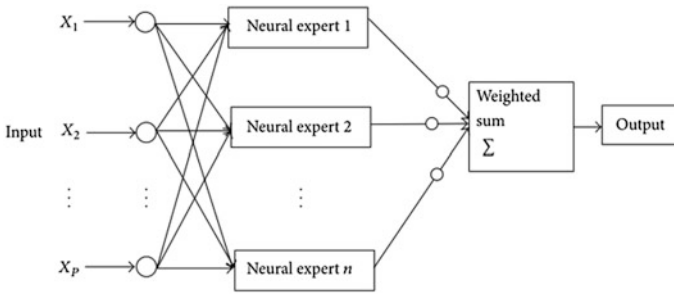
Fig. 2 Presentation of hybrid network for Roodan watershed [17]

hidden, and output layers, were used. The hidden layer is configured into two separated parts, known as neural expert. In other words, the HANN was consisted of a hidden layer configured with nonlinearity and the number of cells in input and output layers (Fig. 2). Usually, the development of network needs transfer functions and training algorithms for hidden and output layers to learn pattern in data. Sigmoild, Linear Sigmoid, and Linear transfer functions were used in the present study with two training algorithms, namely Back propagation and Levenberg–Marquardt [17]. Development of hybrid neural network for Roodan River Basin can be found in [17] in details.

2.5   Criteria for Model's Performance

The performance of SWAT and HANN was evaluated using statistical criteria, namely relative error and absolute error. The relative error offers a relative comparison between the measured and the simulated data such as discharge [13]. In the present study, two methods were used to measure relative error, namely coefficient of efficiency (NS) and percentage of bias (PBIAS) [30]. The value of NS equals to 1 means a complete agreement between the measured and the estimated values. The value of NS equals to 0 presents that all the predicted values are equal to the average value of the observed values. The negative NS value means that the average of the measured data is better than the predicted values. On the other hand, PBIAS is a coefficient to estimate model's capability. A full description of NS and PBIAS is given in [30].

Beside relative errors, absolute errors were used to measure the performance of hydrologic models [31]. In the present study, four methods were used to assess relative error, namely root mean square error (RMSE), the mean-squared error (MSE), the mean relative error (MRE), and mean absolute error (MAE). The RMSE is a dimension value that shows the agreement between the measured and predicted data. RMSE close to zero shows a better performance of model. The MSE value is related to high values (peakflows). MSE should be close to zero for optimal

performance of model. The MRE value is based on the goodness of fit for moderate values. Optimum MRE close to zero shows a better performance modeling. MAE is not weighted toward high-value events (flood, peak flows). Therefore, it calculates all errors from original data without considering the sign [26]. MAE illustrates optimum performance when it is around the zero. Details of the above-mentioned evaluation criteria are discussed in [30, 31].

3   Result and Discussion

3.1   Comparison of SWAT and Hybrid Network

Table 1 summarizes the relative and absolute errors in SWAT and HANN in simulation of stream flow in Roodan River Basin. The table shows that in term of NS, HANN performed better compared to SWAT during model calibration. However, NS during validation was found better for SWAT compared to HANN. SWAT showed a smaller PBIAS in comparison with HANN during both calibration and validation. In terms of RMSE, HANN outperformed SWAT during model calibration (39.4); however, during validation, SWAT performance was better (29.4).

MSE is a better way for evaluating peak flows. Result shows that MSE for HANN was lower during calibration (SWAT = 2631, HANN = 1551). However, during validation, SWAT outperformed HANN in terms of MSE (SWAT = 864, hybrid network = 1036.5). MRE was used to evaluate the performance of models in simulating low-to-moderate flows. Result shows that performance of HANN was better in terms of MRE during model calibration, which was closer to zero (SWAT = 1.6, HANN = 0.88). However, MRE was lower for SWAT during validation (SWAT = 5.95, HANN = 13.4). In terms of MAE, HANN was found to outperform SWAT during both model calibration and validation (HANN = 7.3 − 5.5, SWAT = 11.1 − 5.5).

Some physical properties of catchment have significant influence on low-to-medium flows such as soil features, land cover, and local depression storage.

Table 1 Comparison of SWAT and hybrid network for flow simulation

Index	Calibration–Validation	
	SWAT	Hybrid network
Nash and Sutcliffe coefficient % (NS)	75–64	85–57
PBIAS%	1.5–21.8	4.7–31
RMSE (m^3/s)	51–29.4	39.4–32.2
MSE (m^6/s^2)	2631–864	1551–1036.5
MRE (*100)	1.6–5.95	0.88–13.4
MAE (m^3/s)	11.1–5.5	7.3–5.5

Fig. 3 Measured and simulated daily stream flow (CMS) over calibration
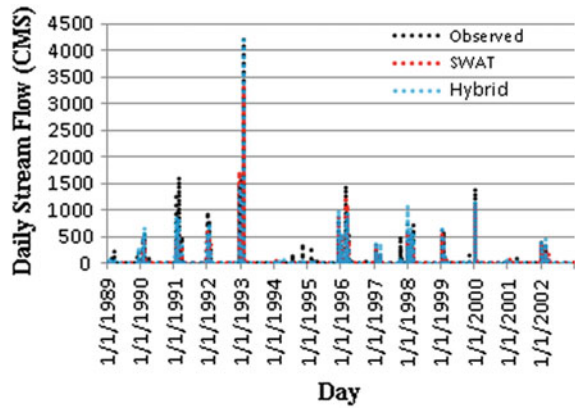
On the other hand, rainfall is considered as the most influential factor for peak or high flows. Therefore, stream flow hydrograph in arid regions is a complex combination of low flows and infrequent peak flows. Therefore, performance of models needs to analyze critically based on various evaluation criteria.

The results show that HANN performed better in terms of NS during model calibration. RMSE, MSE, and MRE were also found closer to zero for HANN in comparison with SWAT during model calibration. On the other hand, SWAT was found to perform better in terms of NS, RMSE, MSE, MRE during model validation. In regard to MAE, both models showed similar performance during model validation. Figure 3 shows the SWAT- and HANN-simulated stream flow in comparison with observed flow during model calibration. The figure shows that both models were successful to simulate an acceptable fluctuation of daily flow. The peak flow during model calibration period was 4209 m^3/s, which were predicted as 3315 and 4184 m^3/s by SWAT and HANN, respectively. Figure 4 shows the SWAT- and HANN-simulated stream flow in comparison with observed flow during model validation. The figure shows that the peak flow during model validation period (1248 m^3/s) was underestimated by both SWAT and HANN. SWAT and hybrid network predicted the corresponding peak flow as 746 and 743 m^3/s, respectively. Highest flows during model calibration and validation are shown in detail in Figs. 5 and 6. The figures show largest flow events for February 1993 and February 2005 during model calibration and validation by SWAT and HANN. Figure 4 shows that HANN outperformed for highest peak flow; meanwhile, both models have similar trend in validation in highest flow event (Fig. 5).

3.2 Pros and Cons of SWAT and HANN

In the present study, SWAT was found advantageous in terms of prediction of stream flow for a long-term period time and meaningful physical parameters guide

Fig. 4 Measured and simulated daily stream flow (CMS) over validation
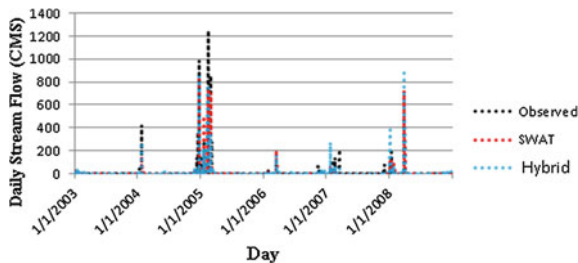
Fig. 5 Measured and simulated daily flow for February 1993
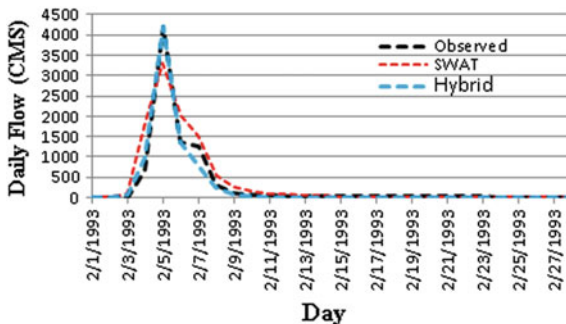
Fig. 6 Measured and simulated daily flow for February 2005
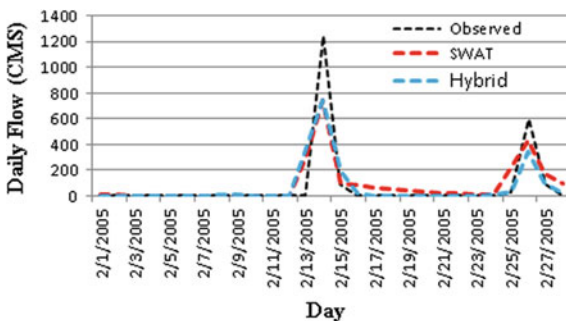
developer for better calibration. The SWAT model is capable to show a visual configuration of Roodan and also it visualizes surface flow besides other water balance component. SWAT can be used as a subsidiary tool with a hydrologist to offer outcomes for monitoring of any management factor such as changing in agricultural area [18]. The drawbacks of SWAT for Roodan might be related to require high-speed digital devices, comprehensive data requirements, and impact of over parameterization in calibration. Moreover, hybrid network is found to be quicker and relatively easier to develop for Roodan on personal device; it does not involve with a collection of variety of data such as SWAT. In addition, HANN needs short time for performing the calculation of simulated data for Roodan. Generally, HANN is capable to model flows with primary knowledge for Roodan

with limited data as input–output pairs. One of the advantages of HANN can be a low cost for Roodan. On the other hand, the disadvantages of HANN are related to low transparency as a data-driven concept for Roodan. Little transparency will cause failure to figure out the interior functions as physically meaning parameters. Another drawback for HANN might be various extensions to be done for Roodan owing to the availability of more options for development based on heuristic circumstances and the outcomes are still unknown for developer. In conclusion, this research suggests the development of current hydrological tools due to comparison and introduction of their applicability in regard to specific regions and objectives.

4   Conclusion

A comparison has been performed for flow simulation on SWAT and HANN. It can be concluded that capability of simulation of flow has been increased with integration of SWAT and semi-automatic calibration (SUFI-2 algorithm). Moreover, HANN is faster for processing and less data demand for application. It can be suggest that SWAT model is more flexible to study the watershed management but HANN model mostly related to the values of flow simulation and hydrological analysis.

References

1. Patra KC (2008) Hydrology and water resources engineering. Alpha Science International Ltd., U.K.
2. World Water Council, Water crisis. Retrieved 20 Dec 2009, from http://www.worldwatercouncil.org/index.php?id=25
3. Foltz RC (2002) Iran's water crisis: cultural, political, and ethical dimensions. J Agric Environ Ethics 15:357–380
4. Shaw EM (1994) Hydrology in practice. Chapman and Hall, London
5. Singh A, Imtiyaz M, Isaac RK, Denis DM (2012) Comparison of soil and water assessment tool (SWAT) and multilayer perceptron (MLP) artificial neural network for predicting sediment yield in the Nagwa agricultural watershed in Jharkhand, India. Agric Water Manage 104:113–120
6. Van Liew MW, Arnold JG, Garbrecht JD (2003) Hydrologic simulation on agricultural watersheds: choosing between two models. Trans ASAE 46(6):1539–1551
7. Anctil F, Perrin C, Andreassian V (2004) Impact of the length of observed records on the performance of ANN and of conceptual parsimonious rainfall-runoff forecasting models. Environ Model Softw 19:357–368

8. Junfeng C, Xiubin L, Ming Z (2005) Simulating the impacts of climate variation and land-cover changes on basin hydrology: a case study of the Suomo basin. Scii China Ser D Earth Sci 48(9):1501–1509

9. Qin XU, Ren L, Yu Z, Bang Y, Wang G (2008) Rainfall-runoff modelling at daily scale with artificial neural networks. In: 4th international conference on natural computation, vol. 2, pp. 504-508, ICNC. 18–20 Oct

10. Parajuli PB, Nelson NO, Frees LD, Mankin KR (2009) Comparison of AnnAGNPS and SWAT model simulation results in USDA-CEAP agricultural watersheds in south-central Kansas. Hydrol Process 23:785–797

11. Xu ZX, Pang JP, Liu CM, Li JY (2009) Assessment of runoff and sediment yield in the Miyun reservoir catchment by using SWAT model. Hydrol Process 23:3619–3630

12. Demirel MC, Venancio A, Kahya E (2009) Flow forecast by SWAT model and ANN in Pracana basin, Portugal. Adv Eng Softw 40:467–473

13. Srivastava P, McNair JN, Johnson TE (2006) Comparison of process-based and artificial neural network approaches for stream flow modeling in an agricultural watershed. J Am Water Resour Assoc 42(3):545–563

14. Morid S, Gosain AK, Keshari AK (2002) Comparison of the SWAT model and ANN for daily simulation of runoff in snowbound un-gauged catchments. In: Fifth international conference on hydroinformatics, Cardiff, UK

15. Al-Damkhi AM, Abdul-Wahab SA, AL-Nafisi AS (2009) On the need to reconsidering water management in Kuwait. Clean Technol Environ Policy 11:379–384

16. Kanae S (2009) Global warming and the water crisis. J Health Sci 55:860–864

17. Jajarmizadeh M, Harun S, Salarpour M (2014) An assessment of a proposed hybrid neural network for daily flow prediction in arid climate. Model Simul Eng Article ID 635018, 10 pages

18. Jajarmizadeh M, Harun S, Abdullah R, Salarpour M An evaluation of blue water prediction in southern part of Iran using SWAT. Environ Eng Manage J (in press)

19. Arnold JG, Moriasi DN, Gassman PW, Abbaspour KC, White MJ, Srinivasan R, Santhi C, Harmel RD, van Griensven A, Van Liew MW, Kannan N, Jha M (2012) SWAT: model use, calibration, and validation. Am Soc Agric Biol Eng 55(4):1491–1508

20. Jajarmizadeh M, Harun Sobri, Akib Shatirah, Sabari NSB (2014) Derivative discharge and runoff volume simulation from different time steps with a hydrologic simulator. Res J Appl Sci Eng Technol 8(9):1125–1131

21. Jajarmizadeh M, Harun S, Shahid S, Akib S, Salarpour M (2014) Impact of direct soil-moisture and revised soil-moisture index methods on hydrologic predictions in an arid climate. Adv Meteorol 2014:8, Article ID 156172

22. Jajarmizadeh M, Kakaei Lafdani E, Harun S, Ahmadi A (2015) Application of SVM and SWAT models for monthly stream flow prediction a case study in South of Iran. KSCE J Civil Eng 19(1):345–357

23. Ahmed Suliman AH, Jajarmizadeh M, Harun S, Darus IZM (2015) Comparison of semi-distributed, GIS-based hydrological models for the prediction of streamflow in a large catchment. Water Resour Manage 29(9):3095, 3110

24. Abbaspour KC, Johnson A, Van Genuchten MT (2004) Estimating uncertain flow and transport parameters using a sequential uncertainty fitting procedure. Vadose Zone J 3 (4):1340–1352

25. Abbaspour KC (2015) SWAT-CUP: SWAT calibration and uncertainty programs, A User Manual

26. Dawson CW, Wilby RL (2001) Hydrological modeling using artificial neural networks. Progress Phys Geogr 25(1):80–108

27. Bowden G, Dandy GC, Maier HR (2005) Input determination for neural network models in water resources applications. Part 1—background and methodology. J Hydrol 301:75–92

28. Kalteh AM, Hjorth P, Berndtsson R (2008) Review of the self-organizing map (SOM) approach in water resources: analysis, modeling and application. Environ Model Softw 23:835–845

29. Parasuraman K, Elshorbagy A, Carey SK (2006) Spiking modular neural networks: a neural network modeling approach for hydrological processes. Water Resou Res 42:1–14
30. Krause P, Boyle DP, Base F (2005) Comparison of different efficient criteria for hydrological model assessment. Adv Geosci 5:89–97
31. Wu JS, Han J, Annambhotla S, Bryant S (2005) Artificial neural networks for forecasting watershed runoff and stream flows. J Hydrol Eng 10(3):216–222

Estimation of Peak Discharges Using Flood Frequency Analysis and Hydrological Modeling System

Jazuri Abdullah, Nur S. Muhammad and Nur A. Mohamad Sharif

Abstract This study presents the methodology to estimate peak discharges using flood frequency analysis (FFA) and hydrological modeling system (HMS). FFA method was performed using two distribution functions, i.e., Gumbel's extreme value distribution (Gumbel's) and lognormal (LN) distribution, while HMS was carried out using the Hydrologic Engineering Center's Hydrologic Modeling System (HEC-HMS) software. Long and reliable daily streamflow and rainfall data (i.e., 50 years) recorded at Sungai Rinching, Selangor, were used. Goodness-of-fit test indicates that the chi-square (χ^2) values for Gumbel's and lognormal distributions are 1.952 and 7.976, respectively, which are significantly less than the $\chi^2_{\alpha,v}$ value of 9.488. However, Gumbel's is chosen to represent the distribution of annual maximum daily streamflow because the χ^2 test value was much lesser as compared to lognormal distribution. The calibration and validation processes were carried out to test the suitability of HEC-HMS software to simulate the streamflow of Sungai Rinching. The relative percentage difference (RPD) estimated for peak discharges from these processes was between 3 and 6 %, and maximum lag times were only 1 h. These results indicate that the model performance is very good. The peak discharges for several average recurrence intervals (ARIs), i.e., 2, 5, 10, 20, 50, and 100 years estimated using FFA and HMS, were also compared. Results show that the peak discharges estimated using HMS for all ARIs (except 2 years) are comparable to the values given by FFA, and the given percentage differences are between 2.7 and 12.2 %. This finding indicates that HEC-HMS may be used as a tool in simulating the daily streamflow and estimate the annual daily maximum streamflow of several ARIs at Sungai Rinching.

J. Abdullah · N.A. Mohamad Sharif
Faculty of Civil Engineering, Universiti Teknologi MARA, Shah Alam,
40450 Selangor, Malaysia

N.S. Muhammad (✉)
Faculty of Engineering and Built Environment, Department of Civil and Structural Engineering, Universiti Kebangsaan Malaysia, Bangi, 43600 Selangor, Malaysia
e-mail: shazwani.muhammad@ukm.edu.my

1   Introduction

Malaysia is located near the equator and experiences two major monsoon seasons
every year, i.e., northeast (from November to March) and southwest (from May to
September). The nature of climate results in total annual rainfall of between 2000 and
4000 mm [1]. As a result, flooding is the most common natural disaster in Malaysia.

Flood frequency analysis (FFA) is the most commonly used method in esti-
mating the severity and recurrence interval of flood events. There are two methods
in FFA, i.e., at-site or direct analysis and regional analysis [2]. The procedures of
using at-site or direct analysis require choosing and fitting appropriate theoretical
probability distribution to the data. Previous researchers concluded that there were
many questions and opinions expressed regarding selecting an appropriate distri-
bution for the flood analysis [2–4]. That include the problems of short data set and
extrapolation beyond the record length, which are errors, inconsistency,
non-homogeneity, and non-stationary, thus affecting the assumptions made when
fitting a distribution to the data [2, 3]. At-site analysis can be performed when the
long record of streamflow is available, but many studies have shown that regional
approach for frequency analysis results in more reliable design estimates [2].

Regional frequency analysis uses data from several sites to estimate the fre-
quency distribution at each site [2, 5]. Regional analysis assumed that the data at
every site in the study area have a standardized variant with the same distribution,
and therefore, they can be combined to produce a frequency distribution with
appropriate site-specific scaling [2, 5–7]. Regionalization also refers to the identi-
fication of homogeneous flood response and the selection of an appropriate fre-
quency distribution at a given location [2, 8]. Additionally, regional approach can
be used to estimate the flooding events at an ungauged site [2, 9].

The Log-Pearson Type III (LP3) distribution gives the best fit to the annual
streamflow data for several sites in USA [2, 10]. The distribution of daily maximum
flow data of the Nyanyadzi River, Zimbabwe, was investigated using 30 years of
observed data [11]. The outcome of the study has revealed the capability of
Gumbel's distribution to predict the flood magnitudes. The analysis shown that
there was no significant difference between the predicted and measured flow
magnitudes. Gumbel's distribution is also best to represent the distribution of daily
maximum discharge of Osse River [12]. The data used for this study were the
maximum annual streamflow for 20 years (1989–2008), collected from the Benin
Owena River Basin Development Authority. In this study, it was concluded that the
Gumbel's distribution was suitable for predicting the expected flow in the river.
Based on the studies on FFA discussed above, the authors decided to test the
capability of lognormal (LN) and Gumbel's distributions in estimation of annual
flood at Sungai Rinching, Semenyih, Selangor.

Hydrological modeling system (HMS) was first started in the nineteenth centuries where the technologies and software system have been widely developed. Examples include Corps Water Management System (CWMS), Hydrologic Engineering Center's Reservoir System (HEC-ResSim), Hydrologic Engineering Center's River Analysis System (HEC-RAS), and Hydrologic Engineering Center's Hydrologic Modeling System (HEC-HMS). These softwares were introduced by US Army Corps of Engineers. One of the main objectives of the system is to assist engineers and hydrologists in providing the most reliable estimation of annual floods. However, there are limited studies that examine the effectiveness and the suitability of the software for flood estimation and compared it with FFA methods.

The HEC-HMS was used to simulate joint event and continuous hydrologic modeling [13]. Their findings indicate that it is necessary to develop an effective modeling system since it was built with many functions that only required a simple observed data. This also helps in increasing the accuracy of modeling. For this case study, the researchers combined the fine-scale event and coarse-scale continuous hydrologic modeling. This study was carried out at Mona Lake watershed, which has an area of 191.64 km^2. The prominent land uses in the study area were residential, forest and agricultural. The condition of the area was estimated to have low runoff potential and high capability of infiltration. The researchers have come out with an idea to strengthen the capability of modeling by implementing the joint Soil Conservation Service Curve Number (SCS-CN) method event and soil moisture accounting (SMA) continuous modeling. HEC-HMS was also used to model runoff in Iranian catchments [14, 15].

This paper presents the methodology to estimate the flood frequency using FFA and HMS. FFA method was performed using two distribution functions, i.e., Gumbel's Extreme Value Distribution (Gumbel's) and LN, while HMS was carried out using the HEC-HMS software. The best-fit distribution function is selected from FFA. The calibration and validation of HEC-HMS were done to evaluate the model performance and estimate the maximum discharge. Additionally, the comparison and performance of each method, in terms of peak discharges with respect to the average recurrence intervals (ARIs), were also presented.

2 Flood Frequency Analysis

2.1 Weibull Plotting Position

Weibull plotting position method was used to represent the non-exceedance probability of the observed data, and the formula is given as follows:[16]

$$P(Q_T \leq q) = \frac{i}{N+1} = 1 - \frac{1}{T} \tag{1}$$

where i is the rank in ascending order, N is the number of observations, and T is the return period in years.

2.2   *Gumbel's Extreme Value Distribution (Gumbel's)*

This distribution is one of the most used probability distribution functions for extreme values in hydrologic and meteorological studies for the prediction of flood peaks, maximum rainfalls, maximum wind speed, and others. According to Gumbel, the probability of occurrence of an event equal to or larger than a value q is expressed as follows [12]:

$$P(Q_T \leq q) = \exp\left[-e^{-(y)}\right] \tag{2}$$

where y is a dimensionless variable given by

$$y = \frac{1.2825(q - \bar{q}) + 0.577}{\sigma_q} \tag{3}$$

where $\bar{q}$ is the mean and σ_q is the standard deviation for annual daily maximum flowrate, q.

Reference [12] provides further explanation on estimating the return period for a certain value of $P(Q_T \leq q)$.

2.3   *Lognormal*

The probability density function of a two-parameter LN distribution is as follows: [16]

$$f(q) = \frac{1}{q\sigma_x\sqrt{2\pi}} \exp\left[\frac{-(\log q - \mu_x)^2}{2\sigma_x^2}\right] \tag{4}$$

where μ_x and σ_x are the mean and standard deviation of the natural logarithms of q.

Reference [16] gives detailed methodology on estimating the return period for a certain value of $f(q)$.

3   Hydrological Modeling System Using HEC-HMS

A specified hyetograph was selected as meteorology model, and the parameters used were runoff curve number (CN), impervious layer (%), and lag time (min) for a certain event to occur. CN value and lag time are the most important parameters for the calibration because they determine the estimation of discharges and time to peak. CN number was selected based on the antecedent moisture condition (AMC).

Table 1 Types of AMC for different types of soil [17]

AMC	Types of soil
I	Soils are dry but not to wilting point. Satisfactory cultivation has taken place
II	Average conditions
III	Sufficient rainfall has occurred within the immediate past 5 days. Saturated soil conditions prevail

Table 2 CN value for suburban and urban land uses [17]

Cover and treatment	Hydrologic soil group			
	A	*B*	*C*	*D*
Open spaces, lawns, parks, etc.				
(i) In good condition, grass covers in more than 75 % area	39	61	74	80
(ii) In fair condition, grass covers in 50–75 % area	49	69	79	84
Commercial and business areas (85 % impervious)	89	92	94	95
Industrial districts (72 % impervious)	81	88	91	93
Residential, average 65 % impervious	77	85	90	92
Paved parking lots, paved roads with curbs, roofs, driveways, etc.	98	98	98	98
Streets and roads				
Gravel	76	85	89	91
Dirt	72	82	87	89

AMC refers to the moisture content in the soil at the beginning rainfall event under consideration [17]. There are three types of AMC conditions which can be shown in Table 1.

Based on the classification of AMC given above, the soil condition of Sungai Rinching can be considered as AMC-II since it was once a cultivated area, which is the average condition for the type of soil. Reference [17] has also listed certain values of CN for different types of land use under AMC-II condition. Variation of CN value is shown in Table 2.

Sungai Rinching was considered as suburban land. Hence, the catchment is assumed to be an open space in fair condition for soil type B that gives the CN value of 69.

4   Results and Discussion

4.1   *Flood Frequency Analysis (FFA)*

Sungai Rinching is located in Semenyih, Selangor, and caters a catchment area of 23.13 km^2. The location of the study area is shown in Fig. 1. It flows through three densely populated areas, namely Kampung Rinching Hulu, Kampung Rinching

Fig. 1 Location of study area

Tengah, and Kampung Rinching Hilir. Sungai Rinching used to be the main source of water supply that is for agricultural activities and human consumptions. Long and reliable daily streamflow record of 50 years, i.e., from 1960 to 2009 was obtained from Department of Irrigation and Drainage (DID), Malaysia.

Weibull plotting position was used to plot the observed data. However, this method may only predict return periods up to $N + 1$ years, where N is the sample size. Following that, two probability distribution methods, i.e., Gumbel and LN, were tested to represent the distribution of annual maximum discharge at the study area. These probability distribution functions were chosen because it may predict
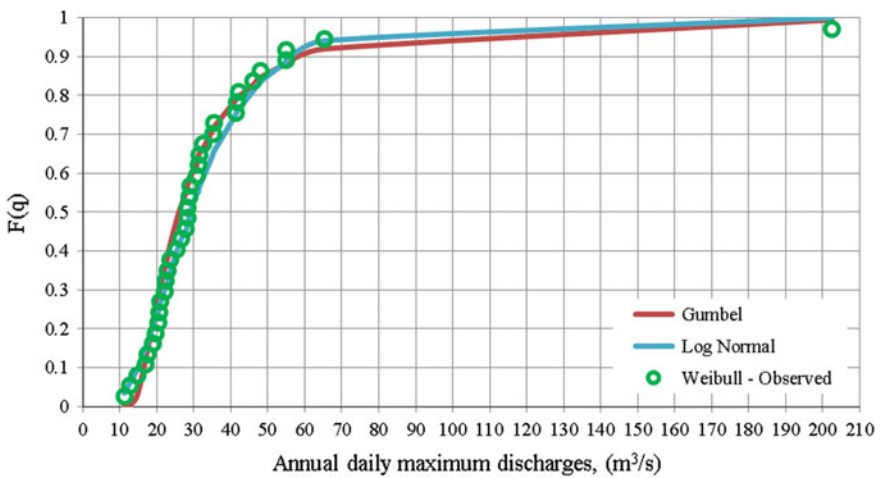
Fig. 2 Plot of cumulative distribution function of annual daily maximum streamflow at Sungai Rinching

Table 3 Chi-square test (χ^2) for Gumbel's and lognormal

Distributions	No. of parameters	χ^2	$\chi^2_{\alpha,v}$
Gumbel's	2	1.952	9.488
Lognormal	2	7.976	

the maximum annual discharge of high return periods, i.e., beyond the $N + 1$ years given by Weibull method. The comparison between Weibull, Gumbel's, and LN is given in Fig. 2.

Goodness-of-fit test using chi-square test (χ^2) was used to determine the best distribution function to represent annual daily maximum discharges at Sungai Rinching. The χ^2 was done according to 5 % significant level ($\alpha = 0.05$), i.e., 95 % confidence interval. Table 3 shows the values of χ^2 test for Gumbel's and LN.

Based on the results given in Table 3, the values of χ^2 test for Gumbel's and lognormal distributions are 1.952 and 7.976, respectively, which are significantly less than the $\chi^2_{\alpha,v}$ value of 9.488. This indicates that both Gumbel's and lognormal distributions are suitable to represent the distribution of annual daily maximum streamflow at Sungai Rinching. However, it is clearly shown in Table 3 that Gumbel's is more suitable because the χ^2 test value was much lesser as compared to lognormal distribution.

Gumbel's distribution is used to estimate the peak discharges for several ARIs, i.e., 2, 5, 10, 20, 50, and 100 years. The results and discussion on that are given after the hydrological modeling system using HEC-HMS.

4.2 Hydrological Modeling System Using HEC-HMS

The calibration and validation of HEC-HMS model were done to check the accuracy and suitability of HEC-HMS to simulate the annual daily maximum discharge. It is important to perform these processes before the estimation of peak discharges for selected ARI.

The calibration for Sungai Rinching was done by using the recorded rainfall and discharge data on November 9, 2002. The simulations were done for 24 h since the data used for simulation were recorded in interval of one hour per day. The assumed value of CN was 83. This value is within the acceptable range of CN, i.e., 52–86. The lag time used was assumed to be 180 min.

With reference to Fig. 3, the calibration of HEC-HMS shows good agreement between the observed and simulated data. The time to peak between simulated and observed discharge is the same which means that the lag time used in this simulation is suitable for Sungai Rinching. The difference between simulated and observed discharges also shows that the gap between these two discharges is satisfactory. From the calibration process, it is concluded that the model performance is very good.
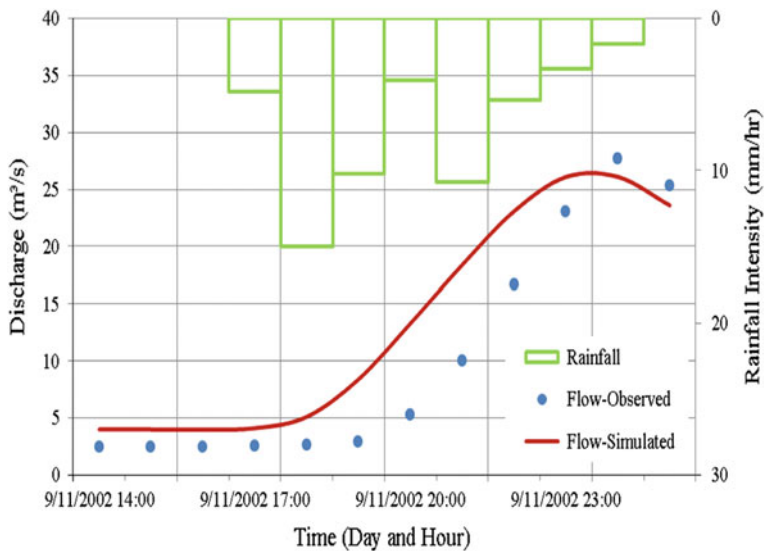
Fig. 3 Model calibration for Sungai Rinching

Further evaluation of the model performance was done by applying the statistical analysis, specifically the relative percentage difference (RPD). Based on the values of RPD, the model performance is very good because the difference between observed and simulated peak discharges is about 6 %. RPD value for time to peak between observed and simulated data is 0 % which means that observed and simulated data have the same time to peak.
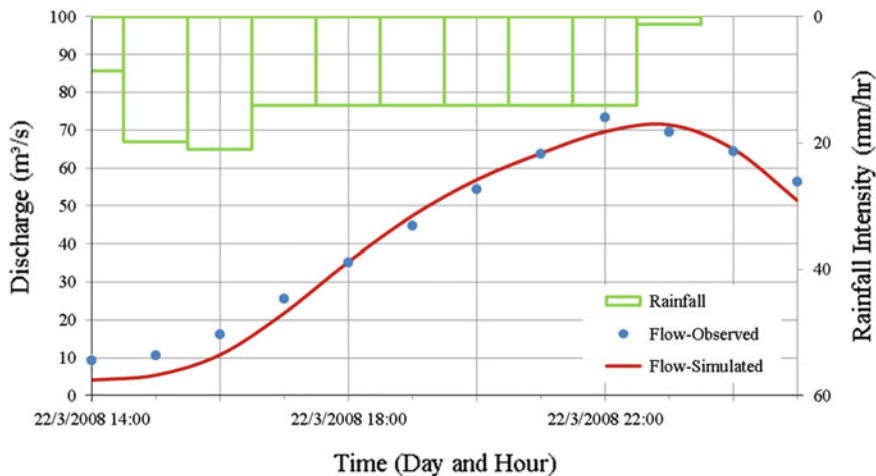
Fig. 4 Model validation for October 1, 2004

Table 4 Calculated value of RPD based on the observed and simulated value

Date of event	Peak discharges (m³/s)			Time to peak (24 h)		
	Obs.	Sim.	RPD %	Obs.	Sim.	RPD (lag time, h)
Calibration						
November 9, 2002	27.7	26.1	−5.81	0:00	0:00	0
Validation						
October 1, 2004	43.1	44.4	2.97	19:00	20:00	01:00
March 22, 2008	73.3	71.4	−2.63	22:00	23:00	01:00

Note Obs. Observed; *Sim.* Simulated; *RPD* Relative percentage difference

Model validation was carried out using by simulating two events, i.e., October 1, 2004, and March 22, 2008. The estimated RPDs for peak discharges are less than 3 %. Additionally, the lag time of time to peak for these events is 1 h. Therefore, it is concluded that the overall performance for model validation is very good. Figure 4 illustrates the observed and simulated discharge for model validation process, while Table 4 gives the estimated RPD for both model calibration and validation processes.

4.3 Estimation of Peak Discharges for Several ARIs Using FFA and HMS

The selected ARIs are 2, 5, 10, 20, 50, and 100 years. Based on the FFA method, the maximum peak discharges at different ARIs are determined using the Gumbel's distribution. For HEC-HMS simulation, the estimated values of peak discharges at different ARIs were determined using rainfall intensity obtained from the intensity–duration–frequency (IDF) curve developed in Manual Saliran Mesra Alam (MASMA). Rainfall intensity is determined based on the duration of rainfall. The maximum estimated discharge for small watershed is between 3 and 5 h [18]. The peak discharge for this study has been assumed to be 4 h (taking an average time between 3 and 5 h). The value of rainfall intensity based on different ARIs was used for the simulation of peak discharges.

Overall, the peak discharges estimated using HMS for all ARIs (except 2 years) are comparable to the values given by FFA. For 2-year ARI, FFA gives a peak discharge of 29.9 m³/s, while HEC-HMS simulated it as 49.4 m³/s that gives a percentage difference of 65 %. Other than that, the differences are between 2.7 and 12.2 %. More interestingly, the peak discharges estimated by HMS for high ARIs, i.e., 50 and 100 years, are close to the values estimated by FFA. Table 5 shows the values of peak discharges estimated by FFA and the difference in percentage for every ARI.

Table 5 Estimated peak discharges using FFA and HMS

ARI (years)	Peak discharges (m³/s)		Difference (%)
	FFA	HMS	
2	29.9	49.4	65.2
5	61.3	68.4	11.6
10	82.1	84.3	2.7
20	102.1	92.4	9.5
50	127.9	117.0	8.5
100	147.3	129.4	12.2

5   Conclusions

The Gumbel's Extreme Value Distribution (Gumbel's) is best to represent the annual maximum daily discharges at Sungai Rinching. Maximum discharges at different ARIs were also estimated using HMS, i.e., HEC-HMS. The calibration and validation processes of HEC-HMS model prove that this model is capable of simulating the discharges at the study area. Model performance was measured using RPD. The RPD values for the calibration and validation process were less than 10 %. Therefore, we conclude that the overall model performance is very good.

The peak discharges estimated using Gumbel's distribution was compared with the values simulated by the HEC-HMS software. The peak discharges estimated using HMS for all ARIs (except 2 years) are comparable to the values given by FFA, and the given percentage differences are between 2.7 % and 12.2 %.

References

1. Suhaila J, Jemain AA (2007) Fitting daily rainfall amount in Malaysia using the normal transform distribution. J Appl Sci 7(14):1880–1886
2. Smithers J (2012) Methods for design flood estimation in South Africa. Water SA 38 (4):633–646
3. Schulze RE (1989) Non-stationary catchment responses and other problems in determining flood series: a case for a simulation modelling approach. In: Kienzle SW, Maaren H (eds) Proceedings of the Fourth South African National Hydrological Symposium. Pretoria, South Africa, SANCIAHS, pp 135–157
4. Smithers JC, Schulze RE (2003) Design rainfall and flood estimation in South Africa. WRC report No. 1060/01/03. Water Research Commission, Pretoria, South Africa, p 155
5. Hosking J, Wallis J (1997) Regional frequency analysis: an approach based on L-moment. Cambridge University, Cambridge

6. Cunnane C (1989) Statistical distribution for flood frequency analysis. WMO-report no. 781 (Operational hydrology report no. 33), p 73
7. Gabriele S, Arnell N (1991) A hierarchical approach to regional flood frequency analysis. Water Resour Res 27(6):1281–1289
8. Kachroo RK, Mkhandi SH, Parida BP (2000) Flood frequency analysis of southern Africa: I. Delineation of homogeneous regions. Hydrol Sci J 45(3):437–447
9. Pilon PJ, Adamowski K (1992) The value of regional information to flood frequency analysis using the method of L-moments. Can J Civ Eng 19(1):137–147
10. Stedinger Vogel RM, Foufoula-Georgiou E (1993) Frequency analysis of extreme events. McGraw-Hill, New York
11. Mujere N (2011) Flood frequency analysis using the Gumbel's distribution. Int J Comput Sci Eng (IJSCE) 3(7):2774–2778
12. Solomon O, Prince O (2013) Flood frequency analysis of Osse river using Gumbel's distribution. Civil Environ Res 3(10):57–59
13. Chu X, Steinman A (2009) Event and continuous hydrologic modeling with HEC-HMS. J Irrig Drain Eng 135(1):119–124
14. Arekhi S (2012) Runoff modeling by HEC-HMS model (case study: Kan Watershed, Iran). Int J Agric Crop Sci (IJACS) 4(23):1807–1811
15. Tahmasbinejad H, Feyzolahpo M, Mumipour M, Zakerhosei F (2012) Rainfall-runoff simulation and modeling of Karun river using HEC-RAS and HEC-HMS models, Izeh district, Iran. J Appl Sci 12(18):1900–1908
16. Rao AR, Hamed KH (2000) Flood frequency analysis. CRC Press LLC, Baco Raton
17. Subramanya K (2013) Floods. In: Subramanya K (ed) Engineering hydrology. McGraw Hill, India, pp 296–331
18. Abdullah J (2013) Distributed runoff simulation of extreme monsoon rainstorms in Malaysia using TREX. Ph.D. thesis, Department of Civil and Environmental Engineering, Colorado State University, CO

Simulation of Estuary Transverse Flow Salinity Intrusion During Flood Event: Case Study of Selangor River Estuary

Nuryazmeen Farhan Haron and Wardah Tahir

Abstract The objective of this paper was to describe the effect of estuarine flooding leading to estuary transverse flow salinity intrusion specifically in the Selangor River estuary. The simulation of Selangor River estuary has been carried out using a multi-dimensional hydrodynamic and transport model. The Selangor River estuary model has been calibrated and validated using data on November 2005 for water-level calibration and from May to June 2014 for salinity validation. The results of the simulation show that the salinity level decreases when the water-level increases due to high fresh water discharge from the river upstream for different return periods of 10, 50, and 100 years.

Keywords Selangor river · Salinity intrusion · Estuary · Estuarine flooding · Return periods

1 Introduction

Selangor river basin can be described as one of the most important freshwater fish production corridors, rich in animal and plant life, also famous for the natural wonder of firefly colony in the riverbanks of the Selangor River downstream specifically at Kg. Kuantan. However, the unbalanced development in the Selangor river basin can cause flooding and many environmental effects, including the

N.F. Haron (✉) · W. Tahir
Universiti Teknologi MARA, Shah Alam, Selangor, Malaysia
e-mail: neemzay@gmail.com

W. Tahir
e-mail: warda053@salam.uitm.edu.my

depletion of salinity level along the estuary. Most of the downstream of Selangor River has been subjected to flooding at various times. Thus, several researches had been conducted on the Selangor River to observe the effect of flooding and other investigation related to the issues such as the generation of flood hazard maps [1], sedimentation [2], physical modeling for flood evaluation [3], salinity intrusion [4, 5], and case study of fireflies [6, 7].

The worst flood experience in the basin is in 1971, and since then minor floods had occurred occasionally. Three types of floods occur in the basin consists of local floods due to high-intensity rainfalls of relatively short duration, general floods (caused by rainfall of longer duration), and tidal floods affecting a number of villages in the lower reaches of Selangor River. Currently, there are no improvements or changes in widening, deepening, or realigning the channel of Selangor River [8]. The Selangor river channel width varies from 40 to 1200 m.

In this research, the simulation of the effect of flood to salinity level along the Selangor River estuary has been carried out. A hydrodynamic and transport model was applied to the study area to simulate the hydrodynamics and salinity intrusion. The Selangor River estuary model has been calibrated and validated using data on November 2005 for water-level calibration and from May to June 2014 for salinity validation. However, the calibration and validation processes were not discussed in details in this paper as the main focus is the model application during flood event.

Hence, this paper presents the results of the simulation of the estuary transverse flow salinity intrusion due to estuarine flooding from river upstream in Selangor River estuary.

2 Study Area

Figure 1 shows the location of the study area that is located in Kuala Selangor. Selangor river basin is adjacent to Klang Valley, located in the northern part of the state of Selangor. The catchment area is about 1960 km^2 with the total length of Selangor River being approximately 120 km. The major tributaries are Sg. Batang Kali, Sg. Kerling, Sg. Rening, Sg. Kubu, Sg. Sembah, Sg. Buloh, and Sg. Gerachi. Tidal influence can be experienced up to 40 km from the river mouth passing the famous firefly habitat area at Kg. Kuantan.

The Selangor River rises in Titiwangsa Range bordering the state of Pahang and flows in an approximately southwest direction before discharging into the Straits of Melaka. The main inhabited areas are in the towns of Kuala Selangor, Batang Berjuntai, Serendah, Rasa, and Kuala Kubu Baru. The Selangor river basin is a favorable and essential recreation and tourism area, providing a green and pristine environment for local residents and those in the Klang Valley.

Fig. 1 Study area. *Source* [9]

3   Selangor River Estuary Model Calibration and Validation

The model of Selangor River estuary has been calibrated using observed water level at Kg. Asahan (Fig. 2) from November 15 to November 27, 2005. The most suitable Manning's coefficient n value used in the calibration is 0.02 indicate by the lowest of mean absolute error (MAE), root-mean-square error (RMSE), and also the R^2 value as compared to other Manning's coefficient n values (Table 1). Besides, the comparison between observed and simulated water level does not show much difference and has the same pattern.

Fig. 2 Location of salinity and water level for Selangor River estuary model
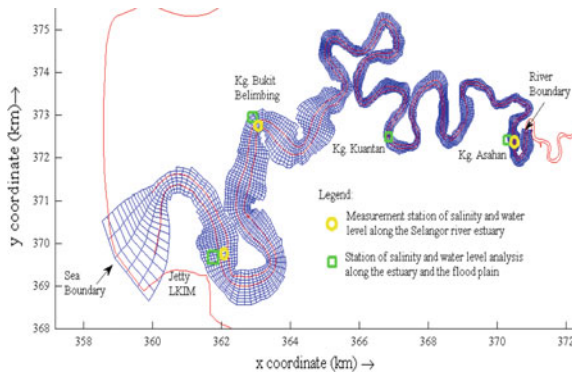
Table 1 Results of statistical test based on MAE, RMSE, and R^2 for different n values at Kg. Asahan station on November 2005

n	0.02	0.03	0.04
MAE (m)	0.32	0.34	0.47
RMSE (m)	0.38	0.42	0.60
R^2	0.88	0.88	0.85

Fig. 3 Simulated salinity versus observed salinity from May 2014 until June 2014 at Kg. Bukit Belimbing Station
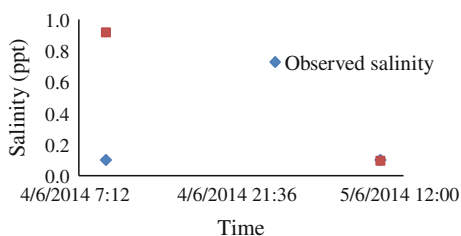
Meanwhile, for the validation process, the measured salinity data at Kg. Bukit Belimbing station and Jetty LKIM Kuala Selangor station from May 2014 to June 2014 have been used. Figures 3 and 4 present the graph of simulated salinity versus observed salinity from May 2014 until June 2014 for validation purpose at Kg. Bukit Belimbing station and Jetty LKIM Kuala Selangor station, respectively.

In both figures, the observed salinity is lower than simulated salinity for several times due to the heavy local rain in Kuala Selangor during the measurement. As a result, the discharge from the river and rainfall has deviated from the reading of salinity. However, from the conditions, it is shown that the high freshwater discharge will dilute the concentration of salinity. Thus, salinity level will reduce.

Fig. 4 Simulated salinity versus observed salinity from May 2014 until June 2014 at Jetty LKIM Kuala Selangor station
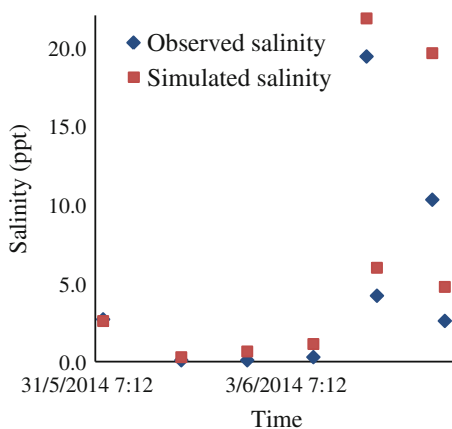
4 Simulation of Different Flood Event

The hydrodynamic and salinity intrusion model was carried out for different return periods of 10, 50, and 100 years in order to determine the changes of water level leads to depletion in the salinity level along the estuary. The maximum flow from 1970 to 2014 has been obtained from DID for Rantau Panjang station. The data were used as an approximation for the Selangor River estuary model as the station is the nearest to the model region. The model region is from the river mouth up to Kg. Asahan (the limit of saline water) since the main focus is to identify the salinity intrusion changes during flood events.

From the simulation of water level and salinity at Kg. Asahan station, it shows that the water level increases while the salinity level becomes zero as the flow increases for different return periods (Fig. 5).

Meanwhile, the simulation of salinity shows the salinity level decreases as the water level increases for 10, 50, and 100 years return periods at Kg. Bukit Belimbing station (Fig. 6) and Jetty LKIM Kuala Selangor station (Fig. 7).

Fig. 5 Comparison of water level and salinity with different flow for 10, 50, and 100 years return periods at Kg. Asahan station
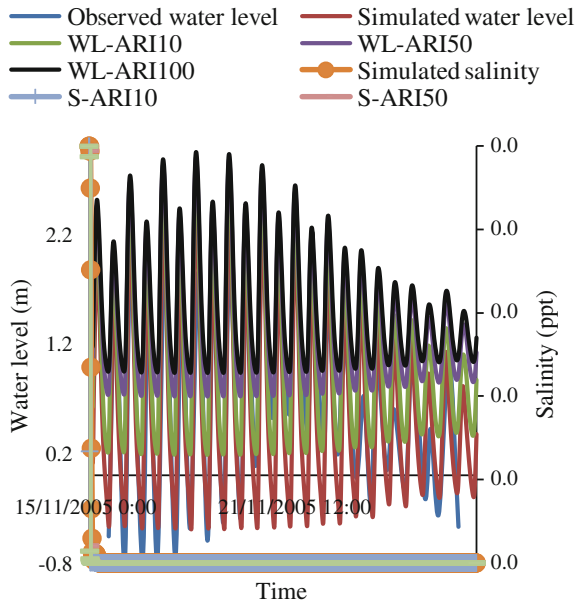
Fig. 6 Comparison of salinity and water level with different flow for 10, 50, and 100 years return periods at Kg. Bukit Belimbing station
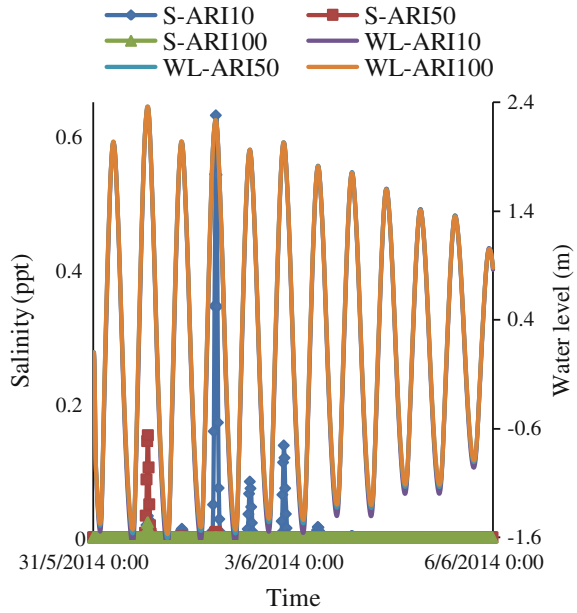
Fig. 7 Comparison of salinity and water level with different flow for 10, 50, and 100 years return periods at Jetty LKIM Kuala Selangor station
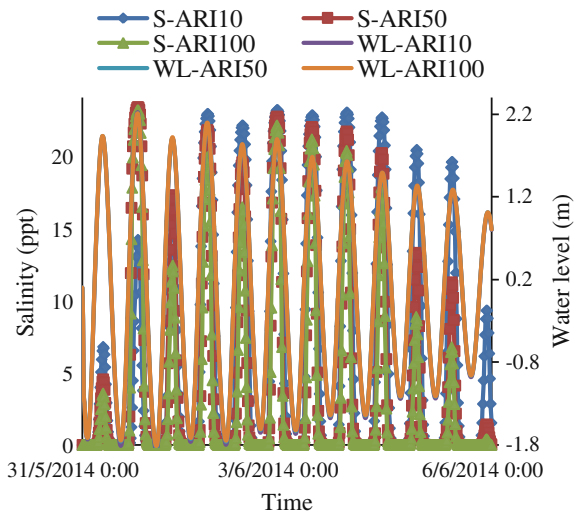
Besides, the flood plain along the Selangor River estuary was also affected by the estuarine flooding and the salinity intrusion. The comparison between the change in water depth and salinity along the flood plain at different return periods is shown in Figs. 8, 9, and 10.

Fig. 8 Comparison of salinity and water depth with different flow of 10, 50, and 100 years return periods at flood plain of Kg. Kuantan
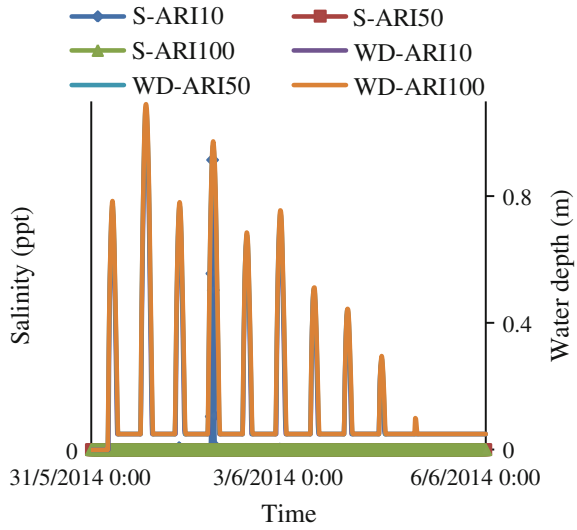
Fig. 9 Comparison of salinity and water depth with different flow of 10, 50, and 100 years return periods at flood plain of Kg. Asahan
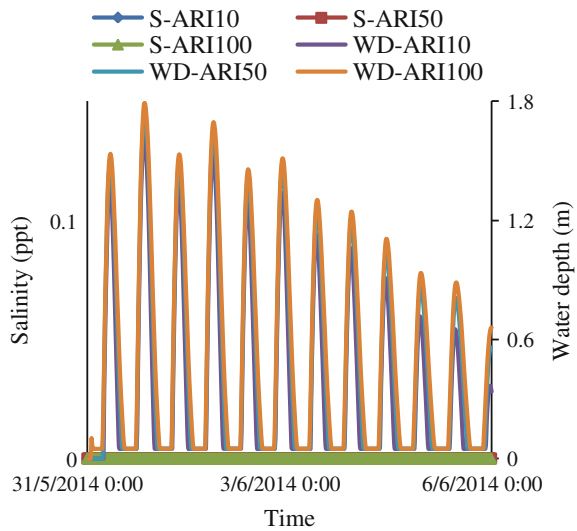
These figures depict the salinity-level drop until zero when the water depth increases due to high freshwater discharge at Kg. Kuantan station, Kg. Asahan station, and Kg. Bukit Belimbing station, respectively.

Fig. 10 Comparison of
salinity and water depth with
different flow of 10, 50, and
100 years return periods at
flood plain of Kg. Bukit
Belimbing
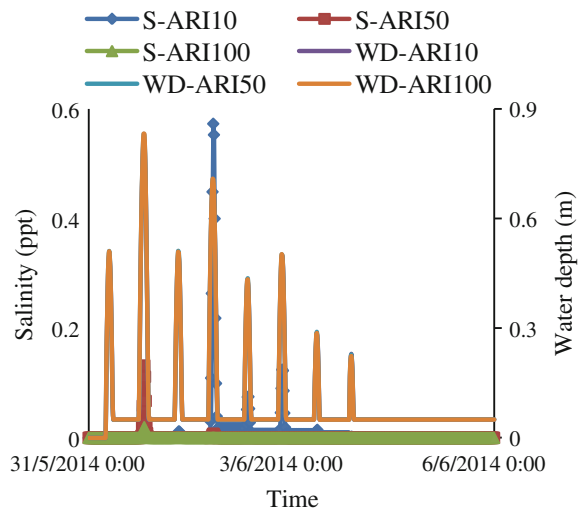
5   Conclusion

The Selangor River estuary model that was calibrated (observed water-level data on
November 2005) and validated (observed salinity data from May to June 2014) has
been applied for salinity and water-level simulations using different flows of 10, 50,
and 100 years return periods along the estuary and the flood plain. From the
simulations, it can be indicated that the salinity level will decrease as the freshwater
inflow increases in the estuarine system including at the flood plain area.

   The salinity depletion may have impact on the environment and ecosystem of the
area. As for example, the berembang trees as the habitat of fireflies at Kg. Kuantan
may be effected. Thus, the model can be used as an aid to environmental monitoring
by being able to predict the extent of salinity intrusion either during normal flow or
during flood event along the estuary as well as at the flood plain.

References

1. Hassan AJ, Ghani AAb, Abdullah R (2006) Development of flood risk map using GIS for Sg.
   Selangor Basin. In: Proceeding of the 6th international conference on ASIA GIS, 9–10 Mac,
   UTM, pp 1–11
2. Ishak AK, Samuding K, Yusoff NH (2000) Water and suspended sediment dynamics in
   Selangor river estuary. In: Proceedings of the Malaysian science and technology congress 2000:
   symposium A, vol II, no. 20, pp 164–171

3. Mohamad MF, Samion MKH, Hamzah SB (2014) Physical modelling for flood evaluation of Selangor river under tidal influence. In: International conference data mining, civil and mechanical engineering (ICDMCME 2014), pp 102–106
4. Ishak AK, Samuding K, Yusoff NH, Abdul Latif J (2002) Salinity intrusions into the Selangor river estuary and its effect on the mangrove species *Sonneratia caseolaris*. In: Proceedings of the seminar R and D MINT 2002: strengthening R and D culture for technology generation, pp 123–130
5. Zainal Abidin MR, Hassan AJ, Awang S, Yuk San L, Hashim N (2006) Salinity intrusion modeling for sungai Selangor. In: Proceedings of seminar on water resources and environment: application of nuclear and related technologies, pp 150–160
6. Kirton LG, Nada B, Khoo V, Phon CK (2012) Monitoring populations of bioluminescent organisms using digital night photography and image analysis: a case study of the fireflies of the Selangor River, Malaysia. Insect Conserv Divers 5(3):244–250
7. Nada B, Kirton LG, Norma-Rashid Y, Cheng S, Shahlinney L, Phon CK (2012) Monitoring the fireflies of the Selangor River. In: Mangrove and coastal environment of Selangor, Malaysia, University of Malaya Press, Malaysia, pp 153–162
8. DID (2012) Generation of flood hazard maps for Sg. Selangor basin: Final Report
9. van Breemen MTJ (2008) Salt intrusion in the Selangor Estuary in Malaysia model—study with Delft3D, University of Twente

Flood Frequency Analysis Based on Gaussian Copula

Mohsen Salarpour, Zulkifli Yusop, Fadhilah Yusof, Shamsudin Shahid and Milad Jajarmizadeh

Abstract Flood duration, volume, and peak flow are important considerations in flood risk analysis and management of hydraulic structures. The conventional flood frequency analysis assumed that the marginal distribution functions of flood parameters follow a certain pattern. However, such assumption is impractical because a flood event is multivariate and the flood parameter distributions can be different. These discrepancies were addressed using bivariate joint distributions and Copula function which allow flood parameters having different marginal distributions to be analyzed simultaneously. The analysis used hourly stream flow data for 45 years recorded at the Rantau Panjang gauging station on the Johor River in Malaysia. It was found that flood duration and volume are best fitted by the generalized extreme value distribution while peak flow by the Generalized Pareto. Inference function for margin (IFM) method was applied to model the joint distributions of correlated flood variables for each pair and the results showed that all the calculated θ values were in acceptable range of Gaussian Copula. By horizontally cutting the joint cumulative distribution function (CDF), a set of contour lines were obtained for Gaussian Copula which represented the occurrence probabilities for the joint variables. Also the joint return period for pair of flood variables was calculated.

Keywords Flood frequency analysis · Gaussian Copula · Bivariate probability distribution

M. Salarpour · S. Shahid · M. Jajarmizadeh
Faculty of Civil Engineering, Department of Hydraulic and Hydrology,
Universiti Teknologi Malaysia, Skudai 81310, Johor, Malaysia

Z. Yusop (✉)
Centre for Environmental Sustainability and Water Security (IPASA),
Universiti Teknologi Malaysia, Skudai 81310, Johor, Malaysia
e-mail: zulyusop@utm.my

F. Yusof
Faculty of Science, Department of Mathematics, Universiti Teknologi Malaysia,
Skudai 81310, Johor, Malaysia

1   Introduction

Detailed information on random yet mutually correlated flood parameters such as flood duration, flood volume, and peak flow is crucial for the design, management, and planning of hydrological structures. A number of flood frequency analysis [1] methodologies has been developed so far to summarize flood characteristics and find their correlations to estimate the severity of flood events using univariate [2–4] and multivariate techniques [5–8]. Both analyses require many restrictive assumptions to be considered [5]. However, the crucial flood characteristics can be presented using multivariate analysis as a joint cumulative distribution function (CDF) and probability density function (PDF). Therefore, multivariate analyses are getting increasingly more popular in recent years for flood frequency analysis [6–8].

The best marginal distribution for the flood parameters aforementioned is not necessarily from the same probability distribution function. This has encouraged the introduction of a Copula concept [9, 10] into flood frequency analysis [11–13] to model the correlations among the flood parameters without taking the type of marginal distributions into consideration. This implies that such joint distribution model is not as restricted as traditional flood frequency analyses. A univariate marginal can be connected to its full multivariate distribution using a Copula. Its model gives more freedom than traditional bivariate models by accommodating various marginal distributions. Therefore, Copula-based flood frequency analysis has emerged as a better option than conventional ones, and its empirical joint distribution has been proven superior to standard join parametric distribution [14, 15]. Copula models have been successfully applied in many fields including survival analysis [16–18], actuarial science [19, 20], and finance [21, 22] though their numbers are still rather limited at this stage.

Generally, Copulas can be parameterized by one or two parameters. Gaussian Copula, a member of Copula family, can be computed and simulated easily and can also be swiftly extended to arbitrary dimensions. Moreover, it can be uniquely defined by the correlation matrix of marginal distributions and therefore only requires calculating pairwise correlations. Gaussian Copula has been used in this study to estimate the joint CDF and joint bivariate return period of three flood parameters of the Johor River in Malaysia.

2   Materials and Methods

2.1   Case Study

The Johor River (Fig. 1) is located in the south of Peninsular Malaysia, covering an area of 2700 km^2. The topography of the catchment is undulating, but quite steep in the upstream. It has a tropical climate with a mean annual rainfall of 2470 mm, mean air temperature of 28.5 °C, and mean relative humidity of 85 %. This river is
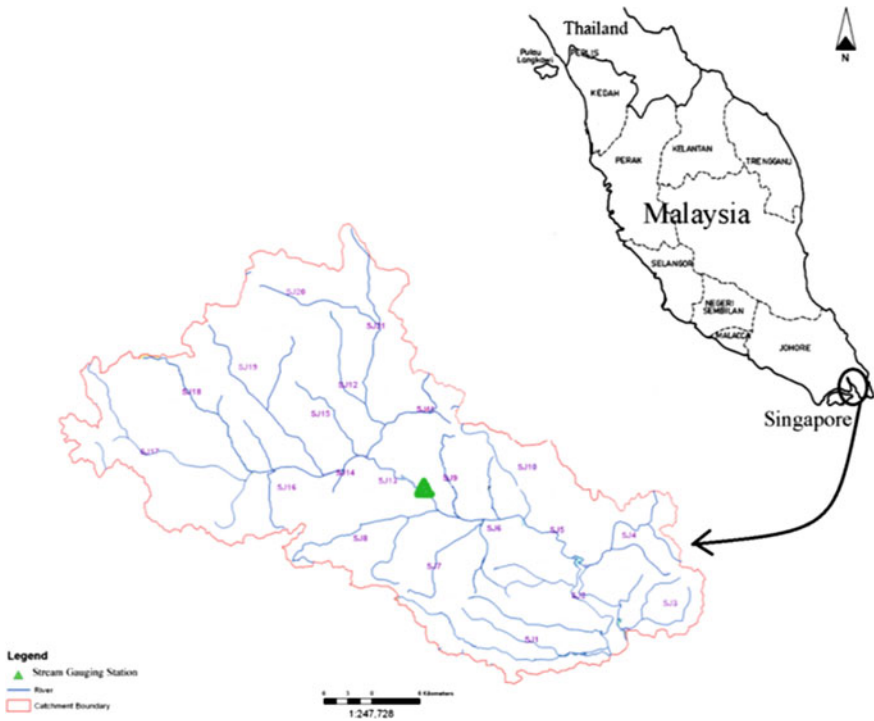
Fig. 1 Location of Johor River in south of peninsular Malaysia

selected since flood is a recurrent phenomenon in the basin. This study utilized 45-year hourly stream flow data of Johor River measured at the Rantau Panjang gauging station (01° 46′ 50″N and 103° 44′ 45″E) by the Department of Irrigation and Drainage (DID), Malaysia.

2.2 Determination of Flood Characteristics

The hourly river discharge data aforementioned were utilized to determine the annual flood peaks and its corresponding volume and duration. The initiation and ending of all flood events were marked using the method of [23, 24]. The peak flow (Q_p) was determined using the flood duration frequency approach [25], where the peak flow corresponds to the maximum amount of flood in each water year. The flood volume (V) is approximately the total water volume, and the flood duration (D) is the time elapsed during the flood event.

2.3 Modeling Peak flow, Flood Duration, and Flood Volume

The distribution of the flood variables was modeled using Generalized Pareto, Pearson, Exponential, Beta, and General Extreme Value distributions. The goodness-of-fit tests measure how well a random sample fits a theoretical PDF. In this study, the Kolmogorov–Smirnov (K-S) goodness-of-fit tests were conducted at a 5 % significance level.

2.4 Copula Function

The function of a Copula is a joint distribution with uniform random variables [26], which can be expressed as:

$$C : [0, 1]^n \rightarrow [0, 1]$$

Within the unit hypercube, every n dimensional hyper cube's probability has to be positive. Sklar's theorem [9] links the Copulas to the multivariate distributions, which means that the Copula can represent each multivariate distribution $F(t_1, ..., t_n)$ as:

$$F(t_1, \ldots, t_n) = C(F_{t_1}(t_1), \ldots, F_{t_n}(t_n)) \tag{1}$$

where $F_{t_i}(t_i)$ is the ith one-dimensional margin of the multivariate distribution. The Copula C becomes unique when the distribution is continuous. Nelsen [10] constructed Copulas from distribution function as:

$$C(u) = C(u_1, \ldots, u_n) = F\left(F_{t_1}^{-1}(t_1), \ldots, F_{t_n}^{-1}(t_n)\right) \tag{2}$$

If the corresponding dependence of a bivariate Copula is symmetrical, it can be expressed as:

$$C(u, v) = C(1 - u, 1 - v) - 1 + u + v \tag{3}$$

When the Copula density is symmetrical with the secondary diagonal of the unit square, i.e., $u = 1 - v$, the Copula density, c, fulfills the following condition:

$$C(u, v) = C(1 - u, 1 - v) \tag{4}$$

2.5 Gaussian (Normal) Copula

The normal Copula [27, 28] takes the form of:

$$C(u, v; \theta) = \Phi_G(\Phi^{-1}(u), \Phi^{-1}(v); \theta) \tag{5}$$

$$= \int\limits_{-\infty}^{\Phi^{-1}(u)} \int\limits_{-\infty}^{\Phi^{-1}(v)} \frac{1}{2\pi(1-\theta^2)^{1/2}} \times \left\{ \frac{-(x^2 - 2\theta xy + y^2)}{2(1-\theta^2)} \right\} dx dy \tag{6}$$

where $\Phi^{-1}(\cdot)$ is the inverse function of the standard normal distribution (CDF) $\Phi(\cdot)$ and θ is the linear correlation coefficient between $\Phi^{-1}(u)$ and $\Phi^{-1}(v)$ restricted to the interval $(-1, 1)$ which is explained in below.

2.6 Parameter Estimation of Copulas

The inference function for margin (IFM) method was used to determine the Copula parameter (θ), which is a parameter used to measure the degree of association between two univariate CDFs, using MATLAB coding in this research. Basically, this method has two steps:

1. Using two margins' log-likelihood functions, estimate α and β for the PDF of $f_x(x; \alpha)$ and $f_y(y; \beta)$, respectively. The two parameters α and β may have $\alpha_1, \alpha_2, \ldots, \alpha_i, \ldots, \alpha_m, i \in [1, m]$ and $\beta_1, \beta_2, \ldots, \beta_i, \ldots, \beta_n, j \in [1, n]$, respectively.
2. Use the estimated α and β to solve the general log-likelihood function to find θ through Eq. 7:

$$\begin{aligned} \ln L[f_{x,y}(x, y; \alpha, \beta, \theta)] = &\sum_{k=1}^{k} \ln C_\theta(F_X(x_k; \alpha), F_Y(y_k; \beta); \theta) \\ &+ \sum_{k=1}^{k} \ln[f_x(x_k; \alpha) + f_Y(y_k; \beta)] \end{aligned} \tag{7}$$

The accepted rang of Gaussian Copula parameter is $(-1 < \theta < 1)$.

2.7 Bivariate Joint Return Periods

For the bivariate case, the joint return period can be characterized in two ways: (i) Return period for $X \geq x$ AND $Y \geq y$, let the corresponding return period

represented by T_{XY}; (ii) Return period for $X \geq x$ OR $Y \geq y$, let the corresponding return period represented by T'_{XY}. The joint return periods, and, or Copula-based flood events can be expressed as follows [13, 29]):

$$T_{x,y} = \frac{1}{P(X \geq x \,\text{AND}\, Y \geq y)} = \frac{1}{1 - F_x(x) - F_y(y) + F_{x,y}(x,y)}$$
$$= \frac{1}{1 - F_x(x) - F_y(y) + C\left[F_x(x), F_y(y)\right]} \qquad (8)$$

$$T'_{x,y} = \frac{1}{P(X \geq x \,\text{OR}\, Y \geq y)} = \frac{1}{1 - F_{x,y}(x,y)} = \frac{1}{1 - C\left[F_x(x)F_y(y)\right]} \qquad (9)$$

Based on the above equations, the meaning of $T_{x,y}$ is the joint return period for variable X equal or greater then a certain value and variable Y equal to or greater than another certain value. On the other hand, the meaning of $T'_{x,y}$ is the joint return period for variable X equal or greater than a certain value or variable Y equal to or greater than another certain value [30].

3   Result and Discussion

3.1   Statistical Analysis

The summary of statistics for the flood parameters is given in Table 1. The observed averages of peak flow, flood duration, and flood volume at the study site were 248 m^3/s, 349 h, and 105 mm, respectively.

Table 2 presents the contribution of the shape parameter (κ), continuous scale parameter (σ), and continuous location parameter (μ) of various distributions used to fit flood variable data. Results of the K-S test showed that the Generalized Pareto distribution is most compatible with peak flow distribution. The best-fit distribution for the flood duration and volume distributions is the Generalized Extreme Value. The Kendall's rank correlations are tabulated in Table 3. The positive value of Kendall's rank correlation shows that the flood variables are dependent and satisfy the first condition of Copula [31].

Figures 2, 3, and 4 present the joint CDF of the peak flow and duration, peak flow and volume, and duration and volume based on Gaussian Copula, respectively. By horizontally cutting the joint cumulative distribution, a set of counter lines are obtained, which are also shown in the figures. It should be noted that for a given joint probability, there may exist more than one possible flood variable combinations. The contour lines of joint cumulative distribution of the peak flow and duration are depicted in Fig. 2. Joint cumulative distribution refers to the probability that a specified value of one variable will be exceeded at the same time with a specified value of a second variable. Therefore, the joint probability graph presented in Fig. 2

Table 1 The summary statistics of flood parameters

	Peak flow (m^3/s)	Duration (h)	Volume (mm)
Maximum	725	600	231
Minimum	77	144	20
Average	248	349	105
SD[a]	164	126	49

[a]Standard deviation. Volume in unit depth (mm) which is the flood volume (m^3) divided by the basin area

Table 2 Fitting result parameters for various distributions of flood variables

Flood variable	Best fitted distribution	Parameters
Peak flow (Q_P)	Gen. Pareto	$\kappa = -0.033905$
		$\sigma = 184.48$
		$\mu = 70.684$
Duration (D)	Gen. extreme value (GEV)	$\kappa = -0.20041$
		$\sigma = 122.45$
		$\mu = 299.35$
Volume (V)	Gen. extreme value (GEV)	$\kappa = -0.074$
		$\sigma = 42.82$
		$\mu = 83.01$

Note Based on the Kolmogorov–Smirnov test, the Generalized Extreme Value distribution is best fitted to flood volume and duration, and Gen. Pareto distribution is the best for peak flow

Table 3 Kendall's rank correlations and Copula linear correlation parameter among flood variables

	Peak flow-Duration	Peak flow-Volume	Duration-Volume
Kendall's rank correlation	0.472	0.015	0.333
θ	0.0165	0.6455	0.4397

refers to the chance of two conditions, namely peak flow and flood duration occurring at the same time. Joint cumulative contours, which are lines of equal probability of the variables, are simultaneous probability values indicated by any point on the contour. The amount of a CDF value is the probability of flood variables which call $P(x)$ to being less than or equal to the specific value. On the other hand, the probability of flood variables to exceed the specific value is $1 - P(x)$.

Figures 2, 3, and 4 show how joint distribution of two flood variables can be determined simultaneously and thus more meaningful for solving many problems of hydrological design. For example, for a given flood peak, it is possible to obtain the
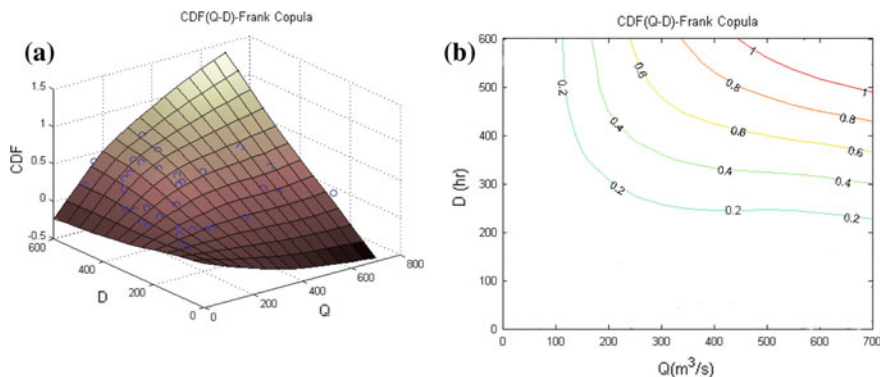
Fig. 2 The joint CDF $f(x, y)$ of peak flow (Q), duration (D), and the contour of $f(x, y)$ based on Gaussian Copula
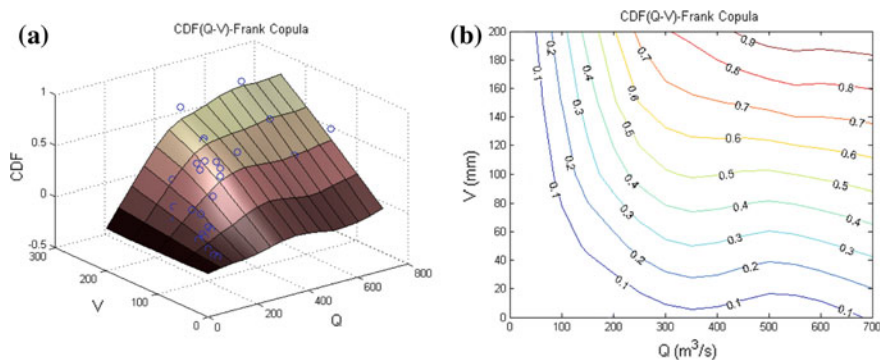
Fig. 3 The joint CDF $g(x, y)$ of peak flow (Q), volume (V), and the contour of $g(x, y)$ based on Gaussian Copula
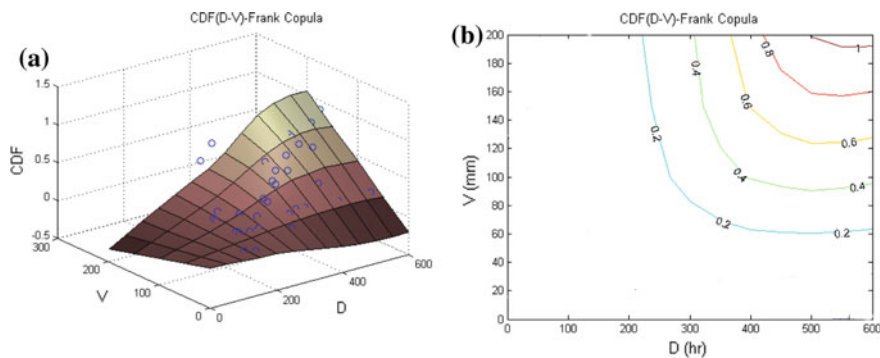
Fig. 4 The joint CDF $h(x, y)$ of duration (D), volume (V), and the contour of $h(x, y)$ based on Gaussian Copula

probability of non-occurrence of various combinations of flood duration and flood volume, and vice versa. In short, the figure allows one to obtain information concerning the occurrence probabilities of flood volume under the condition that a less than or equal to given flood peak or flood duration occurs, and vice versa.

The Copula-based joint CDF of peak flow and flood duration for Johor River based on the Gaussian Copula is shown in Eq. (10):

$$F(x,y) = \int_{-\infty}^{\phi^{-1}\left(1-\left(1-0.04\frac{x-70.684}{184.48}\right)^{\frac{1}{0.04}}\right)} \int_{-\infty}^{\phi^{-1}\left(\exp\left(-\left(1-0.2\left(\frac{y-299.35}{122.45}\right)\right)^{\frac{1}{0.24}}\right)\right)} 0.1592$$
$$\times \exp\left\{-\frac{x^2 - 0.033\,xy + y^2}{1.9995}\right\} dxdy \tag{10}$$

where $\phi =$ CDF of the standard normal and the ϕ^{-1} is the inversed standard normal.

Figure 2 revealed that the probabilities are between 0.2 and 1.0 based on the Gaussian Copula. Furthermore, it is possible to derive the probability of occurrence for each pair of given values of peak flow and duration. For example, for the peak flow values of less or equal to 113 m^3/s and duration less or equal to 229 h, the probability of occurrence is 0.2. Conversely, the probability of occurrence for peak flow exceeding 113 m^3/s and the duration exceeding 228 h is 0.8 (1–0.2).

The probabilities of occurrence of joint peak flow and duration based on the Gaussian Copula are 0.6,0.4, 0.2, and 0, when the peak flows are greater than 168 m^3/s, 241 m^3/s, 339 m^3/s, and 447 m^3/s and the durations greater than 296 h, 363 h, 433 h, and 492 h, respectively. Specifically, the joint probability of occurrence for this combination is close to 0 when the peak flow is greater than 447 m^3/s and duration greater than 492 h. Also, Fig. 2 shows that when the peak flow is equal to 113 m^3/s, the probability of not being exceeded is always 0.2 for all values of flood durations that fall on the 0.2 contour line.

Meanwhile, the Gaussian Copula-based joint CDF of peak flow and flood volume can be calculated as in Eq. 11 below:

$$\phi^{-1}G(x,y) = \int_{-\infty}^{\phi^{-1}\left(1-\left(1-0.03\frac{x-70.684}{184.48}\right)^{\frac{1}{0.04}}\right)} \int_{-\infty}^{\phi^{-1}\left(\exp\left(-\left(1-0.07399\left(\frac{y-83.017}{42.822}\right)\right)^{\frac{1}{0.07}}\right)\right)} 0.2084$$
$$\times \exp\left\{-\frac{x^2 - 1.291xy + y^2}{1.1667}\right\} dxdy$$
$$\tag{11}$$

Figure 3 depicts the contour lines generated from Eq. 11. For hydraulic design and hydraulic infrastructure operation, a combined occurrence of these two flood

characteristics is often important. The joint probability graph presented in Fig. 3 refers to the chance of peak flow and flood volume occurring simultaneously. In Fig. 3a, b, the probabilities are shown in intervals of 0.2 from 0 to 1.0.

The probabilities of joint peak flow and flood volume occurrence based on the Gaussian Copula were 0.8, 0.6, 0.4, 0.2, and 0, when the peak flow were greater than 81, 139, 202, 308, and 428 m^3/s and the flood volume greater than 19, 66, 113, 159, and 183 mm, respectively. It can be mentioned that the joint probability is 0.2 when the peak flow exceed 308 m^3/s and the flood volume is greater than 159 mm. The joint probability is almost zero when the peak flood exceeds 428 m^3/s and flood volume is more than 183 mm. On the other hand, when the peak flow is greater than 81 m^3/s, the probability of occurrence across all flood volumes is anticipated to be always 0.8.

The Copula-based joint CDF of flood duration-flood volume for Johor River based on the Gaussian Copula is calculated as in Eq. 12:

$$H(x, y) = \int_{-\infty}^{\phi^{-1}\left(\exp\left(-\left(1-0.2\left(\frac{x-299.35}{122.45}\right)\right)^{\frac{1}{0.2}}\right)\right)} \int_{-\infty}^{\phi^{-1}\left(\exp\left(-\left(1-0.07\left(\frac{y-83.017}{42.822}\right)\right)^{\frac{1}{0.09}}\right)\right)} 0.1772$$
$$\times \exp\left\{-\frac{x^2 - 0.8794xy + y^2}{1.6133}\right\} \mathrm{d}x\mathrm{d}y$$

(12)

Similar to Figs. 2 and 3, in Fig. 4, the contour lines of joint CDF for flood duration and flood volume based on Eq. 12 are shown. Similarly, it illustrates the chance of a certain amount of flood duration and flood volume occurring at the same time. As shown in Fig. 4, the probabilities of occurrence based on the Gaussian Copula were 0.8, 0.6, 0.4, 0.2, and 0, when the flood duration was greater than or equal to 221, 307, 368, 420, and 496 h while the flood volume was greater than or equal to 66, 96, 129, 159, and 194 mm. These are interpreted in such manner: assuming that the flood duration is greater than or equal to 420 h and the flood volume is not smaller than 159 mm, the joint probability of occurrence is thus 0.2. Also, if flood duration and flood volume are, respectively, smaller than 420 h and 159 mm, the joint probability now becomes 0.8. The probability is at its maximum (i.e., 0) when flood duration exceeds 496 h and flood volume exceeds 194 mm. Also, the probability is consistently 0.2 if the flood volume is less than 66 mm.

Figures 2, 3, and 4, show joint distribution of two flood variables can be determined simultaneously to help in solving many of hydrological design problems is shown. The graphs allow one to obtain information concerning the occurrence probabilities when two variables are recorded at certain values.

The contour lines for specific joint return periods, in which both peak flow and duration are exceeded (*TQD*), peak flow and volume are exceeded (*TQV*), and flood volume and duration are exceeded (*TVD*), have inward bounds as shown in Figs. 5a, 6a, and 7a, respectively, whereas the contour lines for specific joint return

periods, in which either peak flow or duration is exceeded ($T'QD$), peak flow or volume is exceeded ($T'QV$), and flood volume or duration is exceeded ($T'VD$), have outward bounds as shown in Figs. 5b, 6b, and 7b, respectively.

Figure 5a is derived from the Gaussian Copula and shows that for the bivariate joint return periods of 2, 5, 10, 20, 50, and 100 years, both peak flow and flood duration are, respectively, greater than or equal to 230 m³/s and 367 h; 391 m³/s and 447 h; 510 m³/s and 528 h; 623 m³/s and 580 h; 770 m³/s and 630 h; and 874 m³/s and 668 h. Therefore, the joint return period of occurrence of peak flow and flood duration is 50 years when peak flow is greater than 770 m³/s and flood duration is greater than 630 h. In addition, Fig. 5b shows the joint return period of peak flow or flood duration for 2, 5, 10, 20, 50, and 100 years when flood peak exceeds a specific value or flood duration exceeds another specific value.

Historical floods are analyzed by using the graphs given in Figs. 5a, b. The worst flood in the basin during the study period occurred in the year 1995–1996. The flood had a peak flow of 725 m³/s and duration of 192 h. The joint return periods derived from Gaussian Copula for this flood event TQD estimated using Eq. 7; $T'QD$ using Eq. 8 are 38.64 and 0.94 years, respectively. This means that the joint return period of peak flow and flood duration greater than or equal to 725 m³/s and 192 h, respectively, is 38.64 years, and the return period of either peak flow greater than 725 m³/s or flood duration greater than 192 h is only 0.94 year. The summary of bivariate joint return period of flood variables based on the Gaussian Copula from Figs. 5, 6, and 7 is as follow:

From Figs. 5a, 6a, and 7a, it can be noticed that for the same values of peak flow and duration, peak flow and volume, volume and duration, the joint return period of T is much greater than that of T'. For example, in the mentioned year 1995–1996,
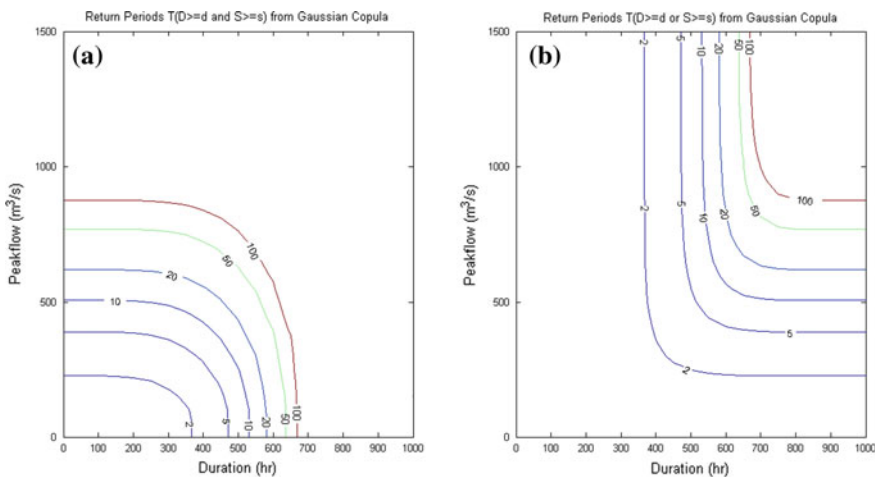
Fig. 5 Joint return periods of peak flow and duration based on the Gaussian Copula: **a** both duration and peak flow are exceeded, TQD (years); **b** either duration or peak flow is exceeded, T' QD (years)
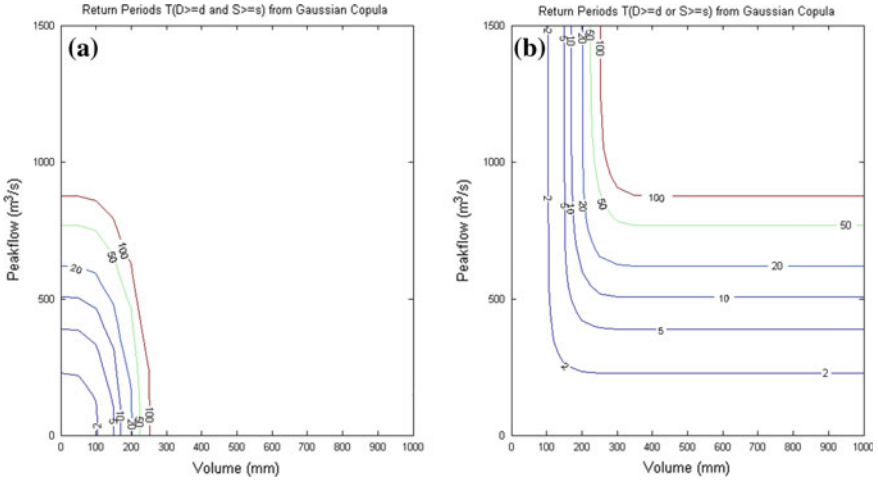
Fig. 6 Joint return periods of peak flow and volume based on the Gaussian Copula for **a** both volume and peak flow are exceeded, *TQV* (years); **b** either volume or peak flow is exceeded, *T'QV* (years)

for annual peak flow of 725 m³/s the corresponding flood duration was 192 h, the joint return periods for this flood event *TQD* is 38.64 years and *T'QD* is 0.94 year. Similar results are observed for joint return periods of volume and duration (i.e., *TVD* is greater than that of *T'VD*) and also joint return periods of peak flow and volume (i.e., *TQV* is greater than that of *T'QV*).
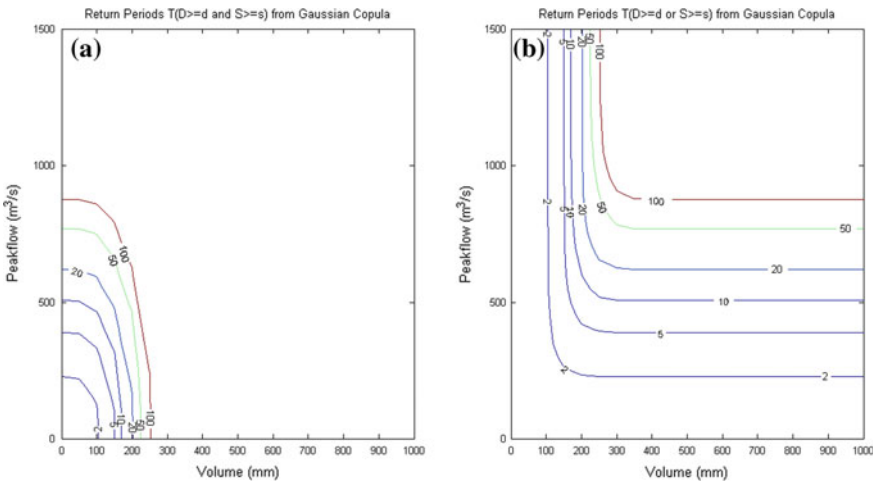
Fig. 7 Joint return periods of flood duration and volume based on the Gaussian Copula: **a** both flood duration and volume are exceeded, *TVD* (years); **b** either duration or volume is exceeded, *T' VD* (years)

4 Conclusion

The concept of Copula has been used in this paper to derive bivariate joint distributions for the Johor River Basin's flood characteristics. The modeling of flood variable function was done using the Generalized Pareto, Pearson, Exponential, Beta, and GEV distributions with their goodness of fit measured using the K-S test. The best fitted distribution functions were used to develop the joint CDFs of peak flow volume, volume duration, and peak flow duration using Gaussian Copula. Moderate correlations were found between peak flow and flood volume (Kendall's $\tau = 0.472$) as well as flood duration and flood volume (Kendall's $\tau = 0.333$). However, the peak flow and flood duration combination had a weak correlation (Kendall's $\tau = 0.015$). Statistically significant correlations between the flood variables are prerequisite for Gaussian Copula bivariate flood frequency analysis. The Copula parameter θ was applied to model the joint distributions of correlated flood variables for each pair based on the IFM method. Results showed that all calculated θ values were within the acceptable range and could be applied to compute the bivariate joint distribution of flood variables for Gaussian Copula families. By horizontally cutting the joint CDF, a set of contour lines were obtained for each Copula family which represented the occurrence probabilities for the joint variables at intervals of 0.2, 0.4, 06, 0.8, and 1.0 were obtained. The joint return periods for pair of flood variables were also calculated. For Gaussian Copula, the bivariate joint return periods of 2, 5, 10, 20, 50, and 100 years for peak flow (m^3/s) equal to or greater than and flood duration (h) equal to or greater than are (230 m^3/s, 367 h), (391 m^3/s, 474 h), (510 m^3/s, 528 h), (623 m^3/s, 580 h), (770 m^3/s, 630 h), and (874 m^3/s 668 h), respectively. For hydraulic design and hydraulic infrastructure operation, a combined occurrence of two flood characteristics is often important. Therefore, it is expected that the results of bivariate Copula frequency analysis could provide a better alternative for water resources management and flood risk assessment. Development of trivariate Copula functions for flood frequency analysis is recommended for future work. For simplicity, this can be achieved by performing bivariate analysis in two stages: first by determining the bivariate of variable pairs and then rerunning the bivariate of the paired variables with another variable. Examples of combinations include the bivariate of peak flow flood volume with flood duration; peak flow duration with flood volume; and flood volume flood duration with peak flow.

References

1. Almedeij J (2002) Modeling rainfall variability over urban areas: a case study for Kuwait. Sci World J 2012:8, Article ID. 980738. doi:10.1100/2012/980738

2. Goodarzi E, Mirzaei M, Ziaei M (2012) Evaluation of dam overtopping risk based on univariate and bivariate flood frequency analyses. Rev Can Genie Civ 39(4):374–387. doi:10.1007/978-94-007-5851-3_6

3. Goodarzi E, Ziaei M, Shu LT (2013) Evaluation of dam overtopping risk based on univariate frequency analysis. In: Introduction to risk and uncertainty in hydrosystem engineering. Springer, Netherlands, pp 101–121

4. Goodarzi E, Shui LT, Ziaei M (2014) Risk and uncertainty analysis for dam overtopping-case study: the Doroudzan Dam, Iran. J Hydro-Environ Res 8(1):50–61. doi:10.1016/j.jher.2013.02.001

5. Zhang L, Singh VP (2012) Bivariate rainfall and runoff analysis using entropy and Copula theories. Entropy 14(9):1784–1812. doi:10.3390/e14091784

6. Requena AI, Mediero L, Garrote L (2013) Bivariate return period based on Copulas for hydrologic dam design: comparison of theoretical and empirical approach. Hydrol Earth Syst Sci Dis 10(1):557–596. doi:10.5194/hessd-10-557-2013

7. Salvadori G, Michele CD (2013) Multivariate extreme value methods. In: Extremes in a changing climate. Springer, Netherlands, pp. 115–162

8. Chen LS, Tzeng IS, Lin CT (2013) Bivariate generalized gamma distributions of Kibble's type. Statistics, (ahead-of-print), 48(4). doi:10.1080/02331888.2012.760092

9. Sklar A (1959) Fonction de répartition à n dimensions et leurs marges. Publications de L' Institute de Statistique. Université de Paris. vol 8, pp 229–231

10. Nelsen R (1999) An introduction to Copulas. Springer, New York

11. Kao SC, Chang NB (2011) Copula-based flood frequency analysis at ungauged basin confluences: Nashville, Tennessee. J Hydrol Eng 17(7):790–799. doi:10.1061/(ASCE)HE.1943-5584.0000477

12. Chebana F, Dabo NS, Ouarda TBMJ (2012) Exploratory functional flood frequency analysis and outlier detection. Water Resour Res 48(4):W04514. doi:10.1029/2011WR011040

13. Reddy MJ, Ganguli P (2012) Bivariate flood frequency analysis of upper Godavari River flows using Archimedean Copulas. Water Resour Manage 26(14):3995–4018. doi:10.1007/s11269-012-0124-z

14. Zhang L, Singh VP (2006) Bivariate flood frequency analysis using the Copula method. J Hydrol Eng ASCE 11(2):150–164. doi:10.1061/(ASCE)1084-0699(2006)11:2(150)

15. Grimaldi S, Serinaldi F (2006) Design hyetographs analysis with 3-Copula function. Hydrol Sci J 51(2):223–238. doi:10.1623/hysj.51.2.223

16. Lee SH, Deng P, Lee EJ (2013) Analysis of multiple myeloma life expectancy using Copula. Int J Stat Probab 2(1):44. doi:10.5539/ijsp.v2n1p44

17. Swanepoel JWH, Allison JS (2013) Some new results on the empirical Copula estimator with applications. Statist Probab Lett 83(7):1731–1739. doi:10.1016/j.spl.2013.03.027

18. Cao C, Kobayashi M (2013) Testing for single against competing risks models in survival analysis. Soc Sci Res Netw. doi:10.2139/ssrn.2202152

19. Zhang L, Duan B (2013) Extensions of the notion of overall comonotonicity to partial comonotonicity. Insur Math Econo 52(3):457–464. doi:10.1016/j.insmatheco.2013.01.009

20. Cossette H, Côté MP, Marceau E, Moutanabbir K (2013) Multivariate distribution defined with Farlie-Gumbel-Morgenstern Copula and mixed Erlang marginals: aggregation and capital allocation. Insur Math Econ 52(3):560–572. doi:10.1016/j.insmatheco.2013.03.006

21. Lim KG (2013) Choice of Copulas in explaining stock market contagion. In: Uncertainty analysis in econometrics with applications. Springer, Berlin, pp 129–140

22. Salazar Y, Ng WL (2013) Nonparametric tail Copula estimation: an application to stock and volatility index returns. Commun Statist Simul Comput 42(3):613–635. doi:10.1080/03610918.2011.650256

23. Hewlett JD, Hibbert AR (1967) Factors affecting the response of small watersheds to precipitation in humid areas. For Hydrol 1:275–290
24. Yusop Z, Douglas I, Nik AR (2006) Export of dissolved and undissolved nutrients from forested catchments in Peninsular Malaysia. For Ecol Manage 224(1):26–44. doi:10.1016/j.foreco.2005.12.006
25. Cunderlik JM, Ouarda TBMJ (2006) Regional flood-duration-frequency modeling in the changing environment. J Hydrol 318(1):276–291. doi:10.1016/j.jhydrol.2005.06.020
26. Cong RG, Brady M (2012) The interdependence between rainfall and temperature: Copula analyses. Sci World J 2012:11, Article ID. 405675
27. Cossin D, Schellhorn H, Song N, Tungsong S (2010) A theoretical argument why the t-Copula explains credit risk contagion better than the Gaussian Copula. Adv Decis Sci 2010:29, Article ID. 546547
28. Notsu A, Kawasaki Y, Eguchi S (2013) Detection of heterogeneous structures on the gaussian Copula model using projective power entropy. ISRN Probab Stat 2013:10p, Article ID: 787141. doi:10.1155/2013/787141
29. Shiau JT, Wang HY, Chang TT (2006) Bivariate frequency analysis of floods using Copulas. JAWRA J Am Water Resour Assoc 42(6):1549–1564. doi:10.1111/j.1752-1688.2006.tb06020.x
30. Shiau JT (2003) Return period of bivariate distributed extreme hydrological events. Stoch Env Res Risk Assess 17(1–2):42–57. doi:10.1007/s00477-003-0125-9
31. De Michiels F, Schepper A (2008) A Copula test space model how to avoid the wrong Copula choice. Kybernetika 44(6):864–878

Part III
Rainfall-Runoff Modelling

Identification of Seasonal Rainfall Peaks at Kelantan Using Fourier Series

Noridayu Mah Hashim, Sayang Mohd Deni, S. Sarifah Radiah Shariff, Wardah Tahir and Janmaizatul Jani

Abstract This study aimed to identify the wet period, peaks of mean rainfall amount per rainy day at Kelantan River basin. Daily rainfall data from 12 selected rainfall stations for the period of 1975–2014 which comprises of three main areas such as inland, river, and coastal are analyzed. The estimated wet period, date, and value at peak of mean rainfall amount per rainy day will be identified using Fourier series and compared with the actual flood events in 2013/2014 and 2014/2015. The findings indicate that duration of wet periods obtained from the results of best fitting justifies the flood event occurred most recently. Moreover, the coastal area of Kelantan also shows the highest probability of rainfall amounts exceeding 60 mm.

Keywords Daily rainfall · Fourier series · Gamma distribution · Generalized linear model · Deviance

1 Introduction

In the analysis of rainfall variability, particularly on the precipitation amounts, the sequence of wet days is becoming important in managing water resources not only in Malaysia but also throughout the world. Identifying seasonal rainfall peak period provides useful information in predicting future climatic events since these variables are closely related to extreme weather events such as floods and landslides.

N. Mah Hashim (✉) · S. Mohd Deni · S.S.R. Shariff
Center for Statistical and Decision Science Studies, Faculty of Computer and Mathematical Sciences, Universiti Teknologi Mara (UiTM), 40450 Shah Alam, Selangor, Malaysia
e-mail: mimimarina_ayu@yahoo.com

W. Tahir · J. Jani
Faculty of Civil Engineering, Universiti Teknologi Mara (UiTM), 40450 Shah Alam, Selangor, Malaysia

Most recently, the widespread flooding which occurred in Kelantan from November to December 2014 contributed to around RM 2.81 billion losses to the country. The flood that drowned most of the areas in Kelantan is seen as the most disastrous flood event in the history of Malaysia, which caused 14 deaths and 319,156 victims evacuated to safety. Thus, it is important to further investigate the chances of heavy flood to occur especially during monsoon seasons.

Rainfall has a seasonal variation which caused frequent changes in rainfall parameters and rainfall amount throughout the year. The variations could be handled by deriving separate parameter sets for each month of the year. Unfortunately, this would cause a large number of parameters to be estimated in the models. Based on some previous studies by Jimoh and Webster [1] for Nigeria and Woolhiser and Pegram [2] for US data set, the Fourier series was found to be the best method in smoothing the model parameter of periodic function. This would then help to describe the rainfall pattern and its temporal variation concisely.

Moreover, the study on comparing and investigating various methods of periodogram analysis was conducted by Kottegoda et al. [3]. The analysis was mainly focused on periodicity and persistency in daily rainfall. Besides that, the optimum number of Markov chain model was also applied in determining the persistency in daily rainfall occurrence.

Gamma distribution is commonly used in modeling rainfall amount of wet days [4]. The parameter of gamma distribution may change throughout the year. A gamma distribution was fit by Buishand using a Fourier series to the mean. Coe and Stern [5] and Stern and Coe [6] applied the Fourier series to model parameter of gamma distributions in analyzing rainfall distribution for several stations in Africa and Sri Lanka. Results from this method will help in providing summarized statistics which would enable the rainfall pattern to be compared between areas (Fig. 1).

The comparison of rainfall patterns between stations on the east and west coasts of Peninsular Malaysia using Fourier series had been conducted by Suhaila and Jemain [7]. The findings indicated that the western areas have a bimodal pattern and best described with two harmonics. On the other hand, four harmonics of Fourier series are required for the stations located in the eastern area which exhibit unimodal pattern of rainfall. Unfortunately, none of the rainfall stations under their study involved Kelantan region which was the most disastrous areas during the flood event occurred in Peninsular Malaysia recently.

Therefore, further analysis on investigating the seasonal rainfall peaks which contributes to flood event at Kelantan will be conducted in this study. In order to model time of dependence throughout the year using Fourier series, the approach taken by Coe and Stern [5] and some other previous researchers in the field will be adopted. A generalized linear model (GLM) will be used to model those rainfall distributions which vary as a function of time of year. Daily rainfall amount as well

Fig. 1 Location of twelve selected rainfall stations at Kelantan

as mean rainfall per rainy day will be analyzed, and the results on different harmonics of the rainfall patterns and seasonal peak periods will be compared based on three different regions at Kelantan such as inland, river, and coastal areas.

2 Data

Daily rainfall data from the selected twelve rain gauge stations at Kelantan were collected from Malaysian Department of Irrigation and Drainage for the period of 1975–2014, which gives a total of 40 years' worth of data. A wet day is defined as a day with a rainfall at least 1 mm.

The data used in this study as shown in Table 1 could be considered a good quality data with less than 21 % missing values throughout the 40-year period. The missing values in the data series for the period of 1975–2014 are estimated using various types of modified weighting methods such as neighboring stations [8, 9], imputation, and log transformation.

It can be seen clearly in Table 1 that the mean rainfall amount ranges between 257.2 and 309.7 mm for all areas. The highest rainfall intensity is 18.3 mm per day that is observed at Ibu Bekalan Tok Uban at the river area. Moreover, further analysis also shows that this area possesses the highest mean number of rainy days throughout a 40-year period of records.

Table 1 The percentage of missing rainfall data and the summary of statistics for twelve selected rainfall stations at Kelantan

No station	Area	Name	Missing (%)	Mean amount (mm)	Intensity (mm/day)	Mean rainy days (day)
4819027	Inland	Gua Musang	0.1	257.30	13.95	165.90
5422046		Ldg. Lapan Kabu	5.9	262.30	15.98	140.60
5722057		JPS Machang	19.0	284.50	14.75	162.90
5821007		K'api Bukit Panau	14.2	278.00	17.00	137.15
6122064		Kota Bahru	0.0	282.20	17.21	133.78
5522047	River	JPS Kuala Krai	1.0	267.00	15.62	146.83
5322044		Kg. Laloh	11.6	263.70	13.42	172.83
5320038		Dabong	9.8	258.10	13.38	168.23
5921009		Ibu Bekalan Tok Uban	0.0	309.40	18.30	142.48
6024074	Coastal	Jabatan Pertanian Bachok	20.3	309.70	15.23	167.20
5824080		Kg Beris	8.8	292.70	15.65	153.68
6121067		Stesen Keretapi Tumpat	1.1	267.10	17.05	126.25

3   Methodology

This section explains on the methodology used to fit Fourier series to daily rainfall data and evaluating the deviances.

Based on the research conducted by Firth [10] and some other researchers, gamma distribution performed slightly better than lognormal model in representing daily rainfall amount [11]. Therefore, gamma distribution was chosen in this study. Supposed the model is fitted to the T days of the year with day $t = t_1, t_2, \ldots, t_T$ and $T = 365$. The amount of rain day t at the year i is $x_i(t)$, $i = 1, 2, \ldots, n(t)$, where $n(t)$ represent the number of years in which day t had rained. The observations follow a gamma distribution with a density function of:

$$f(x) = \frac{\left(\frac{k}{\mu(t)}\right)^k x_i(t)^{k-1} \exp\left(-\frac{kx_i(t)}{\mu(t)}\right)}{\Gamma(k)}, \quad x_i(t) > 0, \ \mu(t) > 0 \tag{1}$$

where $\mu(t)$ is the mean rainfall on day t with a condition that day t is wet and $1/\sqrt{k}$ is the coefficient of variation of the distribution. The mean rain per rainy day may change throughout the year but the coefficient of variation $1/\sqrt{k}$ is assumed to remain constant for all values of t. Stern and Coe [6] suggested that the value of k is estimated based on the between-day deviances. Based on their suggestion, as

reported by Suhaila and Jemain [7], the approximate value of k is obtained based on the proportion of T (days of a year) with respect to residual between-day deviances.

Fourier series is always being chosen as the smoothing function due to its capability in fitting both the unimodal and bimodal seasonal patterns [1, 12]. Moreover, the fitted curves are able to connect at the beginning and end of the year. The independent variables are the functions of the time of year, and the dependent variables are the parameters for the gamma distributions for rainfall amounts. The Fourier series is expressed as follows:

$$g(t) = A_0 + \sum_{j=1}^{m} \left(A_j \sin(jt')B_j \cos(jt') \right) \qquad (2)$$

where j is the harmonic, m is the maximum harmonic required for the series, A_j and B_j are the parameter estimates for Fourier series obtained by using the maximum-likelihood method. The performance of the Fourier series in describing seasonal behavior can be assessed using deviance.

Deviance is the statistical term used to describe or measure the discrepancy or correspondence of fit in the form of log likelihood ratio [11]. In this study, the deviance is divided into two components, namely the 'between-day deviance' and the 'within-day deviance' which had been explained by Suhaila and Jemain [7].

4 Result and Discussion

4.1 Number of Harmonics and Estimated Values of K

Table 2a–c shows the analysis of deviance obtained based on the results of fitting the Fourier series to the observed data for each area, i.e., inland, river, and coastal. The amount of rainfall for each station is combined and averaged according to these areas. Table 2a–c also shows that the total numbers of rainy days are 9435, 8970, and 7683 days for inland, river, and coastal areas, respectively. The results indicate that three harmonics of Fourier series are appropriate to model the mean rainfall per rainy day for the station in inland and river areas. Meanwhile, that of coastal area is found to be more appropriate with two harmonics of Fourier series model. Further analysis on larger number of harmonics is not required since they do not reduce the deviance significantly.

As mentioned previously, the approximate value of k is obtained based on the proportion of T (days of a year) with respect to residual between-day deviances. The estimated value of k for each area is shown in Table 3.

These values will affect the proportion of extreme observations, as it will increase as k decreases. Similarly, the coefficient of variation will also increase as k decreases. The analysis on the shape of gamma distribution based on its parameter value k shows that its lowest value occurs at coastal areas. This indicates that much

Table 2 Analysis of deviance for mean rainfall per rainy days at (a) inland area (b) river area (c) coastal area

Source	Degree of freedom	Deviance	Mean deviance	F	P-value
(a)					
Between day	364	857.94	–	–	–
One harmonic	2	429.22	214.61	279.22	2.2e−16
Two harmonics	2	69.88	34.94	45.46	2.2e−16
Three harmonics	2	55.32	27.66	35.99	5.82e−15
Four harmonics	2	52.39	26.20	34.08	2.87e−14
Residual	354	251.13	0.71	–	–
Within days	9071			–	–
Total	9435		–	–	–
(b)					
Between day	364	743.90	–	–	–
One harmonic	2	356.32	178.16	286.73	2.2e−16
Two harmonics	2	87.94	43.97	70.76	2.2e−16
Three harmonics	2	30.14	15.07	24.25	1.346e−10
Four harmonics	2	37.87	18.94	30.47	6.07e−13
Residual	354	231.63	0.65	–	–
Within days	8606			–	–
Total	8970		–	–	–
(c)					
Between day	364	1577.18	–	–	–
One harmonic	2	749.23	374.62	292.49	2.2e−16
Two harmonics	2	148.00	74.00	57.78	2.2e−16
Three harmonics	2	166.99	83.50	65.19	2.2e−16
Four harmonics	2	67.54	33.77	26.37	2.10e−11
Residual	354	445.41	1.26	–	–
Within days	7319			–	–
Total	7683		–	–	–

Table 3 The estimated values of k

Area	Calculation	Estimate k values
Inland	365/251.13	1.45
River	365/231.63	1.58
Coastal	365/445.41	0.82

larger variations in the mean rainfall per rainy day are observed at the coastal areas compared to the other two areas. River area exhibits the highest k values with almost twice more than the coastal areas, which receive lesser variation in the mean rainfall amount per rainy day.

4.2   Identifying the Seasonal Rainfall Peaks

The summary statistics of the mean rainfall amount at the three different areas based on the selected harmonic of Fourier series is given in Table 4.

Based on the results of the best fitted of two and three harmonics of Fourier series, it shows that the mean rainfall amount ranges from approximately 7–27.3 mm per day. Figure 2a–c describes the fitted curves for the observed mean rainfall values per rainy day at each of the three areas in Kelantan. The quartile thresholds of 25th percentile and the 75th percentile obtained from the fitted curves are used to distinguish between the dry and wet periods. The values that are smaller than the lower quartile could be considered as the dry period, while the values that are greater than the upper quartile are assumed as the wet period. Referring to Fig. 2c, the coastal area exhibits larger variation of mean rainfall per rainy day where more extreme cases occurred toward the end of the year. The findings support the results shown in Table 3 where this area experiences of having the lowest k values. Generally, the months of November and December receive greater amount of rainfall since the mean amount of rainfall per rainy day during these periods was observed above the upper quartile threshold which may be due to Northeast monsoon season. This finding seems to be in agreement with the results obtained by Suhaila and Jemain [7] who reported that the eastern areas of Peninsular Malaysia showed unimodal pattern with the larger amount of rainfall received during this monsoon period.

Table 5 shows the estimated wet period duration, the date, and the value at peak of mean rainfall per rainy day and the actual date of flood events occurred during 2013/2014 and 2014/2015 which consists of three and two wave phases, respectively. The flood events brought about heavy losses, including loss of life in many areas in Kelantan. The findings show that the date at the estimated rainfall peak based on the results of Fourier series falls during the duration of the actual date of flood event at almost all stations except Gua Musang station. There are three stations, Keretapi Bukit Panau, Ibu Bekalan Tok Uban, and Stesen Keretapi Tumpat, which experienced having floods during the two waves phases for the past two years of flood events. Therefore, there is a high possibility of flood event to occur at these stations in the future. The findings obtained here are very useful for monitoring and predicting the extreme future climatic event such as flood and landslides.

Table 4   Summary statistics of mean rainfall per rainy day based on the selected harmonic at three areas

Area	No of harmonics	Min	1st Quartile	3rd Quartile	Max
Inland	3	7.00	8.58	11.80	21.22
River	3	8.21	8.96	12.55	20.84
Coastal	2	8.01	10.48	18.47	27.30

Fig. 2 Observed (*dots*) and fitted (*curves*) rainfall or rainy days for each area and the coefficient of the Fourier series. **a** Inland area with three harmonics and estimate $k = 1.45$, $A_0 = 2.34$, $A_1 = 0.18$, $B_1 = -0.32$, $A_2 = -0.12$, $B_2 = 0.11$, $A_3 = 0.18$, $B_3 = 0.01$; **b** River area with three harmonics and estimate $k = 1.58$, $A_0 = 2.39$, $A_1 = 0.17$, $B_1 = -0.29$, $A_2 = -0.12$, $B_2 = 0.14$, $A_3 = 0.13$, $B_3 = -0.03$; **c** Coastal area with two harmonics and estimate $k = 0.82$, $A_0 = 2.60$, $A_1 = 0.13$, $B_1 = -0.45$, $A_2 = -0.26$, $B_2 = 0.00$
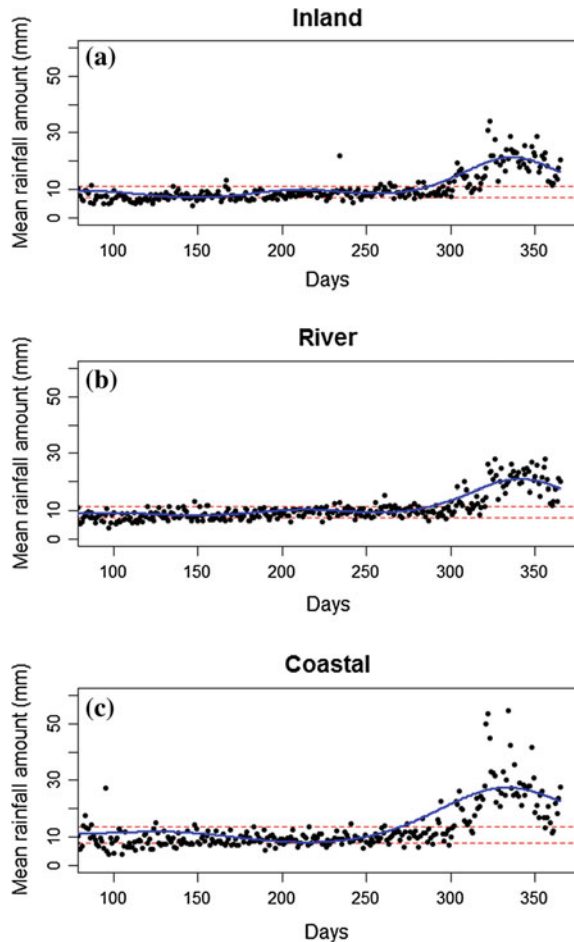
4.3 Comparing Probability of Rainfall Amounts Exceeding Threshold

An amount of 30 mm is a common value recorded at the station in Kelantan especially during December. According to the report of Drainage and Irrigation Department of Malaysia (*Bhgn. Sumber Air dan Hidrologi* 2015), the threshold of 60 m could be considered as heavy rainfall leading to flood occurrence. Using a gamma density function as mentioned previously, together with estimated shape parameter, k, and the fitted mean rainfall values on a particular day, the estimated probability of amounts that exceed 60 mm can be determined.

Table 5 The estimated wet period, the date, the and value at peak of mean rainfall per rainy day and the actual flood events

Area	Station	Wet period duration	Date at peak	Value at peak	Actual flood event	
					2013/2014	2014/2015
Inland	Gua Musang	28 Aug–17 Nov	13 Oct	14.33	–	2nd wave: 14 Dec–3 Jan
	Ldg Lapan Kabu	28 Oct–26 Jan	9 Dec	31.47	2nd wave: 30 Nov–11 Dec	2nd wave: 14 Dec–3 Jan
	JPS Machang	1 Nov–30 Jan	21 Dec	26.91	2nd wave: 30 Nov–11 Dec	2nd wave: 14 Dec–3 Jan
	K'api Bukit Panau	24 Oct–22 Jan	8 Dec	20.90	2nd wave: 30 Nov–11 Dec 3rd wave: 9–14 Jan	2nd wave: 14 Dec–3 Jan
	Kota Bahru	30 Oct–29 Jan	10 Dec	44.65	–	2nd wave: 14 Dec–3 Jan
	Overall (*Inland*)	19 Oct–17 Jan	2 Dec	23.90		
River	JPS Kuala Krai	4 Nov–2 Feb	19 Dec	24.81	2nd wave: 30 Nov–11 Dec	2nd wave: 14 Dec–3 Jan
	Kg Laloh	19 Oct–12 Jan	5 Dec	22.06	2nd wave: 30 Nov–11 Dec	2nd wave: 14 Dec–3 Jan
	Dabong	13 Oct–12 Jan	1 Dec	15.12	–	2nd wave: 14 Dec–3 Jan
	Ibu Bekalan Tok Uban	10 Oct–16 Jan	7 Dec	30.55	2nd wave: 30 Nov–11 Dec 3rd wave: 9–14 Jan	2nd wave: 14 Dec–3 Jan
	Overall (*River*)	22 Oct–21 Jan	7 Dec	19.45		
Coastal	Jbtn Pertan. Bachok	20 Oct–31 Dec	27 Nov	40.82	–	2nd wave: 14 Dec–3 Jan
	Kg Beris	17 Oct–15 Jan	29 Nov	38.26	2nd wave: 30 Nov–11 Dec	2nd wave: 14 Dec–3 Jan
	Stsn K'api Tumpat	24 Oct–2 Jan	28 Nov	25.66	2nd wave: 30 Nov–11 Dec 3rd wave: 9–14 Jan	1st wave: 17–23 Nov 2nd wave: 14 Dec–3 Jan
	Overall (*Coastal*)	17 Oct–15 Jan	29 Nov	30.12		

Two observations can be interpreted: firstly, the percentage of the amount of rain that falls on a particular day that contributes to the threshold values, and secondly, the particular day of the year that has the highest probability of exceeding the threshold values.

Probability of amount exceeding 60 mm is calculated and averaged for the three areas in Kelantan, and the results are given in Table 6. The probability of amount exceeding 60 mm for inland area varies between 11.9 and 23.7 %. A five-day duration, which is from 30 November to 4 December, gives the highest probability with 23.7 % of the amount that falls on these days contributing to more than 60 mm per day. The highest probability for river area is observed during the early December, which is from 5 until 9 December. The percentage of amount starts to

Table 6 Probability of amounts that contribute to more than 60 mm for November and December

Date	Inland	River	Coastal	Date	Inland	River	Coastal
1-Nov	0.119	0.101	0.269	12-Dec	0.222	0.224	0.312
–	–	–	–	13-Dec	0.219	0.223	0.311
25-Nov	0.229	0.208	0.323	14-Dec	0.216	0.221	0.309
26-Nov	0.231	0.211	0.323	15-Dec	0.212	0.219	0.307
27-Nov	0.233	0.213	0.323	16-Dec	0.208	0.217	0.305
28-Nov	0.235	0.216	**0.324**	17-Dec	0.204	0.214	0.302
29-Nov	0.236	0.218	**0.324**	18-Dec	0.200	0.212	0.300
30-Nov	**0.237**	0.220	**0.324**	19-Dec	0.196	0.209	0.297
1-Dec	**0.237**	0.222	0.323	21-Dec	0.191	0.205	0.295
2-Dec	**0.237**	0.224	0.323	22-Dec	0.186	0.202	0.292
3-Dec	**0.237**	0.225	0.323	23-Dec	0.181	0.199	0.289
4-Dec	**0.237**	0.226	0.322	24-Dec	0.176	0.195	0.287
5-Dec	0.236	**0.227**	0.321	25-Dec	0.171	0.191	0.284
6-Dec	0.235	**0.227**	0.320	26-Dec	0.166	0.187	0.281
7-Dec	0.234	**0.227**	0.319	27-Dec	0.161	0.183	0.278
8-Dec	0.232	**0.227**	0.318	28-Dec	0.155	0.178	0.274
9-Dec	0.230	**0.227**	0.317	29-Dec	0.150	0.174	0.271
10-Dec	0.228	**0.226**	0.316	30-Dec	0.145	0.169	0.268
11-Dec	0.225	**0.225**	0.314	31-Dec	0.134	0.160	0.261

The significant of bold indicates the highest probability amount that contributes to more than 60mm for November and December at Inland, River and Coastal

drop from the period of the highest probability at inland and river area to the end of December where only 13.4 and 16 % of the amount on 31 December exceeds 60 mm per day, respectively. The highest probability of amount exceeding 60 mm at coastal area is computed at the end of November until early December, with 32.4 %. The probability then begins to decrease until it reaches the lowest at 26.1 % recorded at the end of December.

These results indicate that the rainfall patterns between the three areas are almost the same. In all cases, the highest probability occurred at the same period of the second wave of the actual flood events in 2013/2014, which is from 30 November until 11 December.

5   Conclusion

The rainfall distribution at twelve rainfall stations which comprises of inland, river, and coastal areas in Kelantan is compared using the Fourier series. The results obtained by using the Fourier series can describe the seasonal variation of the model parameters as well as determining the number of harmonics required at each area. In

addition, the estimated wet period, the dates, and the values at rainfall peaks and the probability of amounts falling that exceed certain threshold values are identified and then compared with the actual flood events during 2013/2014 and 2014/2015. Three harmonics are appropriate for the inland and river areas; meanwhile, the coastal area is more suitable with two harmonics model of Fourier series. In terms of wet periods, October until the early January can be considered as the wettest months with the peak periods are around the end of November until the middle of December.

The fitted curves provide a good summary of statistics and provide useful information for describing the rainfall patterns and variability of studied areas.

References

1. Jimoh OD, Webster P (1999) Stochastic modeling of daily rainfall in Nigeria: intra-annual variation of model parameters. J Hydrol 222:1–17
2. Woolhiser DA, Pegram GGS (1979) Maximum likelihood estimation of Fourier coefficients to describe seasonal variations of parameters in stochastic daily precipitation models. J Appl Meteorol 18(1):34–44
3. Kottegoda NT, Natale L, Raiteri E (2004) Some considerations of periodicity and persistence in daily rainfalls. J Hydrol 296:23–37
4. Edelsten PR (1976) A stochastic model of the weather at Hurley in S.E. Engl Meteorol Mag 105:206–214
5. Coe R, Stern RD (1982) Fitting models to daily rainfall data. J Appl Meteorol 21:1024–1031
6. Stern RD, Coe R (1984) A model fitting analysis of daily rainfall data. J Roy Stat Soc Ser A 147:1–34
7. Suhaila J, Jemain AA (2009) A comparison of the rainfall pattern between stations on the east and west coasts of Peninsular Malaysia using the smoothing model of rainfall amounts. Meteorol Appl 16:391–401
8. Suhaila J, Deni SM, Jemain AA (2008) Detecting inhomogeneity of rainfall series in Peninsular Malaysia. Asia-Pac J Atmos Sci 44(4):369–380
9. Sullivan DO, Unwin DJ (2003) Geographic information analysis. Wiley, Hoboken
10. Firth D (1988) Multiplicative errors: lognormal or gamma? J Roy Stat Soc Ser B 50:266–268
11. McCullagh P, Nelder JA (1989) Generalized linear models. Chapman and Hall, London
12. Garbutt DJ, Stern RD, Dennett MD, Elston J (1981) A comparison of the rainfall climate of eleven places in West Africa using a two part model of daily rainfall. Arch Meteorol Geophys Bioclimatol Ser B 29:137–155

Application of HEC-GeoHMS and HEC-HMS as Rainfall–Runoff Model for Flood Simulation

Salwa Ramly and Wardah Tahir

Abstract Flood modeling and simulation assist in the prediction of the hazard for better flood preparedness and thus reduce flood damages. The study had simulated flood occurrence at the upper Klang–Ampang River Basin which is a flood-prone area near the capital city of Malaysia. Digital elevation model (DEM) for this area was processed in the ArcGIS 10.2 environment using terrain preprocessing tools to delineate the basin, sub-basin, and stream network. Results from the terrain preprocessing were used in the HEC-GeoHMS to extract the hydrologic parameters of the river basin. These hydrologic parameters were used in the estimation of streamflow runoff in HEC-HMS. The study had produced an illustrative and comprehensive representation of the sub-basin with reasonable accuracy indicated by the Nash–Sutcliffe coefficient of 0.86.

Keywords Rainfall–runoff model · HEC-GeoHMS · HEC-HMS

1 Introduction

Flooding is a natural phenomenon caused by various factors. Flooding also varies in terms of size of the affected area, flood duration, and depth of flood. Flooding happens when the normally dry areas have been inundated with water. Among the factors that could cause flood are excessively heavy and prolonged rainfall, urbanization, river erosion, deforestation, and poor drainage systems. Therefore, analysis on flood event is important to understand the response of the catchment to the heavy rainfall and the change of the land use. Nowadays, with the advance of the geographic information system (GIS), analysis of the flood using rainfall–runoff model has been enhanced to get better simulation and result.

Application of GIS in rainfall–runoff model is widely used to estimate the catchment characteristics based on the digital elevation data. Digital elevation

S. Ramly (✉) · W. Tahir
Faculty of Civil Engineering, University Technology MARA, Shah Alam, Malaysia
e-mail: salwaramly@yahoo.com

model (DEM) is a digital model with 3D view representing the terrain of surface catchment or area. DEM is in raster format, and each pixel value of the raster data represents an elevation of the point. There are many techniques to produce the DEM data, and it depends on the resolution needed for the study. Remote sensing is the most common technique used for data collection of digital terrain model (DTM) before its conversion to DEM. However, DEM can also be generated from land surveying techniques or topographic map using GIS program. Most common GIS program is ArcGIS from ESRI. ArcGIS could convert vector data from terrain line in topographic map and produce the DEM as a raster format file. This DEM could be used to determine the catchment characteristics such as streamline and drainage network and delineate the basin and sub-basin [1]. This information could be used as hydrologic parameter value for rainfall–runoff modeling. DEM also has been widely used for flood and drainage modeling, land use studies, and other applications [2–4].

Rainfall–runoff model describes the relationship between rainfall and runoff of a catchment area. The model will estimate the surface runoff in the channel or river system as a response to rainfall input data for the target catchment. There are numerous rainfall–runoff model software programs available, and each has its own advantages and disadvantages. One of the widely used rainfall–runoff model software programs is the HEC Hydrologic Modelling System (HEC-HMS).

The HEC-HMS mathematical model is designed to simulate the complete hydrologic processes of dendritic catchment [5]. The model will simulate rainfall–runoff and routing processes in natural or controlled watershed. It shall predict flow, stage, and timing for giving rainfall input into the basin. Hydrographs from the program are useful for water resources studies such as for flood forecasting, water availability, urban drainage design, or reservoir design. Combination between HEC-HMS and GIS, impact of the land use change in the catchment could be analyzed based on the increment of the stream flow in the river system.

Application of HEC-HMS in the rainfall–runoff model has been used in various objectives of the study. One important objective of the study using HEC-HMS is for flood forecasting. [6] conducted a study on regional-scale flood modeling using radar, GIS, and HEC-HMS/HRAS for the San Antonio River Basin, USA. The study found that the model has the capability to perform hydrologic studies on a regional scale for a large watershed. The other study by Oleyiblo [7] also conducted a study on flood forecasting by using HEC-HMS in Misai an Wan'an catchments in China. From the study, the model predicted peak discharge accurately and the author concluded the HEC-HMS is suitable for flood forecasting at the studied catchments. Besides flood forecasting purposes, HEC-HMS is also suitable to be used in the analysis of the land use change. A study was conducted by Ali et al. [8] on the impacts of land use change on surface runoff of Lai Nullah Basin in Islamabad, Pakistan, using HEC-HMS and GIS data. The simulation of the model shows the effects of land use for future development and suggested the future planning for this catchment should take into account the water management and planning. As a program for rainfall–runoff model, many researchers used

HEC-HMS for streamflow analysis. Other studies by [9–13] used HEC-HMS for streamflow analysis with different approaches based on their research objectives.

The main objective of this work is to develop a framework for rainfall–runoff model by using HEC-HMS program and utilize a GIS input in HEC-GeoHMS to extract the hydrologic parameters at upper Klang–Ampang catchment.

2 Background

2.1 Study Site and Data

Klang River Basin is an important basin in Malaysia located at Kuala Lumpur, the capital and the largest city in Malaysia. This river basin is placed between 101°30′ and 101°55′ E longitudes and 3–3°30′ N latitude. Klang River Basin is highly dense with 1.7 million populations. The main rivers in Klang River Basin are Sungai Klang, Sungai Ampang, and Sungai Gombak. The area of interest of the study is the upper Klang River Basin, which consists of Sungai Klang and Sungai Ampang. Total catchment for this study area is 159.7 km². The altitude ranges from 1430 masl at the upper part of the catchment and low-lying area in the downstream of the river near the city center. Mean annual rainfall for the upper part of Klang catchment is 2600 mm. Figure 1 shows the upper Klang–Ampang catchment with the topographic map of Kuala Lumpur.
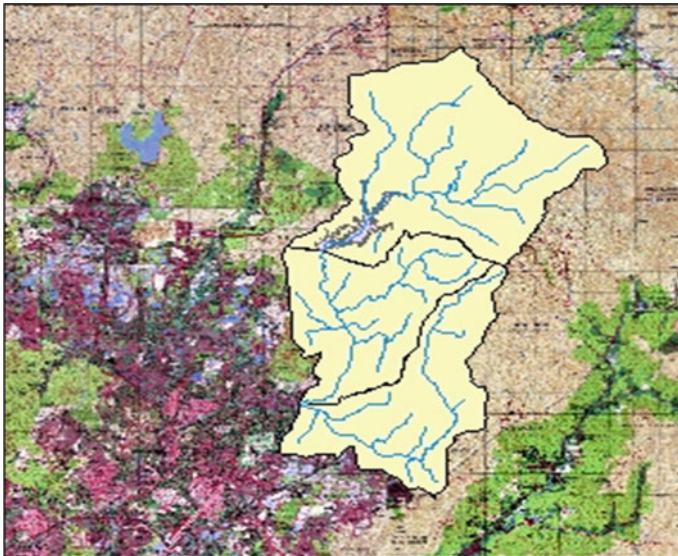
Fig. 1 Study area: Upper Klang–Ampang river basin

There is a dam located at the upstream of the Klang River approximately 10 km from the confluence of Klang–Ampang River. This dam is situated in the forest as its watershed. The concrete arch dam with a spillway in the center is used for water supply purposes and also as flood mitigation for Klang Valley. Downstream areas of the dam are rapidly developing for residential and commercial purposes. The upper Klang–Ampang catchment is selected since it is prone to flood and a large part of the catchment at low-lying area has been well developed with residential and commercial properties.

Land use, soil, rainfall, and streamflow data were obtained from the Department of Irrigation and Drainage (DID). In order to use HEC-GeoHMS, DEM is needed to delineate the watershed. These DEM data were derived from 20-m contour line map produced by JUPEM using ArcGIS program.

2.2 HEC-GeoHMS

HEC-GeoHMS is an extension for ArcGIS (ESRI) released by the US Army Corps of Engineers, Hydrologic Engineering Center (HEC). It is a geospatial hydrology toolkit which allows user to create basin parameters based on topographic data for the use of hydrologic model [14]. Overview of GIS and HEC-HMS is shown in Fig. 2. HEC-GeoHMS is used to derive a river network of basin from the DEM data. It also can delineate basin and sub-basin of the watershed. HEC-GeoHMS creates the drainage network by analyzing the digital terrain data and transforming the drainage paths and watershed boundaries into a hydrologic data structure to represent the drainage network.
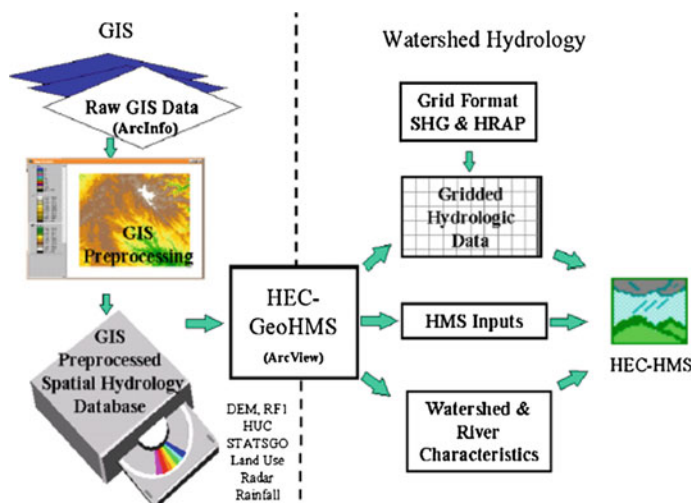
Fig. 2 Overview of GIS and hydrology program [14]

2.3 HEC-HMS

The HEC Hydrologic Modelling System (HEC-HMS) is a hydrologic model designed to simulate hydrologic processes of the dendritic watershed systems [15]. This mathematical model will simulate precipitation–runoff and routing processes in natural or controlled watershed. The spatial data from HEC-GeoHMS could be imported to the HEC-HMS, and the model shall predict flow, stage, and timing for the basin based on the given meteorological dataset and land use information. HEC-HMS uses various hydrologic analysis procedures for continuous or event-based analysis for hydrologic analysis. There are three main components in the HEC-HMS model: basin model, meteorological model, and control specification. The basin model consists of the elements of the basin and sub-basin, the connectivity, and runoff parameter. The meteorological model contains the rainfall and evaporation data, while control specifications consist of the start/stop timing and calculation intervals for run.

3 Methodology

The use of GIS in rainfall–runoff model is useful because it facilitates the development of the basin model. HEC-GeoHMS is integrated with ArcGIS software. It uses ArcGIS and the spatial analyst extension to develop hydrologic parameters as input data for HEC-HMS. The spatial analyst extension will process the terrain based on DEM and stream data. This process is called terrain preprocessing, where the stream network and watershed are created.

3.1 Terrain Preprocessing

Delineation of the catchment and stream network could be done with terrain preprocessing tools. It is one of the many useful tools in the ArcGIS application. There are 10 steps in terrain preprocessing as shown in Fig. 2 to generate the drainage or river network and watershed and sub-basin boundaries. Terrain preprocessing results consist of raster and vector data. These data will be the input for HEC-GeoHMS project setup. Terrain preprocessing also could be done by using Arc-Hydro tools. Reference [14] gives detailed description of the terrain preprocessing steps to create the stream network and delineation of the catchment (Fig. 3).

Fig. 3 Steps for terrain
preprocessing

1. DEM Reconditioning
2. Fill Sink
3. Flow Direction
4. Flow Accumulation
5. Stream Definition
6. Stream Segmentation
7. Catchment Grid Delineation
8. Catchment Polygon Processing
9. Drainage Line Processing
10. Adjoint Catchment Processing
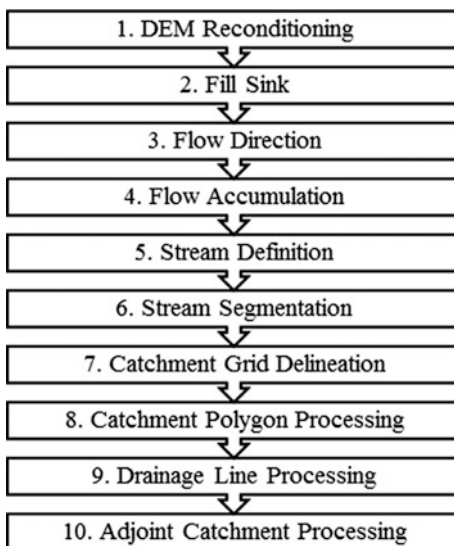
3.2   HEC-GeoHMS

HEC-GeoHMS computes dataset from terrain preprocessing to produce the hydrologic parameters. Hydrologic parameters that could be computed are river length, river slope, basin centroid, longest flow path, and centroid flow path. There are three main steps in HEC-GeoHMS to calculate the hydrologic parameters in the basin (Fig. 4).

Results or datasets in raster and vector formats from terrain preprocessing were used in the HEC-GeoHMS project setup. Raster data are raw DEM, filled DEM, flow direction grid, flow accumulation grid, stream network, stream link grid, catchment grid, and slope grid, while vector data are catchment, drainage line, and adjoint catchment. Once defined the project for HEC-GeoHMS, a new data frame is created and all the terrain preprocessing data were extracted and imported to a new project.

After the new project had been created, the basin processing menu was used to revise or customize the sub-basin delineation, dividing sub-basins, and merging streams. The outlet point of the target study area was defined with located batch

Fig. 4 Steps for
HEC-GeoHMS

1. Project Setup
2. Basin processing
3. Extracting Basin Characteristics
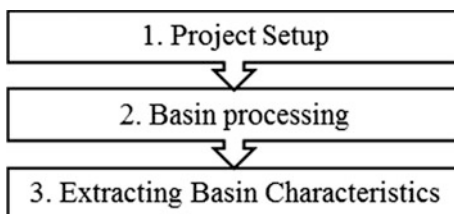
point at the basin. Then, the program defined and generated a new basin based on the defined outlet point.

Extracting the basin characteristics was done using the tools provided. Physical characteristics are extracted river length, river slope, basin slope, longest flow path, basin centroid, centroid elevation, and centroid flow path. These physical characteristics of sub-basins and rivers were used to estimate hydrologic parameters of the basin.

3.3   HEC-HMS

HEC-HMS is designed to simulate the complete hydrologic processes of the watershed. In order to simulate the hydrologic processes, the program needs data on hydrologic parameters of the basin as input data. Hydrologic parameters from the HEC-GeoHMS are essential to be used in this program.

HEC-HMS uses hydrologic parameters from HEC-GeoHMS to develop the rainfall–runoff model. To set up a hydrologic model using this program, there are three main components/models need to be created: basin model, meteorological model, and control specification. Sub-basin and stream data which were derived from HEC-GeoHMS were imported to the basin model as a background map.

In the basin model, elements of the basin such as sub-basins, reaches, junctions, and reservoir were created. This model has three sub-basins, and schematic diagram of the basin model is shown in Fig. 5. SCS curve number was selected as loss method, while transform method used was SCS unit hydrograph.

SCS curve number (CN) estimates precipitation excess as a function of cumulative precipitation, soil cover, land use, and antecedent moisture. Precipitation excess could be calculated by using Eq. (1).

$$P_e = \frac{(P - I_a)^2}{P - I_a + S} \tag{1}$$

P_e accumulated precipitation excess at time t;
P accumulated rainfall depth at time t;
I_a the initial abstraction (initial loss);
S potential maximum retention.

Potential maximum retention, S, is a measurement of the ability of a catchment to abstract and store storm precipitation. There will be no precipitation excess until the accumulated rainfall exceeds the initial abstraction.

According to Ref. [5], the SCS developed a relationship of I_a and S as in Eq. (2):

$$I_a = 0.2S \tag{2}$$

Fig. 5 Schematic of
HEC-HMS model for upper
Klang–Ampang catchment
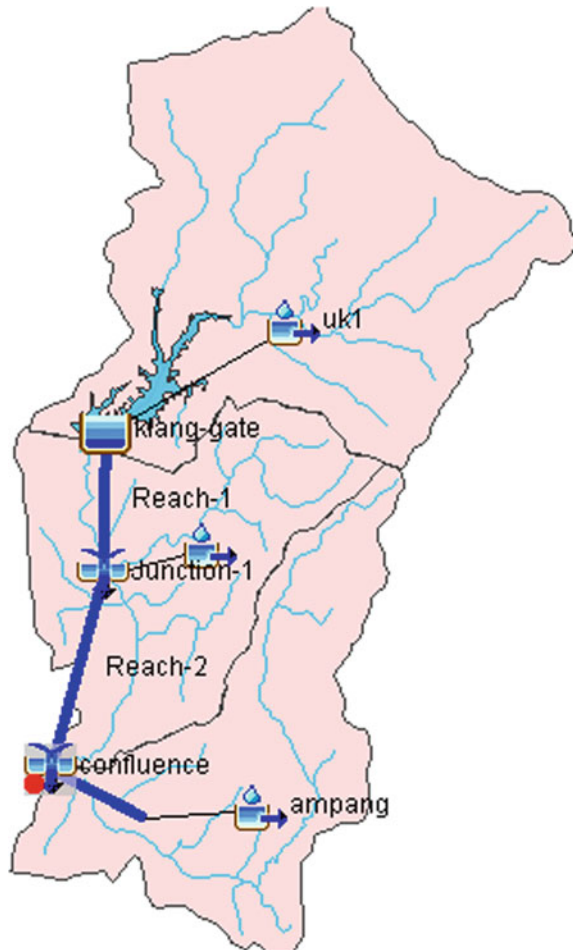
The cumulative excess at time t could be calculated with the Eq. (3):

$$P_{\mathrm{e}} = \frac{(P - 0.2S)^2}{P + 0.8S} \tag{3}$$

The difference between the accumulated excess at the end of and the beginning of the period called as incremental excess for a time interval. The maximum retention, S, and watershed characteristics are related through an intermediate parameter, called as curve number (CN). The relationship between S and CN is shown in Eq. (4):

$$S = \frac{25{,}400 - 254\text{CN}}{\text{CN}} \tag{4}$$

CN values range are 100–30 where value for 100 for water bodies and 30 for permeable soils with high infiltration rates. CV values could be estimated based on appendix A, CN Table in [5] which it was reproduced from the SCS report, Urban hydrology for small watersheds.

Meteorological model was created using observed rainfall and discharge data. The observed historical data of three precipitation stations representing each sub-catchment, and one stream discharge gauge station at the confluence of Klang River and Ampang River was used for model calibration and verification. Five-minute time step was used for the simulation based on the time interval of the available observed data. Observed rainfall and discharge data were added in the time series data manager component as precipitation gage and discharge gage. The meteorological model was set as specified hyetograph method. The control specifications were used to set the time step for the simulation, starting and ending for date and time. Basin model, meteorological model, and control specification were combined before running the program.

4 Results and Discussion

4.1 Terrain Preprocessing and HEC-GeoHMS

Catchment of the upper Klang–Ampang River Basin was delineated by using terrain preprocessing tools in ArcGIS program. The results of each step in the terrain preprocessing are shown in Fig. 6. Output data from terrain preprocessing were used in HEC-GeoHMS for project setup. From the HEC-GeoHMS results, sub-basin areas were extracted and the data are shown in Table 1. These data were used to set up the rainfall–runoff model in HEC-HMS.

4.2 Rainfall–Runoff Model with HEC-HMS

For this study, sub-basins generated in HEC-GeoHMS were combined or merged to make 3 sub-basins: UK1, UK2, and Ampang. The purpose of this combination is to simplify the rainfall–runoff model setup for the beginning of the analysis on the streamflow at the confluence of Klang–Ampang River.

Analysis of the streamflow at the confluence of Klang–Ampang River was done for selected event on May 3, 2011. The model was calibrated and validated with the observed discharge data at the confluence of upper Klang–Ampang catchment. Figure 7 shows the result of simulation run for an event on May 3, 2011. Simulation

Fig. 6 Terrain preprocessing
results for each step

DEM Reconditioning

Fill sink

Flow Direction

Flow accumulation

Stream Definition

Stream segmentation

Catchment grid
delineation

Catchment polygon
processing

Drainage line processing

Adjoint catchment
Processing
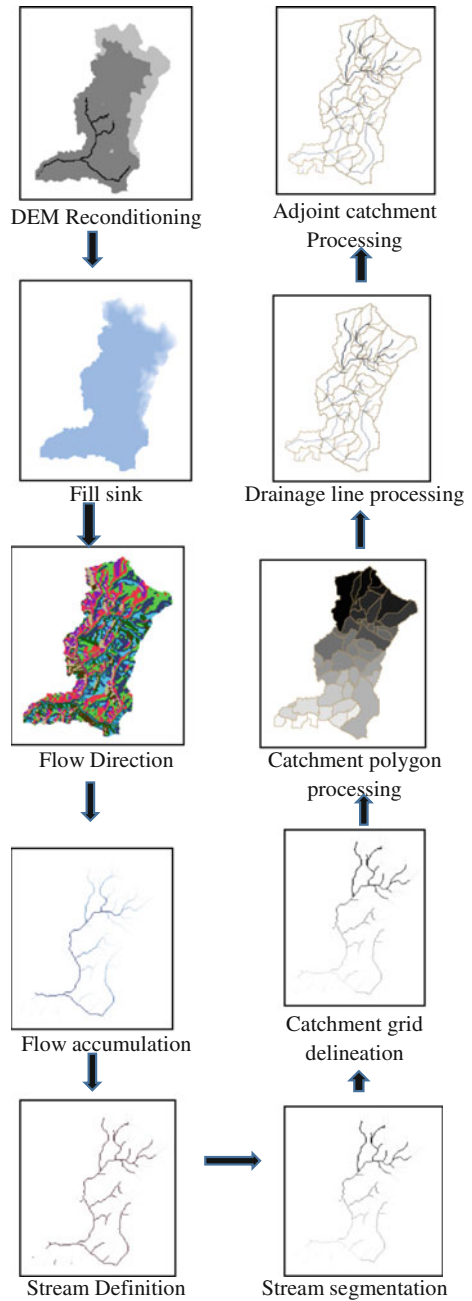
Table 1 Catchment parameter

Sub-basin area	Km^2
UK1	76.94
UK2	41.14
Ampang	41.64
Total	159.72
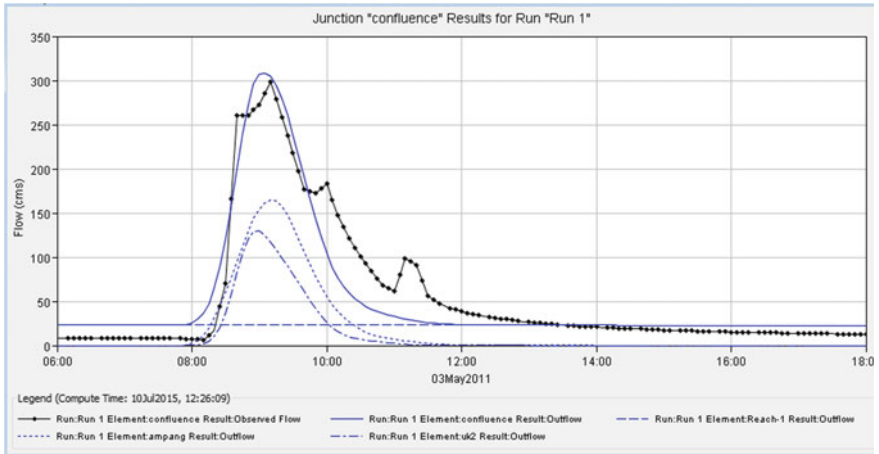
Fig. 7 Simulation result for event May 3, 2011

discharge of 308.7 m^3/s was compared with the observed discharge 298.8 m^3/s. The Nash–Sutcliffe coefficient for this simulation was 0.86, mean absolute error 17.9 m^3/s, and RMS error 25.3 m^3/s. Percentage error between simulation and observed discharge is 3.2 %. This result shows the model gives good simulation on event-based rainfall–runoff analysis study. However, further calibration and verification for other events should be done to this model.

5 Conclusion

This paper presents a methodology and development of rainfall–runoff model by using HEC-HMS program integrated with DEM data as an input for basin model. This model will have the capabilities to perform the hydrologic studies with different objectives and may expand to be a flood forecasting model by providing the further advanced computation in HEC-HMS. As conclusion, HEC-HMS is a useful program and compatible with other programs such as ArcGIS program for rainfall–runoff modeling.

References

1. Djokic D (2008) Comprehensive terrain preprocessing using arc hydro tools, no 5, p 61
2. Zhang W, Montgomery DR (1994) Digital elevation model grid size, landscape representation, and hydrologic simulations. Water Resour Res 30(4):1019–1028
3. Li Z (2014) Watershed modeling using arc hydro based on DEMs: a case study in Jackpine watershed. Environ Syst Res 3(1):11
4. Kabiri R (2014) Simulation of runoff using modifies SCS-CN method using GIS system, case study: Klang watershed in Malaysia. Res J Environ Sci 8(4):178–192
5. Feldman AD (2000) Hydrologic modeling system HEC-HMS technical reference manual, p 155, March
6. Knebl MR, Yang Z-L, Hutchison K, Maidment DR (2005) Regional scale flood modeling using NEXRAD rainfall, GIS, and HEC-HMS/RAS: a case study for the San Antonio river basin summer 2002 storm event. J Environ Manag 75(4):325–336
7. Oleyiblo J (2010) Application of HEC-HMS for flood forecasting in Misai and Wan'an catchments in China. Water Sci Eng 3(1):14–22
8. Ali M, Khan SJ, Aslam I, Khan Z (2011) Simulation of the impacts of land-use change on surface runoff of Lai Nullah basin in Islamabad, Pakistan. Landsc Urban Plan 102(4):271–279
9. Chu X, Steinman A (2009) Event and continuous hydrologic modeling with HEC-HMS. J Irrig Drain Eng 135(1):119–124
10. Zhang HL, Wang YJ, Wang YQ, Li DX, Wang XK (2013) The effect of watershed scale on HEC-HMS calibrated parameters: a case study in the clear creek watershed in Iowa, US. Hydrol Earth Syst Sci 17(7):2735–2745
11. Kabiri R, Chan A, Bai R (2013) Comparison of SCS and Green-Ampt methods in surface runoff-flooding simulation for Klang Watershed in Malaysia. Open J Mod Hydrol 03(03):102–114
12. Adib M, Junaidah A, Wardah T (2010) Flood Estimation studies using hydrologic modeling system (HEC-HMS) for Johor River, Malaysia. J Appl Sci 18028-JAS-ANSI, 10(11) 930–939
13. Basarudin Z, Adnan N, Wardah T, Syafiqah N (2014) Event-based rainfall runoff modelling of the Kelantan river basin. In: IOP conference series: earth and environmental science, vol 18, no 1, p 012084
14. U. S. Army Corps of Engineers, USACE (2010) HEC-GeoHMS geospatial hydrologic modeling extension, Version 5.0 - User's Manual. Davis, CA, pp 1–6
15. Scharffenberg WA (2013) Hydrologic modeling system HEC-HMS—user' s manual, p 442, December

Evaluation of Total Load Equation for Malaysian Mountain Rivers

S.K. Sinnakaudan, M.R. Shukor, M.S. Sulaiman, S.I.H. Ismail, M. Mohammed and R. Che Soh

Abstract Development of total sediment load (TL) equations for Malaysian rivers was first cited in Sinnakaudan et al. [1]. Sinnakaudan et al. [4] proposed an equation which may best predict TL for mountain rivers (MR). In 2011, Sinnakaudan and Sulaiman [3] listed another 22 possible combinations of multiple linear regression TL equations which may be used for MR in Malaysia. However, their performance is not fully verified due to field data constraints. The present paper gives the performance test carried out for the equations with latest 130 sets of data collected from 25 numbers of Malaysian MR. The accuracy of the existing equations was obtained using the discrepancy ratio analysis, which is the ratio of calculated values to the measured values. Overall prediction indicates that Eq. (11) obtained from Sinnakaudan and Sulaiman [3] performs better compared to other equations; however, the percentage prediction is still below 30 %. Thus, a site-specific equation is proposed to be developed based on to correctly predict the sediment transport in MR in Malaysia

1 Introduction

Development of total sediment load (TL) equations for Malaysian rivers was first cited in Sinnakaudan et al. [1]. Much effort has been put to appraise the performance of the proposed equation and similar equations which were derived elsewhere in the world [1, 5]. The limitation of Sinnakaudan et al. [1] in predicting TL for MR leads the avenue to carry out an extensive research in developing a suitable

S.K. Sinnakaudan · M.R. Shukor (✉) · M.S. Sulaiman · S.I.H. Ismail
M. Mohammed · R. Che Soh
Water Resources Engineering and Management Research Centre, Faculty of Civil
Engineering, Universiti Teknologi MARA Pulau Pinang, 13500 Permatang Pauh, Pulau
Pinang, Malaysia
e-mail: drsshan@yahoo.com

TL equation for mountain rivers (MR) in Malaysia. Sinnakaudan et al. [4] proposed an equation which may best predict sediment transport for MR. The performance of the said equation was tested using 55 sets of independent mountain river data [5]. However, the selected equation generally does not yield consistent results when applied to new study areas with diverse morphological and flow characteristics [4].

In 2011, Sinnakaudan and Sulaiman [3] listed 22 possible combinations of multiple linear regression TL equations which may be used for MR in Malaysia. As such, this paper reports the performance test results of the selected 24 equations (including [1, 3]). The reason for selecting all these equations is that it was specifically developed from local rivers data. The equations were tested with the latest 130 sets of mountain river sediment and hydraulic data [5, 6].

Table 1 Study site

No	Study area	
	River name	No of data
1	Sungai Ulu Paip	9
2	Sungai Reyau	9
3	Sungai Abang	1
4	Sungai Giam	1
5	Sungai Semadang	1
6	Sungai Air Putih	4
7	Sungai Sedim (Kg Sedim)	4
8	Sungai Terla	3
9	Sungai Telom	2
10	Sungai Sedim	2
11	Sungai Kemia	3
12	Sungai Sayap	5
13	Sungai Bukit Hijau	1
14	Sungai Lata Tembakah	1
15	Sungai Rasi	1
16	Sungai Rambai	1
17	Sungai Keruak 3B	1
18	Sungai Lubuk Permata	1
19	Sungai Lagus	1
20	Sungai Loh	1
21	Sungai Kacong	1
22	Sungai Besut	2
23	Sungai Lemoi, C. Highlands, Pahang	25
24	Sungai Bertam, C. Highlands, Pahang	25
25	Sungai Telom, C. Highlands, Pahang	25
	Total	130

2 Typical Data Sources

The data used in the present study are collected from 25 MR as listed in Table 1 having diverse catchment characteristics in Malaysia [5, 6]. The collected data were carefully studied, and most reliable 130 numbers of data were used in the analysis. Table 2 shows the typical range of data used in the performance test. It is worth mentioning here that the sampling guidelines given by USGS [7] were adopted where by the suspended load was measured using DH 48 sampler, bedload measured using Helley-Smith sampler, velocity measured using McBirney electromagnetic current meter. The samples are collected by wading techniques for low flow conditions. For medium and high flows, measurement was carried out using suspended bridge. The typical view of the studied reach was given in Fig. 1

3 Existing Total Sediment Load Equations

Twenty-four existing local TL equations as suggested in [1, 3, 4] were selected here for performance test. In this study, equation obtained from Sinnakaudan et al. [1] is denoted as Eq. (1) while equation obtained from Sinnakaudan et al. [4] denoted as Eq. (2). Twenty-two possible combinations of equations from Sinnakaudan and Sulaiman [3] are denoted as Eqs. (3)–(24). The selected equations are listed as below.

$$C_{\mathrm{v}} = 1.811 \times 10^{-4} \left(\frac{VS_{\mathrm{o}}}{\omega_{\mathrm{s}}} \right)^{0.293} \left(\frac{R}{d_{50}} \right)^{1.390} \left(\frac{\sqrt{g(S_{\mathrm{s}} - 1)d_{50}^3}}{VR} \right) \qquad (1)$$

$$C_{\mathrm{v}} = 2.138 \times 10^{-11} \times \left[\frac{\frac{\omega_{\mathrm{s}} d_{50}^{1.117}}{v} \times \Omega^{0.608} \times \xi_i^{-0.336}}{VR} \right] \times \left[(S_{\mathrm{s}} - 1)g\, d_{50}^3 \right]^{1/2} \qquad (2)$$

$$C_{\mathrm{v}} = 2.08 \times 10^{-5} \frac{\left[\left(\frac{V}{\sqrt{g\, d_{50}(S_{\mathrm{s}} - 1)}} \right)^{2.128} \psi^{-0.22} \right]}{VR} \times \left[(S_{\mathrm{s}} - 1)g\, d_{50}^3 \right]^{1/2} \qquad (3)$$

Table 2 Data applicability ranges

Parameter	Summary of sediment database						
	Q, m^3/s	V, m/s	B, m	y_{o}, m	S_0, m/m	d_{50}, mm	TL kg/s
Min	0.15	0.10	5.00	0.13	0.0001	0.34	0.0001
Avg	4.01	0.75	11.5	0.57	0.0154	108.8	3.72
Max	23.9	2.07	21.3	5.88	0.0389	472.5	206.12

Fig. 1 Typical view of the sampling reach at the study area [2]

$$C_v = 1.057 \times 10^{-4} \frac{\left[\left(\frac{V}{\sqrt{g\,d_{50}(S_s-1)}} \right)^{1.582} \left(\frac{d_{50}}{B} \right)^{-0.656} \right]}{\mathrm{VR}} \times \left[(S_s - 1)g\,d_{50}^3 \right]^{1/2} \quad (4)$$

$$C_v = 1.493 \times 10^{-20} \frac{\left[\left(\frac{V}{\sqrt{g\,d_{50}(S_s-1)}} \right)^{1.158} \left(\frac{\omega_s d_{50}}{\upsilon} \right)^{2.129} \right]}{\mathrm{VR}} \times \left[(S_s - 1)g\,d_{50}^3 \right]^{1/2} \quad (5)$$

$$C_v = 4.285 \times 10^{-33} \frac{\left[\psi^{0.106} \left(\frac{\omega_s d_{50}}{\upsilon} \right)^{3.853} \right]}{\mathrm{VR}} \times \left[(S_s - 1)g\,d_{50}^3 \right]^{1/2} \quad (6)$$

$$C_v = 0.029 \frac{[\psi^{-0.106} F^{2.095}]}{VR} \times [(S_s - 1)g\, d_{50}^3]^{1/2} \tag{7}$$

$$C_v = 7.726 \times 10^{-6} \frac{[\psi^{-0.876} \Omega^{0.828}]}{VR} \times [(S_s - 1)g\, d_{50}^3]^{1/2} \tag{8}$$

$$C_v = 0.022 \frac{\left[\left(\frac{d_{50}}{B}\right)^{-0.54} F^{1.635}\right]}{VR} \times [(S_s - 1)g\, d_{50}^3]^{1/2} \tag{9}$$

$$C_v = 1.125 \times 10^{-27} \frac{\left[\left(\frac{\omega_s d_{50}}{v}\right)^{3.179} \Omega^{0.338}\right]}{VR} \times [(S_s - 1)g\, d_{50}^3]^{1/2} \tag{10}$$

$$C_v = 0.011 \frac{[\Omega^{1.451} \eta^{0.118}]}{VR} \times [(S_s - 1)g\, d_{50}^3]^{1/2} \tag{11}$$

$$C_v = 1.102 \times 10^{-4} \frac{\left[\left(\frac{V}{\sqrt{g\, d_{50}(S_s-1)}}\right)^{1.584} \left(\frac{d_{50}}{B}\right)^{-0.66} \psi^{0.005}\right]}{VR} \times [(S_s - 1)g\, d_{50}^3]^{1/2} \tag{12}$$

$$C_v = 1.069 \times 10^{-22} \frac{\left[\left(\frac{V}{\sqrt{g\, d_{50}(S_s-1)}}\right)^{1.185} \left(\frac{\omega_s d_{50}}{v}\right)^{2.486} \psi^{0.155}\right]}{VR} \times [(S_s - 1)g\, d_{50}^3]^{1/2} \tag{13}$$

$$C_v = 0.023 \frac{\left[\psi^{0.008} \left(\frac{d_{50}}{B}\right)^{-0.547} F^{1.638}\right]}{VR} \times [(S_s - 1)g\, d_{50}^3]^{1/2} \tag{14}$$

$$C_v = 5.754 \times 10^{-5} \frac{\left[\psi^{-0.45} \left(\frac{d_{50}}{B}\right)^{-0.719} \Omega^{-0.585}\right]}{VR} \times [(S_s - 1)g\, d_{50}^3]^{1/2} \tag{15}$$

$$C_v = 2.333 \times 10^{-19} \frac{\left[\psi^{0.145} \left(\frac{\omega_s d_{50}}{v}\right)^{2.264} F^{1.221}\right]}{VR} \times [(S_s - 1)g\, d_{50}^3]^{1/2} \tag{16}$$

$$C_v = 2.594 \times 10^{-24} \frac{\left[\psi^{-0.165} \left(\frac{\omega_s d_{50}}{v}\right)^{2.675} \Omega^{0.407}\right]}{VR} \times [(S_s - 1)g\, d_{50}^3]^{1/2} \tag{17}$$

$$C_v = 3.99 \times 10^{-6} \frac{\left[\psi^{-0.362} \left(\frac{y_0}{d_{50}}\right)^{0.761} \Omega^{0.455}\right]}{VR} \times [(S_s - 1)g\, d_{50}^3]^{1/2} \tag{18}$$

$$C_{\mathrm{v}} = 3.855 \times 10^{-4} \frac{\left[\xi_i^{-0.534} \left(\frac{y_0}{d_{50}} \right)^{0.408} \eta^{-0.106} \right]}{\mathrm{VR}} \times \left[(S_{\mathrm{s}} - 1) g \, d_{50}^3 \right]^{1/2} \qquad (19)$$

$$C_{\mathrm{v}} = 1.309 \times 10^{-4} \frac{\left[\left(\frac{V}{\sqrt{g \, d_{50}(S_{\mathrm{s}}-1)}} \right)^{1.64} \left(\frac{d_{50}}{B} \right)^{-0.195} \psi^{-0.229} \eta^{-0.161} \right]}{\mathrm{VR}}$$
$$\times \left[(S_{\mathrm{s}} - 1) g \, d_{50}^3 \right]^{1/2} \qquad (20)$$

$$C_{\mathrm{v}} = 8.511 \times 10^{-5} \frac{\left[\left(\frac{V}{\sqrt{g \, d_{50}(S_{\mathrm{s}}-1)}} \right)^{1.736} \left(\frac{y_0}{d_{50}} \right)^{0.15} \psi^{-0.213} \eta^{-0.156} \right]}{\mathrm{VR}}$$
$$\times \left[(S_{\mathrm{s}} - 1) g \, d_{50}^3 \right]^{1/2} \qquad (21)$$

$$C_{\mathrm{v}} = 0.0285 \frac{\left[\psi^{-0.226} \left(\frac{d_{50}}{B} \right)^{-0.106} F^{1.664} \eta^{-0.158} \right]}{\mathrm{VR}} \times \left[(S_{\mathrm{s}} - 1) g \, d_{50}^3 \right]^{1/2} \qquad (22)$$

$$C_{\mathrm{v}} = 0.0278 \frac{\left[\psi^{-0.23} \left(\frac{y_0}{d_{50}} \right)^{1.727} F^{1.727} \eta^{-0.157} \right]}{\mathrm{VR}} \times \left[(S_{\mathrm{s}} - 1) g \, d_{50}^3 \right]^{1/2} \qquad (23)$$

Table 3 Parameters groups

Parameters class	Dimensionless groups
Mobility	$\Psi = \frac{(S_{\mathrm{S}}-1)d_{50}}{RS_0}, \left(\frac{V}{\sqrt{g \, d_{50}(S_{\mathrm{S}}-1)}} \right), \frac{U_*}{V}, \frac{VS_0}{\omega_{\mathrm{s}}}$
Transport	$C_{\mathrm{v}}, \Phi = \frac{c_v \mathrm{VR}}{\sqrt{g(S_{\mathrm{s}}-1)d_{50}^3}}$
Sediment	$D_{\mathrm{gr}} = d_{50} \left(\frac{g(S_{\mathrm{s}}-1)}{v^2} \right)^{\frac{1}{3}}, d_{50}/B, \frac{U_*}{\omega_{\mathrm{S}}}, \frac{\omega_{\mathrm{S}} d_{50}}{v}$
Hiding exposure	$\xi_i = \frac{1.66667}{\left[\log \left(19 \frac{D_i}{D_{50}} \right) \right]^2}, \eta_i = \left(\frac{P_{\mathrm{e}}i}{\varphi} \right)$
Flow resistance	$\lambda_{\mathrm{S}} = \frac{8gRS}{V^2}, R/d_{50}, y_{\mathrm{o}} = d_{50}$
Incipient motion	$\Omega = \frac{\tau_{\mathrm{b}} U_*}{\rho[(S_{\mathrm{s}}-1)gD_{50}]^{3/2}} F^* = \frac{V}{[g(S-1)D \cos\theta(\tan\phi - \tan\theta)]^{1/2}}$
Conveyance shape	$B/y_{\mathrm{o}}, B^2/A$
Sheltering factor	$\eta = C_1 \left(\frac{D_i}{D_{50}} \right)^{C_2}$
Fractional function	$\Phi_i = P_{\mathrm{ai}}\eta, \ P_{\mathrm{ai}} = \frac{P_i/D_i}{\sum_{i=1}^n P_i/D_i}$

$$C_\mathrm{v} = 1.161 \times 10^{-13} \frac{\left[\xi_i^{-0.326}\left(\frac{\omega_s d_{50}}{\upsilon}\right)^{1.391}\Omega^{0.386}\eta^{-0.047}\right]}{\mathrm{VR}} \times \left[(S_\mathrm{s} - 1)g\, d_{40}^3\right]^{1/2} \quad (24)$$

Generally, the parameters used in Equations fall within eight main groups [8] as shown in Table 3 whereby volumetric sediment concentration, C_v, and transport parameter, Φ, were functioning as independent variables.

4 Results and Discussion

The performances of the selected equations are tested using discrepancy ratio, r which is the ratio between the calculated total bed material load and the measured bed material load [5, 9]. r is expressed as the ratio of predicted TL over measured TL. The values of discrepancy ratios were then averaged, and the test equations

Table 4 Discrepancy ratio result

Equation no.	Number of data fall within r (0.5–2.0)	Percentage (%)
1	13	10.00
2	10	7.69
3	26	20.00
4	21	16.15
5	0	0.00
6	0	0.00
7	0	0.00
8	0	0.00
9	0	0.00
10	0	0.00
11	30	23.08
12	19	14.62
13	0	0.00
14	0	0.00
15	17	13.08
16	0	0.00
17	0	0.00
18	2	1.54
19	23	17.69
20	16	12.31
21	14	10.77
22	0	0.00
23	0	0.00
24	3	2.31

were recommended based on the mean of the discrepancy ratio. The closer the value to unity and smaller the standard deviation, the better suited the TL equation is assumed for the current data set. The summary of the suitability analyses for 24 selected equations is given in Table 4.

Figure 2 shows the overall measured against the predicted total bed material load using the selected 24 equations. Figure 3 shows the performance plot for Eq. (11).
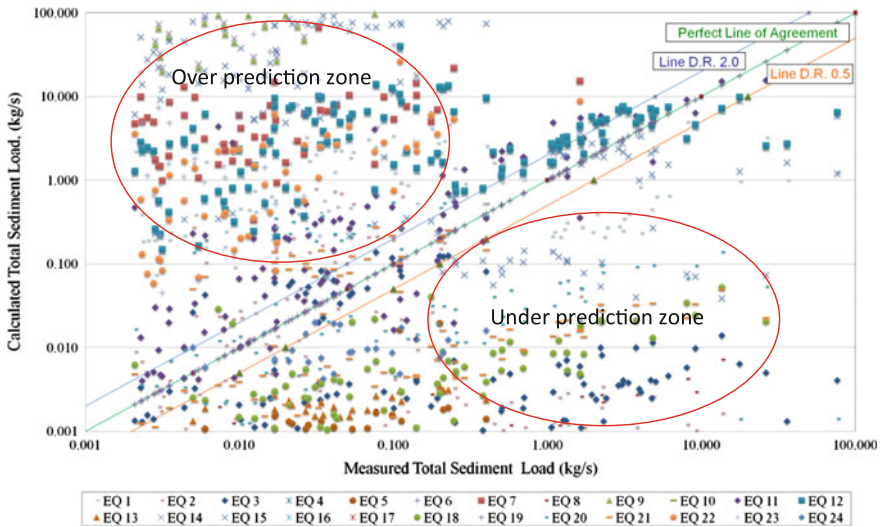
Fig. 2 Overall comparison of measured and predicted TL for selected 24 equations
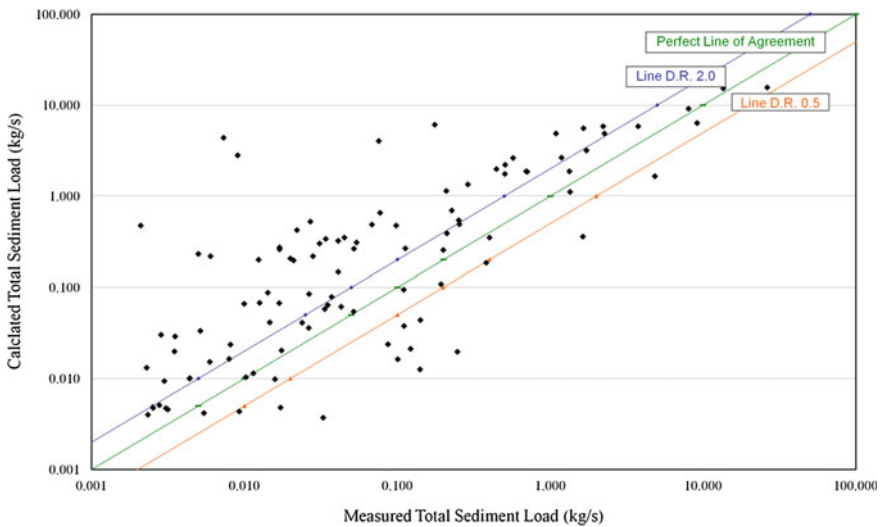
Fig. 3 Comparison of measured and predicted TL using Eq. (11)

It can be seen that almost all equations seemed to overpredict or underpredict the values of TL with some exceptions for Eqs. (3) and (11) which have 26 and 30 data, respectively, lie within the acceptable r, 0.5–2.0.

Equation (11) has the best performance where it shows the 23 % of the variability in the test data followed by Eq. (3) with 20 %. The rest of the equations tested give less favorable predictions as listed in Table 4. It is worth to mention here that the TL Equation suggested in Sinnakaudan et al. [4] does not perform well as compared to other tested equations.

5 Conclusion

The TBML equation performance test reported herein suggests that some careful technical consideration is needed before any of the existing sediment transport formulas can be applied to field design activities. It is evident that equations reported in [1, 3, 4] do not perform well when tested with data from rivers having diverse morphological characteristics. As such, it is proposed that the existing equations to be re-evaluated with larger sets of data and redeveloped to cater various flow and sediment transport regime.

It is hoped that this paper would promote more rigorous work on techniques on field data measurements, finding right sampling equipments and revisit of existing theories to cater mountain river conditions. It is also hoped that hydraulic and sediment transport engineers to evaluate few equations based on specific site conditions before making the final selection. The future direction of the present research is aimed to come out with the site-specific equation for Malaysian MR conditions to correctly predict the sediment transport in Malaysia.

References

1. Sinnakaudan SK, Ghani AAb, Ahmad MSS, Zakaria NA (2006) Multiple linear regression model for total bed material load prediction. J Hydraul Eng 132(5):521–528
2. Sinnakaudan SK, Sulaiman MS (2007) Development of total bed material load equation for high gradient rivers in Malaysia. In: Proceeding of the 10th international symposium on river sedimentation, Moscow State University, Moscow, pp 297–304
3. Sinnakaudan SK, Sulaiman MS (2011) Total bed material load equation development for mountain rivers: worked example. (ISBN: 978–3-8454-3039-3) LAP Lambert Academic Publishing AG & Co. KG

4. Sinnakaudan SK, Sulaiman MS, Teoh SH (2010) Total bed material load equation for high gradient rivers. J of Hydro-Environ Res 4:243–251
5. Sinnakaudan SK (2010) Sediment Transport Modeling (STM) and Flood Risk Mapping in GIS. (ISBN 978-3-8383-4733-2) LAP Lambert Academic Publishing AG & Co. KG
6. Sinnakaudan SK, Abdul Razad AZ (2014) Development of Total sediment load of High Gradient Rivers of Sg. Lemoi, Sg Bertam and Sg. Telom for Ulu Jelai Hydroelectric Scheme in Pahang.TNB Reaserch Sdn. Bhd (unpublished)
7. USGS- United State Geological Survey (2005) Sediment data collection technique, USGS training course–SW1091TC. USA (unpublished), Vancouver
8. Sinnakaudan SK, Sulaiman MS (2008) Influential parameters for sediment transport prediction in headwater streams (Hws). Paper presented at the 8th international conference of hydro-science and engineering, Nagoya Hydraulic Research Institute for River Basin Management, Nagoya, Japan
9. Yang CT (1984) Unit Stream Power Equations for Gravel. J Hydraul Eng 110(HY12):1783–1797

Evaluation of Stochastic Daily Rainfall Data Generation Models

J. Jaafar, A. Baki, I.A. Abu Bakar, W. Tahir, H. Awang and F. Ismail

Abstract In developing countries, data is usually a scarce resource as data collection is an expensive exercise. Therefore, analytical method is required to simulate the actual situations and provide synthetic data for forecasting purposes. This paper will compare several methods of synthetically generating rainfall data based on available data. Several models will be used, including lag-one Markov chain model, two-step model, and transition probability model to generate stochastic daily rainfall data of long-term duration, using data from a catchment in Australia. Three variations of lag-one Markov chain models were used: untransformed, logarithmic transformation, and square root transformation. Two-step model uses Markov chain to model rainfall occurrences and gamma distribution to model rainfall depths. Six variations of the Transition Probability Matrices were used, 3 using Shifted Exponential Distribution and 3 using Box–Cox Power Transformation was adopted to predict the high rainfall depths, and the parameters are determined using maximum-likelihood method on the available rainfall data. The models' results were tested by comparing the statistics of the generated data against those of the available data. Direct comparisons of the means, standard deviations, and skews show satisfactory results. Further comparisons of monthly means, standard deviations, skews, maxima and minima, as well as the lengths of wet and dry spells had also shown satisfactory results. In conclusion, all the models have produced synthetic rainfall data, which are statistically similar to those of the available data. In comparison, the TPM model gave the most accurate results. Therefore, this model may be utilised for synthetic rainfall data generations, which can then be used for forecasting.

Keywords Markov chain model · Rainfall modelling · Stochastic modelling · Transition probability matrices and two-step model

J. Jaafar (✉) · I.A. Abu Bakar · W. Tahir · H. Awang · F. Ismail
Faculty of Civil Engineering, Universiti Teknologi MARA, Shah Alam, Malaysia
e-mail: jurina1106@gmail.com

A. Baki
Faculty of Engineering, Al-Madinah International University, Shah Alam, Malaysia

A. Baki
Envirab Services, P.O. Box 7866, Shah Alam 40730, Malaysia

1 Introduction

Long-term data is desirable to enable the asset managers to sufficiently simulate the many possibilities, including flooding and extreme droughts. In developing countries, data is usually a scarce resource as data collection is an expensive exercise. Generation of synthetic data is one of the methods to enable forecasting to be made. One of the techniques available to produce the synthetic data is the stochastic data generation. Rainfall is regarded as the most basic weather variable, independent of temperature and evaporation [16]. Hence, generation of long-term synthetic rainfall data can provide basic set of weather variables for long-term forecasting.

The hydrological time series consists of two contributing factors: random factors and persistence (stochastically deterministic factor) [26]. Stochastic modelling used the stochastic properties of observed time series to generate long-term time series. The statistical and stochastic properties of the observed time series are assumed to represent the population properties, and the synthetic long-term time series is assumed to come from the same population [10].

There are many stochastic data generation models. This paper compared several models including lag-one Markov chain model, two-step model, and the transition probability Matrices model (TPM).

Lag-one Markov chain models are the most popular variations of rainfall data generation models [2, 24, 31]. Higher-order Markov chain models have also been utilised satisfactorily [12]. The major problem in daily rainfall generation using a single-step runoff generation type model (Lag-one Markov Chain Model by [2]) is the large number of zero values of daily rainfall. Richardson [22] used square root transformation and a multivariate normal distribution truncated at zero to overcome the zeros problems. Baki [4] used logarithmic and square root transformation to overcome this problem. Nevertheless, there is an inherent problem of large number of zeros in the historical data, which introduced skews. Nevertheless, Malek and Baki [17] successfully forecasted stochastic data for Gombak River in Malaysia using non-transformed data.

The two-step model was developed by various researchers to separate the analysis between the occurrences of rainfall and the rainfall depth. Jones et al. [16] and Adam [1] modelled occurrences of daily rainfall using a Markov chain. The wet spells, which is a series of rainfall occurrences, and the dry spells, which is a series of non-occurrences of rainfall, have also been satisfactorily modelled using Markov chains [19, 21, 25]. Baki [5] has modelled rainfall data generation using the two-step model using Markov chain for rainfall occurrences and gamma distribution for rainfall depth. Generally, Baki [5] has achieved satisfactory results, where the statistics of the generated data is comparable to those of the recorded data.

Haan et al. [14] and Taewechit et al. [29] used a multistate Markov chain approach to model the distribution of rainfall. Haan et al. [14] used seven states to describe rainfall behaviour based on rainfall depths. The first state is dry (no rain), and six others are wet (with rainfall). Uniform distributions were assumed for states 2–6 and a shifted exponential distribution for the seventh state (unbounded).

A modified TPM model was developed by Srikanthan and McMahon [26] based on the TPM model of Haan et al. [14]. The exception was that the daily rainfall data is transformed using the Box–Cox power transformation [8] instead of a shifted exponential distribution for the last class. Srikanthan and McMahon [27] used TPM model in their development of automatic evaluation of stochastically generated rainfall data. Srikhathan et al. [28] also used TPM model in their comparison of daily rainfall data generation models. Baki [6] found that in general, all six variations used (three sets of matrices using shifted exponential and three sets of matrices using Box–Cox power transformation) were equally satisfactory as the differences between the six variations are minimal. This was consistent with the past research as Haan et al. [14] found that the number of classes did not affect the accuracy of the TPM model to a great extent. Therefore, the selection between the six variations is not very critical.

The objective of this paper is to compare the performance of those models in generating daily rainfall. Apart from comparing the daily statistics of the generated data to those of the recorded data, further comparisons will also be carried out using monthly and annual statistics, daily maxima, and average lengths of dry and wet spells. The comparison will enable identification of the model that will give the most accurate statistical comparisons between recorded and generated rainfall statistics.

2 Data and Methods

2.1 Data

The catchment selected for this study is Kangaroo Valley, which is located about 150 km south of Sydney and about 50 km west of the east coast of New South Wales, Australia. The map is shown in Fig. 1, and catchment characteristics are as listed below [3]:

- The National Index reference is 215,220.
- The catchment area is 330 km^2.
- The length of the stream (Kangaroo River) is 34.5 km.
- The average slope of the Kangaroo River is 1.35 % or 135 in 10,000.
- The annual rainfall for Kangaroo Valley is 1629.0 mm.
- The annual runoff from the catchment is 934.2 mm.
- The annual pan evaporation is 1773.4 mm.
- The climatic condition for this catchment is temperate.
- The vegetation in the area is a mixture of rainforest, hedgeland, sedgeland, and grassland.

A total of 80 years of daily rainfall data were used. Both regionalised and single-site approaches have been satisfactorily used in rainfall data generation.

Fig. 1 Catchment (after, [3])

Benson and Matalas [7] used regionalised parameters in stochastic runoff data generation. Solomon [23] used regionalised parameters as he found that regionalised parameters were more suitable than single-site parameters because regionalisation reduced operational bias. Baki [4] found that by using the average rainfall for the catchment, continuity of data could be obtained. Hernáez and Martin-Vide [15], Mehrotra et al. [18], and Camberlin et al. [9] had used regionalised approach to satisfactorily model rainfall data. However, Mhanna and Bauwers [20] had satisfactorily generated rainfall data using single-site approach. In this study, the regionalised approach had been adopted using catchment daily average rainfall. Therefore, the use of catchment average rainfall instead of individual stations allows for better approximations of rainfall stochastic properties and processes.

The location of the catchment is shown in Fig. 1. The locations of the rainfall stations are shown in the enlarged inset of Fig. 1. Catchment average rainfall was computed using the Thiessen polygons [30] of available data for the day. For the day with available data from all rainfall stations, the Thiessen [30] polygons will be computed using 6 rainfall stations (as shown in the inset of Fig. 1). For days that have missing data (e.g. if station 1 data is missing), the Thiessen polygons [30] will be computed using the available data only, namely stations 2, 3, 4, 5, and 6. Similarly, if data from stations 1 and 2 are missing, then the Thiessen polygons [30] will be computed using the available data from stations 3, 4, 5, and 6. There are different polygons for different sets of missing data.

Statistics of daily rainfall for this catchment are shown in Table 1. Table 1 shows that the overall means, standard deviations, skews, and coefficient of variations of daily rainfall for this catchment are 4.4, 15.6, 8.1, and 3.5 mm, respectively.

Table 1 Recorded daily rainfall statistics (after [4])

Month	Mean (mm)	Std. Dev. (mm)	Skew (γ)	Coeff. Var. (C_v)	γ/C_v
Jan	4.8	16.4	11.3	3.4	3.3
Feb	5.5	17.5	7.4	3.2	2.3
Mar	5.8	18.2	6.3	3.1	2.0
Apr	4.9	16.5	7.0	3.4	2.1
May	4.8	17.7	7.9	3.7	2.1
Jun	6.1	19.3	5.5	3.1	1.8
Jul	4.6	18.0	8.3	3.9	2.1
Aug	3.1	11.4	8.2	3.7	2.2
Sep	3.1	9.9	6.5	3.2	2.0
Oct	3.7	15.0	9.2	4.1	2.3
Nov	2.9	8.9	6.8	3.0	2.2
Dec	4.1	12.2	7.3	3.2	2.3
Overall	**4.4**	**15.6**	**8.1**	**3.5**	**2.3**

Fig. 2 Plot of serial
correlation against lag [4]

(Kangaroo Valley catchment)
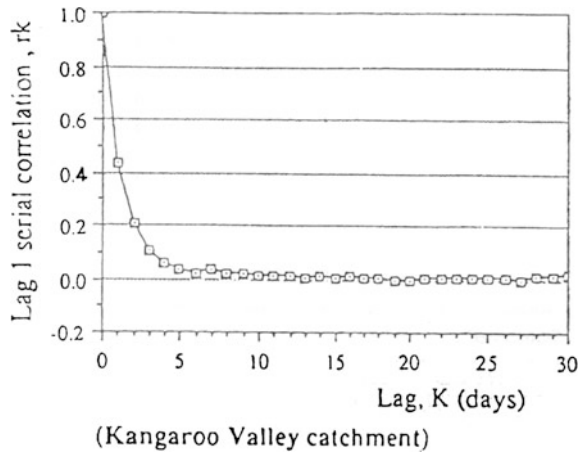
The ratio of skew to coefficient of variation is 2.3, which is close to 2, indicating that gamma distribution can be used to approximate the rainfall distribution [5].

Figure 2 shows a plot of serial correlation coefficient (r_k) plotted against the corresponding lag (k). The lag-one value is $r_1 = 0.436$, while the other r_k values are less than half r_1 [4]. Fisher [13] suggested a value of r_k of 0.349 as the conventional minimum value for stochastic analysis of time series. The lag-one serial correlation coefficient (r1) was shown to be satisfactory for this catchment, while the other r_k values are much lower than the suggested conventional minimum value. Lag-one correlation was adopted for this paper [4].

Figure 3 shows the plot of annual rainfall values [4]. No apparent trend can be observed in the values of annual rainfall for this catchment. Therefore, the random

Fig. 3 Plot of annual catchment rainfall [4]
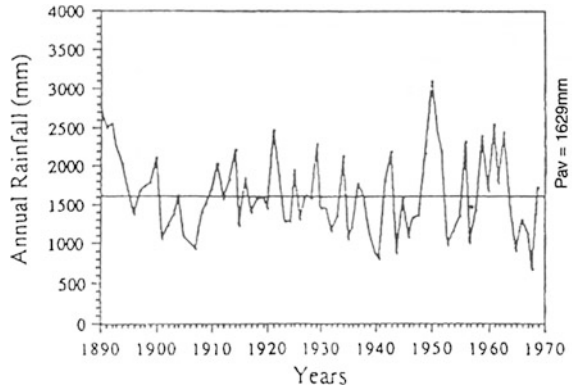
variations are assumed to continue in the future. The stochastic rainfall data generation is therefore assumed to be able to reproduce these random variations [4].

2.2 Lag-One Markov Chain Model

Baki [4] used lag-one Markov chain model in modelling daily rainfall. Earlier applications of lag-one Markov chain model were by Adamowski and Smith [2] and Richardson [22].

In the study by Baki [4], the daily recorded rainfall values were standardised as follows:

$$z_i = \frac{(x_i - \overline{x_i})}{\sigma_i} \tag{1}$$

where z_i is the standardised daily rainfall (mm) for day i, with zero mean and unit standard deviation; x_i is the daily rainfall (mm) for day i; σ_i is the standard deviation (mm) for day i; is the average daily rainfall (mm) for day i, where i ranges from 1 to 366 (including leap years).

The generated rainfall data is given by:

$$z_i = r_i z_{i-1} + t_i \sqrt{(1 - r_i^2)} \tag{2}$$

which gives:

$$x_i = \overline{x_i} + \sigma_i \left[r_i z_{i-1} + t_i \sqrt{(1 - r_i^2)} \right] \tag{3}$$

where x_i is the generated rainfall on day i (mm); $\overline{x_i}$ is the mean recorded daily rainfall of day i (mm); σ_i is the standard deviation of recorded daily rainfall on day i (mm); r_i is the lag-one serial correlation for the whole record; z_{i-1} is the standardised rainfall on day $i-1$; and t_i is the normally distributed random numbers with zero mean and unit variances.

Baki [4] used three variations of the lag-one Markov chain model, untransformed data (referred to as QT), logarithmically transformed data (referred to as LOG), and square root transformation (referred to as SQR). All these three results will be used in the comparison.

2.3   Two-Step Model

The large number of zero values of daily rainfall caused problems to single-step runoff generation type of model to generate daily rainfall data. The two-step model was developed to separate the analysis between the occurrence of rainfall and the rainfall depth. Baki [5] used the two-step model by modelling the occurrences of rainfall using transition probabilities between two classes of events (dry days and wet days). The transition probabilities between the two classes are according to Markov chain probabilities.

The gamma distribution can be used to model rainfall depths during wet days. Table 1 shows that the ratio of daily skew coefficients to coefficient of variation (γ/C_v) of the recorded data is 2.3, which is close to 2. Baki [5] adopted the gamma distribution since the data he used had a ratio (γ/C_v) close to 2. This distribution is also utilised by Jones et al. [16] and Carey and Haan [11].

The gamma distribution is given by:

$$F(x||k) = \int_{o}^{x} \frac{(\lambda_{ik})\eta_{ik}}{\Gamma(\eta_{ik})} U^{(\eta_{ik}=1)} \exp(-\lambda_{ik}U)\mathrm{d}u \tag{4}$$

where U is the uniformly distributed random number between 0 and 1.

In order to find the parameters, λ and η, maximum likelihood can be used. Carey and Haan [11] used maximum likelihood to find the parameters in their study. For example,

$$\eta^* = \frac{0.5000876 + 0.164852y + 0.0544274y^2}{y} \tag{5}$$

in which

$$y = \mathrm{In}\left(\sum_{i=1}^{n}\frac{v_i}{n}\right) - \sum_{i=1}^{n}\frac{\ln v_i}{n} \tag{6}$$

$v_i = i$th observation from a sample of n observations.

Correction for small sample bias can then be made as follows:

$$\eta = \frac{(n-3)\eta^*}{n} \tag{7}$$

The estimate for λ can then be made:

$$\lambda = \frac{\eta}{\sum_{i=1}^{n}\frac{v_i}{n}} \tag{8}$$

Baki [5] used the two-step model, using a first-order Markov chain to model occurrences of rainfall and a gamma distribution to generate rainfall depths during wet days. The parameters of the gamma distribution will be estimated from the recorded wet days. The results from this study will be used in the comparison (referred to as TS).

2.4 Transition Probability Matrices Model

Haan et al. [14] mentioned that persistence and periodicities can be observed in daily weather patterns. The persistence is modelled by a Markov chain. Consider

$$P\left(E_{nj}|E_{n-1j_{n-1},\ldots,}E_{1j_1}\right) = P\left(E_{nj}|E_{n-1j_{n-1}}\right) \tag{9}$$

where for $x_1, x_2, \ldots$ as the observations of daily rainfall, then $E_{i,j}$ ($i = 1, 2,\ldots, c$, and $j = 0, 1, \ldots, c$), where c is the number of classes or states, and if $P(E_{nj}|E_{n-1j})$ does not depend on n, then these transition probabilities (denoted P_{ij}), and the Markov chain is stationary. The transition probability matrices (TPM) is the collection of P_{ij} between classes in $(c + 1) \times (c + 1)$ matrices.

Periodicities mean that the weather pattern undergoes a cyclical behaviour within a year. Within a season, the weather pattern can be assumed to be stationary. Therefore, the TPM can be assumed to be stationary within each season:

$$P_{ij}^{(k)}(i.j = 0, 1, \ldots, c) \quad \text{and} \quad (k = 1, \ldots, s) \tag{10}$$

where k denotes the kth season and s is the total number of seasons.

The probability distributions had to be fitted to each class. It was assumed that the same set of distributions would model each season. Therefore, $(c + 1)$ cumulative distribution functions are used:

$$F_m(x)(m = 0, \ldots, c) \tag{11}$$

where $F_m(x) = P$ (rainfall $< x$ | rainfall belongs to class m).

A uniform distribution was assumed for all wet states, except for the last one. For the highest class, a shifted exponential distribution was found by Haan et al. [14] to be the most suitable:

$$F_{\text{last}(x)} = \exp\left((x - \text{ncl})/\eta\right) \tag{12}$$

where ncl is the lower boundary of the last class and η is a constant found by maximum likelihood:

$$\eta = \bar{x} - \text{ncl} \tag{13}$$

where $\bar{x}$ is the mean daily rainfall greater than ncl.

Haan et al. [14] adopted the months to be the seasons. Seasons follow an annual cycle, and by using months to represent seasons, the cyclical pattern can be satisfactorily represented. Hence, the TPM can be assumed to be stationary within a month. They also adopted 7 classes of daily rainfall states after testing up to 12 classes. These values were found to be satisfactory for the Kentucky basin. Therefore, twelve sets of (7×7) matrices needed to be found from the recorded data.

Baki [6] tested six variations of the TPM model: 6×6 TPM (called SE6), 7×7 TPM (called SE7), and 8×8 TPM (called SE8), all three with shifted exponential distribution for the last class and linear distribution for the other classes, and 6×6 TPM (called BC6), 7×7 TPM (called BC7) and 8×8 TPM (called BC8), all three with Box–Cox power transformation for the last class and linear distribution for the other classes. The last (highest) class has closed lower bound and open upper bound. The class boundaries are shown in Table 2. The results from Baki [6]'s study will be used in the comparison.

Table 2 Class boundaries for TPM model

Class	Lower limit (mm)	Upper limit (mm)		
		6×6	7×7	8×8
1	0.0	0.0	0.0	0.0
2	0.1	0.9	0.9	0.9
3	1.0	2.9	2.9	2.9
4	3.0	6.9	6.9	6.9
5	7.0	14.9	14.9	14.9
6	15.0	∞	30.9	30.9
7	31.0 (for 7×7 and 8×8)	N/A	∞	62.9
8	63.0 (for 8×8)	N/A	N/A	∞

3 Results and Discussion

Ten replicates of generated data were made, each with the same length as the recorded data. The average of the statistical measures of the generated data was compared to those of the recorded data.

Table 3 shows the average of ten replicates of daily means of all models used compared to the recorded data. In general, the statistical measures of daily means of the generated data for all models are satisfactory except for untransformed lag-one Markov chain model (QT). In comparison, all the six variations of the TPM and TS models are more accurate compared to those of the lag-one Markov chain model, in respect to the daily means of the recorded data. In terms of accuracy of the daily means, 7×7 TPM (SE7 with 8 accurate daily means followed by BC7 with 7) gave the best results compared to others (as highlighted in Table 3).

Table 4 shows the average of ten replicates of daily standard deviations compared to the recorded data. Again, the statistics of the generated data for all six variations of the TPM and TS models are more accurate compared to those of the lag-one Markov chain model. In terms of accuracy, the standard deviations for 6×6 and 7×7 TPM (SE6, SE7, BC6, BC7) tend to be lower, indicating that the data generated by the model tend to be more normally distributed, while 8×8 TPM (SE8 and BC8) can generate data that are less normally distributed compared to the recorded data as some of the standard deviations exceeded those of the recorded data. Furthermore, SE8 and BC8 both have 4 accurate daily standard deviations, which are much better than others (SE7 and BC6 both have 2, as highlighted in Table 4).

Table 5 shows the average of ten replicates of daily skews compared to the recorded data. Once again, the statistics of the generated data for all six variations of the TPM and TS models are satisfactory compared to those of the lag-one Markov

Table 3 Mean daily rainfall statistics' comparison

Month	Daily means for recorded and average for the generated data (mm)										
	Rec	Lag-one Markov			2-step	TPM model					
		QT	LOG	SQR	TS	SE6	SE7	SE8	BC6	BC7	BC8
Jan	**4.8**	9.2	5.1	5.4	5.0	4.7	**4.8**	5.0	4.9	**4.8**	4.9
Feb	**5.5**	10.3	6.9	6.2	5.6	5.6	5.4	5.4	5.6	**5.5**	5.7
Mar	**5.8**	11.5	6.7	6.5	6.1	5.9	6.1	6.1	5.6	**5.8**	5.9
Apr	**4.9**	9.7	3.8	5.4	5.2	4.8	**4.9**	**4.9**	4.7	5.0	**4.9**
May	**4.8**	10.3	2.8	5.3	**4.8**	5.1	**4.8**	5.0	4.7	**4.8**	5.0
Jun	**6.1**	11.9	4.9	7.0	6.4	**6.1**	6.2	**6.1**	6.2	**6.1**	6.7
Jul	**4.6**	10.0	2.7	5.2	4.9	4.5	**4.6**	**4.6**	4.7	5.0	4.7
Aug	**3.1**	6.6	2.0	3.5	3.3	3.2	**3.1**	3.2	3.3	3.2	**3.1**
Sep	**3.1**	6.1	2.2	3.5	3.4	3.2	**3.1**	3.2	3.2	**3.1**	3.3
Oct	**3.7**	8.1	2.5	4.1	3.6	3.8	**3.7**	3.9	3.6	3.6	**3.7**
Nov	**2.9**	5.5	2.5	3.3	3.3	**3.0**	3.1	**3.0**	**3.0**	**3.0**	**3.0**
Dec	**4.1**	7.9	3.9	4.6	4.4	4.2	**4.1**	4.4	**4.1**	**4.1**	4.4

Table 4 Daily standard deviations' comparison

Month	Daily standard deviations for recorded and average for the generated data (mm)										
	Rec	Lag-one Markov			2-step	TPM model					
		QT	LOG	SQR	TS	SE6	SE7	SE8	BC6	BC7	BC8
Jan	**16.4**	12.5	21.5	7.2	12.3	13.2	14.3	**15.8**	13.5	14.1	15.4
Feb	**17.5**	13.5	28.7	8.5	12.6	15.3	16.4	16.8	16.0	16.7	**17.4**
Mar	**18.2**	13.6	28.9	8.4	14.4	16.2	**17.9**	19.0	16.3	17.3	17.7
Apr	**16.5**	12.1	16.9	7.0	12.6	14.6	16.2	**16.3**	14.9	16.1	15.6
May	**17.7**	12.9	13.0	6.9	12.5	17.0	16.6	18.4	15.7	16.5	**17.3**
Jun	**19.3**	14.5	22.3	9.2	16.7	18.3	18.9	**19.5**	18.3	18.7	20.0
Jul	**18.0**	13.5	15.3	7.5	13.5	15.4	16.6	17.4	16.0	17.6	**18.2**
Aug	**11.4**	8.7	11.0	5.0	8.8	10.7	10.9	**11.5**	11.1	10.9	10.8
Sep	**9.9**	7.4	9.8	4.6	9.5	9.6	**9.8**	10.3	**9.8**	9.7	10.2
Oct	**15.0**	11.2	11.8	5.7	9.2	12.5	14.3	16.7	13.0	14.4	**14.7**
Nov	**8.9**	7.0	11.3	4.5	**9.0**	8.4	9.5	9.2	8.4	**8.8**	8.7
Dec	**12.2**	10.0	17.4	6.1	11.0	12.4	12.6	14.1	**12.1**	12.7	14.4

Table 5 Daily skews' comparison

Month	Daily skews for recorded and average for the generated data (mm)										
	Rec	Lag-one Markov			2-step	TPM model					
		QT	LOG	SQR	TS	SE6	SE7	SE8	BC6	BC7	BC8
Jan	**11.3**	2.7	**9.3**	2.6	5.5	4.9	6.5	8.1	4.7	5.8	7.4
Feb	**7.4**	2.0	8.3	2.6	4.4	5.1	6.2	**7.3**	4.8	5.8	6.4
Mar	**6.3**	1.4	9.0	2.2	4.9	4.8	5.7	6.7	4.7	5.6	**6.0**
Apr	**7.0**	1.6	10.5	2.2	4.3	5.7	6.4	**7.5**	5.2	5.7	6.4
May	**7.9**	1.7	12.1	2.3	4.3	6.3	6.4	**8.2**	5.3	6.0	7.0
Jun	**5.5**	1.5	9.8	2.3	5.4	4.9	**5.4**	6.1	4.4	4.9	5.0
Jul	**8.3**	2.0	14.0	3.0	4.9	6.2	6.8	8.1	5.3	6.3	**8.2**
Aug	**8.2**	1.9	14.8	2.7	4.8	6.1	7.0	**7.7**	5.7	6.4	7.1
Sep	**6.5**	1.5	11.3	2.2	**6.5**	5.5	6.3	**6.5**	5.2	5.9	6.1
Oct	**9.2**	2.1	12.4	2.6	4.2	6.1	8.8	11.5	7.2	**9.3**	9.0
Nov	**6.8**	2.1	12.1	2.8	**6.7**	5.2	6.5	6.6	4.8	5.9	6.6
Dec	**7.3**	1.8	10.4	2.3	5.5	5.5	6.4	**6.9**	5.0	5.9	**6.9**

chain model, in comparison with the recorded data. In terms of accuracy, the skews for 6 × 6 and 7 × 7 TPM (SE6, SE7, BC6, BC7) tend to be lower, indicating that the data generated by the model tend to be more normally distributed. The 8 × 8 TPM (SE8 and BC8) can generate data that are less normally distributed compared to the recorded data, since some of the skews exceeded those of the recorded data. SE8 has 6 accurate daily skews, followed by BC8 with 4 (as highlighted in Table 5).

By comparing the daily statistics (means, standard deviations, and skews), the TPM models gave the most accurate results compared to the two-step (TS) model

and both TPM and TS are more accurate than the lag-one Markov chain models (QT, LOG, and SQR), especially the untransformed (QT). Within the TPM models, the 7×7 TPM (both SE7 and BC7) gave the best estimates of daily means, but the 8×8 TPM (SE8 and BC8) gave best estimates of daily standard deviations and daily skews. However, the differences between the variations (SE6, SE7, SE8, BC6, BC7, and BC8) are not significant. In general, all six variations were equally satisfactory as the differences between the six variations are minimal. Thus, the findings of Baki [6] were consistent with the past research as Haan et al. [14] found that the number of classes did not affect the accuracy of the TPM model to a great extent. Therefore, the selection between the six variations is not very critical.

In all daily statistical measures, i.e. means, standard deviations, and skews, Tables III, IV, and V show that the trend of the figures given by the TPM model (SE6, SE7, SE8, BC6, BC7, and BC8) follows the trend of the recorded data better than the other models (TS and lag-one Markov). In overall considerations, the TPM is proven to be the most satisfactory model. This finding is consistent with other researches, such as by Srikanthan et al. [28].

Apart from comparing the daily statistical measures (as carried out by [4–6]), other measures were also necessary to be compared. As discussed above, selection between the TPM variations is not critical, and thus, SE8 and BC8 are adopted for further comparison. Since TS has no variations, it is also adopted for further comparison. For the three variations of the lag-one Markov chain model, Baki [4] found that LOG was the most satisfactory variation, and thus, it is adopted for further comparison. Hence, further comparisons were made between SE8, BC8, TS, and LOG.

Figure 4 shows the comparison of daily maxima between recorded data and 4 adopted models. For daily maxima, SE8 was found to be most satisfactorily as it is
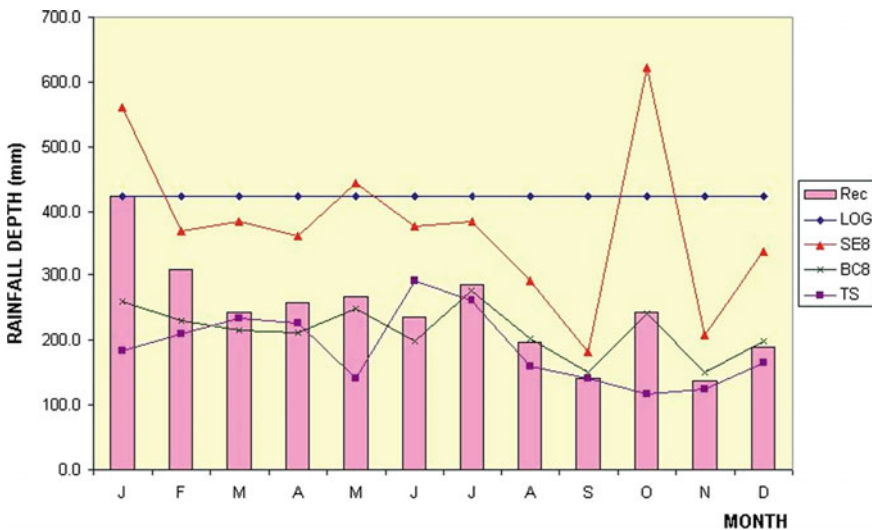
Fig. 4 Comparison of daily maxima
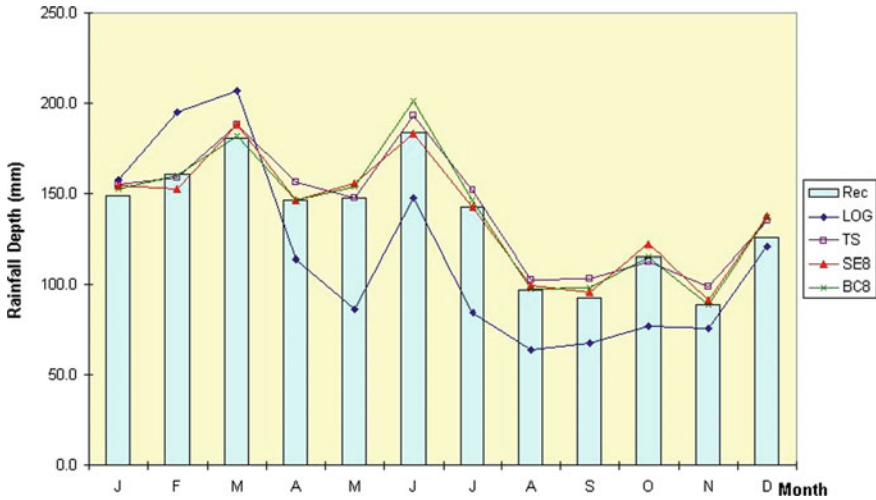
Fig. 5 Monthly means

capable of generated daily maxima greater than the recorded maximum daily rainfall of 423.5 mm. BC8 and TS were also satisfactory in generating the trend, but they tend to have values slightly lower than the recorded maximum. Nevertheless, SE8, BC8, and TS are satisfactory in generating similar trend of daily maxima to the recorded data, hence satisfactory in generating extreme rainfall events. LOG seems to be overestimating the occurrences of daily maxima, with the model generating daily maxima with higher magnitude at higher frequencies compared to other models and also compared to the recorded data.

Figures 5, 6, 7, and 8 show the comparison of monthly statistics. The daily data (recorded and generated) were accumulated on monthly basis, and statistical comparisons were made between the cumulative monthly figures. Figure 5 shows
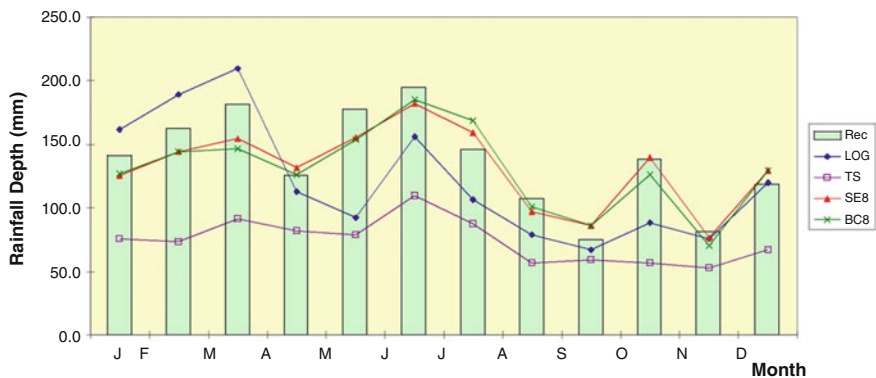
Fig. 6 Monthly standard deviations
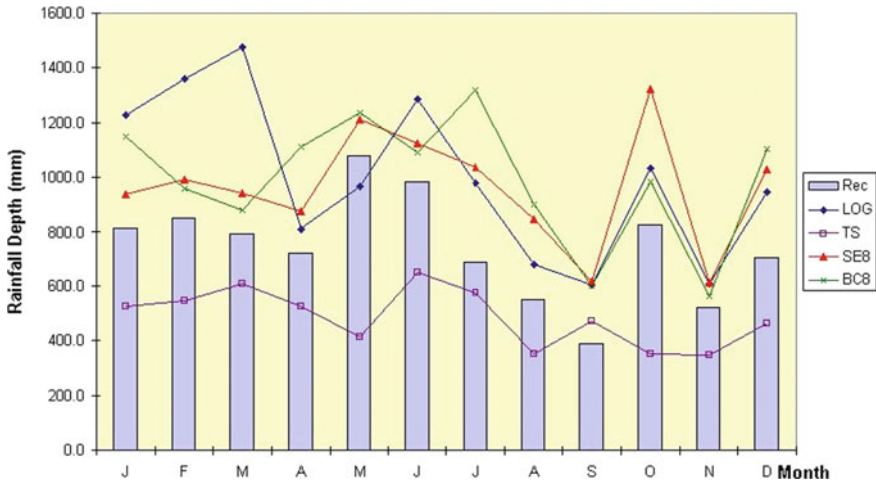
Fig. 7 Monthly maxima
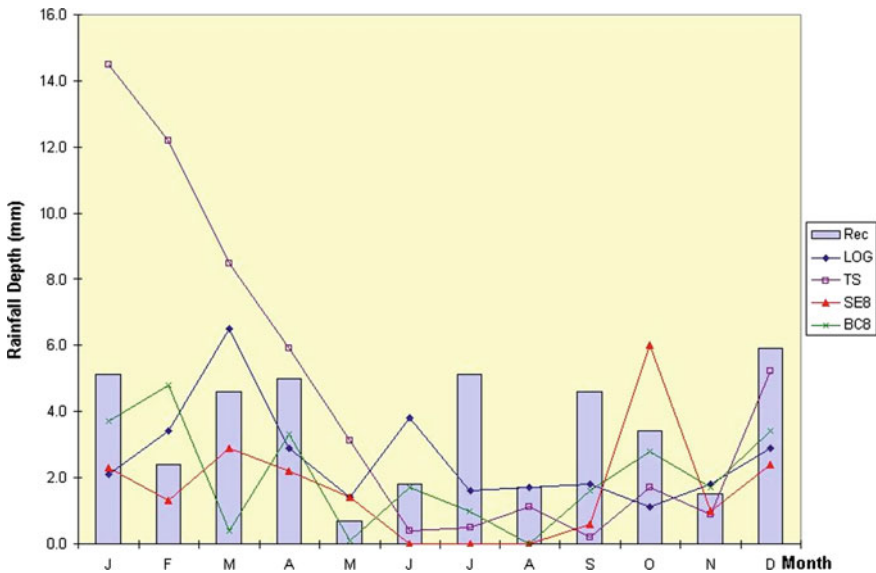
Fig. 8 Monthly minima

that for monthly means, SE8, BC8, and TS were most satisfactory in generating monthly means. Figure 6 shows that SE8 and BC8 were most satisfactory in generating monthly standard deviations, followed by LOG, as TS tends to under-estimate the monthly standard deviations. Figure 7 shows that for monthly maxima, SE8, BC8, and LOG were most satisfactory, while TS tends to generate lower

Table 6 Annual statistical comparison

Measures	Recorded	LOG	TS	SE8	BC8
Mean (mm)	1629.2	1394.8	1703.4	1669.4	1678.1
Std. Dev.(mm)	515.0	457.2	263.6	474.0	499.6
Skew	0.5	0.7	0.3	0.5	0.6
Maximum (mm)	3103.3	3222.5	2617.8	3643.0	3736.5
Minimum (mm)	684.9	358.5	1029.2	574.2	632.8
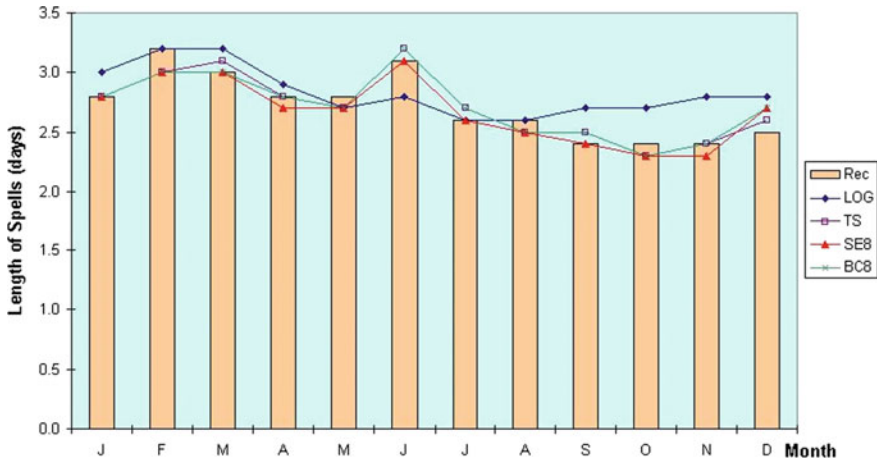
Fig. 9 Average length of wet spells

maxima. Figure 8 shows that for monthly minima, SE8, BC8, and LOG were most satisfactory, while TS tends to generate higher minima during the first quarter. Thus, TS is not able to generate extreme rainfall or drought events.

Table 6 shows the comparison of annual statistics. For annual statistics, SE8 and BC8 are satisfactory in generating annual means, standard deviations, skews, and maxima and minima. TS is only satisfactory in generating annual means, but tends to underestimate the standard deviations, skews, and maxima and overestimate the minima. Thus, TS is unable to reproduce the variations in the recorded data. LOG generated data with lower annual means (14.4 % lower than the annual recorded rainfall), satisfactory standard deviations, skews, and maxima and minima. LOG had the tendency to underestimate the annual rainfall figures.

Figure 9 shows the comparison of average length of wet spells. In terms of sequences of rainfall events, all models were generally satisfactory in reproducing the average lengths of wet spells. Figure 10 shows the comparison of average length of dry spells. LOG tends to underestimate the average lengths of dry spells, while the other three models (SE8, BC8, and TS) are satisfactory. Thus, LOG is unable to model drought events satisfactorily.
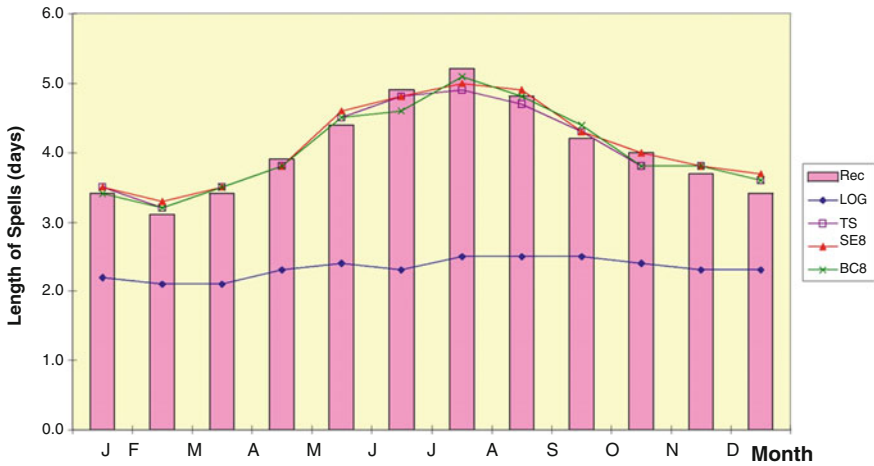
Fig. 10 Average length of dry spells

After further comparisons were made, findings are consistent with the daily statistical comparison (Tables 3, 4, and 5). It is also indicated that the TPM is the most satisfactory model. This finding is consistent with earlier discussions on Tables 3, 4, and 5 and also with other researches, such as by Srikanthan et al. [28]. Thus, TPM can be used to generate stochastic daily rainfall data, which will give synthetic data that is statistically similar to the recorded data.

4 Conclusions

In conclusion, except for QT, all the other models have produced synthetic rainfall data, which are statistically similar to those of the available data. The data generated have similar stochastic properties compared to the recorded data, and statistically, it can be deduced that both samples (recorded and generated sets) come from the same statistical population.

In comparison, the most accurate model is the TPM model for this particular case. It is able to generate data with the closest statistical measures to those of the recorded data. As the data in this case is shown to be persistent over the whole 80-year period, the model can be assumed to be able to forecast the variation in rainfall data. Therefore, this model may be utilised for synthetic rainfall data generations. These synthetic data can then assist in giving possible variations of rainfall over longer period, which would be useful for forecasting.

References

1. Adam RY (2012) Stochastic model for rainfall occurrence using markov chain model. PhD Thesis, Sudan University of Science and Technology, Khartoum, Sudan, unpublished
2. Adamowski K, Smith AK (1972) Stochastic generation of rainfall. J Hydraul Div Am Soc Civil Eng 98(HY11):1935–1945
3. Baki ABM (1996) Objective functions in the optimisation of daily rainfall-runoff modelling. JURUTERA: Mon Bull Inst Eng Malays 9:11–15 (September)
4. Baki ABM (1997) Stochastic rainfall data generation using lag-one markov chain model. J Inst Eng Malays 58(3):55–61
5. Baki ABM (2002) Stochastic rainfall data generation using two-step markov chain model: a case study. In: Proceedings of the 20th conference of ASEAN federation of engineering organisations (CAFEO20), Phnom Penh, Cambodia, vol 1, pp 85–92, 2–4 Sept 2002
6. Baki ABM (2005) Stochastic rainfall data generation using transition probability model. In: Proceedings of the seventh annual IEM water resources colloquium 2005, The Institution of Engineers Malaysia, Petaling Jaya, Malaysia, pp 9-1–9-9, 18 June 2005
7. Benson MA, Matalas NC (1967) Synthetic hydrology based on regional statistical parameters. Water Resour Res 3(4):931–935
8. Box GEP, Cox OR (1964) The analysis of transformations. J Roy Stat Soc B 26(2):211–252
9. Camberlin P, Gitau W, Oettli P, Ogallo L, Bois B (2014) Spatial interpolation of daily rainfall stochastic generation parameters over East Africa. Clim Res 59(1):39–60
10. Campo MA, Lopez JJ, Rebole JP (2012) Rainfall stochastic models, EGU general assembly 2012, held 22–27 Apr 2012 in Vienna, Austria, p 13458
11. Carey DI, Haan CT (1978) Markov processes for simulating daily point rainfall. J Irrig Drai Div Am Soc Civil Eng 104(IR1):111–125
12. Dartidar AG, Gosh D, Dasgupta S, De UK (2010) Higher order markov chain model for monsoon rain over West Bengal, India. Ind J Radio Space Phys 39:39–44 (Febraury)
13. Fisher RA (1958) Statistical methods for research workers, 13th edn. Oliver & Boyd, London
14. Haan CT, Allen DM, Street JO (1976) A Markov chain model of daily rainfall. Water Resour Res 12(3):443–449
15. Hernáez PF-A, Martin-Vide J (2011) Regionalization of the probability of wet spells and rainfall persistence in the Basque Country (Northern Spain). Int J Climatol 32(Issue 12): 1909–1920 (October 2012)
16. Jones JW, Colwick RD, Threadgill ED (1972) A simulated environmental model of temperature. Evaporation Rainfall Soil Moisture Trans Am Soc Agric Eng 15(2):366–372
17. Malek MA, Baki AM (2014) Forecasting of hydrological time series data with lag-one markov chain model. ASEAN J Sci Technol Dev 31(1): 31–37. ISSN: 0217-5460
18. Mehrotra R, Westra SP, Sharma A, Srikanthan R (2012) Continuous rainfall simulation: 2 a regionalized daily rainfall generation approach. Water Resour Res 48:W01536
19. Meshram S, Bisen Y, Kant S, Singh G, Nema AK (2013) Markov chain model probability of dry wet weeks and statistical analysis of weekly rainfall for agricultural planning at Jabalpur. J Environ Ecol 31(3):1250–1254
20. Mhanna M, Bauwens W (2011) Stochastic single-site generation of daily and monthly rainfall in the Middle East. Meteorol Appl 19(1):111–117 (March 2012)
21. Nema AK, Bisen Y, Singh SR, Singh T (2013) Markov chain approach—dry and wet spell rainfall probabilities in planning rainfed rice based production system. Ind J Dryland Agric Res Dev 28(2):16–20
22. Richardson C (1978) Generation of daily precipitation over an area. Water Resour Bull 1 (5):1035–1047
23. Solomon S (1976) Parameter regionalisation and network design. In: Shen HW (ed) Stochastic approaches to water resources. Colorado State University Press, Fort Collins, pp 12.1–12.37
24. Sonnadara DUJ (2012) Modeling daily rainfall using markov chains, annual research sympsium 2012. University of Colombo, Sri Lanka

25. Sonnadara DUJ, Jayawardene DR (2014) A Markov chain probability model to describe wet and dry patterns of weather at Colombo. Theor. Appl Climatol, February 2014. doi:10.1007/s00704-014-1117-z (February)
26. Srikanthan R, McMahon TA (1983) Stochastic simulation of daily rainfall for australian stations. Trans Am Soc Agric Eng 26:754–759
27. Srikanthan R, McMahon TA (2005) Automatic evaluation of stochastically generated rainfall data. Aust J Water Resour 8(2):195–201
28. Srikanthan R, Siriwardena L, McMahon TA (2005) Comparison of two daily rainfall data generation models. Aust J Water Resour 8(2):203–212
29. Taewechit S, Soni P, Salokhe VM, Jayasuriya HPW (2011) Optimal stochastic multi-states first-order Markov chain parameters for synthesizing daily rainfall data using multi-objective differential evolution in Thailand. Meteorol Appl 20(1): 20–31, March 2013 (March 2013)
30. Thiessen AH (1911) Precipitation averages for large areas. Mon Weather Rev 1082 pp
31. Yusuf AU, Adamu L, Abdullahi M (2014) Markov chain model and its application to annual rainfall distribution for crop production. Am J Theor Appl Stat 3(2):39–43

Land Use Change Effects on Extreme Flood in the Kelantan Basin Using Hydrological Model

Arnis Asmat, Shattri Mansor, Nader Saadatkhah, Nor Aizam Adnan and Zailani Khuzaimah

Abstract Land use and land cover (LULC) change results in increased of flood frequency and severity. The increase of annual runoff which is caused by urban development, heavy deforestation, or other anthropogenic activities occurs within the catchment areas. Therefore, accurate and continuous LULC change information is vital in quantifying flood hydrograph for any given time. Many studies showed the effect of land use change on flood based on hydrological response (i.e., peak discharge and runoff volume). In this study, a distributed hydrological modeling and GIS approach were applied for the assessment of land use impact in the Kelantan Basin. The assessment focuses on the runoff contributions from different land use classes and the potential impact of land use changes on runoff generation. The results showed that the direct runoff from developmental area, agricultural area, and grassland region is dominant for a flood event compared with runoff from other land-covered areas in the study area. The urban areas or lower planting density areas tend to increase for runoff and for the monsoon season floods, whereas the inter-flow from forested and secondary jungle areas contributes to the normal flow.

Keywords Kelantan River Basin · Land use · Flood event · Hydrological model

A. Asmat (✉)
Faculty of Applied Sciences, Universiti Technologi Mara (UiTM), 40450 Shah Alam, Selangor, Malaysia
e-mail: arnisasmat@gmail.com

S. Mansor · N. Saadatkhah · Z. Khuzaimah
Department of Civil Engineering, Geospatial Information Science Research Centre (GISRC), Serdang, Selangor, Malaysia

N.A. Adnan
Centre of Studies Surveying Science and Geomatics, Universiti Teknologi Mara (UiTM), 40450 Shah Alam, Selangor, Malaysia

1 Introduction

Flood disasters have been reported in many regions and countries; in many cases, the observed magnitudes and frequency of many contemporary floods have been found to be more severe than in the observed record [1–3]. Recent major floods around the world have raised concerns that floods may have increased due to changes in their controls. Land use changes and variability in climate have received much attention in explaining changes in discharge over time, as river floods are mainly driven by precipitation [4] land use change [5–7]. Any changes in the control parameters will cause changes in the flood magnitude. However, the degree of dependence is not yet clear [8].

There is strong evidence that land use changes can increase surface runoff and flooding [9]. The influence of land use change on surface runoff has been investigated in many studies [5–7, 10]. Changes in land use have involved in the conversion of forestland into cropland or other land uses (e.g., builtup, agricultural, or bare land) [11–13] or grazing land, and urbanization [14, 15]. Urbanization leads to an increase in the impervious area, and, as a result, an increase in the magnitude and frequency of occurrence of floods [16] which had caused infiltration excess occurs when poor infiltration conditions are coupled with high rainfall intensities [14]. The effect of land use change on flood behavior is likely to occur for moderate storms, and this effect is reduced during extreme rainfall events [17]. Several studies reported that as a result of deforestation, landscape moisture that would normally be recycled to the atmosphere through evapotranspiration or retained in vegetation is instead quickly released as increased runoff or subsurface flow [18, 19]. Deforestation may cause increase in overland and river flow due to lower evapotranspiration capacity [20].

In Malaysia, these concerns have been brought to a head in the wake of the devastating floods that occurred in 2014 and inundated much of the floodplain within the Sg. Kelantan. At the end of December 2014, Kelantan River Basin in the Peninsular Malaysia had faced the worst (extreme) floods in decades. Heavy rains since December 17 to January 3 had forced Kelantan people close to the river to flee their homes while Kelantan Basin recorded monthly total rainfall amount exceeded 1200 mm during December 2014. Therefore, the following question immediately arose: How much of those severe flood conditions were actually caused by anthropogenic activities? It may be shown that anthropogenic activities may cause an increase in flood height and flood damage. Does the LULC change (urbanization, deforestation, cultivation) results in increased of flood frequency and severity? How many percent or urbanization especially impervious land cover can cause flood severity? Is the amount and intensity of runoff on catchment scale are strongly determined by the presence of impervious land cover types? To find reasonable answers to these questions, there is an urgent need for estimating the flood using land use changes within the hydrological model parameters.

The idea here is that a model whose parameters depend entirely on catchment characteristics will be able to quantify the impact of land use changes within the hydrological model parameters. Thus, it will enable one to determine the changes that may be expected in flood hydrographs due to changes in land use because of long-term developments (e.g., forest diseases or reforestation of agricultural areas) or short-term developments (e.g., urbanization, industrialization, and highway or airport construction). There is considerable uncertainty about sufficiency of the design flood estimates upon which they were constructed.

Distributed rainfall-runoff model appropriates for extreme flood conditions will be used to generate revised estimates of the flood hydrograph (FH). As part of the population growth, there have been considerable expansion of agriculture and urbanization and associated land use and land cover (LULC) changes, which can be expected to have a significant impact on the runoff processes and therefore the FH. All of these factors can potentially contribute to an increase in the extreme flood estimates.

2 Study Area and Background

2.1 Catchment Area

Kelantan is one of the largest states in Peninsular Malaysia with the huge River Kelantan Basin (Fig. 1). The River Kelantan catchment is located in the north-eastern part of Peninsular Malaysia between the latitudes 4°40′ and 6°12′ North and the longitudes 101°20′ and 102°20′ East. The total area of Kelantan is 15,022 km^2 and about 68.5 % of the population lives in the Kelantan River Basin. The River Kelantan or Sungai Kelantan is one of the major rivers in Malaysia, frequently affected by flooding events [21, 22].

The River Kelantan has two tributary rivers: River Galas and River Lebir. River Galas has two other tributaries known as the River Nenggiri and River Pergau, which contribute about 8000 km^2 or 54 % from the total Kelantan's catchment (i.e., 13,100 km^2). Meanwhile, River Lebir has one tributary known as River Relai, which contributes about 2500 km^2 or 17 % from the total catchment. The average width of the River Kelantan is between 180 and 300 m. From the total catchment area, approximately 95 % is dominated by steep mountainous country (mostly covered with virgin jungle) rising to a height of 2135 m while the remainder is undulating land (mostly covered by rubber and paddy).
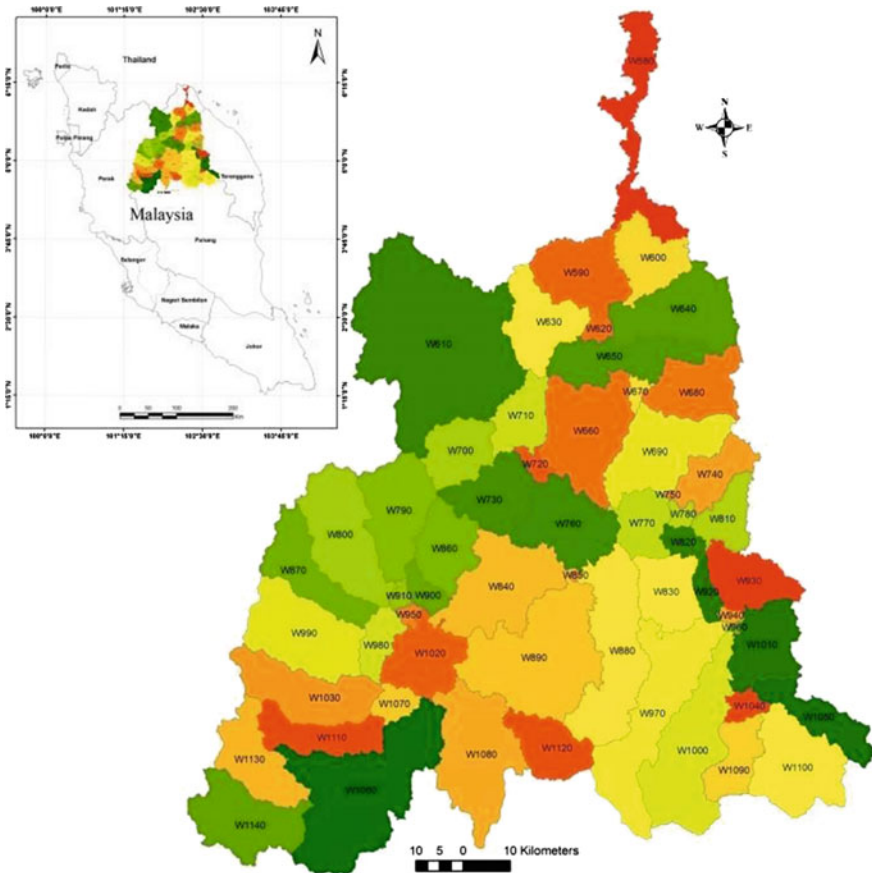
Fig. 1 Location of Kelantan, Malaysia

2.2 Land Use/Land Cover

Kelantan land cover has been defined by reserve forest, which cover an area of 1,078,398.4 ha (71.8 % of Kelantan total land area) mainly located in the upstream area. It is followed by agriculture which covers an area of 309,279.3 ha (20.6 %). Paddy cultivation covers 71,134.0 ha (4.7 %), while urban area and developmental area only cover 22,146.3 ha (1.5 %). The remaining area is covered by orchards and other crops. The distribution of land cover by district in Kelantan for the year 2013 is shown in Fig. 2. Land use change in terms of urban growth has been changing progressively from the 1970s to 1990s with 7 % growth and after the 1990s, there were very slow developments in the area with only 1.4 % growth [23].

Land cover

- Agriculture Station
- Aquaculture
- Banana
- Beach Sand / River Sand
- Cemetery
- Cleared Land
- Cocoa
- Coconut
- Eroded Area
- Floriculture
- Forest
- Herbs & Spices
- Highway / Main Road
- Idle Grasslans / Lallang
- Lake / Pond
- Limestone Hill
- Marshland
- Mine & Ex-Mining Area
- Mixed Horticulture (Village)
- Oil Palm
- Orchard
- Others Crops
- Paddy
- Pasture/ Ruminant
- Poultry & Others
- Power Lines
- Quarry & Ex-Quarry
- Railway
- Reclaimed Area
- Recreational Area
- River / Canal / Waterway / Drain
- Rubber
- Scrub
- Secondary Forest
- Sugarcane
- Swamp Forest / Mangrove Swamp
- Tobacco
- Urban, Residential Etc.
- Vegetables

20   10   0   20 Kilometers

Fig. 2 The distribution of land cover by district in Kelantan for the year 2013

2.3   Climate

Kelantan climate is governed by the regime of the northeast (NE) and southwest (SW) monsoons. According to [24], October–November–December (OND) represents the early and January–February–March (JFM) represents the late stages of the winter monsoon in Malaysia, also known as the NE monsoon. The April–May–June (AMJ) and July–August–September (JAS) seasons represent the early and late stages of the summer monsoon, respectively, also known as the SW monsoon.

The state of Kelantan has a typical equatorial climate characteristic with constantly high annual temperatures, mild wind, and heavy rainfall. Based on Malaysian Meteorological Department (MMD), the annual precipitation over the area varies between 0 and 200 mm in the dry season and 3000 mm in the wet or monsoo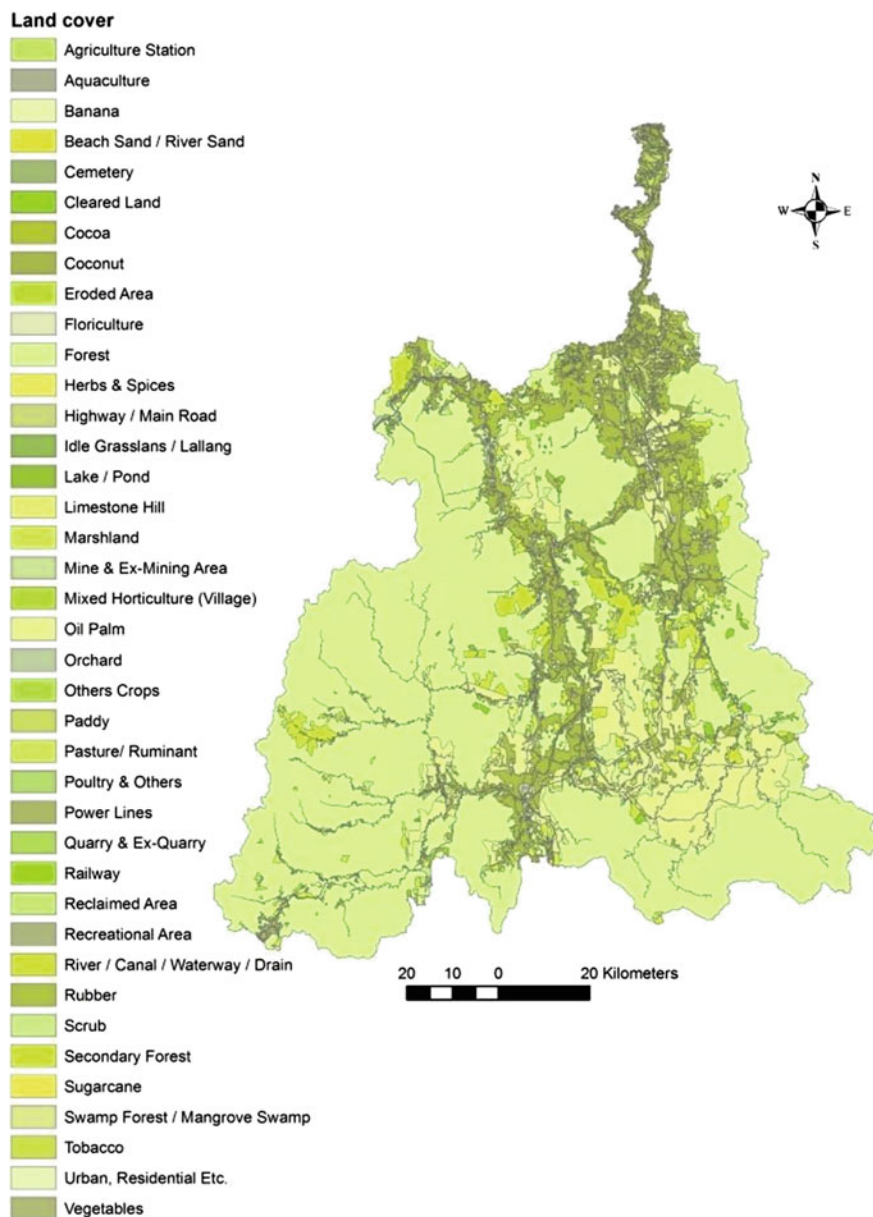n season. The estimated runoff for the River Kelantan catchment is 500 m^3 s^{-1} during 1950–1990. Due to the NE monsoon which brings along heavy rainfall, the River Kelantan often overflows in the period, causing an almost annual recurrence of flood to the state between the end of November till early January [25].

3   Method

3.1   Model Framework

In this paper, the HEC-HMS model based on SCS curve number as rainfall-runoff models was applied to study the impacts of land cover on an extreme flood events in the Kelantan River Basin during December 2014. The HEC-HMS model application was done in conjunction with the HEC-GeoHMS extension in ArcGIS 10. Stream flow estimation was performed on the hourly rainfall data. The aim of this study was to provide a land use sensitivity map using two major frameworks of rainfall-runoff model applications in the Kelantan River Basin. Each model has its own input data sets. HEC-HMS input data include soil type, land use/land cover map, and slope map using SCS-CN values that include the hydrological soil types. Figure 3 represents the flow diagram of the used models in order to perform runoff analysis on a regional scale at the Kelantan River Basin.

3.2   HEC-HMS Model

HEC-HMS is an open-source software for the modeling of the rainfall-runoff process developed by the US Army Corps of Engineering's Hydrologic Engineering Center. The software includes a graphical user interface for the management and analysis of the model data. In HEC-HMS, the rainfall-runoff process in a watershed is represented in a simplified manner.
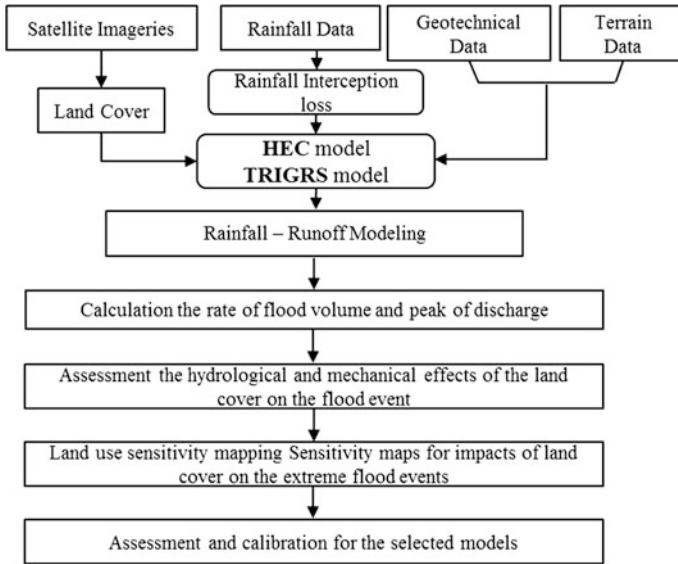
Fig. 3 General framework

This simplified representation of the runoff process does not account for the storage and movement of water vertically within the soil layer. It is however sufficient to model a flood hydrograph as the result of a storm [26]. For modeling purposes, this simplified hydrological cycle is further divided into four components, which are modeled separately.

(i) **Loss Method**: A model to compute the runoff volume is often referred to as the loss method since it accounts for the losses that occur during a rainfall event as a result of infiltration and evapotranspiration. For each time interval in the modeling process, the loss method calculates the amount of water that contributes to the runoff in the river (effective rainfall).

(ii) **Transform Method**: Models of direct runoff are also called transform method, since they convert the effective rainfall over a watershed into a hydrograph at the outlet of the watershed. These models account for the surface roughness and geometry of the watershed.

(iii) **Baseflow Method**: Baseflow models are used to simulate the fraction of the runoff contributed by groundwater.

(iv) **Routing Method**: If the analyzed watershed is divided into sub-watersheds, the flow at the outlet of a certain upstream watershed has to be routed through the river channel in the downstream watershed. The models used to simulate this routing process are therefore called routing methods. They account for the geometry and roughness of the relevant river channel.

3.3 SCS-CN Values

The SCS-CN values have been widely used to compute direct surface runoff. SCS-CN value data developed by Soil Conservation Services (SCS) of USA in 1969 are a simple, predictable, and stable conceptual method for the estimation of direct runoff depth based on storm rainfall depth. It relies on only one parameter, CN. Currently, it is a well-established method, widely accepted for use in USA and many other countries.

The SCS-CN value is based on the water balance equation and two fundamental hypotheses. The first hypothesis equates the ratio of the amount of direct surface runoff Q to the total rainfall P (or maximum potential surface to the runoff) with the ratio of the amount of infiltration F_C and amount of the potential maximum retention S. The second to the potential hypothesis relates the initial abstraction Ia maximum retention.

In determining the CN value, the hydrological soil classification is adopted using four classes A, B, C, and D based on the infiltration and other characteristics. The important soil characteristics that influence the hydrological classification of soils are effective depth of soil, average clay content, infiltration characteristics, and the permeability. The CN values published in Technical Report 55 (TR 55) by USDA [27] were employed as a reference to infer the land use CN values.

3.4 Data Acquisition and Parameterization Procedure

The hydraulic and mechanical data sources were obtained from the Ministry of Agriculture and Agro-Based Industry of Malaysia (MOA), Geological department of Malaysia (JMG), Ampang Jaya Municipal Council (MPAJ), and the Slope Engineering Branch of Public Works Department Malaysia (PWD), as well as data compilation from the previous reported studies and geotechnical boreholes. The properties of the soils are tabulated in Table 1. The mechanical and hydraulic properties were assigned to each cell of the grid map for both the existing and the improved models, as created by the ASCI grid files (Fig. 4).

The rainfall interception loss was calculated based on the land cover maps, and relationships between leaf area index (LAI) and gaps of leaves to ground. Land cover map of Hulu Kelang (see Fig. 4; Table 1) has been used as major data to determine LAI properties for each land class. Under the classification system, nine types of land cover were identified, i.e., primary forest, secondary jungle, rubber, tree cultivation, grass, cleared land, urban area, recreation area, and lake. In particular, Canopy interception method was employed in the present study to determine the precipitation arriving at the vegetation top and LAI characteristic [28]. The LAI of the study area was defined as ranging from 1.49 to 3.99 based on LAI-2000 [29] and linear regression equation from NDVI [30] (Table 1).

Table 1 Characteristics of soils at the Kelantan Basin

Soil name	Group sym.	γs	C′	φ′	Ks	θr	θs
BMU-MUN	SM	18.7	2	35	1.52E−06	0.294	0.339
BHM-TPS-SAN	SC	15.7	5	32	1.61E−07	0.049	0.263
CHS-LKT	SM	18.7	2	35	1.52E−06	0.294	0.339
DRN-MUN-BGR	SM	18.7	2	35	1.52E−06	0.294	0.339
LKI	CL	15.4	21	29	1.64E−08	0.28	0.754
LIK-LSG	CL	15.4	21	29	1.64E−08	0.28	0.754
MLD	CH	13.7	26	23	3.12E−09	0.166	0.873
MUN-SDG	SC	16.8	4	33	1.49E−07	0.05	0.275
PRG	CL	14.1	23	31.5	2.10E−08	0.181	0.842
RGM-BTG	SC	16.8	4	33	1.49E−07	0.05	0.275
RGM-JRA	SC	16.3	11	31	9.61E−07	0.055	0.278
RDU-RSL	SC	16.8	4	33	1.49E−07	0.05	0.275
SGT-KTG	SC	16.3	11	31	9.61E−07	0.055	0.278
STP	CH	13.7	26	23	3.12E−09	0.166	0.873
TYG-CPA-LDG	SC	16.8	4	33	1.49E−07	0.05	0.275
ULD	CL	14.8	22	28	1.84E−08	0.189	0.793

4 Results and Discussion

The initial run of the models are made for the end of December 2014 with land use/land cover. Soil map values obtained from site and land use parameter was chosen to further evaluate rainfall-runoff models at Kelantan River Basin. Land use changes in any catchment affect many processes such as evapotranspiration, resistance to surface runoff, and interception. The input values were initially set based on expected ranges and also based on best fit of outputs. The effect of land cover on the rate of flood event varied between the different catchment areas (Fig. 5).

In the agricultural and developmental area, the land cover changes during the recent 20 years resulted in an enhanced in flood volume [31].

Figure 6 showed the total amounts of precipitation along with the total infiltration losses that resulted in the presented hydrographs in one of catchment area as a sample. 10 days of the modeled rainfall events are considered along with the extreme rainfall intensities of more than 44 mm/hour in the most intense 1 h of the 10 day storm. The absolute loss of a certain event is only a function of the land cover, soil characteristics, and the absolute rainfall depth regardless of the intensity distribution. According to apply both of the models, after the beginning of the rainfall event, no runoff begins until the accumulated precipitation P equals the initial hydraulic conductivity of soil K. After the accumulated rainfall exceeds the initial K, runoff is calculated by subtracting R (water retained in the watershed) from the accumulated rainfall.
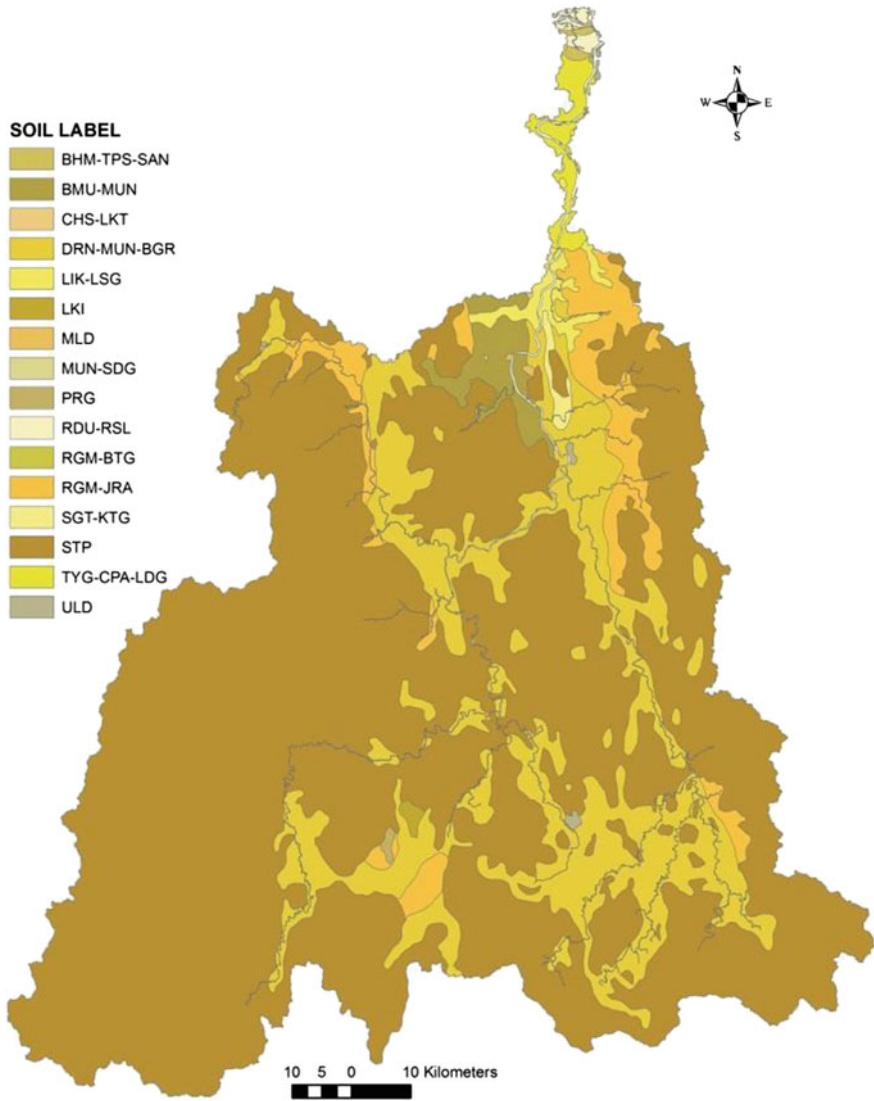
Fig. 4 Soil maps

The effect of land cover on the rate of flood event varied between the different catchment areas. In the agricultural and developmental area, the land cover changes from 1988 to 2013 resulted in enhancing flood volume. Such increments in flood volume are probably due to deforestation and conversion of agricultural land (i.e., rubber and mixed- agriculture). Figure 5 shows the increase of runoff volume as a function of deforestation and urbanization for the study area. The plant cover
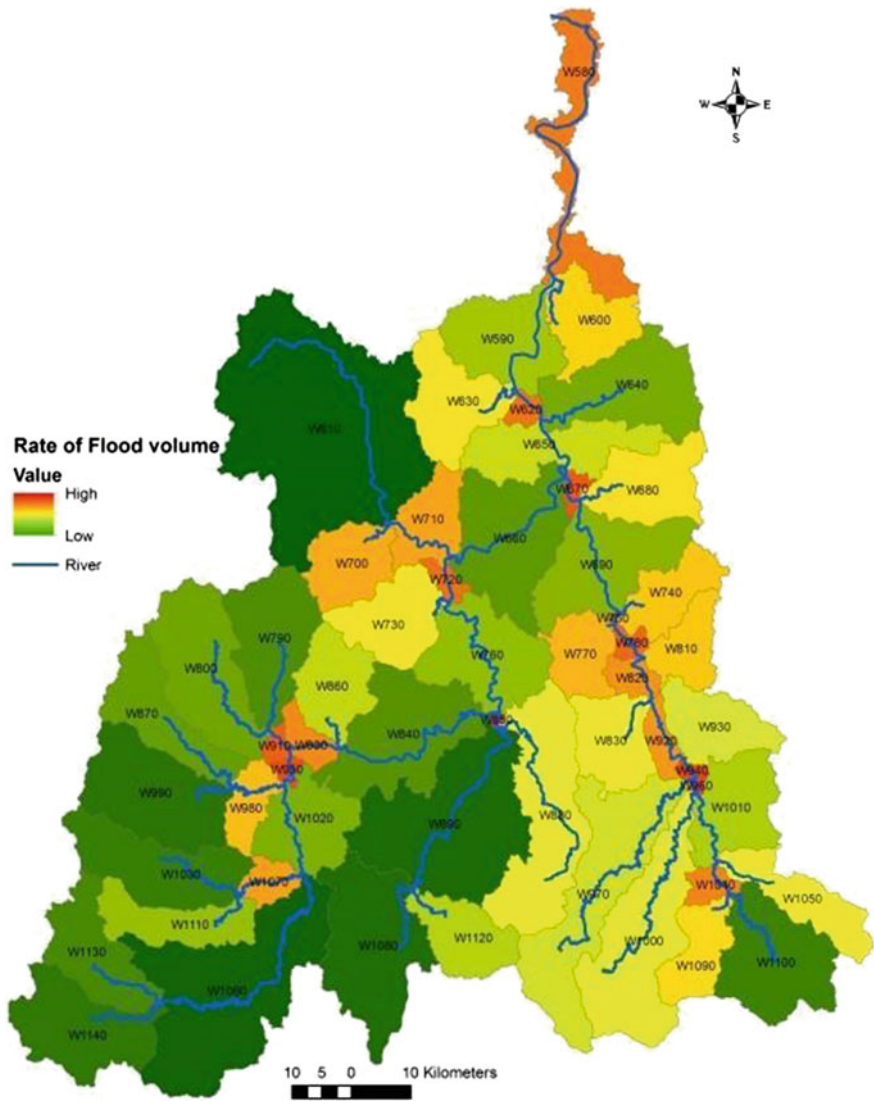
Fig. 5 Potential of flood event on the Kelantan River Basin

change analysis from 1994 to 2013 revealed a moderate percentage of total forest conversion to agricultural area and increase in developmental area.

Figure 7 shows land use change effect on flood flows and critical runoff events were mainly scattered on the agricultural regions and the areas under development. Contribution of different land use types in flood event in percentage of flood volume is illustrated in Fig. 8. In this regard, the fatal debris flows and runoff were caused
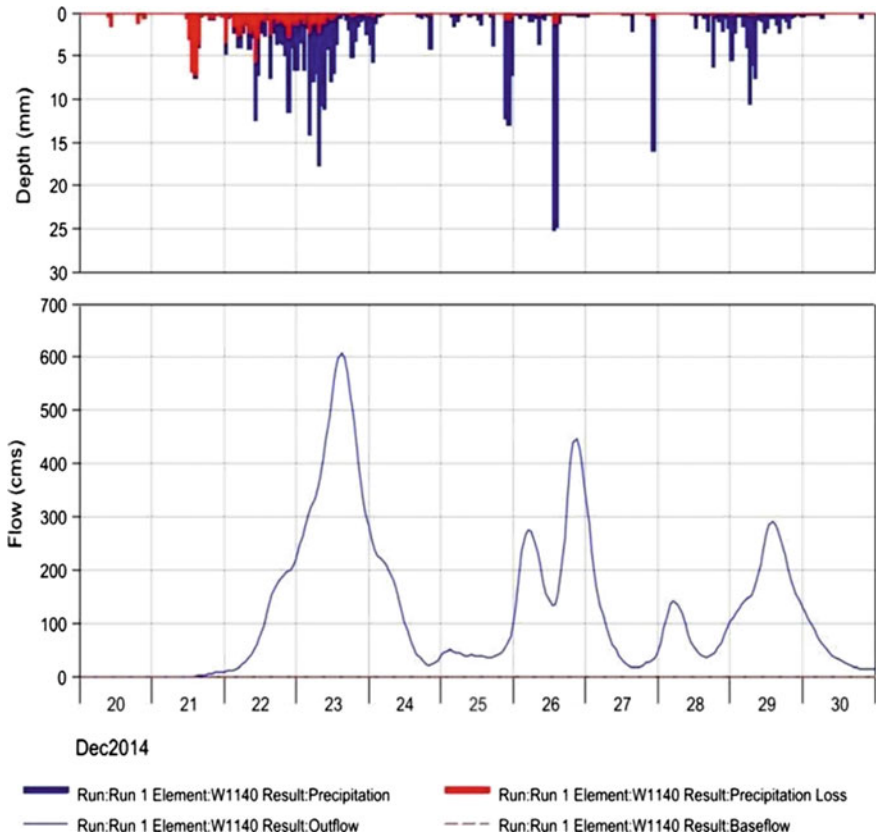
Fig. 6 The total amounts of precipitation along with the total infiltration/losses and rate of flow volume at one of catchment area (w670) at Kelantan Basin

by a combination of extreme rainfall, destruction of natural forest cover (human-caused), and conversion of agricultural plantations in thin, granitic soils.

The area coverage of each land use type acts as a scaling factor in the runoff contributions. Figure 8 shows a summary of the total stream flow contributions from different land use. The results showed that agricultural area contributed in more than 60 % of stream flow using HEC model. The rate of contribution of forest and secondary forest areas at flood events is defined during December 2014 with 40 %. In this regard, the forest clearing means that there is less infiltration/loss because of decrease in porosity and less interception loss water. Conversely, the grassland is a large magnitude of contribution to flood events by 70 %. The increase of grassland allows less infiltration of water due to crusting of the soil which causes higher peak flows and total values of discharge.

The main findings showed that land cover changes caused significant differences in hydrological response to surface water. The increasing of runoff volume at

Fig. 7 Land use changes effect on flood flows

Kelantan River Basin is as a function of deforestation and urbanization, especially the conversion of the forest area to agricultural land (i.e., rubber and mixed-agriculture). Adnan and Basaruddin [7] demonstrated similar finding where forest area plays an important role in controlling water flow and subsequently minimizing the runoff volume in the study area.

Deforestation and conversion to agricultural area caused increase in peak of discharge and flood volume due to lower interception loss and evapotranspiration
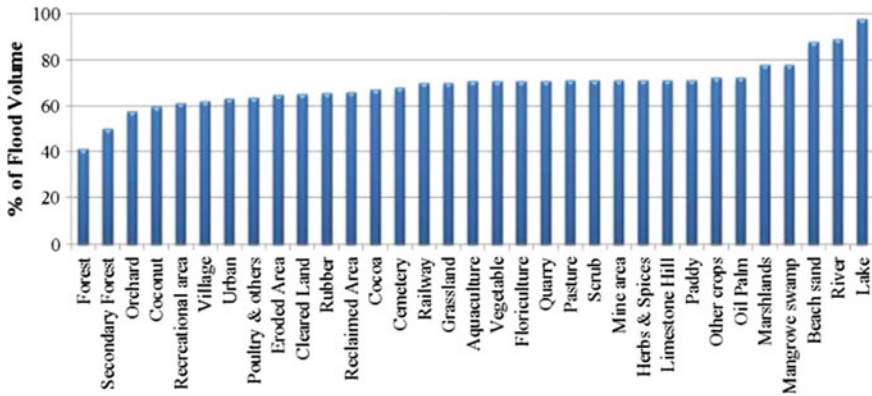
Fig. 8 The percentage of different land use types which contribute to flood volume

capacity. In contrast, urban developmental area leads to a greater impervious ground surface and excess to runoff volume, when less infiltration occurred. The current analysis showed the reliable frameworks to detect the impact of land cover changes in understanding the behavior of the hydrological in catchment areas. However, there are other parameters need be explored further in establishing the relationship of land use and change and peak runoff such as a lag time [32] besides the curve number (CN). Based on absolute sensitivity index analysis, both have the greatest impact on peak discharge and runoff volume, where curve number relates to the capability for soil infiltration and soil storage [13, 33].

5   Conclusion

Change in the land use pattern effect on hydrological processes in watershed affects the natural balance of water flow. LULC change (urbanisation, deforestation, and cultivation) results in increase of flood frequency and severity. The question of how or which anthropogenic activities on a river or within a river basin area cause impacts on flood conditions has not been quantified for Sg. Kelantan Basin. There is a need for comprehensive study on establishing direct relationships between the land use and flood flows to reveal the sensitivity of the land use parameters toward the flood event occurrence.

References

1. Brakenridge GR, Birkett C (2013) Lake storage measurements for water resources management: combining remotely sensed water levels and surface areas. American Geophysical Union Fall, Meeting, San Francisco
2. Pinter N, Ickes BS, Wlosinski JH, van der Ploeg RR (2006) Trends in flood stages: contrasting results from the Mississippi and Rhine River systems. J Hydrol 331:554–566. doi:10.1016/j.jhydrol.2006.06.013
3. Syvitski JPM, Brakenridge GR (2013) Causation and avoidance of catastrophic flooding along the Indus River, Pakistan. GSA Today 23(1):4–10
4. Perdigao AP, Bloschl G (2014) Spatiotemproral flood sensitivity to annual precipitation: Evidence for landscape-climate coevaluation. Water Resour Res, pp 5492–5508
5. Lahmer W, Pfutzner B, Becker A (2001) Assessment of land use and climate change impacts on the mesoscale. Phys Chem Earth Part B 26(7–8):565–575
6. Bathurst JC, Ewen J, Parkin G, O'Connell PE, Cooper JD (2004) Validation of catchment models for predicting land-use and climate change impacts. 3. Blind validation for internal and outlet responses. J Hydrol 287(1–4):74–94
7. Adnan NA, Basaruddin Z (2014) Variation in hydrological response estimation simulation due to land use changes. In: International conference on civil, biological and environmental engineering (CBEE), Istanbul, Turkey, 27–28 May 2014
8. O'Donnell G, Ewen J, O'Connell PE (2011) Sensitivity maps for impacts of land management on an extreme flood in the Hodder catchment, UK. Phys. Chem. Earth 36:630–637
9. Chow VT, Maidment DR, Mays LW (1988) Applied hydrology. McGraw-Hill, New York
10. Shattri M, Saadatkhah N, Arnis A, Zailanai K, Adnan NA (2015) Sensitivity maps for impacts of land cover on the extreme flood events in the Kelantan basin, Malaysia. J Teknol. UTM Press, Penerbit
11. Adnan NA, Atkinson PM (2011) Exploring the impact of climate and land use changes on stream flow trends in a monsoon catchment. Int J Climatol, p 30
12. Xiaoming Z, Xinxiao Y, Manliang Z, Jianlao L (2007) Response of land use/coverage change to hydrological dynamics at watershed scale in the Loess Plateau of China. Acta Ecologica Sinica 27:414–421
13. Wang S, Kang S, Zhang L, Li F (2008) Modelling hydrological response to different land-use and climate change scenarios in the Zamu River basin of northwest China. Hydrol Process 22:2502–2510
14. Moussa R, Voltz M, Andrieux P (2002) Effects of the spatial organization of agricultural management on the hydrological behaviour of a farmed catchment during flood events. Hydrol Process 16(2):393–412
15. Awoniran DR, Adewole D, Sulaiman S. Adegboyega SA, Anifowose Y (2013) Assessment of environmental responses to land use/land cover dynamics in the lower Ogun River Basin, Southwestern Nigeria. Int J Sustain Land Use Urban Plan 1(2):16–31 (ISSN 1927-8845)
16. Tollan A (2002) Land-use change and floods: what do we need most, research or management? Water Sci Technol 45(8):183–190
17. Sriwongsitanon N, Taesombat W (2011) Effects of land cover on runoff coefficient. J Hydrol 410(3–4):226–238
18. IPCC (1996) Climate change 1995. Impacts, adaptations and mitigation of climate change: scientific technical analyses, 1995. Cambridge University Press, UK
19. Wooldridge S, Kalma J, Kuczera G (2001) Parameterisation of a simple semi-distributed model for assessing the impact of land-use on hydrologic response. J Hydrol 254:16–32
20. Niehoff D, Fritsch U, Bronstert A (2002) Land use impacts on storm-run off generation: scenarios of land use change and simulation of hydrological response in a meso-scale catchment in SW-Germany. J Hydro 269:80–93
21. Awadalla S, Noor IM (1991) Induced climate change on surface runoff in Kelantan Malaysia. Int J Water Resour Dev 1991(7):53–59

22. Drainage and Irrigation Department (DID) (2004) Annual flood report of DID for Peninsular Malaysia, Unpublished report. Kuala Lumpur: DID
23. Hassan AAG (2004) Growth, structural change and regional inequality in Malaysia. Ashgate Publishing Ltd., Malaysia
24. Tanggang FT, Juneng I, Ahmad S (2007) Trend and interannual variability of temperature in Malaysia 1961–2002. Theor Appl Chem 89:127–141
25. Drainage and Irrigation Department (DID) (2006). Annual flood report of DID for Peninsular Malaysia. Unpublished report. Kuala Lumpur: DID
26. US Army Corps of Engineers (2000) Hydrologic modeling system (HEC-HMS): technical reference manual. US Army Corps of Engineers, Hydrologic Engineering Center, 149 pp
27. United States Department of Agriculture (USDA) (1986) Urban Hydrology for Small Watersheds. Technical Release 55 (TR-55)—Soil Conservation Service, Engineering Division. USDA, Washington, DC, USA
28. Lawrence PJ, Chase TN (2007) Representing a new MODIS consistent land surface in the Community Land Model (CLM3.0). J Geophys Res 112. doi: 10.1029/2006JG000168
29. LI-COR (1991) LAI-2000 Plant Canopy Analyzer Operating Manual. LI-COR Inc., Lincoln, NE
30. Wang K, Li Z, Cribb M (2006) Estimation of evaporative fraction from a combination of day and night land surface temperatures and NDVI: A new method to determine the Priestley-Taylor parameter. Remote Sens Environ 102:293–305
31. Tuan Pah Rokiah SH, Hamidi I (2011) Land use changes analysis for Kelantan Basin using spatial matrix technique "Patch Analyst" in relation to flood disaster. J Techno-Social 3:1
32. Adnan NA (2010) Quantifying the impacts of climate and land use changes on the hydrological response of a monsoonal catchment, PhD thesis, Southampton University
33. Cunderlik JM, Simonovic SP (2007) Inverse flood risk modelling under changing climatic conditions. Hydrol Process 21(5):563–577

Rainfall Trend Analysis and Geospatial Mapping of the Kelantan River Basin

Nor Aizam Adnan, Sharifah Diyana Syed Ariffin, Arnis Asmat and Shattri Mansor

Abstract Trend analysis was widely used as a tool to detect changes in climatic and hydrologic time series data such as rainfall. Fourteen rainfall stations in the Kelantan River Basin were used to detect trends for each of the sub-basin areas. Two objectives of the study are (i) to quantify the changing trends of rainfall of Kelantan River using statistical tests (i.e., Mann-Kendall test and Sen's slope test) based on monthly, seasonal, and annual time series, and secondly, (ii) to map rainfall trend according to Mann-Kendall test result. Analysis for these two tests revealed that several stations indicated significant increasing and decreasing trends for monthly, seasonal, and annual rainfall time series. The study found that rainfall varies in different months, seasons, and annually as evidenced by the graph and trend maps. Therefore, this information will benefit especially for flood preparation and responses in Kelantan River Basin which annually experiences monsoon flooding.

Keywords Rainfall time series · Mann-Kendall test · Sen's slope estimator · Kriging interpolation

1 Introduction

Statistical methods have been widely implemented to detect time series trends exhibited in hydrometeorological data such as temperature, rainfall, and stream flow. Understanding trends exhibited in hydrological data is crucial for guiding water resource planning and management, and assessing climate variability and

N.A. Adnan (✉) · S.D.S. Ariffin · A. Asmat
Applied Remote Sensing and Geospatial Research Group, Faculty of Architecture, Planning and Surveying UiTM, Shah Alam, Selangor, Malaysia
e-mail: nor_aizam@salam.uitm.edu.my

S. Mansor
Geospatial Information Science Research Center (GISRC), Department of Civil Engineering, Faculty of Engineering, University Putra Malaysia (UPM), Serdang, Selangor, Malaysia

change impacts on water resources [1, 2]. Linear trends of a hydrological time series can be detected using nonparametric statistical tests such as the Spearman's rho, Seasonal Kendall, and Mann-Kendall tests [3]. In particular, the Mann-Kendall test has received great attention because it is the only nonparametric test suitable to be used in climatic and hydrologic studies [4, 5].

The Mann-Kendall test together with Sen's slope test is used to get the trend and slope magnitude. Mann-Kendall test has been applied in order to find any trend of rainfall, temperature, and evapotranspiration time series [6]. Mann-Kendall test is also used for studying the spatial variation and temporal trends of hydroclimatic series. In addition, Mann-Kendall test is used to a set of time-ordered data undergoes an increasing or decreasing trend, within a predetermined level of significant.

At the national scale, a study by Tangang et al. [7] investigated temperature warming trends and interannual variability in Malaysia using linear regression and the Student's *t*-test. The study revealed that the temperature records for most regions in Malaysia are positively influenced by global warming. The study used seasonal temperature data records for over 41 years (i.e., 1961–2002) and found that on a seasonal basis, the temperature has increased by 2.7–4.0 °C over 100 years.

Time series study is one of the major tools for the application involving hydrology and environment which focus on rainfall. It has a strong relationship with the amount of rainfall in that particular place. Among the most effective approaches for analyzing time series data is the model introduced into a map by using GIS technique after undergoes the two statistical tests which are Mann-Kendall test and Sen's slope estimator. The models are used to display the monthly rainfall trends and data and to view the area with peak values of rainfall data. Therefore, this study has two objectives which are first to quantify the changing trend of rainfall of Kelantan River by using statistical tests (i.e., Mann-Kendall test and Sen's slope test) based on monthly, seasonal, and annual time series, and secondly to map rainfall trend according to Mann-Kendall test result.

2 Methodology

2.1 Study Area and Methods

Kelantan is one of the largest states in Peninsular Malaysia, occupying the large Kelantan River Basin. The total area of Kelantan is 15,022 km^2 or 4.4 % of the area of Malaysia. The Kelantan River catchment is located in northeastern Peninsular Malaysia between the latitudes 4°30′ to 6°15′N and the longitudes 101° to 102°45′E and is one of the major rivers in Malaysia, frequently affected by flooding events. It is the longest river in Kelantan State at 248 km and drains an area of 13,100 km^2. The six sub-basins of Kelantan River Basin are Nenggiri, Galas, Lebir and Pergau

located in the upstream area and Kuala Krai and Guillemard Bridge are located in the downstream area [8] (Fig. 1).

Data from the rainfall stations in the parts of Kelantan have been provided by the Department of Irrigation and Drainage (DID) Kelantan. The data include GIS layer of the rainfall station, river networks, and basins of the Kelantan River. The period taken was from 1980 to 2013 or 33 years duration for 14 rainfall stations in the Kelantan River Basin. The data were divided into monthly, seasonal, and annual time series utilizing the mean value for the whole Kelantan River Basin. For seasonal trend analysis, the year was divided into four main seasons: JFM (January–February–March), AMJ (April–May–June), JAS (July–August–September), and OND (October–November–December) [7]. Mean precipitation was calculated for every 3 months and trends were fitted to these data for each rain gauge station. Table 1 shows the availability of rainfall data for the construction and analysis of the rainfall study.
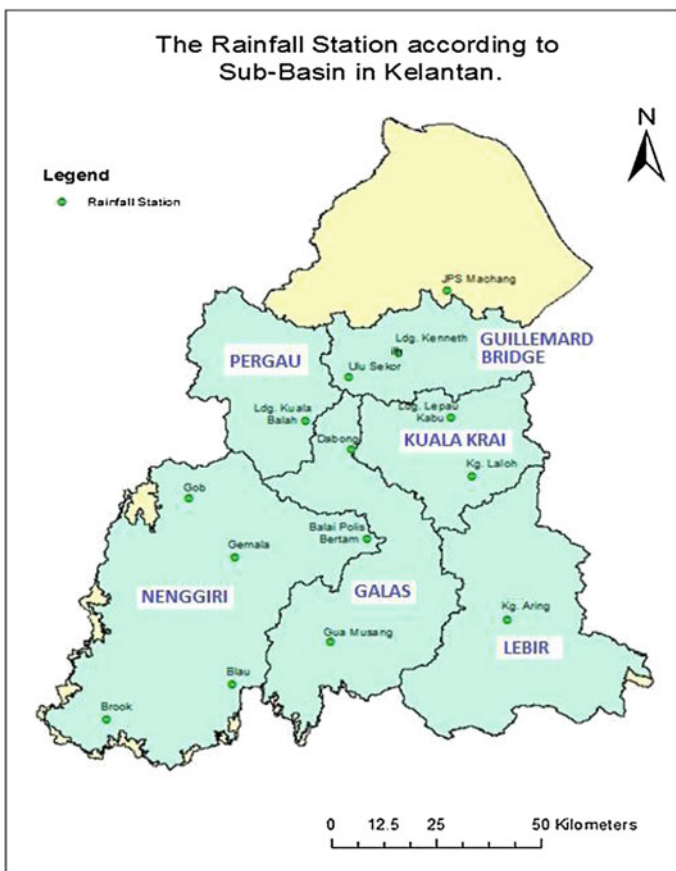

Fig. 1 The rainfall station according to sub-basin in Kelantan

Table 1 Rainfall station and data availability

Station no.	Station	Availability	Missing years
4614001	Brook	1982–2013	1980, 1981
4717001	Blau	1982–2013	1980, 1981
4819027	Gua Musang	1980–2013	–
5017001	Gemala	1982–2013	1980, 1981
5120025	Balai Polis Bertam	1980–2013	–
5216001	Gob	1980–2013	–
5320038	Dabong	1982–2013	1980, 1981
5419036	Ladang Kuala Balah	1980–2013	–
4923001	Kampung Aring	1980–2013	–
5322044	Kampung Laloh	1980–2013	–
5422046	Ladang Lepau Kabau	1980–2013	–
5520001	Ulu Sekor	1981–2013	1980, 1982
5621051	Ladang Kenneth	1980–2013	–
5722057	JPS Machang	1980–2013	1986, 1987, 1988, 1989, 1990

2.2 Trend Detection and Rainfall Distribution Map

Mann-Kendall test is one of a widely used test for observing trend in hydrological data such as rainfall and stream flow data, where positive values show an increase in constituent concentrations over time and vice versa [9]. The trend analysis was done in two phases. First, the presence of a monotonic increasing or decreasing trend was tested with the nonparametric Mann-Kendall test, and secondly, the slope of a linear trend is estimated by the nonparametric Sen's slope estimator. Mann-Kendall test has several advantages such as simplicity, capability of handling non-normal and missing data distributions, and robustness to the effects of outliers and gross data errors [8, 10, 11]. The strength of the trend is proportional to the magnitude of the Mann-Kendall statistics.

Mann-Kendall test has done in a series x_i, where $i = 1,2, \ldots, n - 1$ and x_j where $j = 1,2, \ldots, n$. Each data point x_i is taken as a reference point that compared with the data point x_j. The Mann-Kendall test used the following equation:

$$S = \sum_{k-1}^{n-1} \sum_{j-k=l}^{n} sign(xj - xk) \tag{1}$$

where $i = 1,2, \ldots, n - 1$ and $x_j \, j = 1,2, \ldots, n$.

The values of S and Var(S) are used to compute the test statistics Z as follows:

$$Z = \begin{cases} \frac{S-}{\sqrt{\text{Var}}} & \text{If } S > 0 \\ 0 & \text{If } S = 0 \\ \frac{S+}{\sqrt{\text{Var}}} & \text{If } S < 0 \end{cases} \tag{2}$$
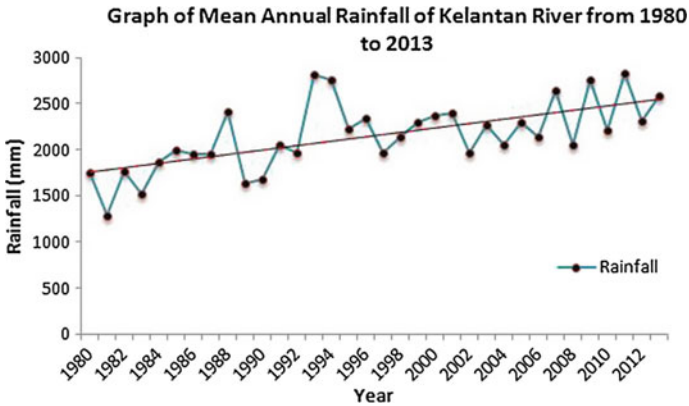
Fig. 2 Mean annual rainfall of Kelantan River from 1980 to 2013

The presence of a statistically significant trend is evaluated by the Z value. Thus, in a two-sided test for the trend, H_1 should be accepted if $|Z| > Z_{\alpha/2}$, where $F_n(Z_{\alpha/2}) = \alpha/2$, F_n being the standard normal cumulative distribution function and α being the significance level for the test. Positive values of Z indicate an upward trend and negative values indicate a downward trend.

Sen's slope test is one of the statistical tests used with Mann-Kendall test to determine the magnitude of changes taking place in that area.

Sen's slope test will indicate the increase and decrease of the slope's magnitude in correspondence with the Mann-Kendall values [12]. The Sen's slope test proves that the true slope can be estimated using a simple nonparametric procedure if linear trend is present.

The result from the statistical tests of the rainfall data will be presented in trend distribution map using an interpolation technique in GIS. Interpolation is the estimation of an unknown quantity between two known quantities or drawing conclusions about missing information based on the available information. Interpolation is very useful because the data surrounding the missing data are available and its trend, seasonality, and longer-term cycle are known. There are several well-known interpolation techniques, including spline and Kriging. However, only Kriging technique was used due to its capability to consider both the distance and the degree of variation between the known data points when estimating the value in unknown areas [13].

3   Results and Discussions

3.1   Rainfall Trend Analysis and Using Mann-Kendall Test and Sen's Slope Estimator

Rainfall trend analysis of Kelantan River according to its river basin has been done for 33 years from 1980 to 2013. Figure 2 represents the rainfall for 33 years from 14 rainfall stations all over Kelantan with maximum annual rainfall occurrence in the year 2011 with the total rainfall of 2826.9 mm and minimum annual rainfall has occurred in the year 1981 with the total rainfall of 1289.5 mm. The average rainfall for this 33 year period is 2152.3 mm. The Mann-Kendal and Sen's slope test were done for the monthly, seasonal, and annual time series as described in the next section.

1. Monthly Trend Analysis

The monthly mean rainfall is subjected to the Mann-Kendall test at each station. The first month of January shows significant trends occurred in Gob, Kg. Aring, Dabong, JPS Machang, Kg. Laloh, Ladang Kenneth, Ladang Kuala Balah, and Ladang Lepau Kabu stations. Figure 3 represents the trend of Z for each station in January and associate Sen's slope trend line. The trend analysis revealed that the Ladang Kenneth holds the most significant trend with 4.23 of Z value and Blau is the least with −0.08. The other monthly time series that have significant trends are indicated in the months of February, March, April, May, September, and December.
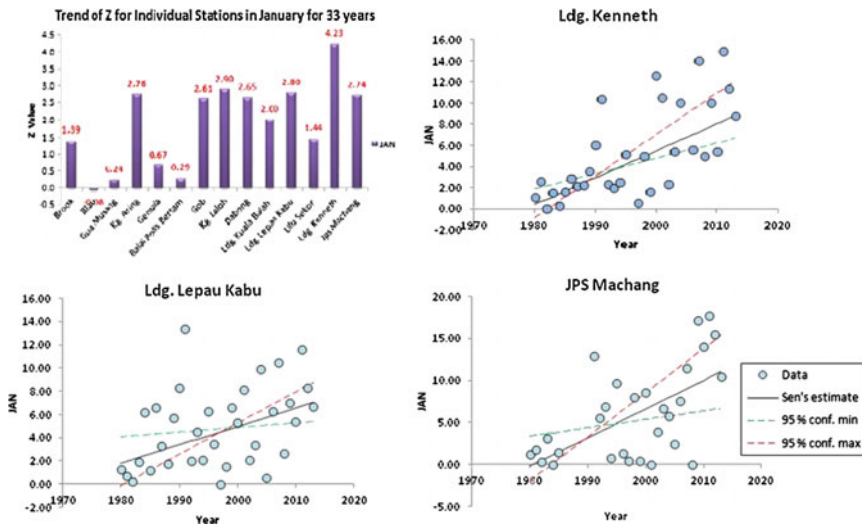

Fig. 3 Trend of Z in January in each of the rainfall stations and increasing trend line for the Ladang Kenneth, Ladang Lepau Kabu, and JPS Machang rainfall stations

However, in September, three stations have showed significant decreasing trends for the stations of Gemala, Gua Musang, and Kg. Aring. The Z test values for these stations Gemala, Gua Musang, and Kg Aring are -2.58, -2.09, and -2.56, respectively.

2. Seasonal Trend Analysis

The seasonal period has been divided into 4 seasons which are January, February, March (JFM); April, May, June (AMJ); July, August, September (JAS); and October, November, December (OND) [7]. From 14 stations, nine stations that used in this study have exhibited significant trends. All the rainfall stations situated in the Guillemard Bridge, Kuala Krai, Lebir, two stations in Neggiri, and one station in Galas evidenced by the significant trends. Most of them occurred during the first season of JFM. Figure 4 shows the Z test value in each station in JFM, AMJ, JAS, and OND seasons.

The AMJ season exhibited increasing significant trends for two stations in the Guillemard Bridge sub-basin. The stations are the JPS Machang and Ladang Kenneth with Z value of 1.76 and 1.70 Z, respectively. Meanwhile, the JAS season is also known as driest season from these four seasons. In the JAS, two stations which are Kg. Aring in Lebir and Ladang Lepau Kabu in Guillemard Bridge sub-basin showed significant decreasing trends. Kg. Aring has the value of -2.90 and Ladang Lepau Kabu has the value of -2.06 (Fig. 4). The last season of OND also has significant increasing trends for two stations which are the JPS Machang
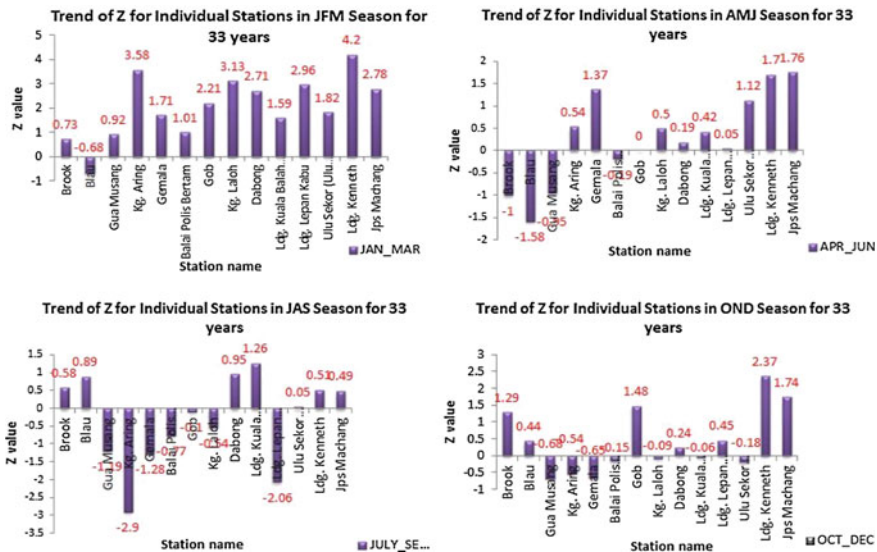

Fig. 4 Z test trend result for all rainfall stations and decreasing trend line for the Gemala, Gua Musang, and Kg. Aring stations

Table 2 Summary of *Z* test result

Rainfall station	Monthly	Seasonal	Annual
Brook	NS	NS	NS
Blau	S− (Feb, May)	NS	NS
Gua Musang	S− (Sept)	NS	NS
Kg. Aring	S+ (Jan, Feb), S− (Sept)	S+ (JFM), S− (JAS)	NS
Gemala	S+ (Mar), S− (Sept)	S+ (JFM)	NS
Balai Polis Bertam	NS	NS	NS
Gob	S+ (Jan)	S+ (JFM)	NS
Kg. Laloh	S+ (Jan, Feb, Apr)	S+ (JFM)	NS
Dabong	S+ (Jan)	S+ (JFM)	NS
Ldg. Kuala Balah	S+ (Jan)	NS	NS
Ldg. Lepan Kabu	S+ (Jan)	S+ (JFM) S− (JAS)	NS
Ulu Sekor	NS	S+ (JFM)	NS
Ldg. Kenneth	S+ (Jan, Feb, Mar, Dec)	S+ (JFM, AMJ, OND)	S+
JPS Machang	S+ (Jan, Mar, Apr, May)	S+ (JFM, AMJ, OND)	S+

NS is not significant trend, *S+* is significant increasing trend, and *S−* is significant decreasing trend

and Ladang Kenneth stations situated in the Guillemard Bridge sub-basin having the *Z* values of 1.74 and 2.87, respectively.

Based on the result, JFM season obviously has the highest *Z* values corresponding to the number of rainfall stations that had the evidence of significant trends. Apart from that, the JAS season for these 33 years had shown that it was the driest season in Kelantan.

3. Annual Trend Analysis

The results of the monthly and seasonal rainfall trends are reflected in the annual rainfall trends. From these 14 rainfall stations, only two revealed an evidence of significant trends for these 33 years. Both Ladang Kenneth and JPS Machang really stressed out the significant increase rainfall in this Mann-Kendall test together with Sen's lope estimator. The JPS Machang is the station with highest significant trends with *Z* value of 3.40 and the Ladang Kenneth with *Z* value of 3.36.

The summary of the trend analysis of rainfall for the monthly, seasonal, and annual is shown in Table 2. The *Z* statistical test showed that the monthly and seasonal time series have many significant trend (with 95 % confidence level) results as compared to the annual data. In brief, the months of JFM and April have increasing significant trends from 1980 to 2013, whereas the months of September indicated a significant decreasing trend of rainfall pattern. In addition, for the seasonal analysis, the season of JFM constitutes a significant increasing trend and the JAS constitutes a significant decreasing trend. Meanwhile, for the annual analysis, only two (2) stations were detected with significant increasing trend (Table 2).
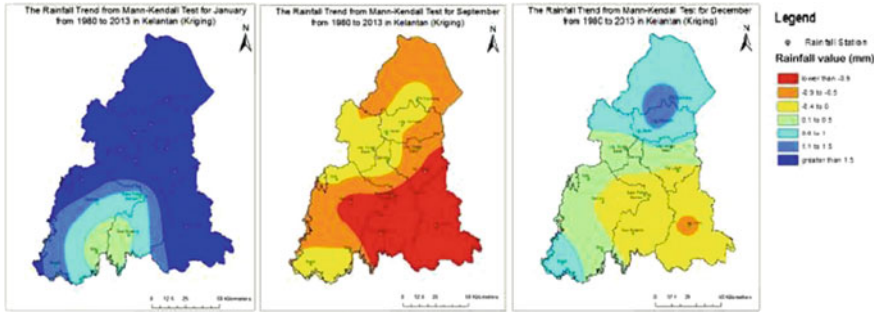
Fig. 5 The rainfall trend from Mann-Kendall test for each station in January, September, and December

3.2   Spatial Map for Mann-Kendall Trend Analysis

The spatial maps were done using the Mann-Kendall (Z test) results for the monthly, seasonal, and annual time series. The values of the test were converted into an attribute table in ArcGIS. To show the map, spatial interpolation for Kriging method is used. According to the previous studies, Kriging is identified as the most promising distribution techniques especially in describing rainfall data.

1. **Monthly Spatial Map**

   This section showed the spatial trend map for the months that only showed significant trends for the whole 33 years. Only seven months, January, February, March, April, May, September, and December, show significant trends while the other 5 months do not have any significant trends. Figure 5 shows the map for months with significant trends. Based on the figures, it really proves that the September is the driest month and December is the wettest month.
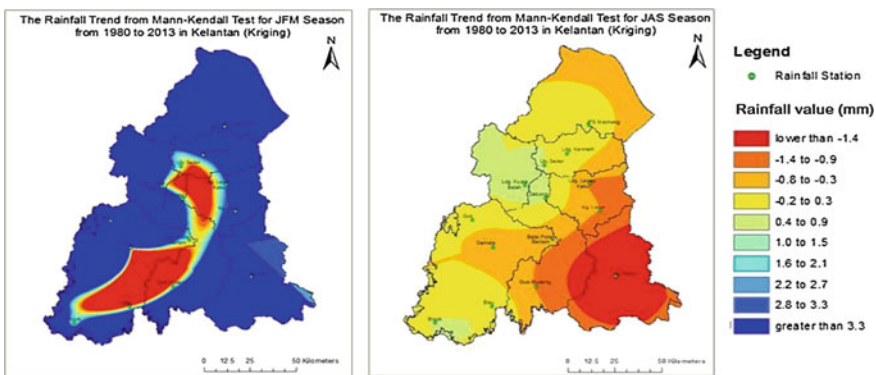
Fig. 6 The rainfall trend for each station in the JFM and JAS seasons

Fig. 7 The rainfall trend for each station in 33 years from 1980 to 2013
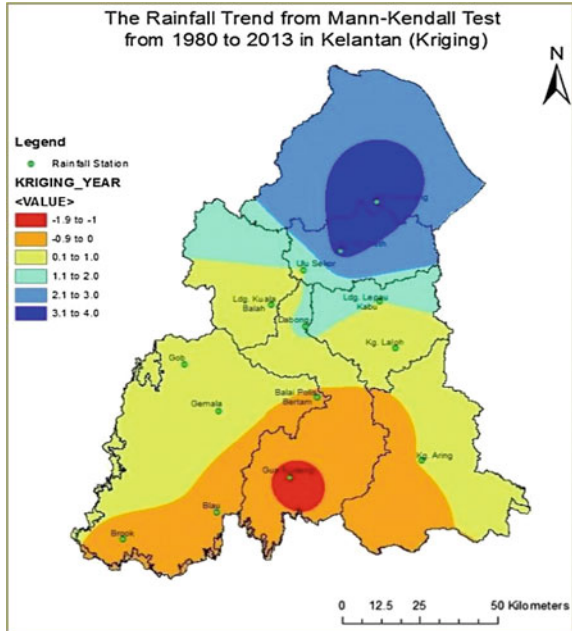
2. Seasonal Spatial Map

The four seasons, which are JFM, AMJ, JAS, and OND, have been mapped spatially based on the Mann-Kendall result of Z statistics. 9 out 14 rainfall stations that used for this study have shown significant trends. Most of the stations have significant trends in the first season of JFM, thus making it the wettest season while JAS is the driest season. Figure 6 shows the spatial map for the seasons using Kriging interpolation method.

3. Annual Spatial Map

The map in Fig. 7 shows the rainfall trend map for the whole 33 years. Based on the 33 years, only two stations revealed an evidence of significant trends. The two stations Ladang Kenneth and JPS Machang are both located in Guillemard Bridge. Gua Musang station is the driest for 33 years.

4   Conclusions

Based on the analysis of the Kelantan River Basin for those 33 years, it can be summarized that the trend is increasing corresponding to its Z values. As the rate of rainfall increases, the Z value also increases, thus leading to significant trends. However, not all stations show the evidence on significant trends. The significant

trends of the station can be either increasing or decreasing. In brief, September has always been the driest month as well as JAS season, which was the driest season. Apart from that, December to January has always been the wettest month in Kelantan. Intense rainfall always occurred during these months. The rainfall keeps on increasing from year to years where it can be predicted that the following years will be higher than the previous years. Therefore, this information will benefit, especially, for flood preparation and responses in the Kelantan River Basin which annually experiences monsoon flooding.

References

1. Mahmud MR, Numata S, Matsuyama H, Hosaka T, Hashim M (2014) Challenge and opportunities of space-based precipitation radar for spatio-temporal hydrology analysis in tropical maritime influenced catchment: Case study on the hilly tropical watershed of Peninsular Malaysia. IOP Conf Ser Earth Environ Sci 18:012001
2. Lei Y, Hoskins B, Slingo J (2011) Exploring the interplay between natural decadal variability and anthropogenic climate change in summer rainfall over China. Part I: observational evidence. J Clim 24(17):4584–4599
3. Kahya E, Kalayci S (2004) Trend analysis of streamflow in Turkey. J Hydrol 289(1–4):128–144
4. Ngongondo C, Xu CY, Gottschalk L, Alemaw B (2011) Evaluation of spatial and temporal characteristics of rainfall in Malawi: a case of data scarce region. Theor Appl Climatol 106(1–2):79–93
5. Taxak AK, Murumkar AR, Arya DS (2014) Long term spatial and temporal rainfall trends and homogeneity analysis in Wainganga basin, Central India. Weather Clim Extremes 4:50–61
6. Yue S, Pilon P (2004) A comparison of the power of the test, Mann-Kendall and bootstrap tests for trend detection. Hydrol Sci J Des Sci Hydrol 49(1):21–37
7. Tangang FT, Juneng L, Ahmad S (2007) Trend and interannual variability of temperature in Malaysia: 1961–2002. Theor Appl Climatol 89(3–4):127–141
8. Adnan NA, Atkinson PM (2010) Exploring the impact of climate and land use changes on streamflow trends in a monsoon catchment. Int J Climatol 9999(9999)
9. Fathian F, Dehghan Z, Bazrkar MH, Eslamian S (2014) Trends in hydrologic and climatic variables affected by four variations of Mann-Kendall approach in Urmia Lake basin, Iran. Hydrol Sci J :140617041244008
10. Xu ZX, Takeuchi K, Ishidaira H, Li JY (2005) Long-term trend analysis for precipitation in Asian Pacific FRIEND river basins. Hydrol Process 19(18):3517–3532
11. Tabari H, Abghari H, Hosseinzadeh Talaee P (2012) Temporal trends and spatial characteristics of drought and rainfall in arid and semiarid regions of Iran. Hydrol Process 26(22):3351–3361
12. Gocic M, Trajkovic S (2013) Analysis of changes in meteorological variables using Mann-Kendall and Sen's slope estimator statistical tests in Serbia. Glob Planet Change 100:172–182
13. Mair A, Fares A (2011) Comparison of rainfall interpolation methods in a mountainous region of a tropical Island. J Hydrol Eng 16(4):371–383

Part IV
Water Quality

Application of 1D Shallow Flow Model for Simulation of Pollution Fate and Streamflow

Nor A. Alias and Lariyah Mohd Sidek

Abstract Numerical models especially two-dimensional (2D) models have long been used in simulating hydrodynamics and its associated processes such as sediment transport, pollutant dispersion, and flooding are caused by overtopping or breaching of river banks. However, due to the complexity of the river geometries, it is still difficult to resolve the problematic river in a 2D manner. Thus, a one-dimensional (1D) component model is needed to analyze complex flow hydrodynamics under flood conditions. As solute transport also greatly impacts the local environment and is closely related to the water quality in shallow water bodies, the prediction of pollutant fate is also included in this paper. Thus, this paper focuses on developing a numerical model to simulate shallow flow hydrodynamics in the context of irregular profiled open channels to predict depth-averaged water level and pollutant transport. The scope of work is limited to the development of a 1D model and verification of the model against benchmark tests and laboratory measurements. Presented in this paper is the development of an integrated model with fully dynamic shallow water equations (SWE's) and the advection–diffusion equation. Results demonstrated are the comparisons between the numerical results and data obtained through experimental procedures or from published analytical solutions in terms of flow depth and solute concentration. Closed agreement is achieved for all tests, and the model was therefore applied in Sungai Penchala, Malaysia.

N.A. Alias (✉)
Faculty of Civil Engineering and Earth Resources, University Malaysia Pahang,
26300 Kuantan, Malaysia
e-mail: azlina@ump.edu.my

L.M. Sidek
Department of Civil Engineering, College of Engineering, UNITEN,
43000 Kajang, Selangor, Malaysia
e-mail: lariyah@uniten.edu.my

1   Introduction

In twenty-first century, due to the continuous development and the influence of climate change, flood risks impact mainly in urban areas and have probably significantly increased. Most countries that are affected by flood disasters took an integrated action in order to overcome or at least minimize the impact of flood risk. In this way, the victims of flood disasters are expected to get early warning of flood events where flood risk management teams are purposely formed to predict the river flow depth in risky areas.

Numerous studies on modeling in open-channel flow, especially on the 2-dimensional (2D) model, have been done; however, there are still deficiencies in the models. As it is difficult to resolve the problematic river reach in a 2D manner, in which there is limitation in signifying rivers with small-scale flow paths in a large-scale flood simulation, developing a 1-dimensional (1D) component with an ability to deal with the complex flow hydrodynamics is thus essential. A 1D model has better capabilities in describing the cross section accurately. The computational cost of 1D models is also lower than the 2D and 3D models. For a large-scale river network, it still consents closely to real-time analysis [1]. However, there is still a subject to debate on the current 1D model. The approximation of the shallow water equations (St. Venant equations) was normally taken to develop most 1D models [2, 3] due to its straightforwardness. This ignored the vital features of the spatially hydraulic variables and caused inability to represent the full dynamics of a flow. Thus, for broader implementation, a high-ability 1D model to solve the more complex hydrodynamics flow especially for the use in urban areas is desired.

Apart from modeling the shallow flow, many of the in situ problems required comprehensive numerical models to simulate the flows together with solute transports. Most of the transport problems were solved using simplified 1D models [4], and it is adequate to represent the solute transport process in 1D equations as the solute is transported or driven by current flow that dominated in longitudinal direction [5]. It was recognized that the solute transport in the river could be correctly modeled if a correct simulation of convection and diffusion is included [6]. Thus, the research objective is to produce a tool that can be used to simulate flow in the context of irregular profile open channels to predict depth-averaged water level and simultaneously predict the fate of pollutant.

2 Model Development

2.1 The Governing Equation

Focus is given on developing a model to simulate shallow flow in irregular beds to predict depth-averaged water level and pollutant transport, especially in the cases pertaining to floods in urban area. The 1D equation used in simulating different types of flow is written in matrix form as (1):

$$\frac{\partial \mathbf{u}}{\partial t} + \frac{\partial (\mathbf{f})}{\partial x} = \mathbf{s} \tag{1}$$

where t is the time and x represents the distance along the flow direction, while vectors $\mathbf{u}$ and $\mathbf{s}$ contain the flow variables and source terms, respectively; however, $\mathbf{f}$ denotes the flux vector in x-direction. Dealing with complex geometry, the 1D channel attached to a floodplain is assumed to have a rectangular cross section [7, 8]. The breadth variation is included to accurately calculate the flow depth (h) and discharge (q). The $\mathbf{u}$, $\mathbf{f}$, and $\mathbf{s}$ are given as in (2):

$$
\mathbf{u} = \begin{bmatrix} \eta \\ uh \\ ch \end{bmatrix} \quad
\mathbf{f} = \begin{bmatrix} uh \\ u^2 h + \frac{1}{2} g(\eta^2 - 2\eta Z_b) \\ uch \end{bmatrix}
$$
$$
\mathbf{s} = \begin{bmatrix} -\frac{q}{b}\frac{\partial b}{\partial x} \\ -\frac{q^2}{bh}\frac{\partial b}{\partial x} - C_f u|u| - g\eta \frac{\partial Z_b}{\partial x} \\ S_c \end{bmatrix}
\tag{2}
$$

where u is velocity, η is free water surface elevation, Z_b is bed elevation, g is the gravity acceleration, b is river width, $C_f = gn^2/h^{1/3}$ is the roughness coefficient of the river bed, and n is the Manning's coefficient. c in the model represents the solute concentration. Equation (1) allows varying channel width and bottom. Riemann solvers are of significant interest (e.g., [9–12]) as widely implemented to model flows with abrupt and discontinuous gradients. By adding the advection–dispersion equation into the model, solute transport and shallow waters flow are simulated simultaneously. This scheme ensures a well-balanced and non-negative (in terms of water depth and solute concentration) solution in simulating cases involving the wet–dry front.

2.2 Numerical Scheme

Due to the advantages of Godunov-type finite-volume schemes, Harten-Lax-Van Leer (HLL) approximate Riemann solver is chosen to be used in the numerical

scheme. The source terms take into account the effects of friction in flow domain. The model is able to handle the wet–dry case over irregular topography. The final expression for the scheme is as in (3):

$$\mathbf{u}_i^{k+1} = \mathbf{u}_i^k - \frac{\Delta t}{\Delta x}\left(\mathbf{f}_{i+1/2} - \mathbf{f}_{i-1/2}\right) + \Delta t\, \mathbf{s}_i \tag{3}$$

where i denotes the cell index, superscript k denotes the new time step, Δx and Δt are, respectively, the cell size and time step, $\mathbf{f_{i+1/2}}$ and $\mathbf{f_{i-1/2}}$ are the interface fluxes. The HLL approximate Riemann solver [13] is adopted for flux calculation due to its superior advantages in providing automatic entropy fix and facilitating wetting and drying. The scheme is improved by employing the second-order Runge–Kutta (RK) method. By combining the Godunov-type finite-volume method with the second-order (RK) method, the time marching equation is (4):

$$\mathbf{u}_i^{k+1} = \mathbf{u}_i^k - 0.5\Delta t\left(\mathbf{K}_i(\mathbf{u}^k) + \mathbf{K}_i(\mathbf{u}^*)\right) \tag{4}$$

where K_i is the Runge–Kutta coefficient at predictor and corrector steps.

In reconstructing the Riemann states, the flow variables at the flux faces were first estimated from the central flow information by a linear interpolation of slope limiter. The reconstruction is adopted to rebuild the face values to attain second-order accuracy in space [14, 15]. Preserving the accuracy and well-balanced property of the proposed scheme, the source terms are split into two parts [16]. Direct discretization by central differences method applied to the geometric and topographic source terms. This technique is compatible to the flux calculation and do not affect the well-balanced scheme. To define numerical fluxes, HLL approximate Riemann solver and the S_L and S_R that represent the left and right speeds are estimated. Based on both faces of Riemann states for local Riemann problem, the wave speeds S_L and S_R are defined by (5).

$$
\begin{aligned}
S_L &= \begin{cases} u_R - 2\sqrt{gh_R} & \text{if } h_L = 0 \\ \min(u_L - \sqrt{gh_L},\, u_* - \sqrt{gh_*}) & \text{if } h_L > 0 \end{cases} \\
S_R &= \begin{cases} u_L - 2\sqrt{gh_L} & \text{if } h_R = 0 \\ \min(u_R - \sqrt{gh_R},\, u_* - \sqrt{gh_*}) & \text{if } h_R > 0 \end{cases}
\end{aligned} \tag{5}
$$

where u_L and u_R are the velocity components while h_L and h_R are the flow depth component of Riemann states calculated for both left and right faces in local Riemann problem. u_* and h_* are denoted in (6).

$$
\begin{aligned}
u^* &= \frac{1}{2}(u_R + u_L) + \sqrt{gh_L} - \sqrt{gh_R} \\
h_* &= \frac{1}{g}\left[\frac{1}{2}\left(\sqrt{gh_L} + \sqrt{gh_R}\right) + \frac{1}{4}(u_L - u_R)\right]^2
\end{aligned} \tag{6}
$$

Having computed all the above-mentioned variables, the HLL flux is computed using (7).

$$f_* = \frac{S_R f_L - S_L f_R + S_L S_R (u_R - u_L)}{S_R - S_L} \tag{7}$$

where f_L and f_R are the left and right flux vectors. Taking east face as an example, (8) is the final corresponding intercell fluxes, f_E^{hll}.

$$f_E^{hll} = \begin{cases} f_L & if \quad 0 \leq S_L \\ f_* & if \quad S_L \leq 0 \leq S_R \\ f_R & if \quad 0 \leq S_R \end{cases} \tag{8}$$

Equations (5)–(8) were used to calculate for the west face. In order to achieve higher-order accuracy, the Riemann states need to be reconstructed which is explained in detail in the following paragraph.

3 Model Validation

The phenomenon of one-dimensional surface flow is observed under various conditions experienced in open channel [16]. In the case of predicting the fate of pollution, presented here also are validation tests on solute transport that include pure advection, pure diffusion, and advection and diffusion of species.

3.1 Open-channel Flow

1. *Tidal Wave Flow and Flow over an Irregular Bed.* Presented here is a test on tidal flow proposed by Bermudes and Vasquez (1994). The tidal flow depth, *H,* is defined as in (9):

$$H(x) = 50.5 - \frac{40x}{L} - 10 \sin \left[\pi \left(\frac{4x}{L} - \frac{1}{2} \right) \right] \tag{9}$$

where the channel length, *L,* is 14,000 m. The initial condition of flow depth and the initial velocity are $h(x,0) = H(x)$ and $u(x,0) = 0$, respectively, while the boundary conditions are as in (10).
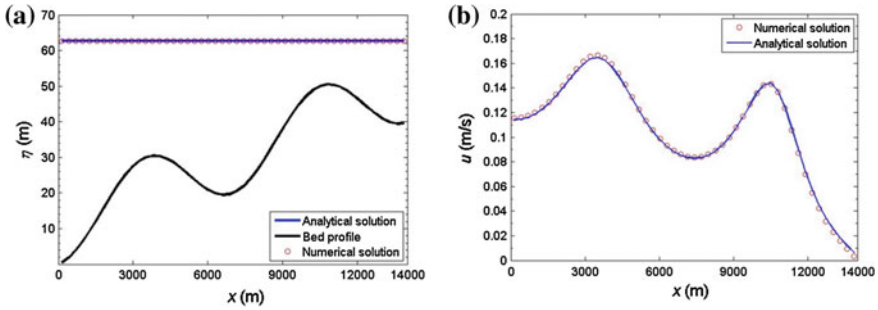
Fig. 1 Tidal wave flow. **a** Comparison of water surface. **b** Comparison of velocity

$$h(0,t) = H(0) + 4 - 4\sin\left[\pi\left(\frac{4t}{86,400} + \frac{1}{2}\right)\right] \text{ and } u(L,t) = 0 \qquad (10)$$

Having simulated using the proposed model, Fig. 1a, b compares the water surface elevation and velocity between both numerical analytical solutions at simulation time, $t = 7552.13$ s. These excellent agreements suggest that the proposed scheme is accurate to be implemented in cases involving the tidal flow problems.

Another test was done to validate the performance of proposed model over irregular bed topography [17]. Replacing the initial condition of tidal flow to $H(0) = 16$, the reach length to $L = 1500$ m, and $H(x) = H(0) - Z_b(x)$, while maintaining the previous boundary conditions as (7), results are plotted as in Figs. 2 and 3.

A comparison of velocities is depicted in Fig. 2, while in Fig. 3 the velocity profile is plotted at a longer simulation time on an irregular bed profile. Again, optimum agreement is obtained between both methods of solution, hence confirming that the developed scheme is also accurate for tidal flow over an irregular topography.

Fig. 2 Velocity profile comparison at $t = 10,800$ s
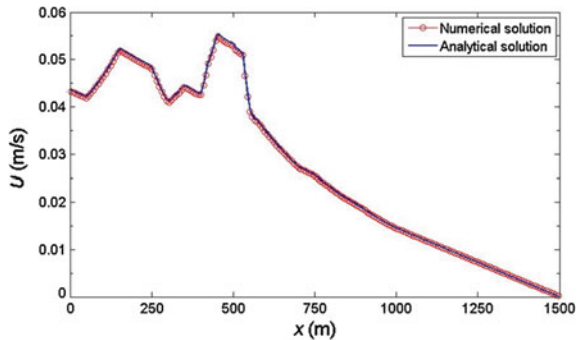
Fig. 3 Velocity profile comparison at $t = 32,400$ s
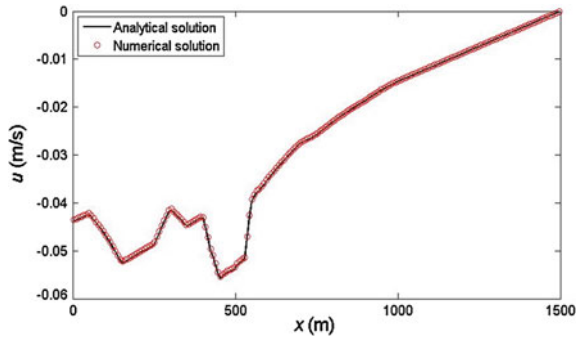
There are errors in numerical solutions; thus, to quantitatively investigate the accuracy of the numerical scheme on shallow flow model, the relative error was calculated. The relative error in the mass conservation of the numerical scheme was computed using (11).

$$q_{\text{err}} = \left(\frac{q_{\text{num}} - q_{\text{anal}}}{q_{\text{anal}}} \right) \times 100\,\% \tag{11}$$

Relative errors calculated for the discharge range from 0.006 to 0.009678. This indicates that the model simulates flow well even if the uneven topography is present.

3.2 Fate of Pollutant

1. *One-Dimensional Pure Diffusion Test.* The one-dimensional pure diffusion test was done in an 8–m-long rectangular channel with a given width of 0.5 m. Analytically, a 1 g of pollutant as defined in (12) was instantaneously injected into the channel.

$$C = \frac{m}{A} \cdot \frac{1}{\sqrt{2\pi\sigma}} e^{-(x-x_0)^2/2\sigma^2} \tag{12}$$

where $m = 10$ g is the mass of the pollutant, and $x_0 = 4$ m is the point where the contaminant is injected. A is the channel's cross section and $\sigma^2 = 2Dt$. Following work that had been done previously [18], different water depths at $h = 1$ m and $h = 2$ m were calculated analytically and solved numerically using the proposed scheme. Figure 4 shows the comparison between both solutions for the concentration for $h = 1$ m and $h = 2$ m at $t = 2$ s and $t = 5$ s after the discharge of the pollutant.
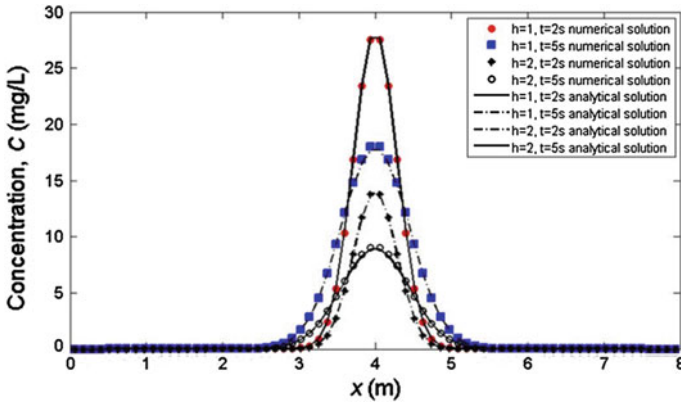
Fig. 4 Comparison of concentration at $t = 2$ s and $t = 5$ s h = 1 m and 2 m

From the plotted lines of concentrations between analytical and numerical solution in Fig. 4, it is clear that the solute transport diffused from the higher to lower concentration regions. The numerical prediction of the concentration profile is in sufficient agreement with the analytical results.

2. *Pure Advection with Transport in Rapidly Varied Flow Regime.* A solute transport in a rapidly varied flow regime is considered in previous example. Here, the performance of the model in a sharp increase and decrease of velocity field is tested. The velocity profile and solute transported in the channel are plotted as in Fig. 5.

If the flow velocity in the channel $u = 0.5$ m/s from the upstream boundary to $x = 3000$ m, then the velocity increased sharply to $u = 1.0$ m/s at distance 3000 m < x < 5000 m. The velocity later was sharply reduced and returned to its initial velocity, $u = 0.5$ m/s, at distance $x = 5000$ m as previously tested [19]. In Fig. 5, after the initial concentration distribution experienced a sharp increase and

Fig. 5 Concentration distribution in rapidly varied flow regime
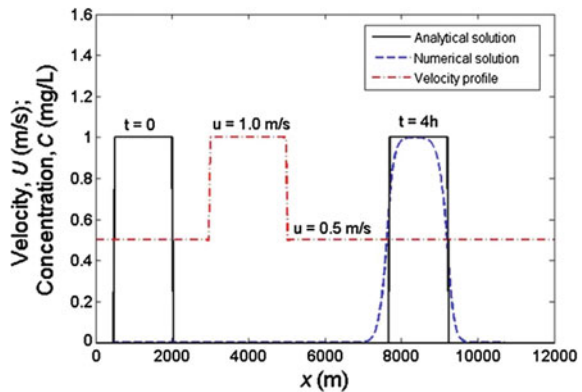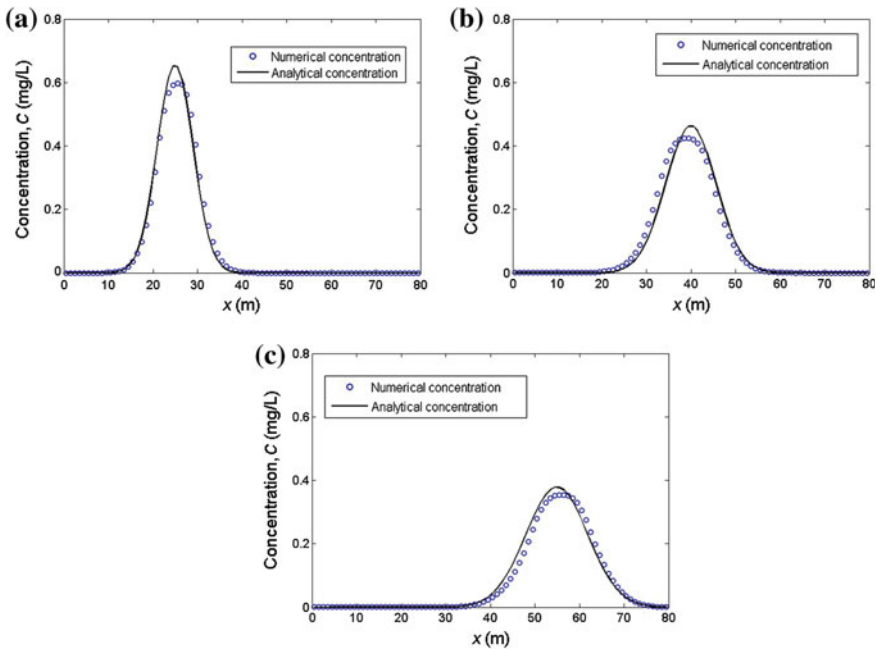
Fig. 6 a–c Comparison of concentration *c* at different time histories. **a** *t* = 20 s, **b** *t* = 40 s, **c** *t* = 60 s

decrease of velocity, the proposed model still provides accurate results after simulation time, *t* = 4 h.

3. *Advection (Convection)–Diffusion.* The integrated model was then used to study the fate of pollutant. The test involved a 1D convective-diffusion problem [19]. Figure 6a–c exhibits the solute concentration at different simulation time.

Numerically, the maximum concentration computed was 0.5982 mg/L and as the time of simulation increased, the maximum concentration was reduced to 0.3537 mg/L. The proposed method seems to provide good accuracy in the convective-diffusion case. From the global relative error analysis, *R* is proportionate with time. The *R* = 0.0949, *R* = 0.10711, and *R* = 0.12836 for *t* = 20, 40, and 60 s, respectively, which may be related to the concentration that is inversely proportionate to the time.

4 Site Implementation

As the results obtained were reliable, it was then implemented to a real-case scenario. Sungai Penchala, which is a densely populated area surrounded by industrial and residential areas situated between Kuala Lumpur and Selangor, was identified

Fig. 7 Bed profile of Sungai
Penchala
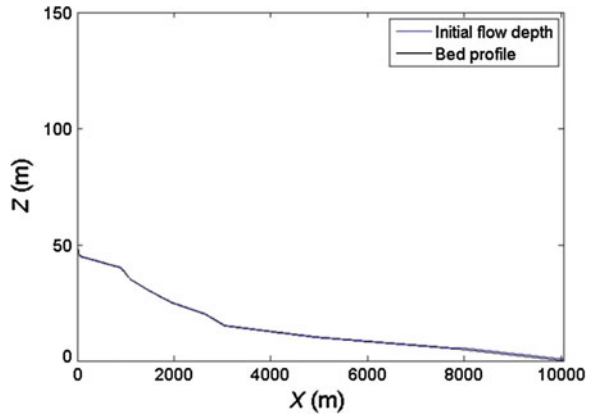
as the potential site study. The river reach is divided into a few sections and the
readings of water level at predetermined locations were recorded. The time histories
for flow depth were predicted numerically using the developed model at 2000 m
interval. The proposed model has been used to validate several benchmark tests and
close agreement has been achieved that confirms the effectiveness of the current 1D
code [13]. Thus, the model was implemented in Sungai Penchala. The 10-km
Sungai Penchala study reach extends from Kiara Park to Kg Ghandi. The model
used the channel geometry contained in field surveys obtained from The
Department of Irrigation and Drainage; the Sungai Penchala topography is plotted
as in Fig. 7.

From the sketch, the Penchala catchment is a hilly terrain. Almost 80 % of
Sungai Penchala is a concrete channel with bed frictional coefficient equal to
0.015 s/m$^{1/3}$. The recorded outflow depth is 0.15 m. Simulation was performed for
7200 s on a uniform grid as in Fig. 8a–d.

The proposed model was applied to predict the flow profile of Sungai Penchala.
Closed and open-end boundaries were set at the upstream and downstream of
Sungai Penchala, respectively. It is a relatively short river but almost 80 % of the
river reach has been channelized with concrete. Following the manual provided by
Manual Saliran Mesra Alam (MSMA), as it flows through residential and com-
mercial areas, the bed frictional coefficient was taken as 0.015 s/m$^{1/3}$. The outflow
depth at the downstream was $h = 0.15$ m as recorded during the survey. No inflow
was imposed during the 7200 s of simulation on a 1-m uniform grid.

The readings of flow depth were done at four selected locations and compared
with numerical prediction by the model. In a 10.5 km reach, the time histories of
flow depth were taken at five locations with 2000 m intervals. Figure 8a–d shows
the time histories of flow depth at five different locations at 2000, 4000, 6000, and
8000 m. The maximum flow depths at these four locations were numerically
simulated and compared with the flow depth measured on site. Figure 9 illustrates
the numerical predictions and experimental measurements in terms of flow depths
along Sungai Penchala. The maximum flow depths predicted numerically by the
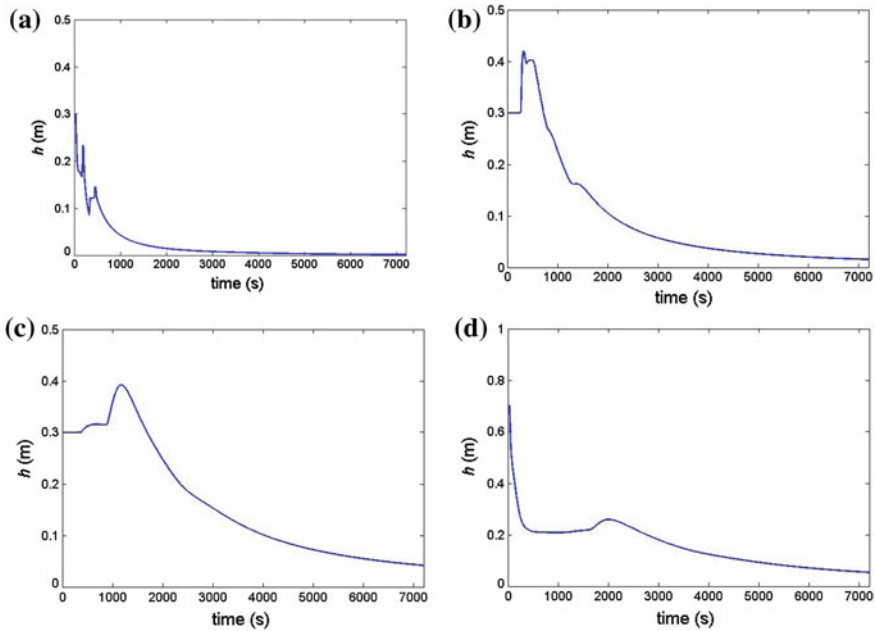
Fig. 8 a–d Time histories of water depth in four points. **a** $x = 2000$ m, **b** $x = 4000$ m, **c** $x = 6000$ m, **d** $x = 8000$ m

model were slightly higher than the maximum measured at G1. A big discrepancy at G2, G3, and G4 might be due to the grid resolution chosen during the simulation. To investigate the cause, a higher grid resolution should be taken into account in further studies. However, whether or not this conclusion can be extended to large-scale simulations over realistic domain topographies remain to be established. The flow model was then integrated with the pollutant transport equation and was subsequently used to study the fate of pollutant on several benchmark tests.

Fig. 9 Comparison of numerical and measured maximum water depth along Sungai Penchala
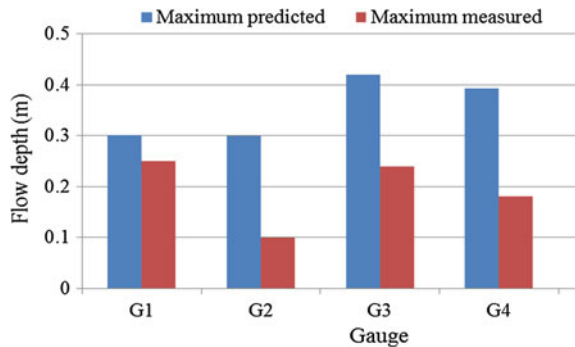
5   Conclusion

The proposed 1D shallow flow model was numerically solved by a Godunov-type finite-volume scheme in conjunction with the HLL approximate Riemann solver for a direct approximation of fluxes through the cell interfaces. The model was validated by a number of benchmark tests, also on a selected site representing a real-case scenario, and results obtained were reliable. The equation used for solute transport model describes passive dynamics of the transported concentration. However, in reality the dynamics is active when the transported materials are chemically reactive or biologically reproductive. Thus, new mathematical formulations such as advection–reaction–diffusion equations are recommended to be included in the future research.

References

1. Gejadze IY, Monnier J (2006) A joint data assimilation-coupling algorithm applied to shallow water flood models. In: Eccomas Cfd 2006: proceedings of the European conference on computational fluid dynamics, Egmond Aan Zee, The Netherlands. Delft University of Technology; European Community on Computational Methods In Applied Sciences (Eccomas), 5–8 Sept 2006
2. Ahmed H, Norio T (2009) Distributed water balance with river dynamic-diffusive flow routing model. J Hydrodyn (Ser B) 21:564–572
3. Wilson MD, Bates PD, Alsdorf D, Forsberg B, Horritt M, Melack J, Frappart F, Famglietti JS (2007) Modeling large-scale inundation of Amazonian seasonally flooded wetlands. Geophys Res Let 34:L15404
4. Pérez Guerrero JS, Pontedeiro EM, Van Genuchten M, Skaggs TH (2013) Analytical solutions of the one-dimensional advection–dispersion solute transport equation subject to time-dependent boundary conditions. Chemical Eng J 221:487–491
5. Chen L, Zhu J, Young MH, Susfalk RB (2009) An integrated approach for modeling solute transport in streams and canals with applications. J Hydrol 378(1):128–136
6. Chevereau G, Priesmann A (1971) Transport of pollutants. In: Practical aspects of computational river hydraulics
7. Bates PD, Roo APJD (2000) A simple raster-based model for flood inundation simulation. J Hydrol 236:54–77
8. Fan P, Li JC, Li QQ, Singh VP (2008) Case study: influence of morphological changes on flooding in Jingjiang river. ASCE J. Hydraul Eng 134:1757–1766
9. Alcrudo F, García-Navarro P (1993) A high-resolution godunov-type scheme in finite volumes for the 2d shallow-water equations. Inter J Numer Meth Fluids 16(6):489–505
10. Anastasiou K, Chan CT (1997) Solution of the 2d shallow water equations using the finite volume method on unstructured triangular meshes. Inter J Numer Meth Fluids 24(11):1225–1245
11. Rogers BD, Fujihara M, Borthwick AGL (2001) Adaptive Q-Tree Godunov-Type scheme for shallow water equations. Inter J Numer Meth Fluids 35(3):247–280
12. Toro EF (2001) Shock-capturing methods for free-surface shallow flows. Wiley, Chichester

13. Harten A, Lax PD, Vanleer B (1983) On upstream differencing and godunov-type schemes for hyperbolic conservation laws. Siam Rev 25(1):35–61
14. Van Leer B (1979) Towards the ultimate conservative difference scheme. V.A second-order sequel to Godunov's method. J Comput Phys 32(1):101–136
15. Qiuhua L, Marche F (2009) Numerical resolution of well-balanced shallow water equations with complex source terms. J Adv Water Res 32(6):873–884
16. Nor A, Lariyah MS (2015) Numerical simulation on the integrated shallow water flow model. In: International conference on advances in civil and environmental engineering
17. Bermúdez A, Vázquez ME (1994) Upwind methods for hyperbolic conservation laws with source terms. J Comput Fluids 23(8):1049–10711
18. Li YN, Huang P (2008) A coupled lattice Boltzmann model for advection and anisotropic dispersion problem in shallow water. J Adv Water Res 31:1719–1730
19. Komatsu T, Ohguishi K, Asai K (1997) Refined numerical scheme for advective transport in diffusion simulation. J Hydraul Eng 123:141–150

Detection and Transportation of Nutrients and Pathogenic Bacteria in Kerayong River Water

Zummy Dahria Mohamed Basri, Zulhafizal Othman, Marfiah Ab. Wahid and Jazuri Abdullah

Abstract Water is one of the most important sources of human life. Rainfall is abundant source that can provide water for human consumption. However, the clean water source cannot be relished, as a result of pollution caused by humans. Development and modernization cause water to become filthy and not suitable to be used directly and require rigorous treatment. Kerayong River that passes through residential and industrial area in Kuala Lumpur also became a victim of water pollution. 6 sampling points along the Kerayong River in this study showed the high rate of ammoniacal nitrogen and phosphorus in the river water, which is 6.92–10.83 mg/L and 2.22–3.53 mg/L, respectively. The presence of nitrate and nitrite concentration can also be detected from 0.09–0.22 mg/L to 0.05–0.17 mg/L, respectively. Pathogenic bacteria such as *Salmonella*, *Shigella, E.coli,* and *Pseudomonas aeruginosa* were detected in concentrations up to 173 cfu/ml in the river water, overcoming the limits. Although only in sampling points 1–4 could detect *Vibrio spp*. with low concentration, but it still needs to be concerned. Overall, the river water is not suitable for use directly without going through the proper water treatment process.

Keywords Nutrient · Pathogenic bacteria · River water · QUAL2 K

Z.D.M. Basri (✉) · Z. Othman · M.Ab.Wahid · J. Abdullah
Faculty of Civil Engineering, UiTM Shah Alam, Kuala Lumpur, Selangor, Malaysia
e-mail: zummy.d@gmail.com

Z. Othman
e-mail: zul_hafizal85@yahoo.com

M.Ab.Wahid
e-mail: marfi851@salam.uitm.edu.my

J. Abdullah
e-mail: jazuri9170@salam.uitm.edu.my

1   Introduction

Water is a basic need of human life and human activities related to the environment. Generally, Malaysia due to high rainfall does not have water shortages. However, water quality in Malaysia shows a deteriorating trend. Water pollution has become an issue that must be addressed immediately. River is known as a natural water channel into which it flows continuously, sometimes a little, sometimes a lot, depending on the frequency of rainfall and the rate where groundwater contributes to the base flow of the watercourse. It is also the water supply system which is distributed to the public [1].

Water quality is directly affected by the amount of waste dumped into the river, where most of the sources of pollution have been caused by human activities. Part of river pollution is also caused by natural resources. Water pollution problem is becoming more serious with the increasing dirty river conditions and filled with garbage. It includes chemicals and other impurities that could not be seen with the eyes. Water quality and sediment in the river are constantly changing. More water pollution problems occur in certain location, especially in urban and industrial areas [2]. Water pollution, however, is not counted as environmental issue recently, as it comes along with the rapid development and modernization [3].

Apart from waste materials such as garbage and waste from industry, the river becomes a place for breeding different kinds of harmful bacteria. The presence of various types of bacteria showed that river water is not suitable to be used directly, without prior treatment. Direct contact with polluted river water will cause water-borne diseases. The 'love our rivers' campaign run on a large scale by the government seems to be deadlocked because people still do not appreciate the natural resources, and everyday activities that cause pollution are becoming more common.

In this study, simulation software QUAL2 K also has been used to model the occurrence of pathogenic bacteria (*E.Coli*) concentration in Kerayong River. QUAL2 K model is a one-dimensional model where river channel is assumed to be well mixed in vertical and lateral direction. It implements the steady-state hydraulics, diel heat budget, and calculates diel water-quality kinetics [4]. It simulates a river by representing a river as a series of reaches which have consistent hydraulic characteristics and these reaches can be divided into a series of elements or difference headwater. Objectives of this study are (1) to determine the concentration of nutrients and pathogenic bacteria present in Kerayong River water and (2) to produce a calibration result on the concentration of pathogenic bacteria *E.coli* transport in Kerayong River water using QUAL2 K.

2 Materials and Method

2.1 Sampling Area

Sungai Kerayong was chosen as a sampling area which is located in Kuala Lumpur. It runs from Pandan Indah to Pantai baru. The sampling site could be categorized as highly urbanized because most of the land is covering with residential areas [5]. Every sampling point has different types of land use, suggesting the occurrence of some local contamination [2]. Figure 1 and Table 1 show the Kerayong River's map with coordinates of six different sampling points.

First sampling point is at Station Outfall Taman Desa (downstream), second point is at Kampung Sri Indah, third point is at Chan Sow Lin, fourth point is at Jalan Maluri, fifth point is at Jalan Kuari, and the last point is at Taman Indah Ampang (Upstream). Distance between point to point is 500 m.

2.2 Sample Collection

Water samples were collected in 500-ml plastic bottles for nutrient analysis and in 50-ml sterile plastic tube for microbiology analysis. Water samples were stored at 4 °C. All the water samples were transported to the laboratory immediately. Analyzed had been done within 24 h of collection.
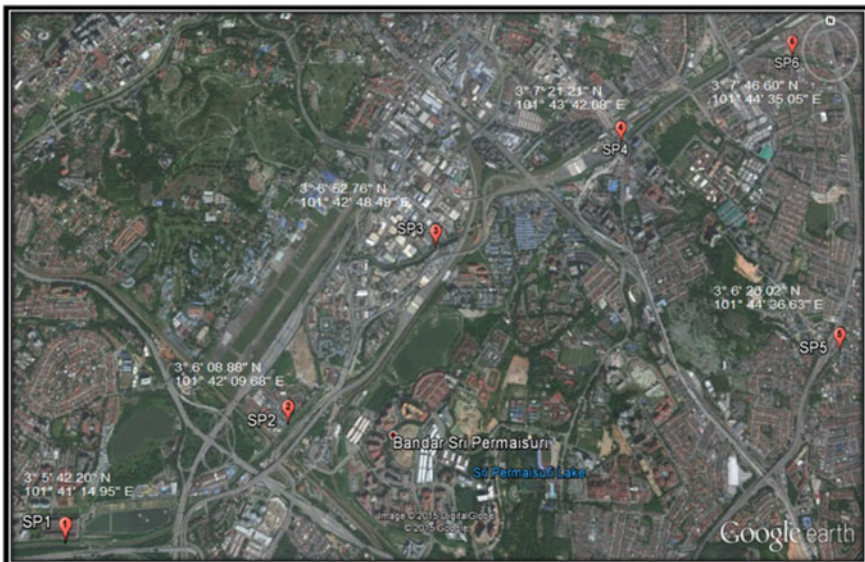

Fig. 1 The map of six sampling points in Sungai Kerayong

Table 1 The coordinates for the six sampling points

Sampling point	Coordinate
1	3° 5′ 42.20″ N 101° 41′ 14.95″ E
2	3° 6′ 08.88″ N 101° 42′ 09.68″ E
3	3° 6′ 52.76″ N 101° 42′ 48.49″ E
4	3° 7′ 21.21″ N 101° 43′ 42.08″ E
5	3° 6′ 26.02″ N 101° 44′ 36.63″ E
6	3° 7′ 46.60″ N 101° 44′ 35.05″ E

2.3 Analysis of Sample

Temperature and pH were measured in situ as field parameter. The nutrients were measured in the laboratory according to standard method. Direct method was used to analyze, enumerate, and identify bacteria. This method included membrane filtration method and standard plate count (SPC). Water sample was collected and then dilutions had been prepared. White membrane with diameter 0.45 µm was removed from the sterile package and was placed into the funnel assembly. 1 mL of the dilutions had been taken out and the sample was put into the funnel. Vacuum is turned on and the sample will pass through the filter completely. After that, the filter membrane is placed in Petri dishes and incubated for 24 h at 35 ± 2 °C.

The colonies of bacteria that grow on the agar were counted. MacConkey agar was used to isolate *Salmonella* (colorless colonies) and *E.Coli* (bright pink colonies). *Salmonella–Shigella* (SS) agar is a selective media used for separation of *Shigella* (colorless colonies). Cetrimide agar is used for identification of *Pseudomonas Aeruginosa* (colorless colonies), while TCBS agar is a medium used to isolate *Vibrio Cholerae* (yellow colonies) and *Vibrio parahaemolyticus* (green colonies).

3 Results and Discussion

3.1 Temperature and PH

pH is used to measure the water acidity or alkalinity. The water considered neutral if the pH value is equal to 7. Some aquatic organisms might die if the water was slightly acidic. Table 2 shows the pH and temperature at all 6 sampling points.

The pH for all sampling sites is more than 7. It is slightly alkalized and considered good enough to support aquatic life. Referring to Malaysia National Water Quality Standards (NWQS), it fulfilled the requirement for class 1. Referring to DOE [6], 6.5–8.5 is acceptable pH range for domestic water supply. Figure 2 shows the calibration result of pH value using QUAL2 K.

From the calibration result of pH value, it shows that the prediction from Qual2 K is quite similar to the actual value obtained from sampling campaign.

Table 2 Temperature and pH

Sampling point	T (°C)	pH
1	28.61	8.13
2	28.28	8.34
3	28.39	8.22
4	28.59	8.23
5	28.86	7.96
6	29.52	8.04

Fig. 2 Calibration results of pH value using QUAL2 K
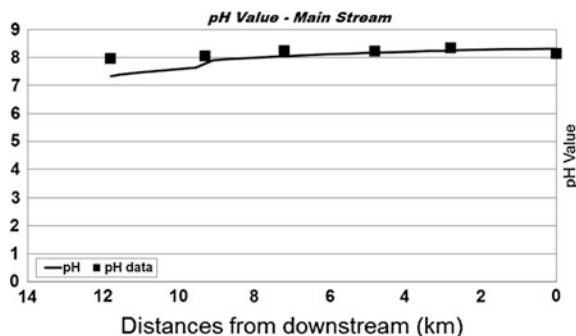
The pH value indicated the decreasing trend from upstream to downstream, perhaps be infected by some factors such as dilution factor and transformation process.

Temperature will directly affect many traits of physical, biological, and chemical characteristics of a water bodies. The temperature recorded in this study fluctuates but not too significant. The table indicates that the results are within the acceptable levels of NWQS Malaysia which ranged from 28.28 to 29.52 °C. The temperature in Kerayong River is quite high compared to Semenyih River in Selangor which ranged from 24.71 to 27.36 °C during dry season [7]. Sampling time, weather condition [8], and location were affected by the increase or decrease of temperature.

3.2 Nutrients

There are four nutrients such as ammoniacal nitrogen, phosphorus, nitrate, and nitrite were tested in Kerayong River (see Table 3). To date, the standard for ammoniacal nitrogen emissions has not been there and the existing sewage treatment plants in Malaysia are not created for ammoniacal nitrogen removal. Nevertheless, according to Indah Water Konsortium, roughly, the public sewage treatment facilities need to comply the stipulated Standard A (15 mg/l) and Standard B (25 mg/L) requirements. In this study, ammoniacal nitrogen detected in river water ranged between 4 and 8.25 mg/l and categorized under Standard A. However, higher ammoniacal nitrogen can be toxic to aquatic life [9].

Table 3 Nutrient detected in Kerayong River

Point	Ammoniacal nitrogen	Phosphorus	Nitrate	Nitrite
1	8.75	2.59	0.10	0.07
2	7.67	2.32	0.18	0.05
3	6.92	3.27	0.21	0.10
4	10.83	3.53	0.22	0.08
5	7.67	2.22	0.09	0.07
6	7.25	3.80	0.41	0.17

The presence of nitrate indicates an important macronutrient in the aquatic environment. It is danger to human because gut can break down the nitrate into nitrite. This situation led to a failure of red blood cells to carry oxygen. Not only to human, but also it can cause serious diseases to aquatic life [10]. The table indicates nitrate and nitrite where upper value ranged from 0.09 to 0.41 mg/l for nitrate concentration (except point 5 with 0.09 mg/l) and from 0.07 to 0.17 mg/l for nitrite (only point 6 was exceeded the limit).

Excessive phosphorus in the water could lead to algae blooms. The presence of algae bloom is harmful to aquatic organisms as it can cause decrease in DO level, and temperature increase would also occur in the water when there is algae bloom. This phenomenon can kill many aquatic organisms [11]. Phosphorus detected in this study ranged from 2.22 to 3.80 mg/l. The highest phosphorus was detected at sampling point 6. Therefore, all detected phosphorus is higher than permissible limit.

3.3 Bacteria Identification

The microbiological quality of river water was determined by enumerating the pathogenic bacteria such as *Salmonella, Vibrios spp, Pseudomonas A., Shigella,* and *E.coli.* Figure 3 shows the concentration of microbiological quality detected in this study.

At sampling point 4, the highest *Salmonella, Shigella, E.coli,* and *Pseudomonas Aeruginosa* were detected with 173, 114, 163, and 155 cfu/ml concentrations, respectively. It indicates that from all sampling points, point 4 was their main reservoir. *Vibrio* could be detected in point 1–4 with highest concentration at point 2. *Salmonella, E.coli, Shigella,* and *Pseudomonas* were detected at all sampling points. *Salmonella spp* were detected in all freshwater river samples, while *Vibrio spp.* were predominantly detected in marine river [12]. All bacterial counts were slightly higher than permissible limit except for *Vibrio spp*.

Figure 4 shows the calibration results of *E.coli* concentration obtained from the Qual2 K software. From the result, the concentration of *E.coli* indicated the upward

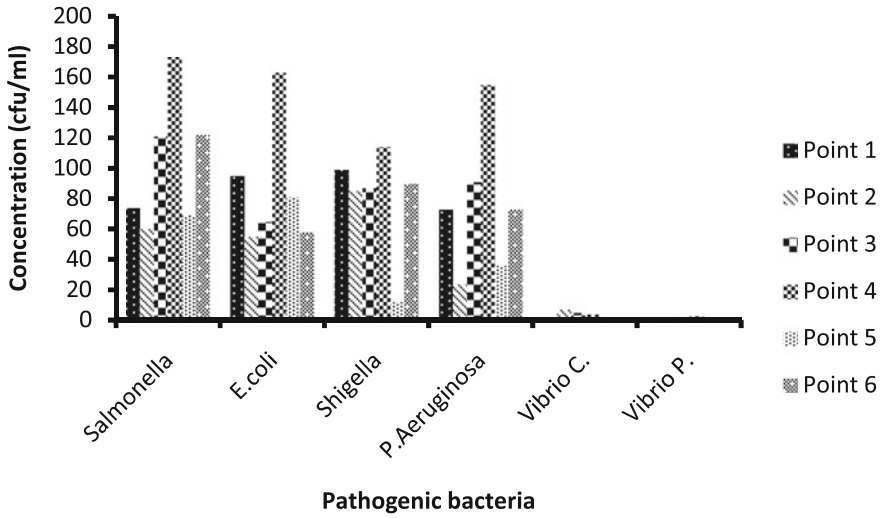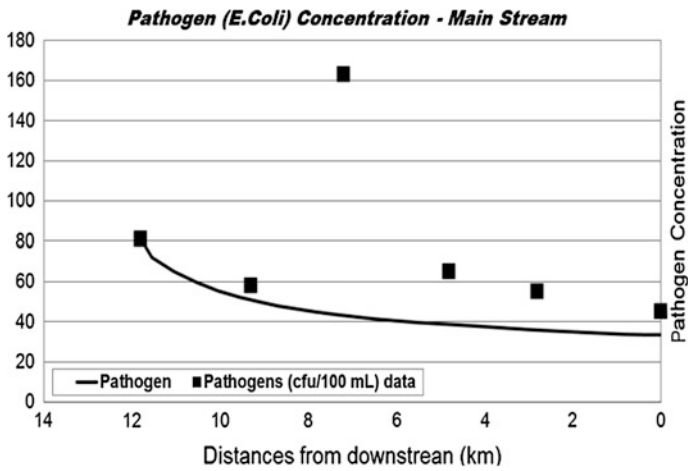**Fig. 3** Pathogenic bacteria detected in Kerayong River

Fig. 4 Calibration result of *E.Coli* concentration using QUAL2 K

trend from upstream to downstream. As shown in the figure, at sampling point 4, the value between prediction and actual showed high percentage of difference, and it may be caused by uncertainty of discharge from various activities along the river which will affect the concentration.

4 Conclusion

1. Ammoniacal nitrogen, phosphorus, nitrate, and nitrite detected in Kerayong River were higher than permissible limit, except nitrate in point 5 and nitrite in point 1, 2, 3, 4, and 5.
2. *Salmonella, Shigella, E.coli,* and *Pseudomonas Aeruginosa* were detected in all sampling points with 24–173 cfu/ml in concentration, while *Vibrio spp*. only detected in points 1–4 with low concentration.
3. Prediction for the concentration of *E.coli* and pH is similar to data collection.

References

1. Koch P (2010) WSO: water sources, 4th edn. American Water Works Association, United States of America
2. Cheung KC, Poon BHT, Lan CY, Wong MH (2003) Assessment of metal and nutrient concentrations in river water and sediment collected from the cities in the Pearl River Delta, South China. Chemosphere 52:1431–1440
3. Maketab M (2008) Water quality models in river management. In: Proceedings of the 1st technical meeting of muslim water researchers cooperation (MUWAREC), December 2008
4. Chapra SC, Pelletier GJ, Tao H (2007) QUAL2 K: a modelling framework for simulating river and stream water quality, Version 2.07, Documentation and User's Manual, Civil and Environment Engineering Dept., Tufts University, Medford, MA., pp 9–10, 15–16, 56, 103
5. Dom NM, Abustan I, Abdullah R (2012) Dissolved organic carbon production and runoff quality of Sungai Kerayong, Kuala Lumpur, Malaysia. Int J Eng Technol 44–47
6. Water resources management and hydrology division department of irrigation and drainage (2009) Study on the river water quality trends and indexes in Peninsular Malaysia, Water Resources Publication No. 21, 2009
7. Al-Badaii F, Shuhaimi-Othman M, Gasim MB (2013) Water quality assessment of the Semenyih River, Selangor, Malaysia. J Chem 2013:1–10
8. Noraini R, Scca G, Johan I, Mohd IJ (2010) Comparative study of water quality at different peat swamp forest of Batang Igan, Sibu, Sarawak. Am J Environ Sci 6(5):416–421
9. Corwin DL, Loague K, Ellsworth TR (1999) Advanced information technologies for assessing nonpoint source pollution in the Vadose zone : conference overview. J Environ Qual 28(2):357–365
10. Davis P, McCuen RH (2005) Storm water management for smart growth, 1st edn. Springer Science and Business Media, Berlin
11. Said D, Stevens K, Sehlke G (2004) An innovative index for evaluating water quality in streams. Environ Manage 34(3):406–414
12. Thong K (2005) Microbiological quality of selected aquatic environments in Langkawi Island. Malays J Sci 24

Trend of Total Phosphorus on Total Suspended Solid Reduction in Constructed Wetland Under Tropical Climate

Nur Emylia Johari, Suhaimi Abdul-Talib, Marfiah Ab. Wahid and Aminuddin Ab. Ghani

Abstract Constructed wetland has the potential to provide significant treatment for quality of stormwater runoff, especially in total suspended solid and total phosphorus concentration. The aim of this research is to investigate the trend of total phosphorus on total suspended solid reduction in constructed wetland in order to enhance the urban stormwater quality. This study was conducted in actual constructed wetland located in Universiti Sains Malaysia (USM) Engineering Campus, Nibong Tebal, Penang, Malaysia. The water samples were taken using grab sampling method from 14 sampling stations for seven months based on 14 stormwater events. The results showed a positive value of Pearson's r as the total suspended solid had a positive correlation with the total phosphorus approximately, $r = 0.78$, which can be considered a large effect on the reduction trend. The coefficient of determination, $R^2 = 0.93$, was obtained from the relationship between total suspended solid and total phosphorus. Thus, the decreasing trend of total suspended solid concentration also showed the decreasing concentration of total phosphorus. The appropriate selection of macrophyte, water depth, and hydraulic residence time are vital to enhance the stormwater quality before discharge to the receiving water body.

N.E. Johari (✉) · S. Abdul-Talib · M. Ab. Wahid
Faculty of Civil Engineering, Universiti Teknologi MARA, Selangor, Malaysia
e-mail: nuremylia88@gmail.com

S. Abdul-Talib
e-mail: ecsuhaimi@salam.uitm.edu.my

M. Ab. Wahid
e-mail: ce_marfiah@yahoo.com

A. Ab. Ghani
River Engineering and Urban Drainage Research Centre, Universiti Sains Malaysia
Engineering Campus, Penang, Malaysia
e-mail: redac02@usm.my

1   Introduction

Particulate matter will enter the river water body through surface runoff due to mainly construction and agricultural activities. It will deteriorate the river water and will disrupt an aquatic habitat through the reduction of light penetration [1]. Particulate matter also can be surrogate to other pollutants such as organic matter, oil and grease, and also nutrient especially phosphorus [2]. The pollutant will attach physically, chemically, and biologically to the particulate matter. The coagulation and sedimentation process will undergo when deal with particulate matter. The settlement of particulate matter will be defined as sediment, and the particulate matter that suspends in water will be called as suspended solid (SS) and will flow according to the water flow. The total suspended solid (TSS) will contain organic and inorganic. According to [3], the accumulation of SS with contaminants was happened as high concentration of organic found in the wetland sediment. Another study reported that removal of nutrient decreases during the high precipitation period where in high precipitation, heavy silt load will attached together with nutrient and organic matter and enter into the water body [4].

Constructed wetland as one of the best management practices has been widely used as treatment system where energy consumed is zero, operation cost is lower, and it is easier for maintenance. Constructed wetland consists of two types, namely horizontal flow and vertical flow. Normally, horizontal flow of constructed wetland will be used as it is economic for stormwater and wastewater [4–6]. [4] Indicate that constructed wetland can remove approximately 82.11 and 84.32 % of total nitrogen (TN) and phosphate, respectively, by using the 1st Edition of MSMA and *Lepironia articulate*. According to [7], the percentage removal of nitrogen in constructed wetland was 22 %. [8] Found that the removal of TSS and total phosphorus (TP) was ranged in between 50–100 % and 24–46 % for each respectively after throughout the constructed wetland by using *Hanguana malayana, Phragmites karka, Lepironia articulate,* and *Typha latifolia*. According to [9], the horizontal surface flow constructed wetland has an open water area and looks as the natural marshes. There are three main zones in constructed wetland, namely inlet zone, macrophyte zone, and open water zone [10].

Macrophyte is one of the key components in constructed wetland in order to enhance the stormwater quality [11]. There are three types of macrophytes or plants that will be used as substrate in constructed wetlands, namely floating plants, submerged plants, and emergent plants. According to [11], macrophyte will provide surface area for microbial growth, will reducing the current velocity and as bed surface stabilization. Therefore, the aim of this research is to evaluate the trend of TP on TSS reduction in constructed wetland to enhancing the urban stormwater quality under tropical climate.

2 Method

The constructed wetlands at Universiti Sains Malaysia (USM) Engineering Campus, Nibong Tebal, Penang, as shown in Fig. 1 had been studied for the trend of TP on TSS reduction in constructed wetland in order to enhance the urban stormwater quality. The USM Engineering Campus has an area about 320 acres and mainly made up of oil palm plantation land and is fairly flat. In Malaysia, USM Engineering Campus was carried out at the national pioneer project based on the 1st Edition of MSMA, namely Bio-Ecological Drainage System (BIOECODS), and the design was continuously improved in the 2nd Edition of MSMA [12]. The series of component was consist in the BIOECODS, namely, ecological swales, online subsurface detentions, dry pond, wet pond, detention pond, constructed wetlands, wading streams and recreational pond. The combination of this component was increased the runoff lag time, reduced the rate and volume of runoff, and also increased the pollutant removal [13, 14]. The source of pollutant that will be carried by stormwater runoff in USM Engineering Campus can be from plant landscaping, plant watering, herbicide, pesticide, fertilizer, car park area, recreational area, and roof top.

Six species of macrophyte had been selected, namely *Eleocharis variegata, Scirpus grossus, Phragmite karka, Typha angustifolia, Lepironia articulate,* and *Hanguana malayana* had been cultivated at constructed wetland. The water sampling was conducted from May 2013 until December 2013 based on rainfall event. Grab sampling method was being applied for 14 sampling stations, and then, the water sample was preserved at freezer prior to analysis. The parameters investigated
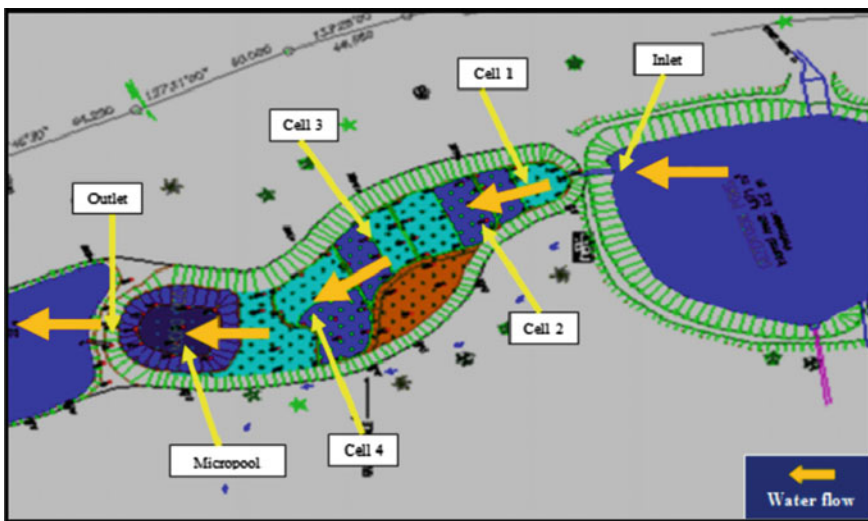

Fig. 1 Constructed wetland at Universiti Sains Malaysia Engineering Campus [15]

in this study are total suspended solid and total phosphorus. In situ measurement was conducted using Marsh McBirney Flo-mate TM Model 2000 for velocity measurement. The laboratory analysis of TSS and TP was carried out at the River Engineering and Urban Drainage Research Centre, REDAC Laboratory, USM, by referring APHA-2540D Standard Method [16] and PhosVer® 3 with acid persulfate digestion method [17], respectively. The testing was conducted in three replicate runs at laboratory by following the standard method which complies with the standard of the American Public Health Association [16]. The percentage of removal on each sampling by rainfall event was determined using the equation as follows:

$$\text{Percentage of reduction}, \% = \frac{C_{\text{in}} - C_{\text{out}}}{C_{\text{in}}} \times 100 \tag{1}$$

where C_{in} and are the concentration of influent and effluent of cell. The Microsoft Excel and Pearson's r will be used for conducting the data analysis.

3 Result and Discussion

The constructed wetland had four cells with different macrophytes and different bathymetry zones as well as velocity for each cell as in Table 1.

Based on the obtained result, the TSS concentration from the inlet zone was in the range of 17.00–34.00 mg/L and the treated water at the outlet zone was in the range of 3.00 mg/L until 11.00 mg/L. The inflow concentration of TSS was characterized by a general trend of decreasing during the period evaluated. Overall performance of constructed wetlands showed the decreasing of TSS concentration which is 71.33 % as shown in Fig. 2.

Table 1 Mean ± standard deviation for velocity throughout the constructed wetland

	Macrophyte	Marsh	Velocity (m/s)
Inlet zone			0.11 ± 0.06
Cell 1	*Eleocharis variegata*	High	0.03 ± 0.01
Cell 2	*Scirpus grossus*	High	0.03 ± 0.01
	Phragmites karka	Low	
Cell 3	*Typha angustifolia*	Low	0.02 ± 0.00
	Scirpus grossus	High	
	Lepironia articulata	High	
Cell 4	*Lepironia articulata*	Low	0.04 ± 0.00
	Eleocharis variegata	Low	
	Eleocharis variegata	High	
	Hanguana malayana	Low	
Outlet zone	*Typha angustifolia*	High	0.12 ± 0.06
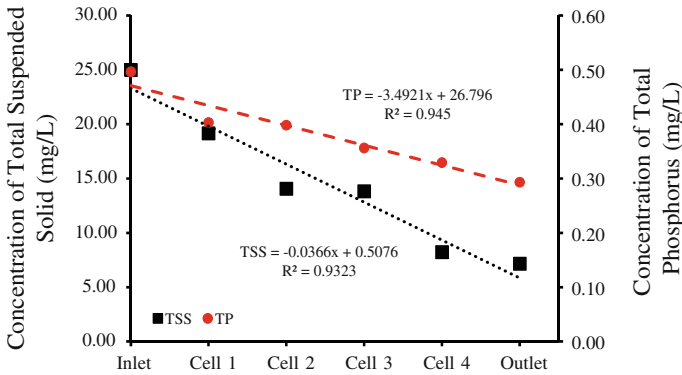
Fig. 2 Trend of total suspended solid and total phosphorus throughout the constructed wetland

The results obtained from this study also showed the effluent concentration of TP at the inlet was in the range of 0.29 mg/L until 0.88 mg/L, while the effluent concentration of TP at the outlet was in the range of 0.20 mg/L until 0.42 mg/L. The effluent concentrations of TP were characterized by a general trend of decreasing, increasing, and decreasing again during the period evaluated. Overall performance of constructed wetland showed the decreasing trend of TP concentration with the percentage removal of 40.94 % as shown in Fig. 2.

The highest removal of TSS and TP concentration were shown from Cell 4 and Cell 1 which is 40.56 and 18.79 % for each, respectively as shown in Table 2.

Pearson's r was used to measure the strength and direction of a linear relationship between two variables. The results showed a positive value of Pearson's r as TSS had a positive linear correlation with the TP approximately, $r = 0.78$, which can be considered a large effect on the reduction trend. Figure 3 shows the relationship between TSS and TP with the coefficient of determination, $R^2 = 0.93$. Therefore, when the concentration of TSS is low, the concentration of TP also will be low. However, based on Table 2, Cell 1 and Cell 2 showed almost the same concentration of TP. This can be predicted to be happening as there were many factors that can affect the concentration of TP as well as for the concentration of TSS.

Table 2 Mean ± standard deviation for TSS and TP throughout the constructed wetland

	TSS (mg/L)	TP (mg/L)
Inlet zone	25.00 ± 6.39	0.50 ± 0.21
Cell 1	19.17 ± 6.01	0.40 ± 0.10
Cell 2	14.06 ± 4.85	0.40 ± 0.08
Cell 3	13.83 ± 7.09	0.36 ± 0.09
Cell 4	8.22 ± 2.80	0.33 ± 0.09
Outlet zone	7.17 ± 2.86	0.29 ± 0.08
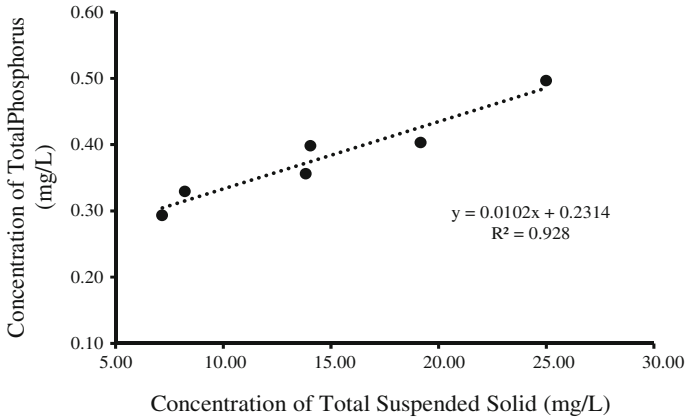
Fig. 3 Relation between total suspended solid and total phosphorus throughout the constructed wetland

The stormwater quality of constructed wetland, in terms of TSS and TP concentration, showed the enhancement with flow length along the constructed wetland. The present of macrophyte species with different bathymetry zone and with the velocity of stormwater where almost stagnant, was led to the reduction in TSS and TP concentration via the sedimentation.

The SS were coagulate with each other and form large particle of SS in low storm water velocity. Despite of this, the slow of storm water moving was given physical settling to SS particles. The large particle will be trapped and settle into the soil as the present of macrophyte and gravel in constructed wetland. Those trapping process seems like a filtration process where SS particle was filtered first in Cell 1, then the rest of non-filter SS particle were flowing into the next cell. Resuspension will give increasing of TSS concentration as well as TP concentration where occur in three mechanisms, namely, wind-driven turbulence, bioturbation, and gas lift [9].

In this study, *Eleocharis variegate* had shown the capability for trapping and filtering the SS particle. According to [11], macrophyte plays an important role in higher TSS removal concentration in constructed wetland because the macrophyte was provided large of surface area, reduce the storm water velocity and reinforced of settling and filtration by the roots. Therefore, when the TSS concentration was decreasing, the TP concentration also showed the decreasing trend. However, further study is needed to determine which part of macrophyte is contributing to a higher removal concentration of TSS and thus will also reduce the TP concentration in constructed wetland.

Next, the macrophyte bathymetry zone also can influence the TSS concentration in terms of high and low marsh zone where were defined by the depth of water. According to [10], the high marsh zone is from 0.30 m below the pool to the normal pool elevation. Therefore, detail study is needed in order to know how the

bathymetry of macrophyte zone will influence the TSS settlement and thus will also affect the decreasing concentration of the TP in constructed wetland.

Besides, hydraulic residence time was also influenced the concentration of TSS. The study reported by [5] showed that hydraulic residence time strongly effects the pollutant removal when higher removal was observed in the small event of rainfall compared to large event of rainfall. Every species may have different characteristic which will influence the hydraulic residence time in order for the SS to settle and trap in constructed wetland.

4 Conclusion

In conclusion, the trend of TP on TSS reduction in constructed wetland can be predicted as the positive value of Pearson's r correlation approximately, $r = 0.78$ with the coefficient of determination, $R^2 = 0.93$ was gave large effect that the TSS had correlated with the TP on the reduction trend. Therefore, when the concentration of TSS has reduced, the concentration of TP also reduces throughout the constructed wetland. *Eleocharis variegate* was found to have removal capability when compared to others. However, further study on factors influencing the water quality treatment in constructed wetland is needed. This study, therefore, offers knowledge to engineers and planners in helping them to make decision for planning, designing, and managing floods and stormwater systems in this area.

References

1. Duncan HP (1999) Urban stormwater quality: a statistical overview. CRC for Catchment Hydrology, Victoria
2. Wu Y, Chen J (2013) Investigating the effects of point sources and nonpoint source pollution on the water quality of the East river (Dongjiang) in South China. Ecol Indic 32:294–304
3. Tu YT, Chiang PC, Yang J, Chen SH, Kao CM (2014) Application of constructed wetland system for polluted stream remediation. J Hydrol 510:70–78
4. Sim CH, Yusoff MK, Shutes B, Ho SC, Mansor M (2008) Nutrient removal in a pilot and full scale constructed wetland, Putrajaya city, Malaysia. Environ Manage 88:307–317
5. Mangangka IR, Egodawatta P, Parker N, Gardner T, Goonetilleke A (2013) Performance characterisation of constructed wetland. Wat Sci Tech 68(10):2195–2201
6. Sundari AS, Retnaningdyah C, Suharjono S (2013) The effectiveness of Scirpus Grossus and Limnocharis flava as phytoremediation agents of nitrate-phosphate to prevent microcystis blooming in fresh water ecosystem. Trop Life Sci 3(1):28–33

7. Lim PE, Wong TF, Lim DV (2001) Oxygen demand, nitrogen and copper removal by free water surface and subsurface flow constructed wetlands under tropical conditions. Environ Int 26:425–431

8. Mohd Noor NA (2009) Water quality modelling of constructed wetlands in Malaysia. Case study BIOECODS, USM. Msc. Thesis, Universiti Sains Malaysia, Penang, Malaysia

9. Kadlec RH, Wallace SD (2008) Treatment wetlands, 2nd edn. CRC Press Inc., Boca Raton

10. Department of Drainage and Irrigation Malaysia or DID (2012) Urban stormwater management manual for Malaysia (MSMA), 2nd edn. Department of Drainage and Irrigation Malaysia (DID), Kuala Lumpur, Malaysia

11. Brix H (1997) Do macrophytes play a role in constructed treatment wetlands? Wat Sci Tech 5:11–17

12. Shaharuddin S, Zakaria NA, Ab. Ghani A, Chang CK (2013) Performance evaluation of constructed wetland in Malaysia for water security enhancement: 2013 IAHR World Congress, Chengdu, China, 8–13 Sept 2013

13. Zakaria NA, Ab. Ghani A, Abdullah R, Mohd Sidek L, Ainan A (2003) Bio-ecological drainage system (BIOECODS) for water quantity and quality control. Int J River Basin Manage, IAHR & INBO 1(3):237–251

14. Ab. Ghani A, Zakaria NA, Abdullah R, Yusof MF, Mohd Sidek L, Kassim AH, Ainan A (2004) BIO-ecological drainage system (BIOECODS): concept, design and construction. In: 6th international conference on hydroscience and engineering (ICHE-2004), 30 May–3 June 2004, Brisbane, Australia

15. Google Maps (2013) Map of Universiti Sains Malaysia Engineering Campus. Retrieved from https://maps.google.com.my/maps?q=campus+engineering+usm&bav=on.2,or.r_cp.r_qf. &bvm=bv.48175248,d.bmk&biw=1280&bih=516&wrapid=tlif137136134591110&um= 1&ie=UTF-8&hl=en&sa=N&tab=wl

16. American Public Health Association (APHA) (2012) American Water Works Association (AWWA) and Water Environment Federation (WEF), Standard Methods for the Examination of Water and Wastewater, 22nd edn. American Public Health Association, Washington D.C.

17. HACH (2013) Water analysis handbook. HACH Company, Loveland, CO, USA

Study of Heavy Metals Concentration from Different Steel-Based Industries Effluents

Ain Nihla Kamarudzaman, Tay Chia Chay, Amnorzahira Amir and Suhaimi Abdul Talib

Abstract A study was conducted to identify and analyze heavy metals concentration in the steel industries effluents. The industrial effluents were collected from three different steel based factories in Shah Alam, Selangor, Malaysia. For each factory, the effluent samples were collected at two different points for determination of heavy metals concentration. Heavy metal concentrations were analyzed using Inductively Coupled Plasma Atomic Emission Spectroscopy. The results showed heavy metals (Cr, Fe, Mn, Ni and Zn) in the untreated effluent at Factory C have the highest concentrations compared with other steel-based factories. Also, the concentration of Fe, Mn and Ni in the treated effluent from Factory C were found above the permissible limits.

Keywords Heavy metals · Industrial effluents · Steel-based industry · Human health · Effluent treatment

A.N. Kamarudzaman (✉)
School of Environmental Engineering, Universiti Malaysia Perlis (UniMAP),
02600 Arau, Perlis, Malaysia
e-mail: ainnihla@unimap.edu.my

T.C. Chay
Faculty of Applied Sciences, Universiti Teknologi MARA (Arau),
02600 Arau, Perlis, Malaysia
e-mail: taychiay@gmail.com

A. Amir
Faculty of Civil Engineering, Universiti Teknologi MARA (Shah Alam),
40450 Shah Alam, Selangor, Malaysia
e-mail: amnorzahira@salam.uitm.edu.my

S.A. Talib
Faculty of Civil Engineering, Universiti Teknologi MARA (Shah Alam),
40450 Shah Alam, Selangor, Malaysia
e-mail: ecsuhaimi@salam.uitm.edu.my

1   Introduction

The steel industry is one of the important industrial sectors in Malaysia. It provides raw materials and components to other sectors such as automotive, construction, fabrication, electrical, computer, and furniture. On average, each steel factory uses about 18000 m^3 of water per day for steel production [1]. Several processes involved in the steel production such as pickling, electrolytic cleaning, furnace, refining, blasting, casting, rolling, and cooling [2, 3]. Each process uses a lot of water and discharges effluent containing a variety of harmful heavy metals [2]. Heavy metals in the effluent generated from steel production include Fe, Ni, Zn, Mn, Cd, Cr, and others metal. The effluents from the steel factory have high concentration of heavy metals due to an accumulation of filtered particles from the filtration process [1].

Heavy metals are toxic and non-biodegradable [4]. It can accumulate in living organisms. Discharge of heavy metals without proper treatment can threaten human health and deteriorate the environment and ecosystems. The effect on human health includes carcinogenic, headache, diarrhea, nausea, vomiting, dermatitis, chronic asthma, coughing, liver failure, and kidney failure [5, 6]. The dissolved or particulate heavy metals generated from industrial effluents can enter the aquatic ecosystems [7].

The effluent from steel factory is discharged into the wastewater holding tank before undergoing some treatments. Treatment technologies such as precipitation, oxidation, reduction, biosorption, coagulation, dissolved air flotation, ion exchange, adsorption, and filtration have been developed in order to remove heavy metals from industrial effluents [1, 8, 9]. In practice, the industrial effluent treatment at factories may involve several combinations of biological, chemical, and physical treatment. However, the cost of operation and maintenance for these treatments could be very high. The objective of this study was to identify and analyze the heavy metal concentrations in the untreated effluents and treated effluents from three different steel-based factories. The study also makes the comparison of performance efficiency of industrial effluent treatment among these factories.

2   Materials and Methods

A. *Sampling of Industrial Effluent*

The industrial effluent samples were collected from three different steel-based factories (namely Factory A, Factory B, and Factory C) located in Shah Alam, Selangor, Malaysia. For each sampling location, samples were taken from two different points, namely from the untreated effluent and the treated effluent outlet. Plastic bottles of 1.0 L were used to collect the industrial effluent samples. The effluent samples were properly labeled and transported to the laboratory and kept refrigerated at a temperature below 4 °C prior to analysis.

Table 1 Specific wavelength for heavy metals analysis [10]	Metals	Wavelength (nm)
	Chromium (Cr)	205.560
	Copper (Cu)	327.393
	Iron (Fe)	238.204
	Manganese (Mn)	257.610
	Nickel (Ni)	231.604
	Zinc (Zn)	213.857

B. *Heavy metals' analysis by ICP-OES*

The analysis of heavy metals such as Chromium (Cr), Copper (Cu), Iron (Fe), Manganese (Mn), Nickel (Ni) and Zinc (Zn) was conducted using Inductively Coupled Plasma—Atomic Emission Spectroscopy (ICP–OES) (Perkin Elmer, USA). The calibration curves were obtained using multi-elements standard solutions. For each sample, the average value of triplicate was taken under specific wavelength as shown in Table 1.

3   Results and Discussions

Table 2 shows the heavy metals concentration in the untreated effluents from three different steel-based factories. It was observed that the concentration of Fe in the untreated effluents from all factories was very high compared to other metals. The results also revealed that the concentration of Cr, Fe, Mn, Ni, and Zn in the untreated effluent at Factory C was considered highest compared with Factory A and Factory B. Furthermore, concentration of these heavy metals also detected above the parameters limits of effluents of Standard B set by the Environmental Quality Act 1974, Environmental Quality (sewage and industrial effluents) Regulations, 1979, Malaysia [11]. The results also showed that the heavy metals

Table 2 Concentration of heavy metals in the untreated effluent from three different steel-based factories

Heavy Metals	Concentration (mg/L)			Permissible limit sets by standard B, EQA 1974
	Factory A	Factory B	Factory C	
Cr	0.016	0.003	0.565	0.05
Cu	ND	0.032	0.265	1.00
Fe	190.48	7.40	664.82	5.00
Mn	1.229	2.564	6.253	1.00
Ni	0.061	0.126	128.77	1.00
Zn	0.028	0.611	15.30	1.00

ND—Not detected
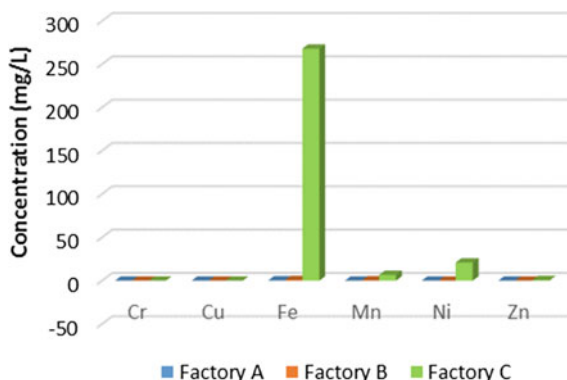
(Fe and Mn) concentration in the untreated effluents from Factory A and Factory B
was higher than the permissible limits of Standard B. However, the values of Cr,
Cu, Ni, and Zn concentrations in the untreated effluents from both factories were
detected below the permissible limits. The operations such as melting, charging,
dumping slag, and tapping steel have generating emission of iron oxides during its
operations [12]. The effects of Fe exposure on human health include respiratory
problems, heart attack, seizures, tissue damage, and depression [13, 14]. Also, the
effects of Mn exposure on human health include behavioral changes, damage of
nervous system, respiratory tract irritant, and lungs problem (associated with
pneumonitis, cough, bronchitis, chronic obstructive lung disease, and decrease in
lung function) [15].

Figure 1 shows the heavy metals concentration in the treated effluents from three
different steel-based factories. The concentration of Cr, Fe, Mn, Ni, and Zn in the
treated effluent from Factory A was reduced to 0.001, 0.376, 0.003, 0.003, and
0.009 mg/L, respectively. For Factory B, the concentration of Cr, Cu, Fe, Mn, Ni
and Zn in the treated effluent was 0.032, 0.001, 0.71, 0.227, 0.019, and 0.024 mg/L,
respectively. For Factory C, the concentration of Fe, Mn, Ni, and Zn in the treated
effluent was reduced to 267.78, 6.55, 20.85, and 0.63 mg/L, respectively. However,
the heavy metals of Cr and Cu in the treated effluent of Factory C were not detected
after treatment. Based on these results, the treated effluents had good results
compared to the untreated effluents. Most of heavy metals concentrations were
reduced after treatment and complies with the Standard B, the Environmental

Table 3 Percentage removal of heavy metals (Fe and Mn) at three different steel-based factories

Heavy Metals	Percentage removal (%)		
	Factory A	Factory B	Factory C
Fe	99.80	90.40	59.72
Mn	99.74	91.16	−4.79
Type of treatment	Several physical–chemical process	Dissolved air flotation (DAF)	Physical–chemical process

Quality Act 1974, Environmental Quality (sewage and industrial effluents) Regulations, 1979, Malaysia. However, the concentration of some heavy metals such as Fe, Mn, and Ni in the treated effluent from Factory C still not complies with the permissible limits of Standard B, EQA 1974.

Table 3 shows the comparison of performance efficiency for heavy metals removal among three factories. However, the study only focused on the removal of Fe and Mn because these parameters have higher concentration compared with others parameter. The result showed that the effluent treatment for the removal of Fe and Mn at Factory A has better performance compared with Factory B and Factory C. This was because the effluent treatment at Factory A consists of combination of physical and chemical processes such as neutralization, oxidation, coagulation, settling, and filtration.

4   Conclusion

Analysis of heavy metals concentration in the untreated and treated industrial effluents from three different steel-based industries was successfully conducted. Most of the heavy metals (Cr, Cu, Fe, Mn, Ni, and Zn) were found in the untreated effluents of steel-based factories. Heavy metals of Cr, Fe, Mn, Ni, and Zn in the untreated effluent at Factory C have highest concentrations compared with other factories and exceeded the permissible limit of Standard B, EQA 1974. However, the results also showed that the effluents treatment process at Factory A, Factory B, and Factory C was effective in reducing the effluent parameters' concentration to the Standard B permissible limits except for some parameters (Fe, Mn, and Ni) at the Factory C.

References

1. Beh CL, Chuah T, Nourouzi MN, Choong TS (2012) Removal of heavy metals from steel making waste water by using electric arc furnace slag. E-J Chem 9(4):2557–2564
2. Gu Y, Xu J, Keller Aa, Yuan D, Li Y, Zhang B, Li F (2015) Calculation of water footprint of the iron and steel industry: a case study in Eastern China. J Clean Prod 92:274–281
3. Sinha SK, Sinha VK, Pandey SK, Tiwari A (2014) A study on the waste water treatment technology for steel industry: recycle and reuse. Am J Eng Res 3(4):309–315
4. Rajeswari TR, Sailaja N (2014) Impact of heavy metals on the environment pollution. J Chem Pharm Sci 3:175–181
5. Kurniawan TA, Chan GYS, Lo W-H, Babel S (2006) Physico–chemical treatment techniques for wastewater laden with heavy metals. Chem Eng J 118(1–2):83–98

6. Singh J, Kalamdhad AS (2011) Effects of heavy metals on soil, plants, human health and aquatic life. Int J Res Chem Environ 1(2):15–21
7. Elkady AA, Sweet ST, Wade TL, Klein AG (2015) Distribution and assessment of heavy metals in the aquatic environment of Lake Manzala, Egypt. Ecol Ind 58:445–457. http://doi.org/10.1016/j.ecolind.2015.05.029
8. Fu F, Wang Q (2011) Removal of heavy metal ions from wastewaters: a review. J Environ Manage 92(3):407–418
9. Willscher S, Mirgorodsky D, Jablonski L, Ollivier D, Merten D, Büchel G, Werner P (2012) Field scale phytoremediation experiments on a heavy metal and uranium contaminated site, and further utilization of the plant residues. Hydrometallurgy 131:46–53
10. Sarojam P (2010) Analysis of Trace Metals in Surface and Bottled Water with the Optima 7300 DV ICP-OES, Perkin Elmer, Inc.
11. Department of Environment (1979) Environmental Quality Act 1974, (Environmental Quality (Sewage and Industrial Effluents) Regulation, Malaysia)
12. Doushanov DL Control of pollution in the iron and steel industry. Encyclopedia of Life Support Systems (Vol. III)
13. Gurzau ES, Neagu C, Gurzau AE (2003) Essential metals—case study on iron. Ecotoxicol Environ Saf 56(1):190–200
14. WHO (2003) Iron in drinking-water. Background document for preparation of WHO Guidelines for drinking-water quality. World Health Organization, Geneva. (WHO/SDE/WSH/03.04/8)
15. Levy BS, Nassetta WJ (2003) Neurologic effects of manganese in humans: a review. Int J Occup Environ Health 9(2):153–163

Adaptation of NoV LAMP Primers by PCR for Highly Sensitive Detection of Noroviruses in Water

**Dzulaikha Khairuddin, Marfiah Ab. Wahid,
Nurul Yuziana Mohd Yusof and Jan Maizatulriah Jani**

Abstract A fast and highly sensitive detection of noroviruses was established by Reverse Transcriptase PCR amplification using primers adapted from loop-mediated isothermal amplification (LAMP) of noroviruses (RT-L-NoV PCR amplification). The amplification was carried out in 30-min early incubation in 50 °C for reverse transcription activity and further 35 PCR short cycles for total finishing time within 60 min with no cross-reactivity with other common environmental species and strains. The LOD of this method was $10^{-15} \times 100$ ng/ulor 1zg/ul of pIDTSMART-NoV gene per reaction which is reported to be the highest sensitivity conventional PCR-based detection method for noroviruses. These early findings give hope for a potentially useful RT-L-NoV PCR amplification assay for a highly sensitive detection of NoV genomes especially in diluted concentration sample like water.

Keywords Noroviruses · PCR · Water contamination

1 Introduction

In the current advances in technology for water and wastewater treatment, water-borne diseases are still a public health and socio-economic problem in both developed and developing countries. Every year, about ~ 2.2 million deaths were reported by World Health Organization (WHO) related to unsafe water, sanitation, and hygiene, and sadly, millions of people are suffering from multiple episodes of non-fatal diarrhea [1]. Noroviruses (NoVs) are the agent of foodborne and water-borne illnesses that raised concern of healthcare professionals and consumers

D. Khairuddin
Malaysia Genome Institute, Jalan Bangi, 43000 Kajang, Selangor, Malaysia

N.Y.M. Yusof
Universiti Kebangsaan Malaysia, 43650 Bangi, Selangor, Malaysia

D. Khairuddin (✉) · M.Ab.Wahid · J.M. Jani
Universiti Teknologi MARA, 40450 Shah Alam, Selangor, Malaysia
e-mail: dzulaikha.k@gmail.com

worldwide. The primary route of NoV transmission is through the fecal–oral route [2]. Their ability producing extensive outbreaks of gastroenteritis attracts media attention around the world. About 58 % of domestically acquired waterborne/foodborne illnesses, 26 % of hospitalizations, and 11 % deaths are attributable to noroviruses in USA [3]. In developing countries, where diarrhea is a leading cause of death in young children, relatively little is known about the etiological role played by NoVs, but estimates indicating that 11.1 million hospitalizations and almost 220,000 deaths occur among children <5 years old each year in such countries have been published recently [4]. The complete scope of waterborne diseases is hard to tackle; however, building capacity to detect, control, and prevent them is an urgent matter especially for a country like Malaysia which has frequent raining and flood seasons. Several studies have shown that norovirus GII was the dominant genotype in watery environment, with the highest concentration among the target enteric viruses. Norovirus GII was also shown to be the most prevalent in environmental, recreational, and bathing waters worldwide: 72 % of surface water in Singapore [5]; 83 % of samples in river water, Spain [6]; 55 % in river water, South Korea [7]; and 63 % in river water, Japan [8]. This statistical prevalence of noroviruses in environment rises the urgency on these studies since noroviruses are now being identified as one of the common causes of diarrhea and still under reported in Malaysia [9]. Although NoVs were frequently associated with the winter season and "remarkably stereotyped as winter vomiting disease" in the temperate zone countries [10], several studies in tropical and subtropical countries showed that NoV infections are associated with the rainy season. Study performed in Ho Chi Minh City suggested that NoVs prevailed at the end of the rainy season and the first half of the dry season [11]. While findings by other study in Thailand [12] Dhaka, and Bangladesh revealed the peak of the NoV infection is during the rainy season [13]. Another study performed in Nicaragua, a tropical climate country in Central America, showed that the highest NoV infections prevailed during the beginning of the rainy seasons [14]. Another study performed in Nicaragua suggested the rainy season as the NoV season [15]. As a tropical country with heavy rainy season every year, Malaysia has high risk in the emerging of NoVs as a cause of sporadic diarrhea in children and the potential of this virus to affect populations lacking proper sanitary conditions especially during flood season. Thus, this detection method would be a basic coverage for early detection and prevention of NoV outbreak. The most widely adopted methods for detection of viruses in water in amplification procedures exploit the polymerase chain reaction (PCR) based on polymerase activity for primer-directed target amplification. The success of PCR amplification is related to its simplicity and cost-effective and has highly efficient exponential process. With the current development in laboratory technology in Malaysia, PCR machine is one of the important equipments available in most laboratories. This progress has encouraged the development of molecular detection method using PCR technology to be adopted in many laboratories. Loop-mediated isothermal amplification (LAMP) is the most currently molecular detection method [16] and has considerable attraction. The method, which targeting 4–6 specific sequences using 4–6 pairs of primers, gives a highly specific and sensitive

detection. The both outer primers designed based on LAMP targeting sequences are exploited to be used as primers for common PCR. Therefore, the objective of this study was to demonstrate norovirus detection by PCR using primers adapted from norovirus LAMP method.

2 Materials and Methods

2.1 NoV (Partial Length) Plasmid Construction as NoV Surrogates

The plasmid designed as synthetic gene in plasmid pIDTSMART-NoV gene (Integrated DNA Technology, USA) contains the target sequences for norovirus detection. The target norovirus sequence in pIDTSMART-NoV plasmid was first amplified with forward primer: 5'-AGGGTGCGCT CCATAGTATT-3' and reverse primer: 5'-GACCCATA CAATTCATGT-3' and inserted into pGEM-T Easy Vector System I (Promega, WI, USA). After selection, plasmid containing the target sequence was treated through linearization using *Spe I* DNA endonuclease (New England Biolab, USA) and then transcribed by using the Ribo-MAXTM Large Scale RNA Production System-T7 (Promega, Madison, USA). The resulting product was purified with the QIAampViral RNA Mini Kit (Qiagen, Hilden, Germany) and serially tenfold diluted for further usage.

2.2 Primer Design

The primers were designed based on the loop isothermal amplification primer (LAMP) adopted from Luo et al. [9] based on the most conserved region of 400 complete and partial RNA-dependent RNA polymerase and the capsid protein gene sequences of NoV GII alignment available in GenBank database. The primers were designed using Software Primer Explorer 4.0 (http://primerexplorer.jp/e/) and produced six primers based on LAMP assay design; however, only the outer primers F3 (5'-GTGGTATGGATTTTTACGTGCC-3') and B3 (5'-GACAACGGGCTC-CAAAGC-3') were used for RT-L-NoV PCR amplification modification.

2.3 RT-L-NoV PCR Optimization

The reverse transcription was first performed in 20 ul of a mixture containing 50 pmol of random nonamer, 20 U of RNase inhibitor (TOYOBO, Osaka, Japan), 100 U of reverse transcriptase (ReverTra Ace; TOYOBO), 2.5 mM concentrations of each deoxynucleoside triphosphate, and 9.5 ul of RNA extract. The RT condition

was 50 °C incubation for 30 min. The RT-L-NoV PCR amplification was optimized based on primer concentrations, annealing temperature (52–59 °C), and incubation time. The L-NoV PCR amplifications were performed in 10 ul reaction containing 10 × GoTaq PCR buffer (Promega, USA), 2 mM dNTPs (New England Biolab, USA), 40 mM MgCl$_2$ (Promega, USA), 0.1U GoTaq DNA polymerase (Promega, USA), 10 pmol/ul F3 and B3 primers (Integrated DNA Technology, USA), and norovirus surrogates (Transcribed RNA) 3ul. The program for RT-L-NoV PCR (Bio-Rad, California, USA) initial denaturation at 95 °C for 2 min, followed by 35 cycles of denaturation at 95 °C for 15 s, annealing at (52–59 °C)for 20 s, and elongation at 72 °C for 30 s, and then final elongation for 2 min at 72 °C. The PCR products were run in 2 % agarose gel and stained using the SYBR Safe (Bio-Rad, California, USA).

2.4 Primers Specificity Test

The primer specificity was validated using 15 commons environmental species: *Burkholderia cepacia*, *B. thailandensis*, *B. pseudomallei, Bacillus subtilis, B. macerans, B. circulans, B. megaterium, Staphylooccus sp., S.epiderminis, S. heamolyticus, E. coli* BL21, *E. coli* Nova Blue, *E. coli* Tuner, *E. coli* DH5α, and *Shinella granuli*. All of these species and strains were run in optimized RT-L-NoV PCR amplification condition concurrently with positive control RT-L-NoV PCR amplification of pIDTSMART-NoV and negative control (sterile dH$_2$O) as DNA template replacement. All PCR products were run in 2 % agarose gel and stained using SYBRSafe (Bio-Rad, California, USA).

2.5 Primers Sensitivity Test

The sensitivity of primers to amplify target region was determined by defining the limit of detection (LOD) of optimized RT-L-NoV PCR amplification on tenfold serial dilution of norovirus synthetic gene. Concentration of plasmid pIDTSMART-NoV was verified using Nanodrop1000 spectrophotometer (Thermo Fischer Scientific, MA, USA) to get starting concentration of 100 ng/ul. The 100 ng/ul of pIDTSMART-NoV was further serially tenfold diluted using sterile distilled water until final dilution of 100 ng/ul × 10^{-18}. One microliter of each dilution was taken as DNA template for RT-L-NoV PCR amplification sensitivity test. The diluted templates were tested in triplicate, and the lowest concentration of genome concentration was taken as the limit when all of the triplicate diluted templates were positive. The RT-L-NoV PCR amplification product was run in 2 % agarose gel and stained using SYBR Safe (Bio-Rad, USA).

3   Results

Several PCR-based methods for detection of noroviruses have been reported in the last decade. This study assessed the relative performance of different primer sets developed from LAMP for the detection of norovirus surrogates using PCR techniques.

3.1   Optimum RT-L-NoV PCR Amplifications

The best annealing temperature for optimum amplification was 55.1 °C using the above-mentioned RT-L-NoV PCR condition with estimated finishing time of 1 h. This rapidity in PCR detection of noroviruses was one of the fastest methods where the available methods were estimated to finish within more than two hours. The expected size of PCR product appeared in the agarose gel is 218 bp.

3.2   Specificity Test of RT-L-NoV PCR Amplification

We tested the specificities of the PCR amplifications using laboratory strains of 15 common environmental species. None of these species and strains tested by RT-L-NoV PCR amplification showed positive amplification. The results are illustrated in Fig. 1.

Fig. 1 Specificity test of RT-L-NoV PCR amplification. Only positive control reaction band of 218 bp appeared in the +ve control reaction using transcribed RNA and showed –ve results (no amplification) in the other reaction. Lane: M, 1-kb DNA marker; +ve, positive control reaction; 1, *Burkholderia cepacia;* 2, *B. thailandensis;* 3, *B.pseudomallei;* 4, *Bacillus subtilis;* 5, *B. macerans*; 6, *B.circulans;* 7, *B.megaterium;* 8, *Staphylooccus sp.;* 9, *S.epiderminis;* 10, *S. heamolyticus;* 11, *Shinella granuli;* 12, *E. coli* BL21; 13, *E. coli* Nova Blue; 14, *E. coli* Tuner; and 15, *E. Coli* DH5a, −ve, negative control
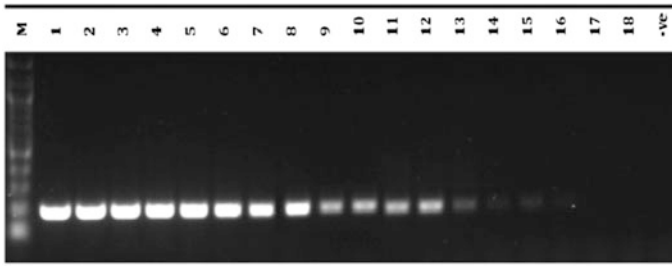
Fig. 2 Sensitivity test of RT-L-NoV PCR amplification. Lowest of detection (LOD) test of RT-L-NoV PCR amplification was $10^{-15} \times 100$ ng/ul equivalent to 1zg/ul. Lane: M, 1 kb DNA marker; 1, $10^{-1} \times 100$ ng/ul; 2, $10^{-2} \times 100$ ng/ul; 3, $10^{-3} \times 100$ ng/ul; 4, $10^{-4} \times 100$ ng/ul; 5, $10^{-5} \times 100$ ng/ul; 6, $10^{-6} \times 100$ ng/ul; 7, $10^{-7} \times 100$ ng/ul; 8, $10^{-8} \times 100$ ng/ul; 9, $10^{-9} \times 100$ ng/ul; 10, $10^{-10} \times 100$ ng/ul; 11, $10^{-11} \times 100$ ng/ul; 12, $10^{-12} \times 100$ ng/ul; 13, $10^{-13} \times 100$ ng/ul; 14, $10^{-14} \times 100$ ng/ul; 15, $10^{-15} \times 100$ ng/ul; 16, $10^{-16} \times 100$ ng/ul; 17, $10^{-17} \times 100$ ng/ul; 18, $10^{-18} \times 100$ ng/ul; −ve, negative control reaction

3.3 Sensitivity Test of RT-L-NoV PCR Amplification

We tested the LOD of RT-L-NoV PCR amplification using tenfold dilution of norovirus synthetic gene. The results showed positive reaction up to $10^{-15} \times 100$ ng/ul of diluted plasmid pIDTSMART-NoV equivalent to 1zg/ul (Fig. 2).

4 Discussion

The establishment of simple, rapid, and reliable methods for detection of noroviruses in water and environment is a fundamental need for preventing acute gastroenteritis outbreaks.

Result presented in this study showed a faster PCR detection achieved by modification in primer adapted from loop-mediated isothermal amplification (LAMP). The LAMP primers designed using the Software Primer Explorer 4.0 (http://primerexplorer.jp/e/) gave advantage by producing hundreds of primer choices. The ability of the software to list all the internal factors for a better choice of primers gives great advantage for a very good primer for a higher efficiency of PCR amplification.

In previous study carried out by Luo et al. [17], these primers has been shown to have no cross-reactivity toward other viruses include the astroviruses, adenoviruses, sapovirus, and rotavirus tested in clinical specimens. Therefore in this study, the ability of these primers was tested to distinguish the noroviruses from the other environmental strains which might be a contaminant in the environment during sampling of water especially during raining and flood seasons.

The ability for the primers to detect to a very sensitive concentration of 1zg/ul of pIDTSMART-NoV is the lowest LOD for conventional PCR detection. The PCR became the method of interest for its reliability in detection and diagnostic method. Furthermore, current technology available in many suburban laboratory permits the application of PCR techniques to be applied for faster and accessible method in a very critical time.

We believed with the current trend of norovirus occurrence worldwide; noroviruses were not only a major causative agents of non-bacterial gastroenteritis in many countries in the temperate zone, but statistics recorded in Singapore showed 72 % availability of the noroviruses in surface water [3]. The prevalence of NoV in Thailand [12] and other tropical countries during and toward end of the rainy season [11, 13–15] urges a great caution to build a capacity to detect, control, and prevent this concern. Monitoring norovirus predominance in Malaysia is also important for updating and comparing global trends of noroviruses infection.

References

1. World Health Organisation, Tessa W, Peter S, Clarissa B, Mickey C, Elizabeth M (2009) Diarrhoea: why children are still dying and what can be done? The Lancet 375(9718):870–872
2. Rabenaeu HF, Sturner M, Buxbaum S, Walczok A, Preiser W, Doerr HW (2003) Laboratory diagnosis of norovirus: which method is the best? Intervirol 46:232–238
3. Scallan E, Hoekstra RM, Angulo FJ, Tauxe RV, Widdowson MA, Roy SL et al (2011) Foodborne illness acquired in the United States-major pathogens. Emerg Infect Dis 17:7–15
4. Patel MM, Widdowson MA, Glass RI, Akazawa K, Vinje J, Parashar UD (2008) Systematic literature review of role of noroviruses in sporadic gastroenteritis. Emerg Infect Dis 14: 1224–1231
5. Aw TG, Gin KYH, Oon LLE, Chen EX, Woo CH (2009) Prevalence and genotypes of human noroviruses in tropical urban surface waters and clinical samples in Singapore. Appl Environ Microbiol 75:4984–4992
6. Calgua B, Fumian T, Rusinol M, Rodriguez-Manzano J, Mbayed VA, Bofill-Mas S, Miagostovich M, Girones R (2013) Detection and quantification of classic and emerging viruses by skimmed-milk flocculation and PCR in river water from two geographical areas. Water Res 47:2797–2810
7. Lee C, Kim SJ (2008) The genetic diversity of human noroviruses detected in river water in Korea. Water Res 42:4477–4484
8. Kishida N, Morita H, Haramoto E, Asami M, Akiba M (2012) One-year weekly survey of noroviruses and enteric adenoviruses in the Tone River water in Tokyo metropolitan area, Japan. Water Res 46:2905–2910
9. Zuridah H, Sufiyan Hadi M, Teh LK, Zed Zakari AH (2011) Molecular characterization of norovirus from acute gastroenteritis patients in Malaysia. African J Microbiol Res 5(18): 2733–2736
10. Greer Amy L, Drews Steven J, Fisman David N (2009) Why "winter" vomiting disease? Seasonality, hydrology, and norovirus epidemiology in Toronto, Canada. EcoHealth 6(192–199):2009. doi:10.1007/s10393-009-0247-8

11. Hansman GS, Doan LTP, Kguyen TA, Okitsu S, Katayama K, Ogawa S, Natori K, Takeda N, Kato Y, Nishio O, Noda M, Ushijima H (2004) Detection of norovirus and sapovirus infection among children with gastroenteritis in Ho Chi Minh City, Vietnam. Arch Virol 149:1673–1688. doi:10.1007/s00705-004-0345-4

12. Kittigul L, Pombubpa K, Taweekate Y, Diraphat P, Sujirarat D, Khamrin P, Ushijima H (2010) Norovirus GII-4 2006b variant circulating in patients with acute gastroenteritis in Thailand During a 2006–2007 Study. J Med Virol 82:854–860

13. Dey SK, Nguyen TA, Phan TG, Nishio O, Salim AFM, Rahman M, Yagyu F, Okitsu S, Ushijima H (2007) Molecular and epidemiological trend of norovirus associated gastroenteritis in Dhaka City, Bangladesh. J Clin Virol 40:218–223

14. Bucardo F, Nordgren J, Carlsson B, Paniagua M, Lindgren P, Espinoza F, Svensson L (2008) Pediatric Norovirus diarrhea in Nicaragua. J Clin Microbiol 2573–2580

15. Bucardo F, Reyes Y, Svensson L, Nordgren J (2014) Predominance of norovirus and sapovirus in nicaragua after implementation of universal rotavirus vaccination. PLoS ONE. doi:10.1371/journal.pone.0098201

16. Notomi T, Okayama H, Masubuchi H, Yonekawa T, Watanabe K, Amino N (2000) Loop-mediated isothermal amplification of DNA. Nucleic Acids Res 28:E63

17. Luo J, Xu Z, Nie K, Ding X, Guan L, Wang J, Xian Y, Wu X, Ma X (2014) Visual detection of norovirus genogroup ii by reverse transcription loop-mediated isothermal amplification with hydroxynaphthol blue dye. Food Environ Virol 6:196–201

Detection of Polycyclic Aromatic Hydrocarbons (PAHs) in Municipal Wastewater Treatment Plant at Klang Valley

**Rosadibah Mohd-Towel, Amnorzahira Amir
and Suhaimi Abdul-Talib**

Abstract Two different types of wastewater treatments are explained in this chapter. All the six parameters were under the standards A and B compared to EQA 1974. However, it does not confirm that PAHs were treated and not exist in the effluent. The possibilities of a low-ring of polycyclic aromatic hydrocarbons (PAHs) exist in both municipal wastewater were analyzed using gas chromatography–mass spectrometry (GC-MS). The main PAHs exist are naphthalene, phenanthrene, and anthracene. 9,9′-Biphenanthrene, octacosahydro, phenanthrene, 4,5-dimethyl, anthracene, anthracene, 9-cyclohexyltetradecaydro, 2-ethyl, phenanthrene, 9-ethyl, phenanthrene, 9,10-bis (chloromethyl) were detected. Municipal wastewater sample B contained 9,9′-Biphenanthrene, octacosahydro, anthracene and phenanthrene, 4,5-dimethyl, 2(3H)-Naphthalenone and 1,8,9-trihydroxyanthracene. The sources of these compounds may come from tobacco smoke and ingestion of food contaminated with combustion products, dandruff shampoo, detergents, and mothballs. This toxic compound may cause skin irritation and lower body's system for fighting disease after both short- and long-term exposure. Wastewater that contains PAHs required an effective technology in order to completely remove in the system. This study also provides baseline assessment on the existence PAHs in the municipal wastewater treatment plan and possible activities that released PAHs into wastewater.

Keywords PAHs · Wastewater

R. Mohd-Towel (✉)
Faculty of Civil Engineering, University Teknologi MARA, Shah Alam, Selangor, Malaysia
e-mail: rosadibah7@gmail.com

A. Amir
Faculty of Civil Engineering, University Teknologi MARA, Institute for Infrastructure Engineering and Sustainable Management (IIESM), Shah Alam, Selangor, Malaysia
e-mail: amnorzahira@salam.uitm.edu.my

S. Abdul-Talib
Faculty of Civil Engineering, University Teknologi MARA, Canseleri Tuanku Syed Sirajuddin, Shah Alam, Selangor, Malaysia
e-mail: ecsuhaimi@salam.uitm.edu.my

1   Introduction

Polycyclic aromatic hydrocarbons (PAHs) consist of carbon–hydrogen bond to form one or more in benzene ring which reduce water solubility and volatility with increasing molecular weight. They are persistent pollutant formed from natural (e.g., volcano) and anthropogenic (e.g., industrial effluent) sources.

In recent years, studies on PAHs have been increasing because of high toxicity, and it can be harmful to human and animals [1]. Exposure of PAHs to human may cause carcinogenic and mutagenic effects (e.g., mutagenic effect to mice) [2]. Studies on PAHs reported that PAHs can be discovered in the form of liquid (water) [3], solid (soil or sand) [4], and air [5] at a long distance from their sources. Due to high hydrophobicity in water and stable structure, it was abundantly found in sediment and seawater, especially coastal area in Malaysia [6, 7].

However, there is limited study on PAHs in municipal wastewater and their sources. Therefore, this study was conducted to identify the existence of PAHs in municipal wastewater at Klang Valley. In this study, we collected two samples from two different sites municipal wastewater and compared the findings with the effluent standard from Environmental Quality Act (EQA) 1974. This study also identify the potential low-ring PAHs detected in both municipal wastewater. Understanding the source of PAHs is a crucial and suitable remediation method must be provided.

2   Materials and Methods

2.1   Sampling Collection and Preparation

Wastewater samples were collected at two different sites which have different activities. Municipal wastewater A was collected from College Mawar at University Teknologi MARA, Shah Alam. The source of this wastewater was from student hostels, Science and Technology tower, cafeteria, and surrounding office buildings. The municipal wastewater B was collected from the Klang Valley area, and the source of wastewater is from residential area, restaurants, office buildings, and commercial area (e.g., shopping mall and hotel).

All the samples were collected and transferred into the Duran scotch 500-mL bottle. The samples were kept in icebox at temperature 4 °C and delivered to laboratory for further analysis.

2.2 Water Quality Parameter

Six parameters were used to measure the quality of wastewater treatments A and B: measurement of pH, biochemical oxygen demand (BOD), chemical oxygen demand (COD), suspended solid (SS), oil and grease, and ammoniacal nitrogen (AN). PAHs was measured using Metrohm pH meter, Nessler Method (Method 8038), DR 2800 (HACH), and USEPA solid-phase extraction method 10300.

2.3 Polycyclic Aromatic Hydrocarbons Extraction

Wastewater samples were filtered prior to the sample extraction method using 0.45-μm-pore-sized filter and extracted using solid-phase extraction (SPE) by using Supelco Visiprep™ DL. 12-port Visiprep™ DL manifold was connected with electric aspirator to achieve a vacuum condition. 6-mL Supelclean™ Envi™-18 SPE tubes (0.5 g) were connected to separate low-ring PAHs from wastewater samples. Four steps were followed to extract PAHs from wastewater samples which are condition, sample loading, washing, and elution. In the condition step, 2 mL methanol (Friendemann Schmidt) was used to reactive the surface of SPE membrane tubes. It was followed by 3 mL sample loading. SPE tubes were washed with 4 mL methanol. 9 mL acetonitrile HPLC grade (Friendemann Schmidt) was used for elution step. The elution was collected in the 10 mL vial before concentrating with a rotary evaporator.

2.4 Sample Concentrate

Samples were transferred to rotary flask and attached to the adjust-lever rotary evaporator model (BUCHI, Switzerland). Acetonitrile (226 mbar) was gently removed from the sample by evaporation from heating bath at 55 °C. The remaining 1 mL of sample was transferred to 2 mL amber vial for the gas chromatograpy mass spectrometry (GC-MS) analysis.

2.5 Gas Chromatography–Mass Spectrometry (GC-MS) Analysis

Clarus 600 GC-MS was used to analyze the concentration of PAHs in the samples. The sample was injected into SLB™-5-MS-fused silica capillary column (30 × 0.25 mm × 0.25 μm) (Sigma-Aldrich) using helium as the carrier gas at constant rate 1.0 ml/min. The samples were analyzed with the full scan for 36-min.

Table 1 The effluent concentration compared to the EQA 1974

Parameter	Effluent standard		Municipal wastewater	Municipal wastewater
	A	B	A	B
BOD	20	50	55.5	15.4
COD	120	200	458	207
Suspended solid	50	100	40	30
pH	6.0–9.0	5.5–9.0	6.57	6.71
Oil and grease	N.d[a]	10	0.033	0.0242
AN	20	50	0.75	1.06

[a]N.d. (Not detectable)

3 Results and Discussion

Table 1 shows a comparison of results between water quality from municipal treatment plant A and B and effluent standard provided by Environmental Quality Act 1974.

BOD results for wastewater treatment plant A and B were 55.5 and 15.4 mg/L, respectively. Result of BOD from municipal wastewater treatment plant A was significantly higher compared to effluent standards A and B, while BOD from municipal wastewater treatment plant B was significantly lower compared to the effluent standards. This result suggests that effluent from STP probably contains a high concentration of microorganism compared to effluent from a municipal wastewater treatment plant B. A previous study has reported that low BOD in effluent probably due to wash down by microorganisms in the effluent during the treatment process [8].

COD results in both samples were over the limit of effluent standard. Results of municipal wastewater treatment plant A was 458 mg/L and for municipal wastewater treatment plant B was 207 mg/L. This results might be due to the treatment used in this site. The anaerobic treatment is preferable to treat high incoming COD [9]; however, both treatment plants were operated using aerobic treatment method.

Concentration of suspended solid was lower compared to guideline from EQA standard A and B where 40 and 30 mg/L for municipal treatment A and B, respectively. This might happen due to the efficiency of settling time for both treatment plants. This is because both treatment plants used activated sludge. Similar results showed that the aeration tanks make the treatment efficient to remove the suspended solid where it will settle down to the bottom tank in the clarifier [8].

The pH values 6.57 and 6.71 are detected in municipal wastewater treatments A and B, respectively. Both readings are in the range of limit standards A and B. pH result plays an important role in the microorganism base treatment, especially in Malaysia.

Table 2 The PAHs detected in the municipal wastewater

Site/structural suggestions	
Municipal wastewater treatment plant A	Municipal wastewater treatment plant B
9,9′-Biphenanthrene, octacosahydro	9,9′-Biphenanthrene, octacosahydro
Phenanthrene, 4,5-dimethyl	Anthracene
Anthracene	Phenanthrene, 4,5-dimethyl
Anthracene, 9-cyclohexyltetradecaydro	2(3H)-Naphthalenone
Anthracene, 2-ethyl	1,8,9-trihydroxyanthracene
Phenanthrene, 9-ethyl	Phenanthrene, 9,10-bis(chloromethyl)

From both samples, concentration of oil and grease was very low, that is 0.033 and 0.0242, respectively. This results indicates that the primary treatment from both sites was slightly efficient due to the low concentration of oil and grease detected. Removal of oil and grease at the primary stage was very important because it will disturb the subsequent treatment.

Ammoniacal nitrogen results show significantly lower in both municipal wastewaters. 0.75 and 1.06 mg/L from wastewater treatments A and B, respectively. These results indicate that the treatment has efficiency to remove the ammoniacal nitrogen. This is proved by [10] where ammoniacal nitrogen concentration was low due to activated sludge treatment base in wastewater treatment. Ammoniacal nitrogen gives impacts to the environment due to nitrite and nitrate production which cause the nitrification to the receiving water body [10].

Table 2 shows the PAHs exist in the wastewater samples from municipal wastewater treatments A and B. Results of water quality in both samples were under the limit standard A and B however, this finding do not indicate that PAHs were completely removed in this samples. Therefore, PAHs were tested to determine the possibilities of existence of low-ring PAHs in the samples.

In the municipal wastewater A, 9,9′-Biphenanthrene, octacosahydro was detected. The sources of this compound might come from the fumes from the vehicle exhaust, coal, coal tar, and burning trash [11]. This results same as [12] where the activities are same. One this compound was inserted into human or animal body, it will extent and target to the fat tissue. A study has been reported laboratory animals have tumor when their food was contaminated with phenanthrene [12].

At the same time, phenanthrene, 4,5-dimethyl was also detected. This result shows that phenanthrene was a dominant compound detected in the wastewater. These results are similar reported from [13]. The sources of this compound are same as phenanthrene where the main compound is phenanthrene but combined with another compound.

Anthracene was detected in the municipal treatment plant A. This compound was also detected by [14] at the coastal sediment at Klang street. This result indicates that anthracene was a persistent compound found in the wastewater and also in the sediment. Anthracene is a common compound that mixed in dandruff shampoo, eczema and psoriasis remedies, detergents, and mothballs. In addition,

anthracene might be present in the food where the food was grown in the contaminated soil or air contains PAHs. In addition, cooking meat or food at high temperature using grilling or burning increases the amount of PAHs in the food [15]. However, the impact of PAHs specifically anthracene to the human is not reported, but harmful effects on skin, body fluids, and body's system for fighting disease after both short- and long-term exposure to animals were reported [15].

At the same retention time, anthracene, 9-cyclohexyltetradecaydro and anthracene, 2-ethyl were detected. These compounds are actually similar as anthracene but combine with another compound. The sources and impact of this compound were same as anthracene.

Phenanthrene, 9-ethyl and phenanthrene, 9,10-bis (chloromethyl) was also detected. This compound indicated that phenanthrene was connected to the other compounds. This result shows that phenanthrene has high possibilities to attach compounds to create another complex compound.

From the result of municipal wastewater sample B, 9,9′-Biphenanthrene, octacosahydro was detected. This compound indicates that two phenanthrene structures have combined to the other compounds. These results were similar reported from [16]. The results show that this compound was common in wastewater as in other countries.

Anthracene was detected in municipal wastewater B. The sources and impact of anthracene were same as above. Phenanthrene, 4,5-dimethyl was also detected. This compound indicates phenanthrene has been attached to the other. The sources and impact are same as phenanthrene.

2(3H)-Naphthalenone was detected in the sample. These results show that naphthalene exists in high concentration sample. This result is similar to [11] from urban wastewater. The sources of naphthalene might come from food and beverage (including additives and contaminants), fragrance/essential oil, bathroom deodorants, detergent, shampoo, and mothballs. The effect of naphthalene can cause damage to the skin, such as skin irritation, manifested as redness and swelling [15].

At the same time, 1,8,9-trihydroxyanthracene was also detected in the sample. This compound was detected as anthracene but attached with other compounds. Sources of this compound might come from tobacco smoke and ingestion of food contaminated with combustion products, dandruff shampoo, eczema and psoriasis remedies, detergents, mothballs, and heavy oils. The effect of this compound is same as anthracene as above-mentioned.

4   Conclusion

This study investigated the potential low-ring of PAHs detected in the municipal wastewater. The results for both wastewater samples were compared to EPA 1974 effluent standard. Most of the results were under the limit for standard A and B however, this finding does not indicate that PAHs were completely removed in the system. The quality of wastewater from both samples significantly affected by

human activities and intensive urbanization. Naphthalene, phenanthrene, and anthracene were the dominant compound detected. The existence of PAHs were due to various activities such as from tobacco smoke and ingestion of food contaminated with combustion products, dandruff shampoo, detergents, and mothballs. The effect of these PAHs can be seen as skin irritation, lower body's system for fighting disease after both short- and long-term exposure. The urgency of treatment of PAHs in the municipal wastewater is needed. This finding could also provide basic knowledge on the predominant low-ring PAHs exist in the selected municipal wastewater treatment plan.

References

1. Michael JC, Tisha KH, Henry T (2005) Chapter 1 The utility of zebrafish as a model for toxicological research. Environ Toxicol 6:3–41
2. Claxton LD, Houk VS, Hughes TJ (1998) Genotoxicity of industrial wastes and effluents. Mutat Res 410(3):237–243
3. Chen B, Xuan X, Zhu L, Wang J, Gao Y, Yang K, Shen X, Lou B (2004) Distributions of polycyclic aromatic hydrocarbons in surface waters, sediments and soils of Hangzhou City, China. Water Res 38(16):3558–3568
4. Sany BT, Salleh A, Hajjartabar M, Tehrani GM (2012) Ecological risk assessment of poly aromatic hydrocarbons in the North Port, Malaysia, vol 33, pp 130–135
5. Jamhari AA, Sahani M, Latif MT, Chan KM, Tan HS, Khan MF, Mohd Tahir N (2014) Concentration and source identification of polycyclic aromatic hydrocarbons (PAHs) in PM10 of urban, industrial and semi-urban areas in Malaysia. Atmos Environ 86:16–27
6. Nasher E, Heng LY, Zakaria Z, Surif S (2013) Concentrations and sources of polycyclic aromatic hydrocarbons in the seawater around Langkawi Island, Malaysia. J. Chem. 2013:1–10
7. Sakari M, Zakaria MP, Mohamed CAR, Lajis NH, Chandru K, Bahry PS, Shahbazi A, Anita S (2010) Historical profiles of polycyclic aromatic hydrocarbons (PAHs), sources and origins in dated sediment cores from Port Klang, Straits of Malacca, Malaysia, vol 34, no 1, pp 140–155
8. Department of Environmental Quality (2014) Activated sludge process control training manual for wastewater
9. Chan YJ, Chong MF, Law CL, Hassell DG (2009) A review on anaerobic-aerobic treatment of industrial and municipal wastewater. Chem Eng J 155(1–2):1–18
10. AWWA (2002) Nitrification, EPA United States. Environ Prot
11. Rule KL, Comber SDW, Ross D, Thornton a, Makropoulos C, Rautiu R (2006) Sources of priority substances entering an urban wastewater catchment-trace organic chemicals. Chemosphere 63(4):581–591
12. Barron MG, Heintz R, Rice SD (2004) Relative potency of PAHs and heterocycles as aryl hydrocarbon receptor agonists in fish. Mar Environ Res 58(2–5):95–100
13. Zhong Y, Luan T, Lin L, Liu H, Tam NFY (2011) Production of metabolites in the biodegradation of phenanthrene, fluoranthene and pyrene by the mixed culture of Mycobacterium sp. and Sphingomonas sp. Bioresour Technol 102(3):2965–2972

14. Tavakoly Sany SB, Hashim R, Salleh A, Rezayi M, Mehdinia A, Safari O (2014) Polycyclic aromatic hydrocarbons in coastal sediment of klang strait, malaysia: distribution pattern, risk assessment and sources. PLoS ONE 9(4):e94907
15. Mumtaz MM, George JD (1996) Toxicological profile for polycyclic aromatic hydrocarbons. U.S. Department of Health and Human Services, August, pp 1–487
16. USEPA (1980) Sources of toxic compounds in household wastewater

Assessment of Chlorine Contact Tank Based on Tank Configuration and Baffle Factor

A. Yahya, M. Ab Wahid and W.K. Lee

Abstract Disinfection is the most important process in water treatment in the concern of water quality and quantity. Hydraulic efficiency is a vital component in evaluating the disinfection capability of a contact system. The objective of this study is to determine free residual chlorine, fluoride, and chloride in chlorine contact tank (CCT) and to evaluate disinfection efficiency. Disinfection efficiency of a WTP could be determined when $CT_{achieved} \geq CT_{required}$ which demonstrates that sufficient disinfection has been met and vice versa. Based on detection test result obtained from the in situ test, all five WTPs have complied with the maximum allowable standards for free residual chlorine as outlined by National Standard for Drinking Water Quality. As the CT rules ($CT_{achieved} \geq CT_{required}$) have been complied, the disinfection process for four WTPs was found efficient whereby the disinfection process in the CCTs was sufficient. The information obtained on disinfection ability of the existing water treatment plant would be useful for design improvement and cost-effectiveness in water treatment.

Keywords Disinfection · Hydraulic efficiency · Chlorine contact tank · Free residual chlorine · Disinfection efficiency

A. Yahya (✉) · M. Ab Wahid · W.K. Lee
Faculty of Civil Engineering, Universiti Teknologi Mara, 40450 Shah Alam, Selangor, Malaysia
e-mail: ddilayahya@gmail.com

M. Ab Wahid
e-mail: marfi851@salam.uitm.edu.my

W.K. Lee
e-mail: leewei994@salam.uitm.edu.my

1   Introduction

Disinfection is the most important process in water treatment when concerning about the water quality and quantity involved in the process. By improving the hydraulic efficiency of the systems, smaller dose of the disinfectant is allowed to be used, thus reducing the formation of the potential carcinogens [1]. In recent years, there are several studies and works have been reported and compiled as part of an ongoing process to determine the efficiency of disinfection system in the water treatment plant and complying the World Health Organization (WHO) standard and operation. The purpose of this study is to further analyse the chlorine contact tank (CCT) of different configuration and evaluate the disinfection efficiency for future improvement in regard to the contact systems.

Based on the WHO, the CCT is required to be equipped with a unit process of disinfection. Chlorine disinfection requires 15–30 min contact time (CT) to ensure that adequate pathogen is killed. Traditional CCT is basically designed to minimize short circuiting by using high length-to-width ratios or serpentine flow paths. However, these design practices do not always produce ideal plug flow conditions given that the contact tank configuration does not alone control chlorine mixing, distribution, and CT. Hydraulic efficiency is an important factor to determine disinfection ability. However, limitation in the parameters is used to estimate hydraulic efficiency, i.e. residence time distribution (RTD) curve and hydraulic efficiency indicators (HEIs) resulting in the black box analysis.

Even though the water quality produced and distributed to the consumers by the plants were complied with the National Standard for Drinking Water Quality, Ministry of Health, Malaysia, the disinfection efficiencies and compliance of the treatment plants were crucial for future improvement. Therefore, investigation on current scenarios of WTP design in Malaysia is necessary in order to alleviate disinfection ability and further improve the water quality.

2   Water Treatment Plant in Malaysia

Generally, most of water treatment plants in Malaysia utilize conventional water treatment system that consists of processes such as aeration, coagulation, flocculation (involves aluminium-based chemicals known as alum), sedimentation, filtration, chlorination, fluoridation, and pH correction (involves lime). In Malaysia, there is one water service company that manages the treatment and distribution of water to public. As for the state of Melaka, SAMB is currently operating with a full capacity of nine water treatment plants. The public water supply of Melaka began over a century ago when piped water supply for the Melaka town was constructed by the Corps of Royal Engineers around 1898. An impounding reservoir was built at Ayer Keroh, located about seven miles from the town, and the water was piped only to a limited reticulation serving mainly the centre portion of Melaka town.

Later, new reservoirs and treatment plants were built in order to cater the ever-increasing demands in line with the development growth [2].

Local guidelines in water treatment plant design were available in Malaysia since 1989 and further developed in order to meet requirements for the improvement in line with the growth of technologies. The "JKR Design Criteria and Standards for Water Supply Systems" in three volumes were first published by the Office of the Director of Water Supplies, JKR Headquarters, Kuala Lumpur, in early 1989. Later in 1994, Malaysian Water Association (MWA) published a manual with title "MWA Design Guidelines for Water Supply Systems" based on an adaptation of the JKR Design Criteria and Standards for Water Supply Systems. However, the proposed guideline is still in the review process and has yet to be published.

3 Chlorine Contact Tank

Chlorine disinfection process requires 15–30 min CT to provide adequate period as to destroy any pathogen in the water. Reuse applications typically require additional time. Dechlorination requires only 30 s of mixing and CT to quench residual chlorine. Traditional CCT is designed to minimize as well as shorten circuiting by using high length-to-width ratios or serpentine flow paths. These design practices, however, do not always produce ideal plug flow conditions, and the contact tank configuration does not alone control chlorine mixing, distribution, and CT. Distribution chambers and feed channels should also be taken into consideration when trying to comprehend the total performance of a chlorination system.

4 Disinfection Efficiency Parameters

Disinfection efficiency parameters are consisting of baffling factors, tank configuration, and CT values. Based on previous studies, the inclusion of baffles can significantly improve the hydraulic performance of a contact tank. Complex simulation using computer software, i.e. CFD simulations were performed based on different baffle options to establish the relation of hydraulic efficiency with a number of baffles [3]. Figure 1 shows the relation of Morrill Index with a number of baffles.

Baffling is used in many contact tanks (disinfection segments) to increase the CT of the disinfectant with the water. USEPA provides guidelines developed from tracer studies for determining baffling factors based on the baffling description. The baffling factor is taken as the ratio of T/TDT. A contact system (or more precisely a disinfection segment) is any tank or pipe system used to achieve CT between a detention time to a more realistic value of the "CT" of the contact system. Baffling factors are listed in Table 1 in order to ensure that appropriate baffling factors are assigned.
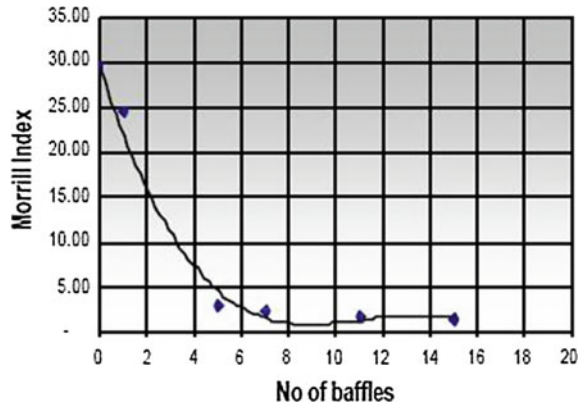
Fig. 1 Number of baffles versus Morrill Index

Table 1 Baffling factors [4]

Baffling condition	Baffling factor	Baffling description
Unbuffled (mixed flow)	0.1	None, agitated basin, very low length-to-width ratio, high inlet and outlet velocities
Poor	0.3	Single or multiple unbaffled inlets and outlets, no intra-basins baffles
Average	0.5	Baffled inlet or outlet with some intra-basin baffles
Superior	0.7	Perforated inlet baffle, serpentine, or perforated intra-basin baffles, outlet weir, or perforated launders
Perfect (plug flow)	1.0	Very high length-to-width ratio (pipeline flow), perforated inlet, outlet, and intra-basin

A reliable and accurate method to determine the BF of a disinfection system is through the use of a tracer study. During a tracer study, a tracer chemical is injected into the influent [4]. A resident time distribution (RTD) curve is then generated by plotting the concentration of tracer at the chlorine contact system outlet as a function of time. Figure 2 shows an example of an RTD curve of a step-dose tracer input for a hypothetical contact system.

An example for the flocculation basin which design with baffle is shown in Fig. 3. Figure 3 shows two stages of flocculation basin with (A) perforated inlet wall followed by horizontal flocculation paddles. Then (B), water passes from the first chamber into the second chamber through horizontal slats. Horizontal paddles are again employed on a second chamber. Ozone, chlorine, or chlorine dioxide applied prior to this point for disinfection credit would certainly benefit from a baffling factor of 0.7 or higher for this basin design [5].

Application of baffle for another unit process is visualized in Fig. 4 that shows a rectangular clarifier with perforated inlet baffle wall. The design is intended to

Fig. 2 Example of a residence time distribution (RTD) curve at the outlet of a hypothetical disinfection segment with the tracer injected as a step dose. Note time T has been normalized by TDT
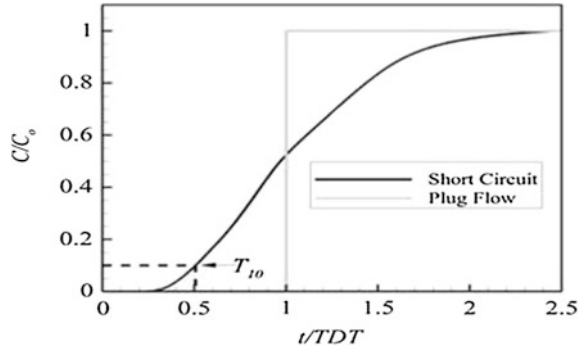
Fig. 3 Two-stage flocculation basin (BF = 0.7) [5]

uniformly distribute the flocculated water across the basin to provide uniform settling time and to minimize short circuiting. Sludge collection pipes (white colour) are visible at the bottom of perforated inlet wall as shown in the left of Fig. 4. On the right of Fig. 4, the jet stream (red arrows) of the flocculated water can be seen entering the basin through the holes. This design would be credited with a baffling factor of 0.7 or better for the purposes of calculation of CT [5].

Fig. 4 Clarifier with perforated inlet baffle wall [5]

5 Contact Time (CT) Values

CT values are defined as disinfectant concentration (C) times theoretical retention time (T). The CT rule was adapted as a more representative value of the actual contact time. More representative CT can be selected from T_{10} value. A very short T_{10} value occurred at a tank with inactivation based on the CT_{10} value. However, by increasing the T_{10} value, the hydraulic efficiency of the contact tank could be modified. Although the actual CT was represented by the T_{10} value, the disadvantage is that the values can only be determined after the tank was built [3].

There were many ways in determining the CT. Tracer tests can be conducted to confirm plug flow for adequate disinfection, and compliance of a disinfection process can be evaluated by the CT method to Interim Enhanced Surface Water Treatment Rule (IESWTR). IESWTR specifies that CT should be the minimum detention time experienced by 90 % of the water passing through the disinfection basin (T_{10}) [6]. If the tracer studies are not available and expensive to be conducted, the CT of CCT may be estimated using the hydraulic characteristics of the tank and baffling factors. However, T should be determined by conducting a tracer study wherever possible. In a simple pipe flow or an ideal tubular (plug flow) reactor, the CT can be calculated as simply as poor hydraulics and a short CT. A tank with a low T_{10} value should therefore be operated at an elevated disinfectant dose rate in order to maintain the same level of

$$T = V/Q$$

where V is the volume of the pipe section and Q is the volumetric flow rate of water in the pipe [6].

CT is also be determined by acceptable limits or minimum requirement sets by the state agency whereby the contact time (CT) values are required based on CT values for 3-log inactivation of Giardia cysts by free chlorine [7] as shown in Table 2.

Table 2 CT values for 3-log inactivation of Giardia cysts by free chlorine [7]

Chlorine concentration (mg/L)	Temperature = 25 °C						
	pH						
	<6.0	6.5	7.0	7.5	8.0	8.5	9.0
	3-log inactivation of Giardia (min mg/L)						
<0.4	24	29	35	42	50	59	70
0.6	25	30	36	43	51	61	73
0.8	26	31	37	44	53	63	75
1.0	26	31	37	45	54	65	78
1.2	27	32	38	46	55	67	80
1.4	27	33	39	47	57	69	82
1.6	28	33	40	48	58	70	84
1.8	29	34	41	49	60	72	86
2.0	29	35	41	50	61	74	88
2.2	30	35	42	51	62	75	90
2.4	30	36	43	52	63	77	92
2.6	31	37	44	53	65	78	94
2.8	31	37	45	54	66	80	96
3.0	32	38	46	55	67	81	97

6 Detection Test for Free Residual Chlorine, Fluoride, and Chloride

Free residual chlorine, fluoride, and chloride detection test results were evaluated with the maximum acceptable value of National Standard for Drinking Water Quality by Ministry of Health (MOH) that obligated for compliance to all water companies in Malaysia. The standard maximum acceptable values are shown in Table 3.

For the purpose to carry out the detection test, five WTPs under the jurisdiction of SAMB which is located in Melaka were selected. Technical site visit and in situ test have been conducted to these 5 WTPs on 19 and 20 May 2015. In situ testings have been carried out at several water treatment plants, namely:

1. Bukit Sebukor Water Treatment Plant
2. Merlimau Water Treatment Plant

Table 3 Maximum acceptable value of National Standard for Drinking Water Quality by Ministry of Health [10]

Item	Parameters	Maximum acceptable value (mg/L)
1	Free residual chlorine	0.2–5.0
2	Fluoride	0.4–0.6
3	Chloride	250

Table 4 Chlorine contact tank configuration data

Item	WTP	Chlorine contact tank (CCT) dimension			CCT volume, V (m^3)
		Length, L (m)	Width, W (m)	Depth, D (m)	
1	Bukit Sebukor	20.75	15.95	4.50	1489
2	Merlimau	54.50	13.75	5.30	3972
3	Gadek	30.50	14.50	5.50	2432
4	Bertam I	38.58	14.00	5.50	2971
5	Bertam II	14.00	8.75	5.50	674
Item	WTP	CCT outlet pipe Ø (m)	Area of outlet pipe (m^2)	Peak velocity, V (m/s)	Peak flow, Q (m^3/s)
1	Bukit Sebukor	0.50	0.20	1.0	0.20
2	Merlimau	0.90	0.64	1.0	0.64
3	Gadek	0.70	0.38	1.0	0.38
4	Bertam I	0.90	0.64	1.0	0.64
5	Bertam II	0.85	0.57	1.0	0.57

3. Gadek Water Treatment Plant
4. Bertam 1 and II Water Treatment Plant

Free residual chlorine, fluoride, and chloride of treated water were determined by carrying out detection test at selected water treatment plants. The detection test was conducted at the CCT unit process. Evaluation of disinfection efficiency of the water treatment plant was carried out through the CT calculated based on results obtained from the detection test. Then, Calculated CT were analysed with minimum CT required in order to evaluate the efficiency of the disinfection process of the selected water treatment plant for future improvement. Based on the disinfection efficiency result, a conclusion will be made based on evaluation and analysis carried out.

Samples were generally taken at the dosing inlet, outlet of the CCT, and in between inlet and outlet. Minimum three samples were taken for analysis. Chlorine detection test was carried out in situ, while fluoride and chloride detection tests are carried out within 12 h after samples were taken. Based on CCT configuration data obtained from all five plants, the volume of the CCT and peak flow at CCT outlet were calculated and are summarized in Table 4.

The detection test was carried out by using Spectometer DR 2800 and the method referred is provided by the manufacturer which is HACH and calibrated by Arachem (M) Sdn Bhd. The method which is Method 8021, 8029, and 8113 were applied for free residual chlorine, fluoride, and chloride detection test, respectively.

7 Evaluation of Disinfection Efficiency

CT disinfection measures the effectiveness of a disinfection process. To inactivate viruses and bacteria, the minimum disinfection CT before reaching the first customer should be measured. Hence, actual CT values ($CT_{achieved}$) obtained from the results were evaluated based on minimum CT required ($CT_{required}$) for efficient disinfection as specified in Table 2. $CT_{achieved}$ was calculated by multiplying the free residual chlorine concentration (C) with the CT (T) as follows:

$$CT_{achieved} = \text{Concentration of Free Chlorine (C, mg/L)} \\ \times \text{contact time (T, Minutes)}$$

Based on Table 1, regarding to the analysis of contact tank configuration from all 5 WTPs and case studies by CBCL and Terry, the chosen baffling factor, BF = 0.3, adopted in this research study suited the baffle description. For the site-specific calculation, nominal detention time is calculated as follows [8]:

$$\text{Nominal Detention Time} = \frac{\text{Lowest Operating Volume (m}^3)}{\text{Peak Flow (m}^3/\text{min)}}$$

Therefore, the CT value was calculated as follows:

$$\text{Contact Time (CT), minutes} = \text{Nominal Detention Time } X \\ \text{Baffling Factor (BF)}$$

8 Results and Data Analysis

Based on the detection test result, CT values for each WTP were calculated and evaluated according to a minimum required CT in the evaluation of disinfection efficiency. As for the comparison with the MOH standard, average results for each parameter of all WTPs are considered and shown in Table 5. Generally, all five WTPs have complied with MOH standard for free residual chlorine and chloride whereby the test results for both parameters were within the range of limits set by the MOH. However, for fluoride, there was only one WTP that has complied with the MOH standard which is Gadek WTP. The average test result of fluoride for Merlimau WTP is 0.9 mg/L, exceeded the limits of 0.6 mg/L. Meanwhile, the average test results of fluoride for Bukit Sebukor and Bertam I and II were 0.2 and 0.3, respectively, which were lower than MOH standard 0.4 mg/L.

Based on detection test carried out, the direction of water flow in the CCT at accessible points from the inlet to an outlet can be determined based on the concentration of parameters obtained. Figures 5, 6, 7, and 8 illustrated the flow path of the water in the CCT. Generally, the concentration of tested parameters was found

Table 5 Compliance of parameters tested based on evaluation with National Standard for Drinking Water Quality

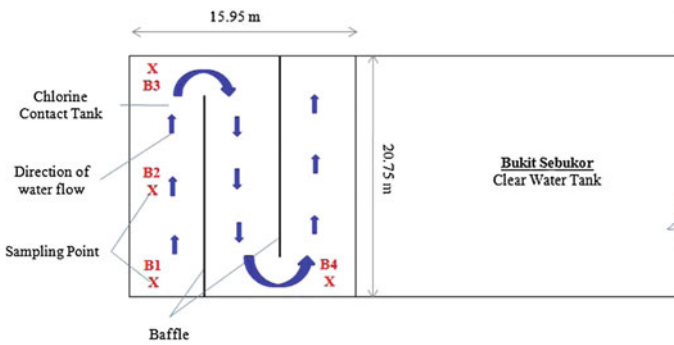| Item	Parameter	MOH standard	Average test result (mg/L)		
			Bukit Sebukor	Merlimau	Gadek
1	Free residual chlorine	0.2–5.0	2.08	1.76	2.68
2	Fluoride	0.4–0.6	0.2	0.9	0.4
3	Chloride	250	32.43	18.18	20.03
Item	Parameter	MOH standard	Average test result (mg/L)		
			Bertam I		Bertam II
1	Free residual chlorine	0.2–5.0	2.80		1.60
2	Fluoride	0.4–0.6	0.2		0.4
3	Chloride	250	25		38.7

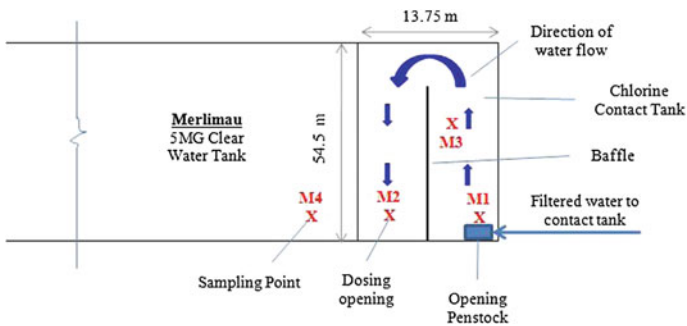**Fig. 5** Tank configuration of Bukit Sebukor WTP

Fig. 6 Tank configuration of Merlimau WTP

reduced along the pathways from the inlet to the outlet which showed that concentration of chlorine for disinfection is reduced due to the reaction to inactivate disease-causing organisms.
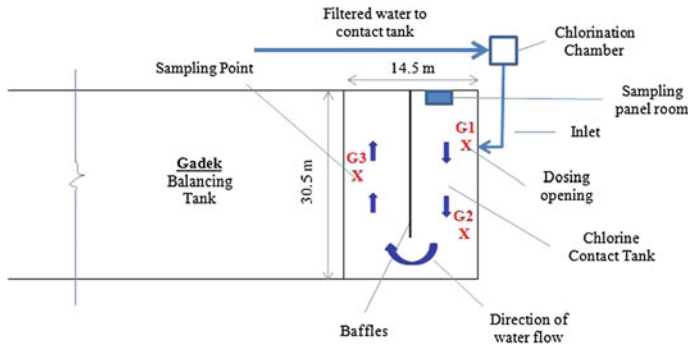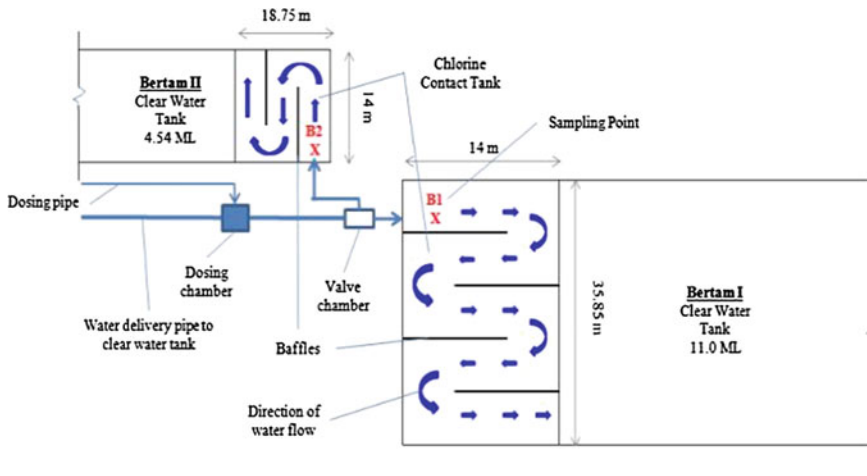
Fig. 7 Tank configuration of Gadek WTP

Fig. 8 Tank configuration of Bertam I and II WTP

Contact time (T) calculated based on the detection test results from selected WTPs is shown in Table 6. Comparison between $CT_{achieved}$ and $CT_{required}$ will show whether the disinfection requirement was met which is efficient when $CT_{achieved} \geq CT_{required}$ [9].

Based on the calculated CT which is $CT_{achieved}$ as shown in Table 6, disinfection efficiency of a WTP could be determined when $CT_{achieved} \geq CT_{required}$ which demonstrates sufficient disinfection have been met and vice versa [9]. There are two values which represent CT disinfection, namely the $CT_{achieved}$ and $CT_{required}$. Here, in this study, $CT_{achieved}$ has been calculated and analysed based on free residual chlorine concentration obtained from detection test which was conducted and based on site-specific CCT configuration as shown in Table 6. For $CT_{required}$, the value is

obtained from Table 2 based on the removal of micro-organism in the raw water that is targeted Giardia concentration in treated water [9].

Based on the in situ water quality tests, average temperature and pH for all five WTPs are 25 °C and 6.5, respectively, and are adopted in the selection of Giardia CT tables from EPA Guideline Manual as $CT_{required}$. Hence, $CT_{required}$ adopted for comparison with the $CT_{achieved}$ in evaluating the disinfection efficiency is shown in Table 2 at $T = 25$ °C and pH = 6.5. Through the findings obtained from the calculation shown in Table 6, $CT_{achieved}$ for Bukit Sebukor, Merlimau Gadek, and Bertam I was found to record higher levels than $CT_{required}$. As the CT rules

Table 6 Contact time calculation and evaluation

Item	WTP	Free residual chlorine at outlet (mg/L)		CCT volume, V (m3)	Peak flow, Q (m^3/s)
1	Bukit Sebukor	1.42		1489	0.20
2	Merlimau	1.45		3972	0.64
3	Gadek	2.55		2432	0.38
4	Bertam I	2.80		2760	0.64
5	Bertam II	1.60		674	0.58
Item	WTP	Nomina detention time, TDT = V/Q (minutes)		Baffling factor (BF)	Contact time (T), (minutes) = $T \times$ BF
1	Bukit Sebukor	124		0.3	37.23
2	Merlimau	103		0.3	31.03
3	Gadek	107		0.3	32.01
4	Bertam I	72		0.3	21.56
5	Bertam II	19		0.3	5.81
Item	WTP	CT Values (min mg/L) [$CT_{achieved}$]	Required CT; 3 log inactivation of viruses by free chlorine at $T = 25$ °C and pH = 6.5 [7] [$CT_{required}$]		
1	Bukit Sebukor	52.87	33		
2	Merlimau	44.99	33		
3	Gadek	81.61	37		
4	Bertam I	60.38	37		
5	Bertam II	9.30	33		
Item	WTP	Disinfection efficiency; 1. $CT_{achieved} \geq CT_{required}$: efficient 2. $CT_{achieved} < CT_{required}$: not efficient [7]			
1	Bukit Sebukor	Efficient			
2	Merlimau	Efficient			
3	Gadek	Efficient			
4	Bertam I	Efficient			
5	Bertam II	Not efficient			

($CT_{achieved} \geq CT_{required}$) have been complied, the disinfection process for four WTPs was found efficient whereby the disinfection process in the CCTs was deemed sufficient.

9 Conclusion and Recommendation

In this paper, the efficiency of disinfection process in the water treatment plant and the existing CCT design compliance specifically in Melaka, Malaysia, was evaluated in this study. For the purpose of this study, the detection test for drinking water quality parameters, i.e. free residual chlorine, fluoride, and chloride, has been conducted at five selected water treatment plants in Melaka. Based on the detection test results obtained from the in situ tests, all five WTPs are in line with the maximum allowable standards for free residual chlorine as outlined by the National Standard for Drinking Water Quality and the results would further be analysed in order to evaluate the disinfection efficiency.

Baffling factor of the CCT of all five WTPs was identified as 0.3 based on Table 2.2 and contact tank configuration analysis. Baffling Factor, BF = 0.3 is suited for baffled tank for open surface concrete tanks. Furthermore, the adoption of BF = 0.3 was made based on the observation of baffling condition for all WTPs due to poor baffling condition and single unbaffled outlet and inlet. Other than that, the baffling factor has also been identified through observation on the other related case studies by CBCL and Terry on other BF factors as guidance. Comparison between $CT_{achieved}$ and $CT_{required}$ measures the effectiveness of a disinfection process whereby if the $CT_{achieved} \geq CT_{required}$, the disinfection is efficient because the required disinfection has been met, otherwise appropriate actions must be taken to ensure sufficient disinfection requirement are met.

The evaluation of disinfection efficiency in disinfection process would be useful in alleviating the hydraulic efficiency of disinfection: design, construction workmanship, equipment, etc. The information obtained on disinfection ability of the existing water treatment plant would be useful for design improvement and cost-effectiveness in water treatment.

Based on the findings in the study, there are a few recommendations that should be shared to enhance the outcome of future research works. There are several suggestions:

1. Disinfection process requirement should always be adhered to all guidelines and standards so that the disinfection efficiency could be maintained.
2. More experimental tests, especially tracer test, should be regularly conducted in order to obtain precise CT in the evaluation of disinfection efficiency.
3. Improve the compilation of documents for every water treatment plant so that important information about the plant, i.e. complete as-built drawing, process design data and water quality data are made available for researchers or personnel to conduct the necessary tests at ease.

4. Increase operator's competency in the requirement of disinfection efficiency for cost-effectiveness in operation, maintenance, and compliance with the guideline.
5. Collaboration between researchers and operators in the evaluation of disinfection efficiency of the existing water treatment plant for ongoing improvement.

References

1. Jordan MW, Subhas KV (2010) Evaluation of hydraulic efficiency of disinfection systems based on residence time distribution curve. Environ Sci Technol 44(24):9377
2. MWA (1999) Malaysia water industry report. Malaysian Water Association, Kuala Lumpur
3. Walt JJ (2000) Is a chlorine contact tank really that simple? A CFD investigation into the hydraulics and kinetics of chlorine decay
4. Colorado Department of Public Health and Environment (2014) Baffling factor guidance manual determining disinfection capability and baffling factors for various types of tanks at small public water systems. Water Quality Control Division Safe Drinking Water Program Version 1.0
5. Terry LE (2014) Coagulation, flocculation, and clarification of drinking water. Hach Company, LIT2141
6. Alok B (2006) Hydraulics of chlorine contact tanks. Kansas State University Manhattan
7. EPA Guidance Manual (2003) Disinfection profiling and benchmarking, USA
8. Washington State Department of Health (2011) Chlorine contact time for small water systems. Division of Environmental Health, Office of Drinking Water, DOH, pp 331–343
9. Brock R (2002) CT disinfection made simple. Alberta Environment, Alberta
10. MOH (2004) National standard for drinking water quality. Engineering Service Division, Ministry of Health, Malaysia

Part V
Weather and Climate

Effect of Climate Change to Flood Inundation Areas in Bertam Catchment, Pahang

N.A.A. Aziz, M.A. Malek, A.S.M. Jaffar and R. May

Abstract Bertam catchment is increasingly becoming a main concern area on flood disaster caused by the dam release. Further research is required to be conducted at this area. The objective of this study is to determine future flood inundation area at the downstream of Bertam catchment for several scenarios as a result of dam release and climate change. The scenarios are current land use with and without climate change scenarios and future land use with and without climate change scenarios. InfoWorks RS, Geographical Information System (GIS) application and Auto CAD was utilized in this study to develop river modeling. The current land use used in this study is referring to 2010, and future land use refers to 2025. The climate change parameters used in this study are rainfall using climate change factor (CCF) derived by NAHRIM as input data. The design storm used in this study is 24 h storm duration and 100-years Annual Recurrence Interval (ARI). The results obtained using four scenarios show the differences of inundation areas. The model is validated based on actual maximum flood depth on site which is 1.2 m. The highest percentage of inundation area is when the water depth is greater than 1.2 m. For current land use, the difference in inundation area between with and without climate change scenarios is 12.6 %, while for future land use the difference is about 12.80 %. The finding of this study shows that impact of climate change has exaggerated the effect of water release from the dam to the downstream catchment.

N.A.A. Aziz (✉) · M.A. Malek
Department of Civil Engineering, Universiti Tenaga Nasional, Bandar Baru Bangi, Malaysia
e-mail: nurulamira_aziz@yahoo.com

M.A. Malek
e-mail: Marlinda@uniten.edu.my

A.S.M. Jaffar
RBM Engineering Consultant, Kuala Lumpur, Malaysia
e-mail: sharmyjaffar@yahoo.co.uk

R. May
Faculty of Civil Engineering, Universiti Teknologi MARA, Shah Alam, Malaysia
e-mail: kh.raksmey@gmail.com

1   Introduction

Bertam catchment is increasingly becoming a main concern area on flood disaster. A complete and urgent research is required to be conducted at this area. Bertam catchment is usually dry. No flooding event has occurred at this area for more than a decade. However, due to the effect of chaotic climate change currently experienced in Malaysia, recent extended long duration of rainfall within the catchment has caused an overflow of water at Sultan Abu Bakar Dam and high runoffs from different subcatchments. Sultan Abu Bakar Dam was designed to channel the water to Jor Dam. Nevertheless, during the incident of flood, the capacity of water is beyond the designed estimations. During the overstorage at the dam reservoir, the water was released in order to prevent the dam failure. However, when the water was discharged from the dam, an incident occurred at the downstream of the dam. In that incident, as reported by Bernama, about 80 houses located on the fringes of the Bertam River were swept away by strong currents after the release of water from the dam [1]. Lack of technical knowledge on the hydrological regime within the catchment of Sultan Abu Bakar Dam and Bertam Valley would leave the authorities and public unprepared to cope with unforeseen phenomena such as the flood tragedy on October 23, 2013, in Ringlet and Bertam Valley in Cameron Highlands. The mud flood tragedy was caused by a series of events, including heavy rainfall, river choked with rubbish, and an increase in water levels at the Sultan Abu Bakar Dam that reached critical levels. Besides, the impact of climate change would exaggerate the effect of water release from the dam to the downstream catchment. In this study, InfoWorks RS, GIS application, and AutoCAD were utilized to produce flood hazard map. In order to enhance the model to be approximately similar to actual scenario, land use and rainfall were incorporated as input to the model. Hydrological assumptions made in this model were based on actual site conditions. In addition, this study focuses on determining future flood inundation areas at the downstream of Bertam catchment on several scenarios as a result of dam release and climate change.

2   Background

Cameron Highlands is the smallest district in Pahang State. It is situated within the Main Range at an elevation between 1000 and 1830 m above sea level. It experiences a tropical climate. Its mean annual rainfall is 2400 mm though there are two distinct periods of maximum and minimum monthly rainfall. The primary maximum rainfall occurs in October and November, whereas the secondary maximum occurs in April and May.

The idea of developing Cameron Highlands as a hill resort was first proposed in 1887; but it was only in 1930 that the road was constructed from Tapah. Most of the larger tea estates had been established by early 1930s, as was several market gardens. For several decades, this pattern of land use remained basically the same due to the restrictions imposed by the terrain. The most widespread land use is the tea estates which were mostly located between 1100 and 1600 m above sea level, while land above 1600 m is mainly forest except in inaccessible areas where holiday homes were built.

In early 1970s, there were changes in land use due to the increase of tourism industry and an amplification of agricultural activities. Moreover, the number of holiday homes has been increased besides large hotels and other recreational facilities such as golf courses. The expansion of agriculture for the production of temperate-type vegetables and flowers has also been on the growth since 1982, with many of the new farms situated on steep slopes. There was a shift in emphasis in the early 1990s, from vegetable farming to flower gardening, though this trend has reversed in more recent years [2].

3 Location of Study

Bertam catchment is located in Cameron Highlands, Pahang. The size of the catchment is about 108 km^2. It is considered a small catchment with short river reach. It is a mountainous area and considered as a developing rural area [3]. There are six rainfall stations available in this catchment. Nevertheless, the downstream of the catchment is ungauged where no river flow data are available. The land use of this study area includes roads, highways, municipal, utility and related, garden vegetables and floriculture, grass idle/weeds, forest, and clearings.

4 Methodology

The data used in this study were obtained from National Hydraulic Research Institute Malaysia (NAHRIM), Town and Country Planning Department (TCPD), and Department of Irrigation and Drainage (DID).

There are six rainfall stations available at the upstream of Bertam catchment. However, only two stations were selected to be used in this study which is Ladang Teh Boh (Industrial Area) Station and Gunung Brinchang Station. Ladang Teh Boh (Industrial Area) Station is found to be the nearest rainfall station to the downstream and it is used for the actual case analysis, while Gunung Brinchang Station was used for other scenario analyses. Table 1 shows the numbers and names of rainfall stations available. The downstream of Bertam catchment is found to be ungauged. Current and future land use maps obtained from TCPD were delineated to match the catchment. Figures 1 and 2 show the current and future land use maps used in this

Table 1 List of rainfall stations

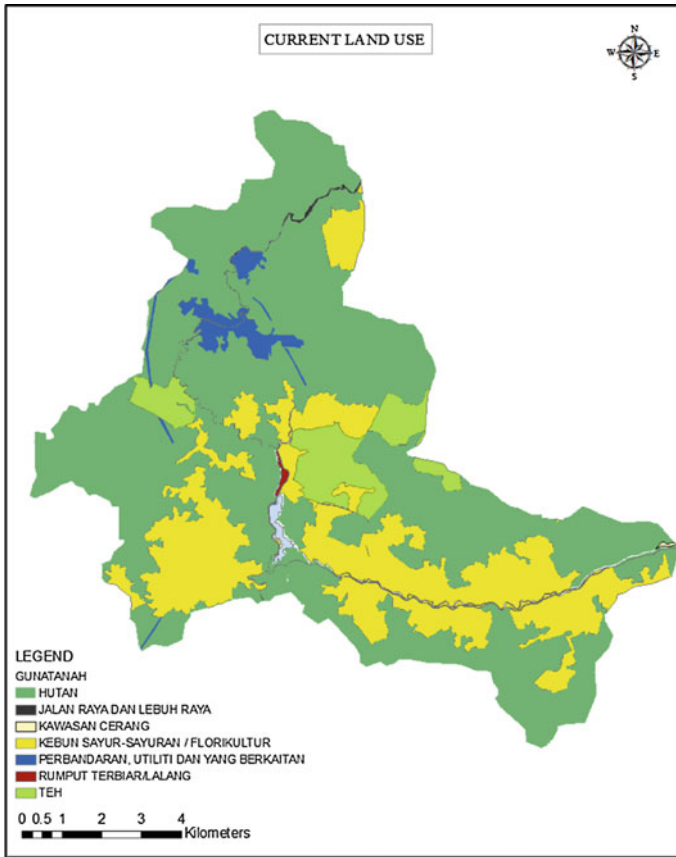| Rainfall station no.	Rainfall station name
4414036	Ladang Teh Boh (industrial area)
4414037	Ladang Boh (Bhg. Boh)
4414038	Ladang Boh (Bhg. Selatan)
4513033	Gunung Brinchang
4514031	Ladang Teh Blue Valley
4514032	Ladang Teh Sg. Palas

Fig. 1 Current land use map at Bertam catchment in 2010 (TCPD)

study. For example, the farming area (yellow) in 2010 is found to be reduced in future land use map 2025. This is probably due to the increase in forest area in future map 2025. The area for facilities (red) is found to be increase in future land use map 2025. In addition, actual case scenario in this study was used actual rainfall
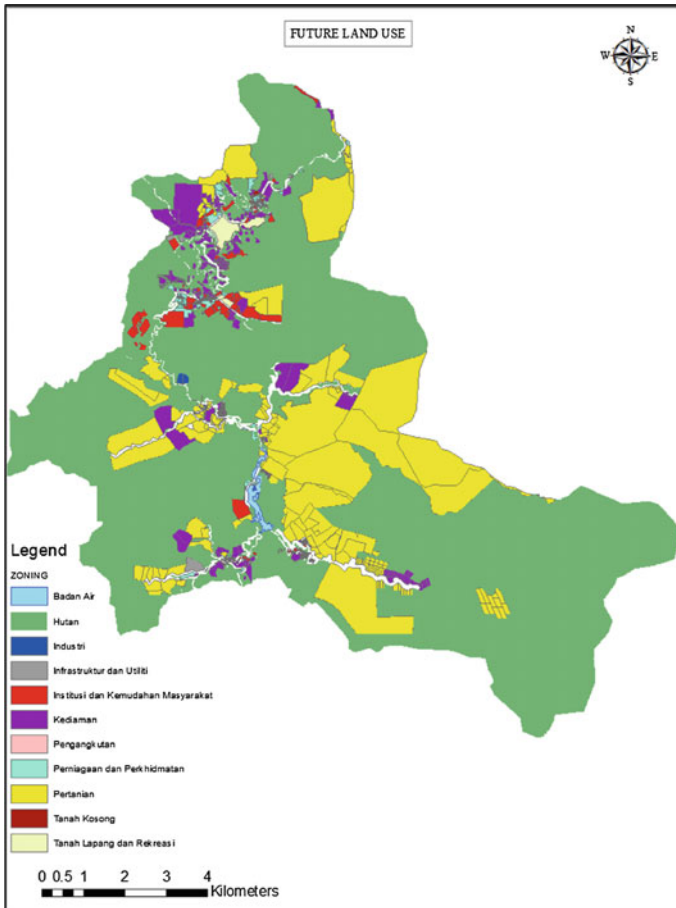
Fig. 2 Future land use map at Bertam catchment in 2025 (TCPD)

on October 22, 2013 to October 23, 2013, while other scenarios were using design rainfall adopted from HP1. The data used in this study include rainfall, land use, river cross section, structure information (bridges), and ground data (3D floodplain terrain data). Moreover, the parameters used are curve number (CN), hydrograph peak time (T_p), and Manning's roughness coefficient (n). Geographical Information System (GIS) was used to create analysis and display all types of geographically or spatially reference data. In addition, GIS is used in all stages of flood hazard map to support and expedite data processing and analysis. AutoCAD was used to analyze the structure information such as bridges.

The catchment was delineated using GIS. Before performing the model simulation, hydrological analysis needs to be conducted. The hydrological analysis includes CN and hydrograph peak time (T_p). CN was calculated using weighted

average as in Eq. 1. In this study, CN value was determined based on land use or land cover types. The value of CN was referred in TR-55 [4].

$$\text{Weighted CN} = \frac{\text{Total Product}}{\text{Total Area}} \tag{1}$$

T_p were obtained by delineating the length, area, and elevation from the sub-catchments identified using GIS. The value of T_p was then determined as in Eq. 2.

$$T_\text{p} = 0.067\,T_\text{c} \tag{2}$$

where T_c = time of concentration.

In hydrodynamic flow model development, one-dimensional energy or continuity and momentum equation (St. Venant equation) should be solved numerically along the flow reach. In this process, Manning's surface roughness parameter is required. Manning's roughness coefficient is the key component to hydraulic model calibration. It is usually selected from the available literature and depending on modeler's experience on surface characteristics [5]. In this study, Manning's roughness coefficient used in river channel and floodplain area for both current and future conditions is between 0.03 and 0.05. The river is classified as natural river.

United Nations Framework Convention on Climate Change (UNFCC) has defined climate change as *change of climate which is attributed directly or indirectly to human activity that alters the composition of the global atmosphere and which is in addition to natural climate variability observed over comparable time periods* [6]. The Intergovernmental Panel on Climate Change 2014 (IPCC 2014) defines climate change as *a change in the state of the climate that can be identified (e.g., by using statistical tests) by changes in the mean and/or the variability of its properties, and that persists for an extended period, typically decades or longer* [7]. In this study, climate change factor (CCF) obtained from NAHRIM was used to obtain future design rainfall. According to NAHRIM (2013), climate change load factor is defined as the ratio of the projected design rainfall for the future to the control period (historical). In this study, the calculation on return periods of maximum daily rainfall events with return periods of 2, 5, 10, 20, 25, 50, 100, and 200 years used generalized extreme value (GEV) and extreme value type 1 by means of on-site approaches. The probability and magnitude of events that are further extreme than any that exist in a given data series may be characterized by extreme value analysis which is a statistical method. In example, to estimate the return level of an event with a return period 1 in 100 years, a 20-year observation record could be used. The magnitude of future design rainfall or rainfall intensity is represented as Eq. 3.

$$I_F = \frac{\lambda' T^k}{(d+\theta)^\eta} = \text{CCF}_{1d} \times \left(I_H = \frac{\lambda T^k}{(d+\theta)^\eta} \right) \tag{3}$$

Then, flood hazard map is produced using InfoWorks RS. Flood hazard map is the map that shows the potential flooding areas based on three probabilities (low, medium, and high). Flood hazard map is considered as a non-structural measure in flood mitigation. It is pertinent to the community within the study area. It is a combination of various flood parameters to produce danger level such as depth and velocity. The information from flood hazard map is represented by various color schemes used. The flood hazard map can be used as a planning tool, to create awareness and emergency responses. Data needed for flood hazard map include catchment characteristics, river alignment, river cross section, and 3D elevation [8].

InfoWorks RS is the combination of advance International Species Information System (ISIS) flow simulation engine, GIS functionality, and database storage within a single environment. It brings together the source data and hydraulic modeling into unique product. By using InfoWorks RS, planners and engineers can conduct fast, accurate modeling on key elements for river and channel systems and view the model data and results in better perspectives.

In addition, InfoWorks RS provides model management in the field of water engineering where it allows a full audit trail to be maintained on the modeling process from source data to final outputs. This software allows data from a wide range of sources to be brought together in a rapid and flexible way. It includes modeling solution for open channels, floodplains, embankments, and hydraulic structures. In this module, rainfall–runoff simulation using both event-based and conceptual hydrological methods is available. InfoWorks RS presents full interactive views of data using geographical plan views, sectional view, long sections, spreadsheet, and time-varying graphical data. The original data can be accessed from any graphical or geographical view. Furthermore, this software contains comprehensive diagnostic error checking and warning and rapid access to the full online documentation that is integrated with the help system. The animated result presentation is shown in geographical plan, long section, and cross-sectional views. It includes full dynamic flood mapping as well as results reporting and analysis using tables and graphs.

Shallow water or St. Venant equation as in Eq. 4–8 used in this model can be explained as motion of water body flowing in open channels, which expresses conservation of mass and momentum. Conservation of mass leads to the continuity equation which establishes a balance between the rate of water-level rise, wedge, and prism storages. Conservation of momentum leads to the dynamic equation which establishes a balance between inertia, diffusion, gravity, and friction forces. The effect of wind, meanders, or some other forces may also be included, but this effect is usually small [9].

$$\frac{\partial Q}{\partial x} + \frac{\partial A}{\partial t} = q \tag{4}$$

$$\frac{\partial Q}{\partial t} + \frac{\partial}{\partial x}\frac{\beta Q^2}{A} + gA\frac{\partial H}{\partial x} - gAS_{\mathrm{f}} = 0 \tag{5}$$

$$S_{\mathrm{f}} = \frac{Q|Q|}{K^2} \qquad (6)$$

$$K^2 = \frac{A^2 R^{\frac{4}{3}}}{n^2} \qquad (7)$$

$$R = \frac{A}{P} \qquad (8)$$

where q is the lateral inflow (m³/s), Q is the discharge (m³/s), A is the area, g is the gravity, S_{f} is the so-called friction slope, K is the channel conveyance calculated according to Manning's equation, R is the hydraulic radius, p is the length of wetted perimeter, and n is the Manning's roughness coefficient.

5   Model Calibration

Prior to performing this simulation, the model of the study area needs to be calibrated. In this study, the model was calibrated with data from the actual flooding event on October 23, 2013. Data of 1-h rainfall is used in this calibration starting from October 22, to October 23, 2013, where the nearest rainfall station is selected (Ladang Teh Boh (Industrial Area) Station). Tenaga Nasional Berhad (TNB) has estimated the flow of water release from the dam on October 23, 2013, is about 30 m³/s. The value of the tested flow in this study ranges at 30, 70, and 100 m³/s. It is found that different values of flow will produce different water depths at the event location. In this study, it is found that the results of 70 m³/s flow produce the corresponding water depth of 1.2 m similar to the water depth marked on site. Figure 3 shows the comparison of flood depth at 30, 70, and 100 m³/s. Hence, it is found that the flow at the actual event is approximately 70 m³/s. Figure 4 shows the flood map produced on the actual flooding event of October 23, 2013.

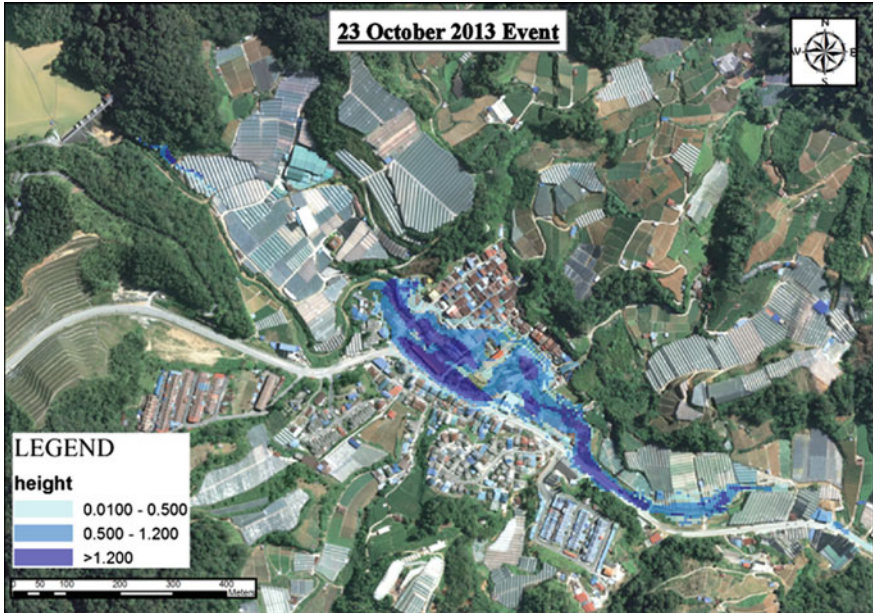**Fig. 3** Comparison of flood depth for various flood simulations
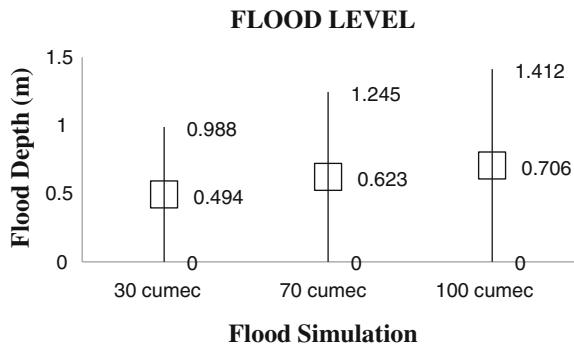
Fig. 4 Flood map of actual flooding event on October 23, 2013

6   Results and Discussion

There were four scenarios of the flood hazard map simulation conducted in this study. The scenarios are current land use without climate change, future land use without climate change, current land use with climate change, and future land use with climate change. Current land use and future land use without climate change is the baseline in this study. The flood hazard map produced in this study covered 5 km length from the dam to the downstream of Bertam catchment. The inundation area is calculated in 5 km length from the dam. In addition, sensitivity analyses were performed in order to identify the suitable design storm duration for this study. It is found that 24-h storm duration and 100-year ARI produce the maximum water level and it is therefore used for further analysis in this study. Flood hazard maps for various cases produced in this study are shown in Figs. 5, 6, 7, and 8.

The summaries of inundation areas and its percentage according to flood depth simulated in this study are summarized in Tables 2 and 3.

The results on four scenarios in Tables 2 and 3 show the increasing of inundation areas. The effect of climate change can be seen by comparing the inundation area in scenarios 4 and 5 with baseline scenarios (2 and 3). The highest percentage of inundation area is when the water depth is greater than 1.2 m. As for current land use, the difference in inundation area affected by climate change when the water depth is greater than 1.2 m is about 12.6 %, while for future land use the difference
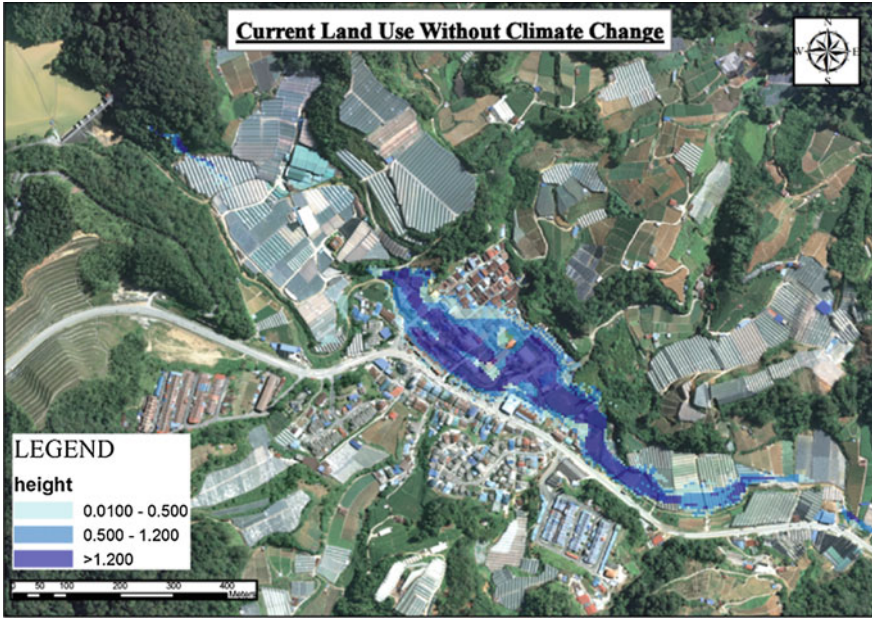
Fig. 5 Flood hazard map for current land use without climate change
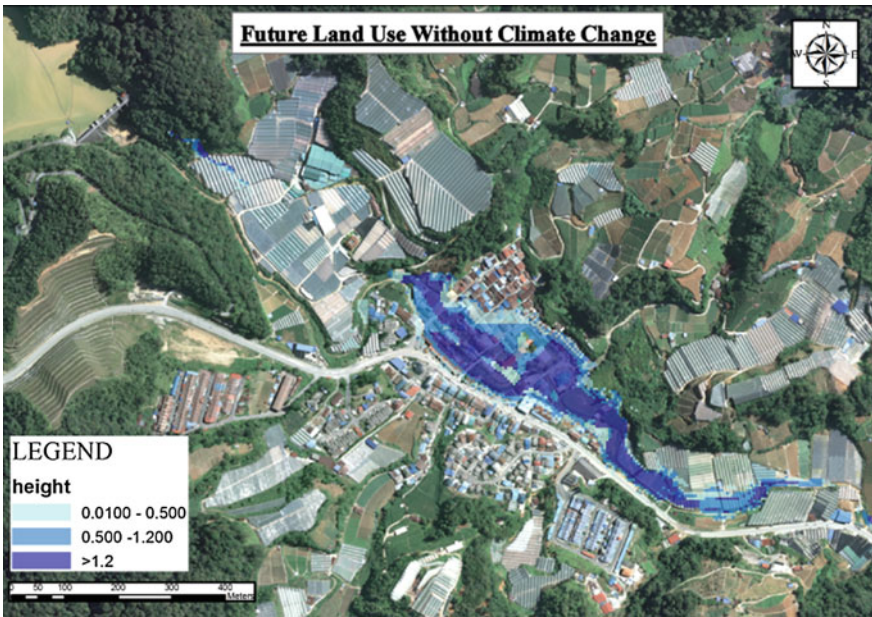

Fig. 6 Flood hazard map for future land use without climate change
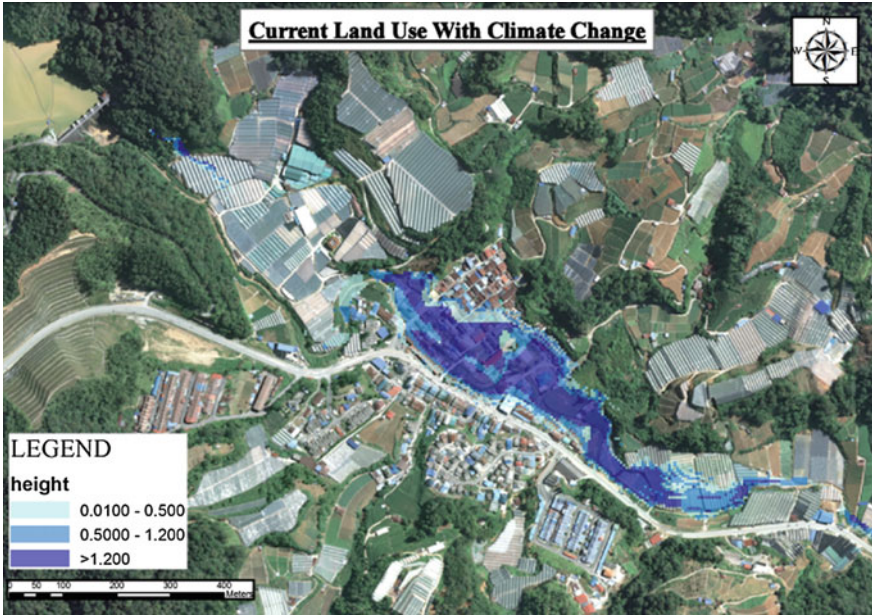
Fig. 7 Flood hazard map for current land use with climate change
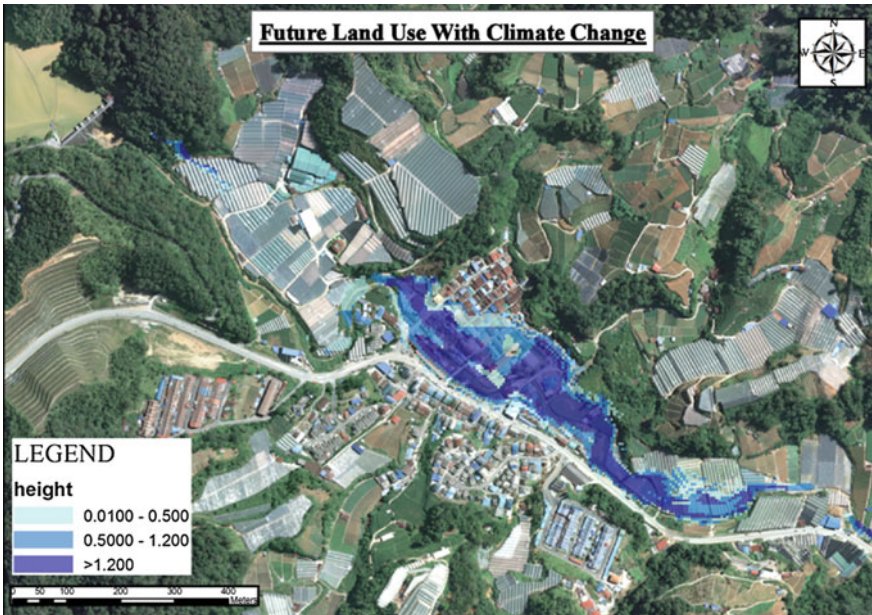

Fig. 8 Flood hazard map for future land use with climate change

Table 2 Summary of inundation areas

Water depth (m)	(1) Actual case October 23, 2013	(2) Current land use without climate change	(3) Future land use without climate change	(4) Current land use with climate change	(5) Future land use with climate changes
	Inundation area (m²)				
0.0100–0.500	33,525	43,100	43,975	45,675	48,350
0.500–1.200	62,475	59,425	59,225	62,625	67,525
>1.200	76,450	172,900	190,675	223,000	246,650
Total	172,450	275,425	293,875	331,300	362,525

Table 3 Summary on percentage of inundation areas

Water depth	(1) Actual case October 23, 2013	(2) Current land use without climate change	(3) Future land use without climate change	(4) Current land use with climate change	(5) Future land use with climate changes
	Percentage of inundation area (%)				
0.0100–0.500	19.44	15.65	14.96	13.79	13.34
0.500–1.200	36.23	21.58	20.15	18.90	18.63
>1.200	44.33	62.78	64.88	67.31	68.04

is about 12.80 %. This trend shows that climate change has contributed to the increasing inundation areas.

7 Conclusion

Flood hazard map simulation has been performed in this study by using InfoWorks RS. Comparison on four scenarios was carried out. From this study, it can be concluded that major contributor to the flooding event on October 23, 2013, is believed to be from the dam release. According to the results obtained from this study, the future flood inundation areas will be further exaggerated by the impact of climate change at the study area. This is supported by the increase in inundation areas of flood as shown in Tables 2 and 3.

In order to reduce the flood disaster, mitigation measures need to be considered. Flood hazard maps can be used as a non-structural mitigation measures, an early warning tool for planning and decision-making. This will assist the relevant

authorities to design various flood structural mitigation measures such as river widening, deepening, bunds, and temporary ponds.

In addition, further study can be conducted by considering the effect of sedimentation to the flood hazard areas.

References

1. Bernama N, 23 October 2013
2. Raj J (2002) Land use changes, soil erosion and decreased base flow of rivers at Cameron Highlands, Peninsular Malaysia. In: Geological society of Malaysia annual geological conference 2002, Kota Bharu Kelantan
3. Zakaria N, Jahaya MF, Ying Ying T, Abdul Rahman MR, Mohamad M (2013) The analysis of dry deposition of acidifying substances between urban and developing rural stations of malaysian meteorological department from 2007–2010. Malaysian Meteorological Department and Ministry of Science, Technology and Innovation, Malayisa
4. United States Department of Agriculture (USDA), Natural Resources Conservation Service (NRCS) and Conservation Engineering Division (1986) Urban hydrology for small watershed. USDA, United States
5. Philips JV, Tadayon S (2006) Selection of manning's roughness coefficient for natural and constructed vegetated and non-vegetated channels, and vegetation maintenance plan guidelines for vegetated channels in Central Arizona. U.S. Geological Survey Scientific Investigations Report, Arizona, US
6. United Nations (1992) United Nations framework convention
7. Intergovernmental Panel on Climate Change (2014) Climate change 2014 (impacts, adaptation and vulnerability). IPCC, Cambridge, United Kingdom
8. Sam WW, Zulkifli MN, Seng CH (2012) Flood mapping as a planning and management tool. Putrajaya
9. Wallngford, Info works RS guide, Wallingford

The Use of Radar Rainfall Inputs for Runoff Estimation in Upper Klang River Basin, Malaysia

R. Suzana and S.H. Abu Bakar

Abstract Flooding is a natural disaster that often occurs in Malaysia due to its heavy rainfall distribution. Many incidents of floods attributed to the extreme downpour caused massive problems. The capability of gauge to receive data of the torrential precipitation is affected and need to be addressed. Thus, the deployment of radar helps to retrieve better rainfall data due to spatial and temporal factors. Radar has the advantages of detecting rainfall amount with higher resolution and covers larger areas. In addition, radar can also access hilly and ungauged areas with the ability to detect cloud movement and lead to estimation of precipitation. The improved radar rainfall as quantitative precipitation estimation (QPE) has been applied in the rainfall–runoff modeling with grid-based soil conservation service curve number (SCS-CN) method and GIS utilization. The outcomes demonstrate good agreement between simulated data and observed data for selected events.

Keywords Radar rainfall · Quantitative precipitation estimation (QPE) · Curve number method

1 Introduction

In most locations, rain gauge stations are available as rain measurement techniques. Although the results are nearly accurate, they also experience problems such as no coverage for certain remote regions, point measurement is not representative of area, different in gauge designs and also the wind effect. Lack of rain gauge in certain locations provides difficulty in assessing rainfall data. In fact, according to Corral et al. [1], a density of about 1 rain gauge per 200 km^2 is still insufficient to study the rainfall characteristics over time and space.

R. Suzana (✉) · S.H. Abu Bakar
Faculty of Civil Engineering, Universiti Teknologi MARA, 40450 Shah Alam, Selangor, Malaysia
e-mail: suzana_ramli@yahoo.com

Rainfall estimation by meteorological satellite is also favorable; since it has good space and time resolutions, observations made are in near real time and consistent. The potential use of meteorological satellite for flood forecasting has been discussed by Wardah et al. [2, 3]. But on the other hand, satellite measurement can be misleading because it measures cloud top properties instead of rain, having too coarse spatial and temporal resolution, and large data are needed to complete the forecasting. Joss and Waldvogel [4] explained that the advantage of using radar for precipitation measurements is the coverage of a large area in real time. At the same time, radar also experiences difficulty in achieving an accurate estimation for hydrological applications. Suzana et al. [5] found that the radar rainfall estimates can be improved by improving the Z–R relationship, while Wardah et al. [6] and Sharifah Nurul Huda et al. [7] studied on Kriging interpolation and Kalman filtering application in improving radar rainfall estimates by removing noises for Klang River basin. After all, the biggest advantages of weather radar are the ability to detect cloud and precipitation structure and also the process of the rainfall system itself by providing real-time regional information [8]. It has been more than 50 years that weather radar is being utilized as a substitute tool to improve rainfall measurement in hydrology [9]. In Malaysia, weather radar that is operated by the Malaysian Meteorological Department (MMD) provides observation of the weather such as detection of the microburst and monitors rainfall distribution especially for the flight aviation. The utilization of weather radar in quantitative precipitation estimates (QPE), however, is still at the early stage especially in hydrological modeling work. The study on radar in hydrological application recently shows that the radar has potential value in developing better rainfall measurement products.

2 Case Study and Data Collection

For the purpose of rainfall–runoff estimation, only the upper part of Klang river basin is included in this study with 468 km^2 area and 120 km of length. The upper section is under jurisdiction of three local authorities: Ampang Jaya, Ulu Langat, and Gombak. The focus of the study area is located in Gombak where the area is about 116 km^2 and 34.6 km in length. 50 % of the upper land had been developed for residential and commercial areas as well as for industrial zone. The remaining land is reserved for forestry. To be specific and for validation purposes, Sungai Gombak has been chosen to be the case study for radar rainfall application in order to compare the stream flows with Department of Irrigation and Drainage (DID) results. With catchment size of 116 km^2 and river length of 34.6 km, the river was reported to experience series of flood events. MMD and DID provide the meteorological data for the year 2009 from Doppler radar and rain gauges, respectively.

Nine rain gauges have been selected (see Table 1) to be calibrated and validated for rainfall–runoff calculation using grid-based curve number method in a few storm events for Klang river basin. Malaysian Remote Sensing Agency (MACRES)

Table 1 Selected rain gauges

No.	Station's name
1	JPS KL
2	JPS Ampang
3	Lading Edinburgh
4	Ibu Pejabat km 11, Gombak
5	Empangan Genting
6	Kg. Sg. Tua
7	Km 16, Gombak
8	Kg. Sg. Sleh
9	Air Terjun Sg. Batu

Table 2 Data used for rainfall–runoff modeling

Data	Source	Scale
Rainfall data and	DID	Hourly data
Radar data	MMD	Raw CAPPI data (15 min interval)
Flow data	DID	Hourly data
Soil type data (map)	JUPEM, DOA	1:25,000
Land use data (map)	DOA	1:25,000
Topography map	JUPEM	1:25,000
Satellite images	MACRES	30 m resolution

supplies the latest satellite image for the land use mapping using SPOT-5 (270/343/8) Pansharp All Bands. The satellite image is converted to digital image using ERDAS IMAGINE by GIS to produce land use map. For the purpose of obtaining curve number, CN for this model, land use map will be used together with soil map at scale 1:25,000. The summary of data used for the rainfall–runoff model is given in Table 2.

3   Methodology

Using Arc View from GIS, the upper basin of Klang River is delineated by digitizing manually the contour and river layer maps. The area has been delineated into nine subcatchments according to rain gauge stations selected. Delineation work utilizes Thiessen polygon method to obtain each subcatchment. A 1 × 1 km grid size has been chosen for simulation work. Each subcatchment is discredited into cells as shown in Fig. 1.

Each cell will have their own CN index after integrating the soil type and land use maps by layering them in GIS. Using the curve number map obtained by using GIS, the ultimate objective of this research is to estimate the surface runoff and peak
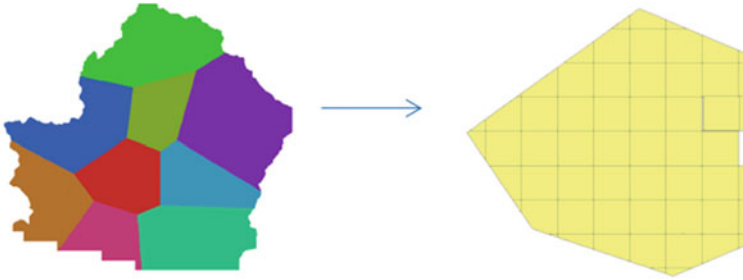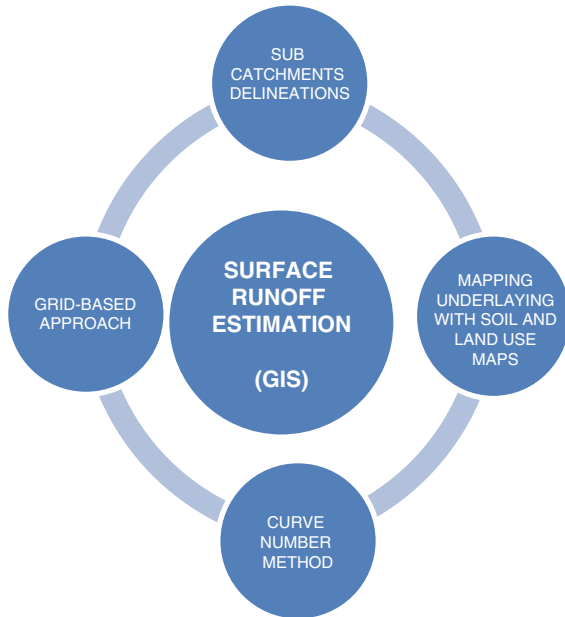
Fig. 1 Delination of upper Klang river basin into subcatchment and gridding into cells

Fig. 2 Processes for surface
flow estimation

discharge of upper Klang river basin by using SCS-CN [10] formula. According to [11], the SCS-CN method is following water balance concepts where the ratio of actual amount of surface runoff to maximum potential runoff is equivalent to the ratio of actual infiltration to the potential maximum retention. Thus, by using the SCS-CN grid-based approach in producing the CN for upper Klang river basin, surface runoff, and flow calculations have been initiated. The processes are being depicted in Fig. 2. Six events have been selected from year 2009 and 2012 (due to radar data availability) to investigate radar performance in SCS-CN method using GIS. For the purpose of validation with DID data, since there is no data recorded for surface runoff, the validation between surface runoff data with radar and gauges was calculated based on SCS-CN formula. In order to compare the DID data, only

stream flow records are available and for upper Klang river basin, Sungai Gombak has been selected due to its existing historical data available and numerous flood occurrences reported. The stream flow data are taken at site 3116433 Jalan Tun Razak.

4   Results and Discussion

The main parameter for SCS-CN method is precipitation. Hence, for surface runoff and flow estimation, rainfall data from 5 selected gauge stations in Sungai Gombak catchment were selected. Six events were selected into rainfall–runoff modeling by using SCS curve number method with GIS integration and grid-based approach. This model utilized only rain gauge data from 5 subcatchments to calculate surface runoff depth in mm. SCS-CN method needs data from curve number map and rain data and then simulated by using Arc View 9.3 of GIS.

From the results, the over and underestimation can be expected in surface runoff and peak discharge of Sungai Gombak catchment due to inappropriate usage of Z–R equations especially in 2009. The results show that the radar measurement in 2012 was better than data collected in 2009 due to radar equipment calibration (antenna) and maintenance done in IRIS hardware. The absence of radar data in 2010 and 2011 was due to radar antenna problems including the malfunction of software system. After several modification works done by VAISALA, improvement on radar data in KLIA is finally can be observed.

Site 3116433 Sungai Gombak at Jalan Tun Razak is the only active stream flow station available for Sungai Gombak catchment. The events were selected based on the amount of rainfall recorded which exceeded 20 mm/h and availability of radar data.

Soil conservation service curve number (SCS-CN) method is applied due to its appropriateness in GIS grid-based model. Curve number method is a simple and straightforward method that enables spatially distributed infiltration calculations. It determines runoff over an area based on land use, soil type, and land cover characteristics. Curve number method determines storm runoff over an area based on land use, soil type, and group as well as land cover type. In this method, it assumes that that ratio of actual retention to actual storage is equal to the ratio of actual direct runoff to rainfall minus abstraction. Important information for curve number includes soil cover type, soil treatment, soil hydrological condition, and antecedent moisture condition where those parameters can be obtained from maps, tables, or diagrams.

Table 3 depicts the peak discharge estimation with gauge, current radar data with Marshall Palmer equation, and also radar data with new Z–R relationships. The results for newly modified Z–R equations were underestimated when being evaluated against gauge and current radar data. The radar data were modified using Z–R relationships of monsoon season (e.g., inter-northeast for event in September and October) according to the date of event.

Table 3 Peak discharge estimation for new Z–R relationships in UKRB

Event	Q simulated (m³/s)			Observed flow from DID (m³/s)
	Radar (MP)	New Z–R	Gauge	
12092012	13.07	2.93	14.98	16.43
22092012	20.61	6.55	19.06	11.89
13102012	53.89	17.20	42.48	25.85
21102012	52.28	16.24	39.43	17.15
14052009	192.53	34.11	38.59	18.46
18112009	145.83	5.17	19.72	5.49

Fig. 3 Peak discharge for different events
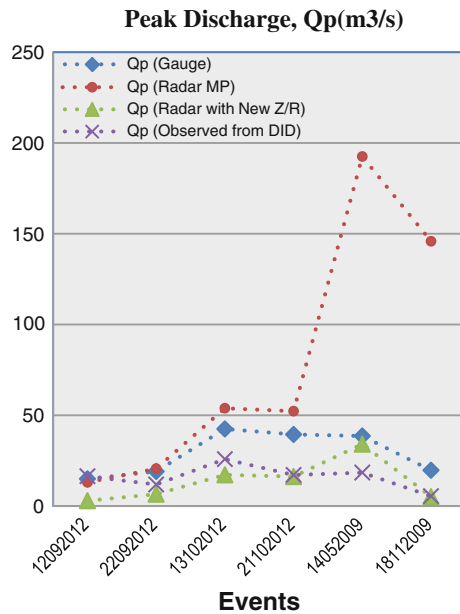
Using the estimated value from surface runoff calculation, for validation purposes, the peak discharge for Sungai Gombak catchment was determined by using SCS method. The results were validated against peak flow data observation from DID as shown in Table 3.

From Fig. 3, it can be shown that the peak runoff from Sungai Gombak catchment calculated using radar data with Marshall Palmer equation exhibits higher estimation when compared to data from gauge stations. The flow estimation increases slightly for events in 2012 while in 2009, the pattern of the graph depicts distinct difference between the two datasets where Doppler radar data overestimated the gauge values. In 12092012, the estimated stream flow shows that radar data gave smaller value than gauge data with 12.8 %. The peak runoff difference from events 22092012, 13102012, and 21102012 are 8, 26.9, and 32.6 %, respectively.

For the year 2009, the two selected events show huge disparity where the peak discharge using Doppler radar data enhanced by approximately five times higher than the gauge data. It means that the radar data collected in year 2009 was very distinctive compared to radar data in 2012 which demonstrate data consistency. The factors suggested for this excessive collected radar values are mostly coming from radar equipment modification and maintenance problems.

References

1. Corral C, Sempere-Torres D, Berenguer M (2008) A distributed rainfall-runoff model to use in Mediterranean Basins with radar rainfall estimates. In: Proceeding of ERAD 2008—the fifth European conference on radar in meteorology and hydrology. Helsinki, Finland
2. Wardah T, Abu Bakar SH, Bardossy A, Maznorizan M (2008) Use of geostationary meteorological satellite images in convective rain estimation for flash-flood forecasting. J Hydrol 356(3):283–298
3. Wardah T, Zaidah I, Suzana R (2009) Geostationary meteorological satellite-based quantitative rainfall estimation (GMS-rain) for flood forecasting. Malays J Civ Eng 21 (1):1–16
4. Joss J, Waldvogel A (1990) Precipitation measurement and hydrology: radar in meteorology. D. Atlas (ED.). Am Meteorol Soc 557–606
5. Suzana R, Wardah T (2011) Radar hydrology: new Z/R relationships for quantitative precipitation estimation in Klang river basin, Malaysia. Int J Environ Sci Dev 2(3)
6. Wardah T, Sharifah Nurul Huda SY, Deni SM, Azwa B (2011) Radar rainfall estimates comparison with kriging interpolation of gauged rain. In: Colloquium on humanities, science and engineering, CHUSER 2011 IEEE Colloquium, Art. No. 6163877, pp 93–97
7. Sharifah Nurul Huda SY, Wardah T, Suzana R, Hamzah A, Muhammad Faiz MS (2012) Improved estimation of radar rainfall bias over Klang river basin using a Kalman filtering approach. In: 2012 IEEE Symposium on business, engineering and industrial applications (ISBEIA), Art. No. 13285358, pp 368–373
8. Peng L, Xingyuan S, Wenwen T (2009) A study on quantitative radar rainfall measurements by the method of set-pair analysis. In: Proceeding of IEEE global congress on intelligent systems. doi:10.1109/GCIS.2009/75
9. Uijlenhoet R (2001) Raindrop size distributions and radar reflectivity-rain rate relationships for radar hydrology. Hydrol Earth System Sci 5:615–627
10. US Soil Conservation Service (1986) Urban hydrology for small watersheds (Technical Release 55), US Department of Agriculture (USDA)
11. Subramanya K (2004) Engineering Hydrology (2nd Edition): Tata McGraw Hill, New Delhi

Estimation of Design Rainstorm for Rural and Urban Area Using Gumbel's and Log-Pearson Type III Method

M.R. Nur Liyana and A.M. Intan Shafeenar

Abstract Growing population and migration in Selangor and Kuala Lumpur led to changes in the usage and management of lands which affect the hydrologic cycle within the area. Every year, flood has been reported in those areas and occurred in a random and unpredictable manner. One of the alternatives to prevent future occurrence of flood is by predicting the design rainstorm, and it is the responsibility of the department of irrigation and drainage to estimate the future hydrological events. Intensity–duration–frequency curve is one of the methods to estimate the rainstorm event of a particular location. Rainfall data are needed to be obtained via installation of rain gauge at a rainfall station before the data are analyzed. In this study, four separate rainfall data of urban and rural areas at intervals of 15, 30, 45, 60, 180, 360, 720, 1440, and 4320 min were recorded to be analyzed. The data were analyzed using two commonly used methods, namely the Extreme Value Type I (Gumbel's) and Log-Pearson Type III method. Intensity–duration–frequency (IDF) curves for every station were plotted using results obtained from both methods, and an empirical formula for the design of rainstorm was developed. Accuracy of both methods was compared by using goodness-of-fit test, which aims to identify the most suitable method to be carried out. Applications of empirical formula will be useful for engineers to design rainstorm in water resource planning in order to prevent flood in future.

Keywords Flood · Rainstorm · Intensity–duration–frequency

1 Introduction

Over the past century, most of the regions in the state of Selangor, which is located at the central of the west coast of Peninsular Malaysia, have become an urban area due to increased migration of the rural population, migrating into the cities. These

M.R. Nur Liyana (✉) · A.M. Intan Shafeenar
Faculty of Civil Engineering, Universiti Teknologi Mara, Shah Alam, Selangor, Malaysia
e-mail: liyanaamanda505@gmail.com

cities have become the major foundation not only to provide employment, services, and shelter, but also the center of learning and technology development which ultimately turns into an avenue to generate higher income. However, the urbanization and development change the management and usage of lands which eventually affect the hydrological characteristics in many ways. Selangor itself experiences hydrological effects when high rainfall intensity occurs in many of its regions, thus becoming one of the significant contributing factors to flood event. Flood mitigation and management aim to mitigate and reduce the likelihood and the impact of flood. One of the approaches that can be done is through development in flood management program with respect to 5 strategies including prevention of damages caused by flood, protection by reducing the likelihood of the impact of flood, and preparedness by informing the public about the risk.

The objectives of this study are to develop empirical formulas of design rainstorm for selected rainfall stations in Selangor and Kuala Lumpur using Gumbel's and Log-Pearson Type III method, to assess the difference of IDF curve between Extreme Value Type 1 (Gumbel's Method) and Log-Pearson Type III method, and to compare the results for rural and urban area in Selangor and Kuala Lumpur. The scope of this study includes four (4) stations in rural areas and four (4) stations in urban areas in Selangor. Rainfall data collected for this study were set to an interval of 15, 30, 45, and 60 min, 3, 6, 12, and 24 h, and 3 days extracted from department of irrigation and drainage (DID). The data are analyzed to determine design rainstorm using Gumbel's and Log-Pearson Type III method, and the results are compared. Developing empirical formula for design rainstorm is based on intensity–duration–frequency (IDF) curves.

It is important to estimate the probability of future hydrological event such as flood, by studying the statistical distribution of such event within an observed time series with the assumption that this distribution will remain unchanged in the future. Studies need to be done to ensure the suitable method and statistical distribution to be used to find accuracy of the result. Apart from that, the application of empirical formula to design rainstorm is useful to design flood and rainstorm event, as a part of flood mitigation measures.

2   Development of Intensity–Duration–Frequency (IDF) Curve

The rainfall intensity–duration–frequency (IDF) relationship is one of the most commonly used tools in water resource engineering, either for planning, operating, and designing water resource projects, or for the protection of various engineering projects (e.g., highways) against floods. IDF curve relationship gives the idea on estimating and forecasting the hydrological events such as storm durations for various amount and durations. The estimation and use of IDF curves rely on the hypothesis of rainfall series stationarity, namely that intensities and frequencies of extreme hydrological events remain unchanged over time [1].

Mansel [2] stated in their study that a critical characteristic of IDF curves is that the intensities are indeed averaged over the specified duration and do not represent the actual time histories of rainfall.

IDF curve is applied in designing storm sewers, which is the commonly constructed urban drainage system. Behzad [3] in his research stated that the rational method is commonly used to estimate the peak flows resulting from storms of specific return periods. The equation of rational method is shown in Eq. (1) below:

$$Q = C.i.A \tag{1}$$

where Q = peak flow rate required for a size of storm sewer, C = coefficient of runoff, and i = rainfall intensity obtained from IDF curve or empirical formula.

Coefficient of runoff, C, is determined using empirical formula based on soils and land use of the area. Less vegetation area or urban area has higher runoff coefficient compared to preurban and rural area. Equation used to determine the coefficient of runoff, C, is shown below:

$$C = \frac{\text{Total Runoff}}{\text{Total Rainfall}} \leq 1 \tag{2}$$

Rainfall intensity obtained from IDF curve is in depth per unit time (mm/h) with duration known as T_d and return period of T_r. The empirical formula of IDF curve is developed by Alhassoun [4] to estimate the design rainfall intensity of Riyadh region.

3   Rainfall Data Collection

The eight rainfall stations in Selangor were selected based on the rainfall station list which is available at DID Malaysia Web site since DID is the authority responsible for measurement and data collection of any hydrological activities in Malaysia. The data extracted from DID were based on 9 intervals of time from 15 min to 3 days for each year available for each rainfall station that was selected. The data duration for Damansara Station is the shortest since the data available are only for year 2008. The longest data duration available is at Hulu Langat rainfall station, which is 21 years starting from year 1993 to 2013. It is important to get the longest years of data duration of rainfall to get the most accurate estimation to design rainstorm.

4   Rainfall Data Analysis

The mean rainfall data for each time interval of 15, 30, 45, 60, 180, and 360 min were used for the analysis. The data from four rural areas and three urban areas were extracted from DID Ampang for the longest years available for each stations.

The data need to have more than 10 years of period to ensure the accuracy of the obtained results; some of the data are missing due to certain factors including damage or fault in rain gauge during the period. The missing data can be estimated using the data at neighboring stations [5].

5 Estimation of Missing Data

When working with hydrological data, missing data situation often happened. However, the missing data can be filled by the estimation values using normal ratio method. This method is used if any surrounding gauges have the normal annual precipitation exceeding 10 % of the considered gauge [6]. The missing rainfall data are estimated by using Eq. (3) below:

$$P_x = \frac{1}{M} \sum_{i-1}^{m} \left[\frac{N_x}{N}\right] P_i \tag{3}$$

5.1 Extreme Value Type 1 (Gumbel's Method)

Most of intensity frequency function can be generalized using Gumbel's distribution as given in Eq. (4) below:

$$K_T = \frac{\sqrt{6}}{\pi} \left\{ 0.5772 + \ln\left[\ln\left(\frac{T}{T-1}\right)\right] \right\} \tag{4}$$

where K_T is the frequency factor corresponding return period of T. Equation (5) shows simplification of T in terms of K_T.

$$T = \frac{1}{1 - \exp\left(-\exp\left[-0.5772 + \frac{\pi K_T}{\sqrt{6}}\right]\right)} \tag{5}$$

Selected duration and return period are identified to express the equation of frequency precipitation, X_T, as stated in Eq. (6) below:

$$X_T = X_{\text{ave}} + K_{T\sigma} \tag{6}$$

where σ is standard deviation of the rainfall data corresponding to duration T_d. To calculate the standard deviation, σ, of P rainfall data, Eq. (7) is used.

$$\sigma = \left[\frac{1}{n-1} \sum_{i=1}^{n} (X_i - X_{\text{ave}})^2 \right]^2 \tag{7}$$

Finally, to calculate rainfall intensity, I (mm/h) for every return period T is calculated using Eq. (8).

$$I_t = \frac{X_T}{T_d} \tag{8}$$

where T_d is the duration in hours.

5.2 Log-Pearson Type III Method

The procedure to calculate rainfall intensity using Log-Pearson Type III distribution method is given as follows:

Assuming X is the variate of a hydrologic series of stations, then the series of Z variates using Eq. (9) are obtained first.

$$Z = \log X \tag{9}$$

Calculate mean value of Z using Eq. (10) below:

$$\acute{Z} = \frac{1}{n} \sum_{i=1}^{n} Z \tag{10}$$

where n is the number of years of recorded data and $\acute{Z}$ is the mean of Z value.

Calculate standard deviation, σ, of the Z variate sample using equation below:

$$\sigma = \sqrt{\frac{\sum (Z - \acute{Z})^2}{(n-1)}} \tag{11}$$

Calculate coefficient of skew of variate Z and C_s using Eq. (12):

$$C_s = \frac{n \sum (Z - \acute{Z})^3}{(n-1)(n-1)(\sigma)^3} \tag{12}$$

Value K_T is then obtained based on the value of C_s from table in hydrology as presented in Table 1 by using interpolation method (when necessary). Value of Z_T was then obtained from Eq. (13) below:

Table 1 Full result of rainfall intensity (mm/h) for various durations (min) for station 3018101 Empangan Semenyih, Hulu Langat, using Gumbel method

Return period (years)	15	30	45	60	180	360	720	1440	4320
2	131.272	103.316	85.952	73.958	29.551	15.686	8.097	4.325	2.075
5	150.248	117.752	99.001	84.941	35.373	18.631	9.770	5.154	2.508
10	162.813	127.310	107.642	92.214	39.229	20.581	10.878	5.702	2.794
25	178.686	139.386	118.557	101.401	44.099	23.044	12.278	6.396	3.156
50	190.462	148.344	126.655	108.218	47.712	24.871	13.316	6.910	3.424
100	202.151	157.237	134.694	114.984	51.299	26.686	14.347	7.420	3.691

$$Z_T = \acute{Z} + K_{T\sigma} \tag{13}$$

After finding Z_T by using above equation, the corresponding value of X_T is obtained by using Eq. (14) as follows:

$$X_T = \text{antilog}(Z_T) \tag{14}$$

Finally, rainfall intensity is calculated using Eq. (8) that was stated previously.

5.3 Empirical Formula of IDF for Design Rainstorm

Elsebaie [7] stated that the IDF formulae are the empirical equations representing a relationship between maximum rainfall intensity as a dependant variable and other parameters of interest, for example, the rainfall duration and frequency as independent variable. The steps and procedure of developing empirical formula of IDF curve relationship were simplified as follows.

The original equation of rainfall intensity is converted in the form of power law relation as follows:

$$I = \frac{CT_r^m}{T_d^e} \tag{15}$$

Logarithm function is applied to get the equation as below:

$$\log I = \log K - e \log T_d \tag{16}$$

where

$$K = CT_r^m \tag{17}$$

and value of e represent the slope of the line.

Natural logarithm of K value found from Gumbel's or Log-Pearson Type III method is calculated as well as the natural logarithm of rainfall period T_d.

The values of log I and log T_d are plotted on y-axis and x-axis, respectively, for all the time intervals for both methods.

By using the graph (log I vs. log T_d) or mathematical calculation, the value of e for all the time intervals is identified and the average value is calculated using the equation below:

$$e_{ave} = \frac{\Sigma e}{n} \tag{18}$$

where n indicates number of return period (years) value noted as T_r.

From the graph, the value of log K is identified for each time interval where log K represents the y-intercept value as per Gumbel's or Log-Pearson Type III method. The equation is converted into a linear equation to become:

$$\log K = \log C + m \log T_r \tag{19}$$

Graph of log K versus log T_r is plotted on x-axis and y-axis, respectively, to determine the parameter value of C and m as C represents the y-intercept of the linear equation by the antilog value and m indicates the slope value of the graph.

5.4 Goodness-of-Fit Test

Chi-square test is used to determine the goodness-of-fit test for observed data and expected data for both methods, Gumbel's and Log-Pearson Type III. Observed value for this study is the result of rainfall intensity obtained from IDF curve, and expected value is the result obtained using empirical formula and calculation. For a five percent level of significance equal to α, the critical value is found from readily available chi-square tables and $\chi^2 >$ constitutes the critical region [7]. For this study, the chi-square test for comparing observed and expected frequencies is defined as follows (Table 2):

Table 2 Full result of rainfall intensity (mm/h) for various durations (min) for station 3018101 Empangan Semenyih, Hulu Langat, using Log-Pearson Type III method

Return Period (years)	15	30	45	60	180	360	720	1440	4320
2	128.015	97.323	79.643	67.937	27.908	14.610	7.566	4.128	1.953
5	138.551	105.628	87.169	73.697	31.064	16.020	8.373	4.434	2.163
10	158.074	120.515	100.810	84.829	37.384	19.163	10.198	5.317	2.636
25	170.754	130.618	110.168	91.805	41.484	20.911	11.226	5.679	2.903
50	179.481	137.669	116.744	96.544	44.326	22.051	11.902	5.887	3.079
100	187.696	144.415	123.068	100.953	47.010	23.076	12.512	6.055	3.237

$$x^2 = \sum \frac{(\text{Observed Value} - \text{Expected Value})^2}{\text{Expected Value}} \qquad (20)$$

The observed data are close to expected data when the value of χ^2 is small, which represents a good fit.

5.5 *Analysis and Result*

From the full results of rainfall intensity for various durations of all stations in this study, it shows that Hulu Selangor has the highest average rainfall intensity followed by Shah Alam, Kuala Selangor, Puchong, Hulu Langat Sabak Bernam, and Petaling by using both methods, Gumbel's and Log-Pearson Type III. However, average rainfall intensity using Log-Pearson Type III is slightly higher compared to Gumbel's method for both rural and urban area. The highest average of rainfall intensity is 90.32 mm/h for Gumbel's methods and 98.41 mm/h for Log-Pearson Type III method, and both values are from Hulu Selangor rainfall station. The lowest rainfall intensity is from Petaling in which the average value of rainfall intensity is 54.59 mm/h for Gumbel's and 51.91 mm/h for Log-Pearson Type III method. High rainfall intensity can lead to flooding because a lot of rainfall in a short amount of time, which means there will not be enough time for much of the rain to infiltrate into the ground and soils, thus leads to increase surface runoff and increase the discharge in the river leading to floods. From the result obtained, it shows that the area of Hulu Langat has higher possibility of flood occurrence. The overall result shows that rural and urban areas do not show much difference in terms of rainfall intensity result.

From the calculation and analysis made, the procedure of Gumbel's method is simpler compared to Log-Pearson Type III method, but the same procedure and equations are used to determine empirical formula in designing rainstorm for both methods. However, comparison had been made to determine the goodness of fit using chi-square test, and the results were plotted into a histogram to give clearer comparison. From the test, both methods were compared due to the accuracy of IDF curve with empirical formula of design rainstorm. By using chi-square formula to determine the variable of χ^2, the result was later compared with significant level that was determined earlier from the table provided. From the average results, the results of Gumbel's method show the best fit when the value of χ^2 for most of the rainfall stations and return period show closer to significant level compared to result of Log-Pearson Type III method. For rural area, however, they do not show much difference in terms of results for both methods, especially at earlier return period. Percentage of error was calculated to show clear view of the comparisons of both methods. The error was calculated based on the average data of observed value and empirical value obtained from the IDF curve and empirical formula, respectively (Figs. 1 and 2).
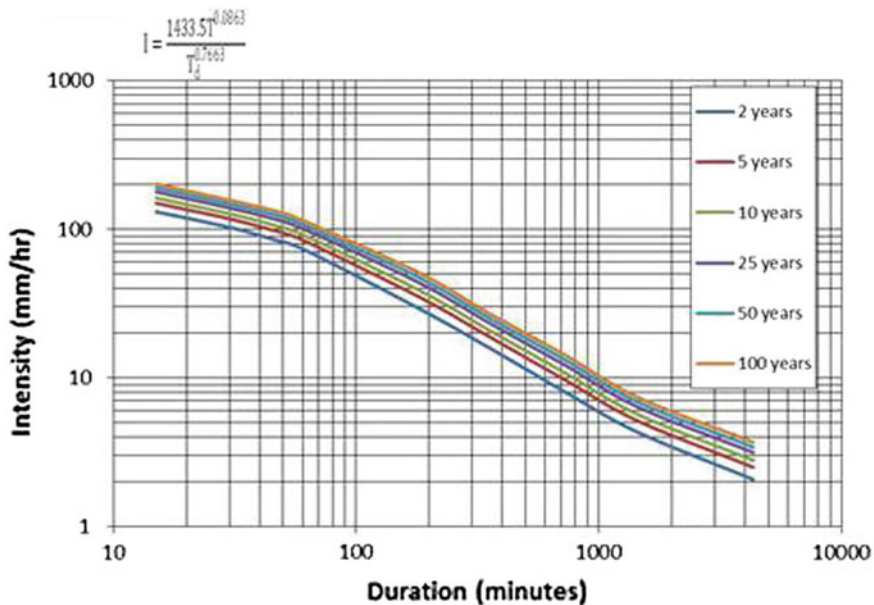
Fig. 1 IDF curve with empirical formula for Gumbel's method for station 3018101 Empangan Semenyih, Hulu Langat
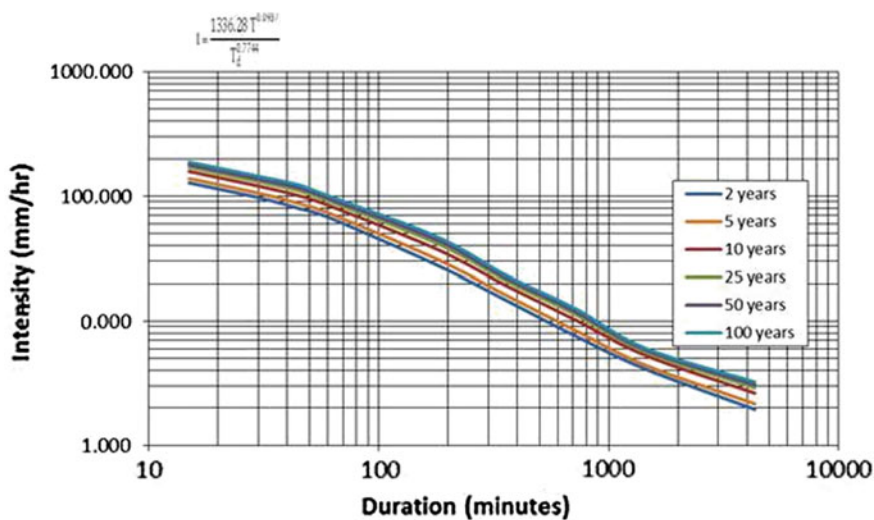

Fig. 2 IDF curve with empirical formula for Log-Pearson Type III method station 3018101 Empangan Semenyih, Hulu Langat

6   Conclusion

It has been shown that not much difference of rainfall analysis results for both rural and urban areas. Comparison of Gumbel's and Log-Pearson Type III method shows that in general, Log-Pearson Type III gives higher values of rainfall intensity for both rural and urban area. However, not many differences were indicated from both methods. In terms of accuracy, Gumbel's method gives a better fit result when tested using chi-square test as the value is closer to the significant level.

Estimating design rainstorm is an important study in the planning and management of floodplains. Planning for design rainstorm does not guarantee that the area will be protected from flood for the amount of years it is designed for; however, it is a safety measurement that must be taken into concern, and the return period varies depending on various requirements.

7   Recommendation

Selangor and Kuala Lumpur are the states in peninsular Malaysia that are experiencing flood each year. Therefore, it is important to estimate design rainstorm since the urbanization and topographic factors of these two states influence the rainfall distribution. It is recommended to analyze the duration of historical recorded data for more than 30 years. This is to ensure the accuracy of the data, and the results can be improved to be more precise.

Rain guage located at every rainfall station needs to be frequently maintained to avoid any missing data which might affect the result of design rainstorm if there are too many missing data occured. Apart from that, complete data will save a lot of time during analysis when estimation of missing data step can be skipped.

Extreme Value Type I (Gumbel's) method is recommended to be used in practical since it gives more accurate results compared to Log-Pearson Type III. In fact, most DID in Malaysia is using Gumbel's method to estimate design rainstorm and develop IDF curve.

To develop accurate empirical formula, it is recommended to use more than two distribution methods to determine rainfall intensity. Another method that can be used is lognormal distribution method. Further studies need to be done whenever there are more data to be verified and, IDF curve needs to be updated.

References

1. Duchesne S, Caya D, Mailhot GTA (2007) Assessment of future change in intensity–duration–frequency (IDF) curves for Southern Quebec using the Canadian Regional Climate Model (CRCM). J Hydrol 347:197–210
2. Mansel MG (2003) Rural and urban hydrology. Thomas Telford Publishing, London

3. Behzad T (2011) Establishment of intensity-duration-frequency curve for precipitation. EMIS 7370:7–10
4. Alhassoun SA (2011) Developing an empirical formulae to estimate rainfall intensity in Riyadh Region. Civil Engineering Department, College of Engineering, King Saud University, Saudi Arabia, pp 81–89
5. Subramanya K (2009) Engineering hydrology, 3rd edn. Mc Graw Hill, Singapore
6. De Silva RP, Dayawansa NDK, Ratnasiri MD (2007) A comparison of methods used in estimating missing rainfall data. J Agric Sci 3:101–108
7. Elsebaie IH (2011) Developing rainfall intensity–duration–frequency relationship for two regions in Saudi Arabia. Civil Engineering Department, College of Engineering, King Saud University, Saudi Arabia, pp 131–141

Analysis of Rainfall Trend and Temporal Patterns: A Case Study for Penchala River Basin, Kuala Lumpur

M.F. Chow, H. Haris and L.M. Sidek

Abstract Changing of rainfall pattern and trend has increased the flooding risk in urban areas in the recent decades. This study aimed to examine the rainfall trends and its temporal rainfall pattern in Penchala River basin. Rainfall data of 5-min interval from 2005 to 2014 were obtained from Department of Irrigation and Drainage Malaysia (DID). The Mann-Kendall (MK) test was used to detect the trends of rainfall while average variability method (AVM) was used to derive the rainfall temporal pattern in the studied river basin. The historical rainfall data in Penchala River basin show a downward trend in the past 10 years, especially in February. Meanwhile, positive trends were detected in October, November, and December. Most of the rainfall events in Penchala River basin are categorized as advanced and intermediate type pattern. Higher fraction of rainfall occurs at the early part of storm event in the Penchala River basin, compared to that of Kuala Lumpur region.

Keywords Flooding risk · Mann-Kendall test · Rainfall trends · Temporal pattern · Urban flood

1 Introduction

The increasing occurrence of flooding at the recent decades motivates more scientists throughout the world to study the changes of rainfall pattern due to climate change. Numerous studies found significant positive trends in rainfall in United States of America [1], central Argentina [2], northern and central Italy [3, 4], and the central region of Australia [5]. However, some parts of the world show a

M.F. Chow (✉) · H. Haris · L.M. Sidek
Center for Sustainable Technology and Environment (CSTEN), Universiti Tenaga Nasional, Jalan IKRAM-UNITEN, 43000 Kajang, Selangor, Malaysia
e-mail: Chowmf@uniten.edu.my

decreasing trend in rainfall such as Nigeria [6], northern China [7], Kenya [8], Sicily [9], Southeast Asia region [10], India [11], and Sri Lanka [12].

In recent years, Malaysia has experienced several extreme storm and drought events such as severe floods over the east coast and southern part of Peninsular Malaysia in December 2004 and 2006, respectively [13]. These events have raised concern in researches on the rainfall pattern which have gradually changed over the years. Generally, studies on the characteristics of extreme rainfall that are associated with flood frequency include duration, intensity, frequency, seasonality, variability, trend, and fluctuation [14].

Design flood estimation is often required design storm duration, rainfall mean intensity of an average recurrence interval (ARI) event, and rainfall temporal pattern. A temporal rainfall pattern is used to represent the typical variation of rainfall intensities during a typical storm and gives the proportion of total rainfall over certain time interval within a given rainfall duration. It is expected that design rainfall temporal pattern obtained from the local rainfall station will increase the reliability of design flood estimation.

In Malaysia, most of the rainfall events are categorized as convective thunderstorms. Urban area is always experiencing flash flood due to heavy storms during afternoon. Sometimes, flood estimation is not accurate if based on regional rainfall temporal pattern [15]. Thus, there is a need to derive a set of design rainfall temporal in a particular urban area based from local rainfall stations. The localize rainfall stations can reflect the local rainfall characteristics in rainfall temporal patterns. Hence, the objective of this study was to examine the rainfall trends and its temporal rainfall pattern in Penchala River basin. The results from this study can be used to assess the flood risk within the Klang River basin in the near future.

2 Methodology

2.1 Study Site

This study focuses on Penchala River basin which located in the Klang River basin. Figure 1 shows the location of the selected catchment. The catchment area is about 290.3 km^2, and majority of the catchment is hilly terrain with predominantly low-to-medium density residential development. The characteristics of the Penchala River basin are summarized in Table 1. Data of 5-min duration rainfall from 2005 to 2014 at Jalan 222 station which located at the center of Penchala River basin were collected from the Department of Irrigation and Drainage Malaysia (DID).
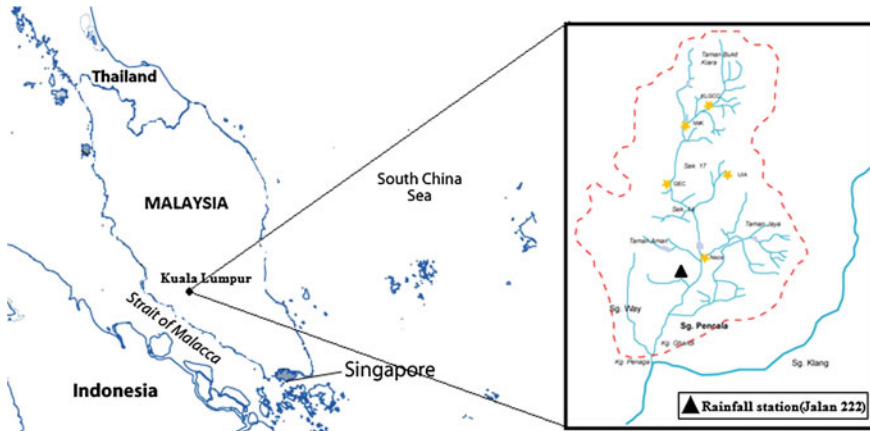
Fig. 1 Location of study site

Table 1 Characteristics of the Penchala River basin

Item	Characteristic
Area	290.3 km^2
Population (2010)	398,310
Population density	1372 person/km^2
Main land uses	Commercial, industrial, and residential

2.2 Mann-Kendall Test

The nonparametric Mann-Kendall test (MK) was used since it is robust against non-normality, missing, and censored data (i.e., data below the detection limit) [16, 17]. Briefly, this test computes the Mann-Kendall statistics S_i (Eq. (1)) and its variance VAR(S_i) (Eq. (2)) within monthly grouped data before summing for all k seasons to give the seasonal statistics S' (Eq. (3)).

$$S_i = \sum_{k=1}^{n_i=1} \sum_{I=k+1}^{n_i} \mathrm{sgn}(x_{il} - x_{ik}) \tag{1}$$

where $l > k$, n_i is the number of non-missing observations for month i, and

$$\mathrm{sgn}(z) = \begin{cases} 1, & \text{if } z > 0 \\ 0, & \text{if } z = 0 \\ -1, & \text{if } z < 0 \end{cases}$$

$$\text{VAR}(S_i) = \frac{1}{18}\left[n_i(n_i - 1)(2n_i + 5) - \sum_{j=1}^{m} t_j(t_j - 1)(2t_j + 5)\right] \qquad (2)$$

where m is the number of groups of tied (equal-valued) data in month i, and t_j is the size of the jth tied group.

$$S^t = \sum_{j=1}^{k} S_i \qquad (3)$$

is asymptotically normally distributed with mean value zero. Variance VAR(S′) (Eq. (4)) extended by the covariance COV (S_iS_g) between months I and g according to (Hirsch 1984)

$$\text{VAR}(S^t) = \sum_{i=1}^{k} \text{VAR}(S_i) + \sum_{i=1}^{k} \text{COV}(S_iS_g) \qquad (4)$$

To test the null hypothesis (H_0) of no trend against either upward or downward trend (two-tailed test) at the σ level of significance, H_0 is rejected if the absolute value of the standardized test statistics (MK stat) is greater than $Z_{1-\sigma/2}$, derived from cumulative normal distribution. A positive (negative) value of MK_{stat} indicates an upward (downward) trend. Trend slopes comprising the period 2005–2014 were calculated as the rainfall change between years for all seasonal blocks derived from the individual slope estimates Q_i for each of the k seasons [18].

$$Q_i = \frac{(x_{il} - x_{ik})}{l - k} \qquad (5)$$

2.3 Temporal Rainfall Pattern Analysis

Average variability method (AVM) was used to develop the temporal rainfall pattern in Penchala River basin since this method was being used in developing temporal rainfall patterns for Peninsular Malaysia as describe in the HP No. 1 [19]. The standard duration recommended in MASMA 2nd edition for design rainfall temporal pattern is 10, 15, 30, 60, 120, 180, and 360 min. The required time interval and number of time intervals are listed in Table 2. Ten most intense rainfall events of each duration were selected from the rainfall dataset at Jalan 222 station. The total rainfall then were divided into respective time interval to give amount of rainfall in each time period. The rainfall periods were ranked, and the percentage of rainfall in period of each rank was calculated and listed in order of magnitude. The average value for rank of each period's rainfall was obtained and given assigned ranks based on these average values. This is for the determination of chronological

Table 2 Recommended standard duration for design rainfall

Standard duration (min)	Time interval (min)	No of time intervals
10	5	2
15	5	3
30	5	6
60	5	12
120	15	8
180	15	12
360	30	12

order of the average heaviest period, second heaviest period, and so on. The mean value for the percentage of rain in period of each rank was also calculated. These average percentages of rainfall are a reasonable estimate of the percentages that would occur in the periods of the burst of rainfall of average variability. Lastly, the chronological sequence of these periods was determined by considering the most intense rainfall within the storms should be assigned to the period whose average rank is the lowest.

3 Results and Discussion

3.1 Monthly Precipitation Trends

In order to study the trend of rainfall, the mean annual and monthly values for rainfall in the Penchala River were calculated and compared. The time series of annual rainfall at station Jalan 222 from 2005 to 2014 are plotted in Fig. 2. The average monthly rainfall at Penchala River basin is plotted in Fig. 3. The monthly rainfall pattern shows two periods of maximum rainfall separated by two periods of
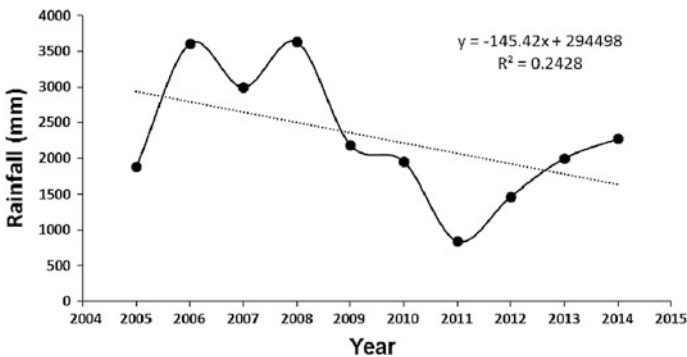

Fig. 2 Time series of annual rainfall for Jalan 222 rainfall station
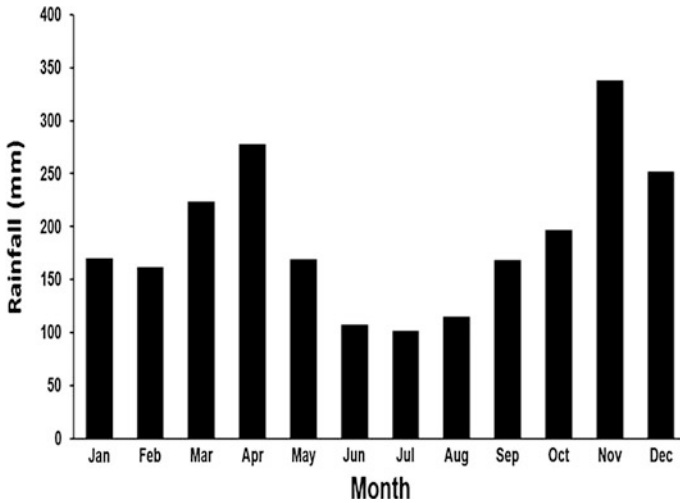
Fig. 3 Average monthly rainfall at Jalan 222 station from 2005 to 2014

minimum rainfall. The primary maximum generally occurs in November–December while the secondary maximum generally occurs in March–April. Meanwhile, the primary minimum occurs in June–July with secondary minimum in February. The trends of annual and monthly rainfall were tested using seasonal Kendall's test, while the Theil's slope method was used for calculating the magnitude of the trends. The yearly and monthly trends results are summarized in Table 3. The monthly and annually rainfall in the Penchala River basin exhibited negative trends from 2005 through 2014. Annual rainfall at the Penchala River

Table 3 Monthly total rainfall and maximum daily rainfall trends

| Month	Total monthly rainfall			Maximum daily rainfall		
	S	p	Slope	S	p	Slope
Jan	−19	0.107	−25.6	−11	0.371	−4.0
Feb	−25	0.032	−17.0	−21	0.074	−3.0
Mar	−21	0.074	−31.8	−20	0.089	−2.8
Apr	−13	0.283	−28.8	−14	0.2448	−7.0
May	−11	0.371	−11.0	−7	0.591	−1.8
Jun	−17	0.152	−31.0	−18	0.128	−6.9
Jul	−17	0.152	−9.2	−26	0.025	−2.8
Aug	−3	0.858	−1.6	−7	0.591	−0.8
Sep	−9	0.474	−13.0	−5	0.720	−1.7
Oct	1	0.834	0.4	1	0.834	0.6
Nov	5	0.5913	15.5	−3	0.858	−0.5
Dec	9	0.371	6.6	2	0.789	0.5
Annual	−9	0.474	−166.9	−11	0.371	−4.0
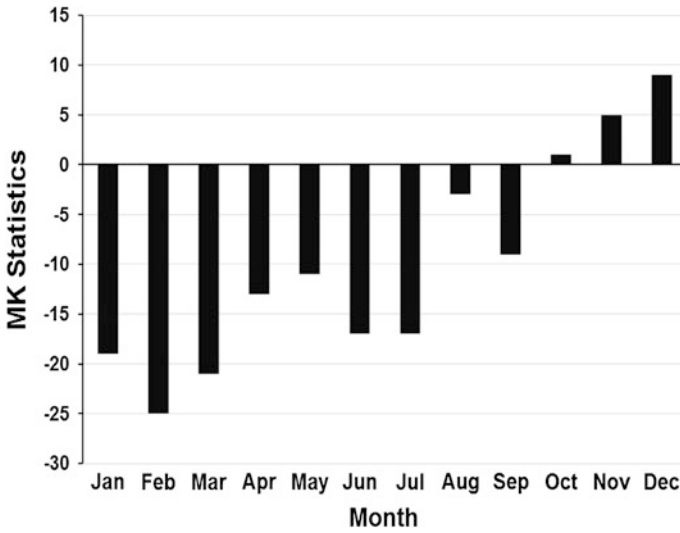
Fig. 4 Mann-Kendall test's statistics for monthly rainfall trends

basin decreased from 2005 through 2014 (slope = -166.9 mm year^{-1}, $p = 0.474$). The MK test for monthly rainfall over the whole basin reveals downward trends from January to September and upward trends in October, November, and December (Fig. 4). Statistically significant downward trend (slope = -17.0 mm month^{-1}, $p = 0.032 < 0.05$) was detected in February as shown in Table 3. The upward trend of rainfall in November and December is of considerable importance for a flood hazard. The maximum daily rainfall in each month was analyzed, and the results are summarized in Table 3. Downward trend was detected for most maximum daily rainfall in each month with statistically significant downward trend detected in July (slope = -2.8 mm month^{-1}, $p = 0.025 < 0.05$). Though many studies had reported that intense precipitation had increased in many regions of the mid and high latitudes of the northern hemisphere, but the maximum daily rainfall seems decreased in the Penchala River basin.

3.2 Temporal Rainfall Patterns

Ten most intense rainfall for each duration of 10, 15, 30, 60, 120, 180, and 360 min were selected to develop the temporal rainfall pattern in Penchala River basin. The temporal rainfall pattern based on data from 2005 to 2014 at the Penchala River basin is shown in Fig. 5. The results revealed that most of the rainfall events are categorized as advanced and intermediate type pattern. A comparison is made between temporal rainfall pattern developed in this study with that of Kuala Lumpur
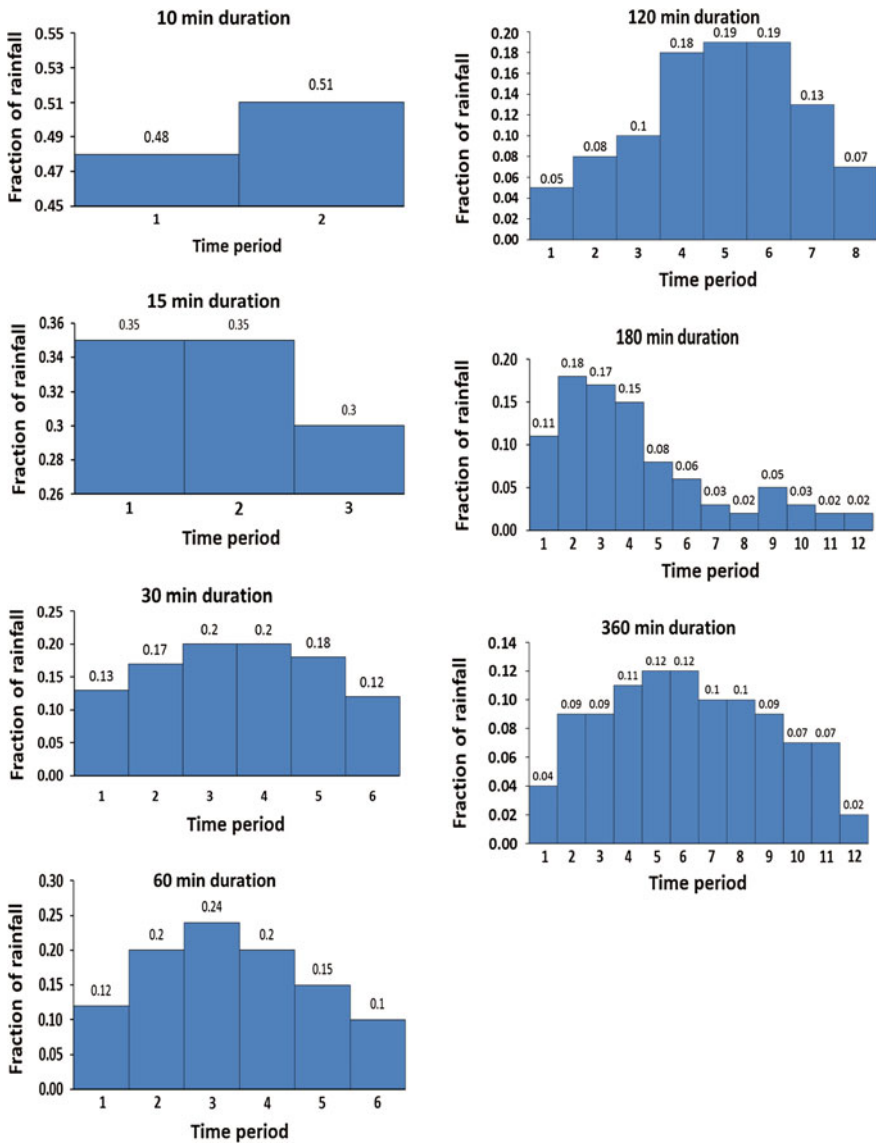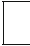
Fig. 5 Temporal rainfall pattern for Penchala River basin

region as developed by National Hydraulic Research Institute of Malaysia (NAHRIM) [20], and the results are tabulated in Table 4. It can be seen that fraction of rainfall is higher at the early part of storm event in Penchala River basin compared to that of Kuala Lumpur region.

Table 4 Comparison of temporal rainfall pattern between Pencala River basin and Kuala Lumpur region

Duration (min)	No of time periods		Fraction of rainfall in each time period											
15	3		0.35	0.35	0.30									
			0.18	*0.45*	*0.37*									
30	6		0.13	0.17	0.20	0.20	0.18	0.12						
			0.10	*0.16*	*0.40*	*0.16*	*0.11*	*0.07*						
180	12		0.11	0.18	0.17	0.15	0.08	0.06	0.03	0.02	0.05	0.03	0.02	0.02
			0.05	*0.06*	*0.08*	*0.10*	*0.10*	*0.18*	*0.12*	*0.10*	*0.09*	*0.06*	*0.05*	*0.03*
360	12		0.04	0.09	0.09	0.11	0.12	0.12	0.10	0.10	0.09	0.07	0.07	0.02
			0.03	*0.05*	*0.09*	*0.10*	*0.11*	*0.16*	*0.12*	*0.10*	*0.10*	*0.09*	*0.04*	*0.02*

Pencala River basin

Kuala Lumpur region

4 Conclusion

This study is carried out to examine the rainfall trends and its temporal rainfall pattern in Penchala River basin. The rainfall in Penchala River basin shows a downward trend in the past 10 years, especially in February. The MK test for rainfall trend from 2005 to 2014 reveals that significant downward trend is detected in February. Meanwhile, positive trends were detected in October, November, and December. The results exhibited that the dry season (e.g., February) has the tendency to get drier while wet season is getting wetter in the Penchala River basin. Even if the total amount of annual rainfall does not change significantly, the enhancement in the seasonal precipitation cycle could have marked consequences for the frequency of droughts and floods. The results of temporal rainfall pattern analysis revealed that most of the rainfall events are categorized as advanced and intermediate type pattern. Higher fraction of rainfall occurs at the early part of storm event in the Penchala River basin, compared to that of Kuala Lumpur region.

References

1. Karl TR, Knight RW (1998) Secular trends of precipitation amount, frequency and intensity of the United States. Bull Am Meteorol Soc 79(2):223–241
2. Lucero OA, Rozas D (2002) Characteristics of aggregation of daily rainfall in a middle-latitudes region during a climate variability in annual rainfall amount. Atmos Res 61:35–48
3. Brunetti M, Buffoni L, Maugeri M, Nanni T (2000) Precipitation intensity trends in Northern Italy. Int J Climatol 20:1017–1031
4. Brunetti M, Colacino M, Maugeri M, Nanni T (2001) Trends in the daily intensity of precipitation in Italy from 1951 to 1996. Int J Climatol 21:299–316

5. Gallant AJE, Hennessy KJ, Risbey J (2007) Trends in rainfall indices for six Australian regions: 1910–2005. Aust Meteorol Mag 56:223–239
6. Hess TM, Stephens W, Maryah UM (1995) Rainfall trends in the North East Arid Zone of Nigeria 1961–1990. Agric For Meteorol 74:87–97
7. Gong D-Y, Shi P-J, Wang J-A (2004) Daily precipitation changes in the semi-arid region over northern China. J Arid Environ 59:771–784
8. Kipkorir EC (2002) Analysis of rainfall climate on the Njemps Flats, Baringo District, Kenya. J Arid Environ 50:445–458
9. Cannarozzo M, Noto LV, Viola F (2006) Spatial distribution of rainfall trends in Sicily (1921–2000). Phys Chem Earth 31:1201–1211
10. Manton MJ, Della-Marta PM, Haylock MR, Hennessy KJ, Nicholls N, Chambers LE, Collins DA, Daw G, Finet A, Gunawan D, Inape K, Isobe H, Kestin TS, Lefale P, Lyu CH, Lwin T, Maitrepierre L, Ouprasitwong N, Page CM, Pahalad J, Plummer N, Salinger MJ, Suppiah R, Tran VL, Trewin B, Tibig I, Yee D (2001) Trends in extreme daily rainfall and temperature in Southeast Asia and the South Pacific: 1961–1998. Int J Climatol 21:269–284
11. Kothyari UC, Singh VP (1996) Rainfall and temperature trends in India. Hydrol Process 10:357–372
12. Herath S, Ratnayake U (2004) Monitoring rainfall trends to predict adverse impacts—A case study from Sri Lanka (1964–1993). Glob Environ Change 14:71–79
13. Juneng L, Tangang FT, Reason CJC (2007) Numerical case study of an extreme rainfall event during 9–11 December 2004 over the east coast of Peninsular Malaysia. Meteorol Atmos Phys 98:81–98
14. Ologunorisa ET, Diagi PN (2005) Extreme rainfall and its implication for flood frequency in the Western Niger Delta a case study of Warri. Niger J Trop Geogr 1
15. Desa MMN, Niemczynowicz J (1996) Spatial variability of rainfall in Kuala Lumpur, Malaysia: long and short term characteristics. Hydrol Sci J 41(3):345–362
16. Hirsch RM, Slack JR, Smith RA (1982) Techniques of trend analysis for monthly water-quality data. Water Resour Res 18:107–121
17. Gilbert RO (1987) Statistical methods for environmental pollution monitoring. Van Nostrand Reinhold, New York (ISBN 0-471-28878-0)
18. Sen PK (1968) Estimates of the regression coefficient based on Kendall's Tau. J Am Stat Assoc 63:1379–1389
19. Department of Irrigation and Drainage Malaysia (DID) (1982) Hydrological procedure No. 1: estimation of the design rainstorm in Peninsular Malaysia (Revised and updated), Malaysia
20. Department of Irrigation and Drainage Malaysia (DID). 2010. "Hydrological Procedure No.1: Estimation of the Design Rainstorm in Peninsular Malaysia (Reviewed and updated)". Malaysia